Formulation and Evaluation of Polymeric Nanoparticles as Carriers of Rosuvastatin Calcium for Oral Administration"

Dissertation submitted to

THE TAMIL NADU Dr. M. G. R. MEDICAL UNIVERSITY

CHENNAI-32

In partial fulfillment of the requirement for the

Degree of

MASTER OF PHARMACY IN PHARMACEUTICS

Submitted By Miss. T. Suganya

(Reg.No-26108608)

APRIL 2012

DEPARTMENT OF PHARMACEUTICS

COLLEGE OF PHARMACY

MADURAI MEDICAL COLLEGE

MADURAI – 625 020

Dr. Mrs. AJITHADAS ARUNA, M.Pharm., PhD.,
Principal,
College of Pharmacy,
Madurai Medical College,
Madurai– 625020.

CERTIFICATE

This is to certify that the dissertation entitled**, "Formulation and Evaluation of Polymeric Nanoparticles as Carriers of Rosuvastatin Calcium for Oral Administration"** was done by **Miss. T. Suganya** in the Department of Pharmaceutics, Madurai Medical College, Madurai – 20, in partial fulfillment of the requirement for the Degree of Master of Pharmacy in Pharmaceutics, is a bonafide work carried out by her, under the guidance and supervision of **Prof. Mr. A. Abdul Hasan Sathali**, **M.Pharm., (Ph.D).,** Professor and Head, in the Department of Pharmaceutics, Madurai Medical College, Madurai-20 during the academic year 2011 – 2012.

This dissertation is forwarded to the Controller of Examinations, The Tamilnadu Dr. M.G.R. Medical University, Chennai.

Place : Madurai

Date :

(AJITHADAS ARUNA)

Prof. Mr. A. Abdul Hasan Sathali, M.Pharm., (Ph.D).,
Professor and Head,
Department of Pharmaceutics,
College of Pharmacy,
Madurai Medical College,
Madurai-625020

CERTIFICATE

This is to certify that the dissertation entitled **"Formulation and Evaluation of Polymeric Nanoparticles as Carriers of Rosuvastatin Calcium for Oral Administration"** submitted by **Miss. T. Suganya** in partial fulfillment of the requirement for the Degree of Master of Pharmacy in Pharmaceutics is a bonafide work carried out by her, under my guidance and supervision during the academic year 2011 – 2012 in the Department of Pharmaceutics, Madurai Medical College, Madurai-20.

I wish her success in all his endeavors.

Place : Madurai

Date :

(A. Abdul Hasan Sathali)

ACKNOWLEDGEMENT

The Almighty, I am thankful and grateful to You for constant support not only for my project but for all the achievements in my life. I bow down to You with both the hands folded.

I am very grateful to my **Parents** for their love and faith in me that "I can do" added huge courage to my spirit.

It is my pleasure to express my respectful regards and thanks to our Dean **Dr. A. EDWIN JOE M.D., F.M., B.L.,** Madurai Medical College, Madurai for providing all kinds of supportive facilities required to carry out my project work.

It is my privilege and honour to extend my gratitude to **Dr. AJITHADAS ARUNA, M.PHARM, Ph.D.,** Principal, College of pharmacy, Madurai Medical College, Madurai for her support to carry out my project work.

It is a great pleasure for me to acknowledge all those who have contributed towards the conception, origin and nurturing of this project. The person whose picture comes first in my mind is that of my esteemed guide **Prof. A. ABDUL HASAN SATHALI, M.Pharm., (Ph.D**), Professor and Head, Department of Pharmaceutics, Madurai Medical College, Madurai for his guidance, timely advice, kind co-operation, understanding and constant inspiration throughout the course of the study. It is with affection and reverence that I dedicate often beyond the call of duty; it was pleasure of working under his guidance.

I owe my thanks to **Mr. C. Pandian, M.Pharm., Mr. R. Senthil Prabhu, M.Pharm.,** and **Mrs. D. Uma Maheswari, M.Pharm.**

I also extend my thanks to our department staffs **Mrs. Geetha, D.M.L.T., Mrs. Mumtaj D.M.L.T.,** and **R.Chitravalli** for their contribution and kind co-operation throughout my project work.

I take privilege to convey my thanks to **Mrs. Lavanya Anbu**, Pharma Information Centre, Chennai for her help in collection of references in accordance with my dissertation work.

I express my heartiest thanks to **Mr. Saravanan B.Pharm., Safetab life Science, Mr. G. Manikandan B.Pharm., MS., Dr.Reddy's lab, Mr.V. Srinivasan M.Pharm., Orchid Pharma** and **United Scientifics** for providing drugs and chemicals to carry out my project work.

I take this privilege to convey my thanks to **Mrs. Manimegalai, M.Sc., M.Phil., Technical officer USIC – M.K.University,** for her help in carrying out **FT - IR** studies in accordance with my dissertation work.

I convey my sincere thanks to **JSS College of Pharmacy, Ooty** for their help in carrying out the **DSC** studies in accordance with my dissertation work.

I extend my thanks to **Dr. Jonat, M.V.S.C** Veterinary Assistant Surgeon, Central Animal House, Madurai Medical College, Madurai for his valuable assistance during *ex vivo* intestinal permeation studies.

I wish to acknowledge **Mr. Shaun Praveen, Karunya University, Coimbatore** for his help in particle size analysis in accordance with my dissertation work.

I convey my sincere thanks to **Agricultural University, Coimbatore** for their help in carrying out the **TEM** studies in accordance with my dissertation work.

My sisters **Mrs. V. Lavanya David** and **Ms. T.Karunya** have been a driving force behind me for my accomplishments and achievements.

"A Friend in need is the Friend Indeed": I would like to give a special thank to **Mr.S.Ganesan, Mr.S.Kathiravan, Mr.V.Palanivel, Mr.T.Prakash, Mr.D.RajivGandhi, Ms.R.Revathi, Mr.V.Selvaraj, Mr.J.Varun and Ms.B.Yuganya** for their ever appraising support and who helped me when I needed someone desperately.

My gratitude goes to my seniors **Ms.A.Gokila, Mrs.R.Kavitha, Ms.K.Priyanka, Ms. P. Shanmugapriya and Ms.T.Sangeetha** for their guidance during the project.

Very special thanks to all my juniors **Ms. C. Deepa, Ms. M. Gomathi, Mr. M. Gopinath, Mrs. J. Jayalakshmi, Mr. L. Magesh kumar, Mr. P.Manikandan, Ms. N. Nisha, Mr. I. Semdurai, Ms N.Surya devi and Ms. V.Susila devi** for making my stay a pleasant one in MMC, Madurai.

I also extend my thanks to all the staff members and P.G. Students of Department of Pharmaceutical Chemistry and Pharmacognosy for their Co-operation.

I am extremely thankful to the staff of **Shanlax Publications, Madurai** for their kind co-operation during my dissertation work.

CONTENTS

LIST OF TABLES

LIST OF FIGURES

ABBREVIATION

Abbreviation	Expansion
nm	Nanometer
λ_{max}	Wavelength with maximum absorbance
%	Percentage
IR	Infra red spectra
H	Hour
GIT	Gastrointestinal tract
PCS	Photon correlation spectroscopy
SEM	Scanning electron microscopy
TEM	Transmission electron microscopy
UV	Ultra violet spectroscopy
DSC	Differential scanning Calorimetry
PBS	Phosphate buffer saline
AUC	Area under the curve
Cmax	Maximum drug concentration in Plasma
T_{max}	Time at peak plasma drug concentration
Ka	First order Absorption rate constant
Ke	Excretion rate constant of the drug in urine
Vd	Volume of distribution
EL 100	Eudragit L100
ES 100	Eudragit S100
NP's	Nanoparticles
PVA	Polyvinyl alcohol
PDI	Polydispersity Index

CHAPTER-I

NANOTECHNOLOGY: A BOON TO DRUG DELIVERY

1.1 Introduction

Size reduction is a fundamental unit operation having important applications in pharmacy. It helps in improving solubility and bioavailability, reducing toxicity, enhancing release and providing better formulation opportunities for drugs. In most of the cases, size reduction is limited to micron size range, for example, various pharmaceutical dosage forms like powder, emulsion, suspension etc. Drugs in the nanometer size range enhance performance in a variety of dosage forms. Major advantages of nanosizing include (i) increased surface area (ii) enhanced solubility (iii) increased rate of dissolution (iv) increased oral bioavailability (v) more rapid onset of therapeutic action (vi) less amount of dose required (vii) decreased fed/fasted variability and (viii) decreased patient-to-patient variability.

The word 'nano' is derived from Latin word, which means dwarf. Nano size refers to one thousand millionth of a particular unit thus nanometer is one thousand millionth of a meter (i.e. $1nm = 10^{-9}$ m).

Nanotechnology is the science that deals with the processes that occur at molecular level and of nanolength scale size. There are numerous examples from nature like DNA, water molecules, virus, red blood corpuscles (RBC) etc., which are of nanodimensions; even our history has numerous examples which prove that we have exploited the advantages of technology in one or other form. Figure 1 depicts various examples from nature and pharmaceuticals which are operated at various dimensions of nanolength scale. The term nanotechnology has been most commonly used in other fields of science like electronic, physics and engineering since many decades. Nanotechnology has shown tremendous

progress in these fields. However, biomedical and pharmaceutical fields remain yet to be explored.

Nanotechnology is a multidisciplinary field, convergence of basic sciences and applied disciplines like biophysics, molecular biology, and bioengineering. It has created powerful impact in various fields of medicine including cardiology, ophthalmology, endocrinology, oncology, immunology etc., and to highly specialized areas like gene delivery, brain targeting, tumor targeting, and oral vaccine formulations. Nanotechnology provides intelligent systems, devices and materials for better pharmaceutical applications.

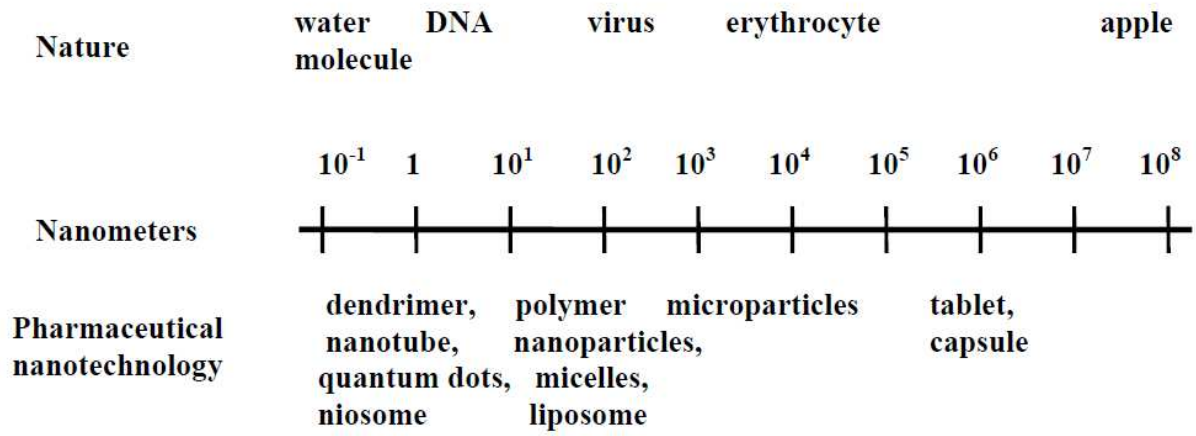

Figure 1 Dimensions of Nanotechnology

1.2 Nano-Definitions

Important nano-definitions are described below:

- **'Nanoscience'** can be defined as study of phenomenon and manipulation of materials at atomic and molecular scales.
- **'Nanotechnology'** is related to design characterization, production and applications of structures, devices and systems by controlling shape and size at nanometer scale.

- **'Pharmaceutical nanotechnology'** embraces applications of nanoscience to pharmacy as nanomaterials, and as devices like drug delivery, diagnostic, imaging and biosensor.
- '**Nanomedicine'** is defined as submicron size (<1um) modules, used for treatment, diagnosis, monitoring, and control of biological system.

Pharmaceutical nanotechnology has provided more fine-tuned diagnosis and focused treatment of disease at a molecular level. Pharmaceutical nanotechnology is most innovative and highly specialized field, which will revolutionize the pharmaceutical industry in near future. Pharmaceutical nanotechnology presents revolutionary opportunities to fight against many diseases. It helps in detecting the antigen associated with diseases such as cancer, diabetes mellitus, neurodegenerative diseases, as well as detecting the microorganisms and viruses associated with infections. It is expected that in next 10 years market will be flooded with nanotechnology-devised medicine.

1.3 Opportunities and Scope

In view of post GATT (General Agreement of Trade and Tariff) scenario pharmaceutical industries are focusing towards their research on nanotechnology because developing new chemical entity (NCE) is very time consuming and expensive affair and most of drugs will be off patent very soon causing huge revenue loss. Applications of nanotechnology to pharmacy that provide intelligent and smart drug delivery systems is expected to emerge as most important and powerful tool as alternate to conventional dosage form. These nano-intelligent drug delivery systems need little investment while expected to be a high profit making deal due to new patent-protection for current or soon-to-be off-patent drugs. A recent report claimed that 23 major pharmaceutical patents would expire by 2008 leading to revenue loss of US $ 46 billion and by 2011, US $ 70-80 billion loss is expected as various drugs go off-patent (Baba, 2007). Therefore most of industrial research interest lies in fact to exploit the

newer technology to develop drug delivery system of available drugs in order to reduce or overcome their shortcoming like high toxicity, instability in biological environment, poor bioavailability, and low therapeutic concentration at site of action, which rendered them poor candidates in currently available dosage forms.

Now days most of the industries have realized the potential applications of nanotechnology in pharmacy and are making their efforts in research and development in this area. Recent data depicts that global investment on nanotechnology reached US $ 12.4 billion in 2006. The data presented below suggests the global interest over nanotechnology investment and related issue (Figure 2).

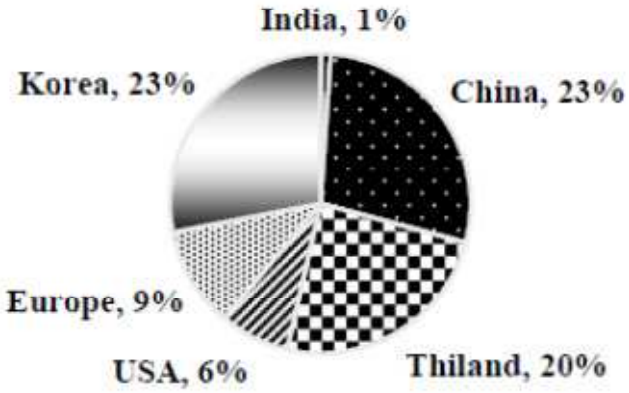

Figure 2 Global investment on nanotechnology (9 billion US $, 2005)

Novel drug delivery comprises of a number of features of nanotechnology, which make it a suitable tool to address major issues. The scope of pharmaceutical nanotechnology is very wide from smart material for tissue engineering to intelligent tools for delivery of drugs and diagnostics, and more recently, artificial RBC etc. Current applications of nanotechnology in pharmacy are development of nanomedicine, tissue engineering, nanorobots, advance

diagnostic, as carrier of diagnostic and therapeutic modalities and as biosensor, biomarker, image enhancement device, implant technology, bioactive surfaces etc. A large number of nanosystems, which have been investigated in pharmacy to date, are liposomes, dendrimers, metallic nanoparticles, polymeric nanoparticles, carbon nanotubes, quantum dots, nanofibres etc.

1.4 Pharmaceutical Nanotechnology Based Systems

Pharmaceutical nanotechnology provides two basic types of nanotools viz. nanomaterials and nanodevices, which play a key role in realm of pharmaceutical nanotechnology and related fields.

1.4.1 Nanomaterials are biomaterials used, for example, in orthopedic or dental implants or as scaffolds for tissue-engineered products. Their surface modifications or coatings might greatly enhance the biocompatibility by favoring the interaction of living cells with the biomaterial. These materials can be sub classified into nanocrystalline and nanostructured materials.

1.4.2 Nanocrystalline materials are readily manufactured and can substitute the less performing bulk materials. Raw nanomaterials can be used in drug encapsulation, bone replacements, prostheses (artificial mechanical devices to replace body parts lost in injury and or by birth e.g. artificial limbs, facial prosthetics and neuroprosthetics etc.), and implants.

1.4.3 Nanostructured materials are processed forms of raw nanomaterials that provide special shapes or functionality, for example quantum dots, dendrimers, fullerenes and carbon nanotubes.

1.4.4 Nanodevices are miniature devices in the nanoscale and some of which include nano- and micro-electromechanical systems (NEMS/ MEMS), microfluidics (control and manipulation of micro or nanolitre of fluids), and microarrays (different kind of biological assay e.g. DNA, protein, cell, and antibody). Examples include biosensors and detectors to

detect trace quantities of bacteria, airborne pathogens, biological hazards, and disease signatures and some intelligent machines like respirocytes (Figure 3).

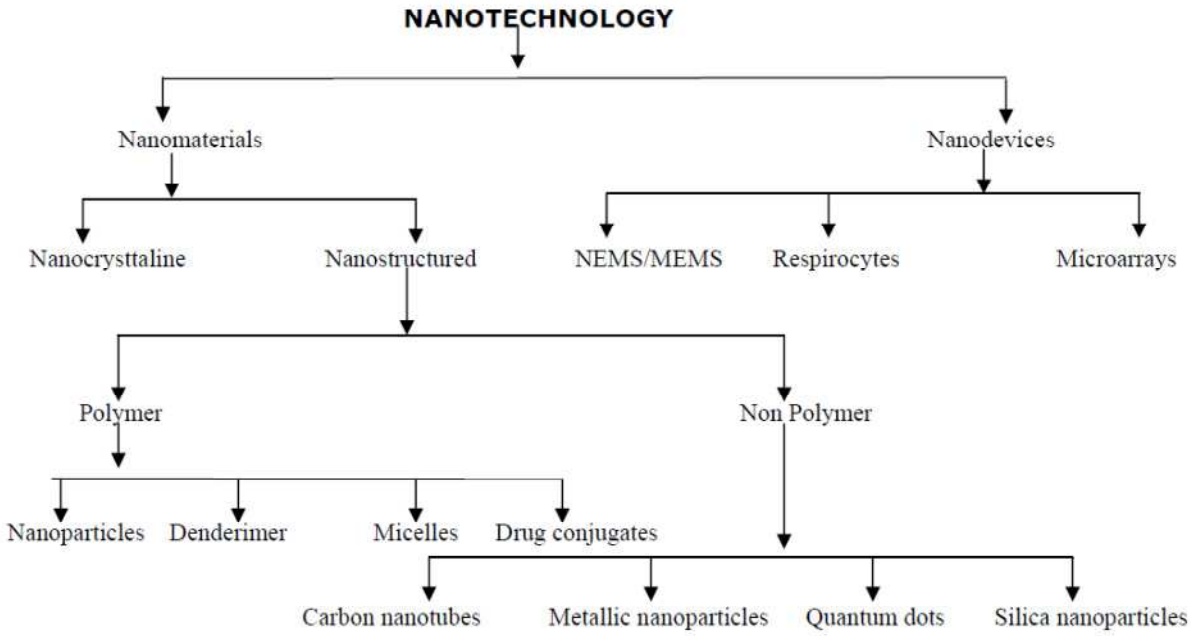

Figure 3 Schematic diagram of various types of pharmaceutical nanosystems

A brief discussion of various types of pharmaceutical nanosystems is presented below:

1.4.4.1 Carbon nanotubes: Carbon nanotubes are hexagonal networks of carbon atoms, 1 nm in diameter and 1–100 nm in length, as a layer of graphite rolled up into a cylinder. There are two types of nanotubes: single-walled nanotubes (SWNTs) and multi-walled nanotubes (MWNTs), which differ in the arrangement of their graphene cylinders (Figure 4).

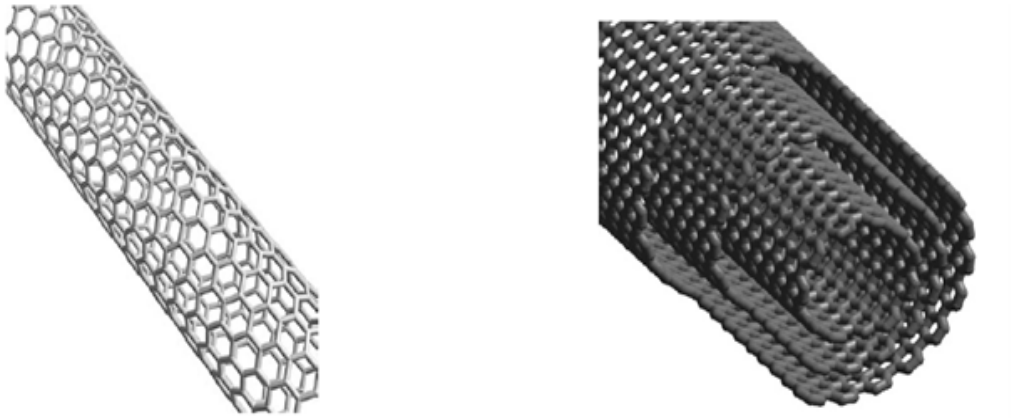

(a) Single walled (SWNTs) (b) Multi walled (MWNTs)

Figure 4 Structure of Carbon nanotubes

These are small macromolecules that are unique for their size, shape, and have remarkable physical properties. Nanotubes offer some distinct advantages over other drug delivery and diagnostic systems due to very interesting physicochemical properties such as ordered structure with high aspect ratio, ultra-light weight, high mechanical strength, high electrical conductivity, high thermal conductivity, metallic or semi-metallic behavior and high surface area (Sinha and Yeow, 2005).

1.4.4.2 Quantum dots: Quantum dots (QDs) are semiconducting materials consisting of a semiconductor core (CdSe), coated by a shell (e.g., ZnS) to improve optical properties, and a cap enabling improved solubility in aqueous buffers. They are neither atomic nor bulk semiconductors. Their properties originate from their physical size, which ranges from 10–100 Å in radius. Due to their bright fluorescence, narrow emission, broad UV excitation and high photo stability QDs have been adopted for *in vitro* bioimaging for real time monitoring or tracking of intracellular process for longer time (Figure 5). Quantum-dots have a large impact on some important development in different medical areas like diagnostic tools

(magnetic resonance imaging, MRI), *in vitro* and *in vivo* detection and analysis of biomolecules, immunoassays, DNA hybridization, development of non-viral vectors for gene therapy, transport vehicles for DNA, protein, drugs or cells, time graded fluorescence imaging of tissue, labeling of cells and as therapeutic tools for cancer treatment.

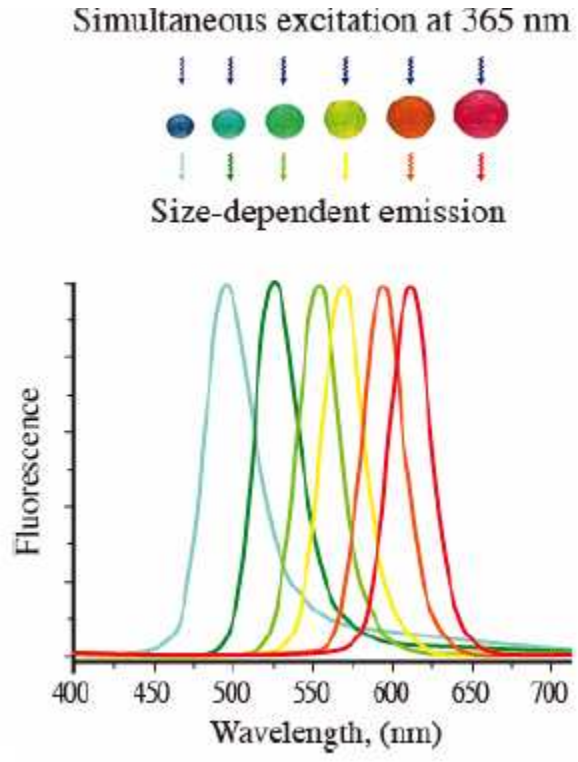

Figure 5 Size dependent representation of a quantum dots

1.4.4.3 Dendrimers: Dendrimers are hyper branched, tree-like structures and have compartmentalized chemical polymer. Dendrimers contain three different regions: core, branches, and surface (Figure 6). The macromolecule constituents radiate in branching form from the central core, creating an internal cavity as well as a sphere of end groups that can be tailored according to requirements (Khopde et al., 2001). They can be tailored or modified into biocompatible compounds with low cytotoxicity and high biopermeability. They bear promising properties for delivery of bioactive ranging from drugs, vaccines, metal, and genes to desired sites. Their hollow interior provides space to incorporate drugs and other bioactive

physically or by various interactions to act as drug delivery vehicles. Most important applications of dendrimers are solubilization, gene therapy, dendrimers based drug delivery, immunoassay and MRI contrast agent. Dendrimers is ideal carrier for drug delivery due to advantages like very low size (1-5 nm), feasibility to develop with defined molecular weight, very low polydispersity index (ratio of weight average molecular weight (Mw) to number average molecular weight (Mn) of polymer), good entrapment efficiency and offering surface for functionalization. They can be modulated for target-specific drug delivery but their toxicity profile renders them not very popular system for use as delivery means.

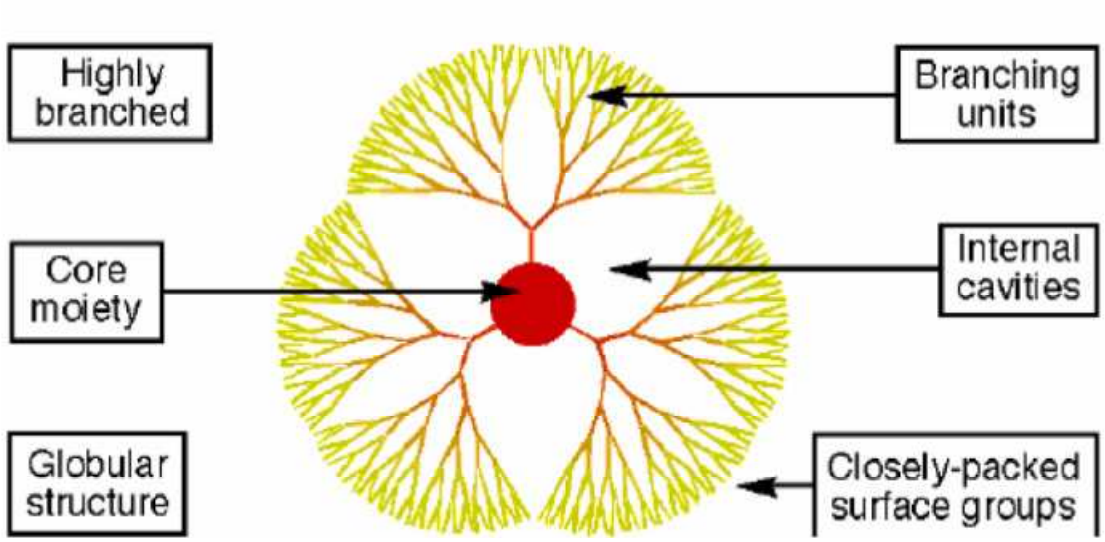

Figure 6 Schematic representation of a dendrimer showing core, branches, and surface

1.4.4.4 Polymeric nanoparticles: Polymeric nanoparticles (Figure 7) provide an alternative to above-mentioned nanosystems due to some inherent properties like biocompatibility, nonimmunogenicity, nontoxicity and biodegradability. These are colloidal carrier, 10 nm - 1μm in size, consisting of synthetic or natural polymers. Polymeric nanoparticles are a broad class comprised of both vesicular systems (nanocapsules) and matrix systems (nanospheres). **Nanocapsules** are systems in which the drug is confined to a cavity surrounded by unique polymeric membrane whereas **Nanospheres** are systems in which the drug is dispersed

throughout the polymer matrix. The various natural polymers like gelatin, albumin and alginate are used to prepare the nanoparticles; however they have some inherent disadvantages like poor batch-to-batch reproducibility, prone to degradation and potential antigenicity.

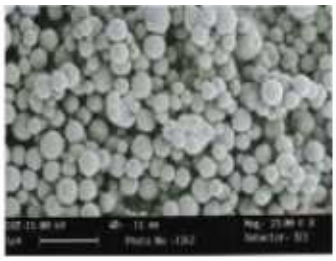

Figure 7 Scanning electron microscopy image of polymer nanoparticles
(Adopted from Senthilkumar *et al.,* 2007)

Synthetic polymers used for nanoparticles preparation may be in the form of preformed polymer e.g. polyesters like polycaprolactone (PCL), poly lactic acid (PLA) or monomers that can be polymerized *in situ* e.g. polyalkyl cyanoacrylate. The candidate drug is dissolved, entrapped, attached or encapsulated throughout or within the polymeric shell/matrix. Depending on the method of preparation, the release characteristic of the incorporated drug can be controlled. Polymeric nanoparticulate systems are attractive modules for intracellular and site specific delivery. Nanoparticles can be made to reach a target site by virtue of their size and surface modification with a specific recognition ligand. Their surface can be easily modified and functionalized.

1.4.4.5 Metallic nanoparticles: Metallic nanoparticles are emerging as good delivery carrier for drug and biosensor. Although nanoparticles of various metals have been made yet silver and gold nanoparticles are of prime importance for biomedical use (Figure 8). Their surface functionalization is very easy and various ligands have been decorated onto the surface. A large numbers of ligands have been linked to nanoparticles including sugars, peptide, protein and DNA. They have been used for active delivery of bioactive, drug

discovery, bioassays, detection, imaging and many other applications due to surface functionalization ability, as an alternative to quantum-dots.

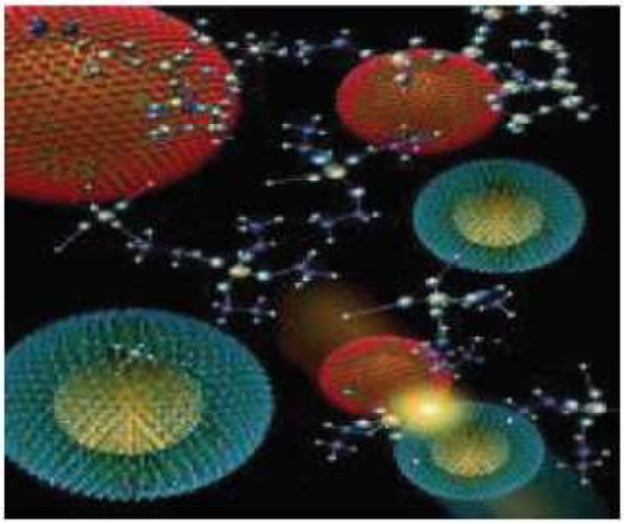

Figure 8 Surface functionalized gold nanoparticles

1.4.4.6 Liposomes: Liposomes have been extensively explored and most developed nanocarriers for novel and targeted drug delivery. These closed vesicles are formed when dry phospholipids are hydrated (Figure 9). Liposomes are classified into three basic types based on their size and number of bilayers. Multilamellar vesicles (MLVs) consist of several lipid bilayers separated from one another by aqueous spaces. These entities are heterogeneous in size, often ranging from a few hundreds to thousands of nanometers in diameter. On the other hand, both small unilamellar vesicles (SUVs) and large unilamellar vesicles (LUVs) consist of a single bilayer surrounding the entrapped aqueous space. SUVs are less than 100 nm in size whereas LUVs have diameters larger than 100 nm.

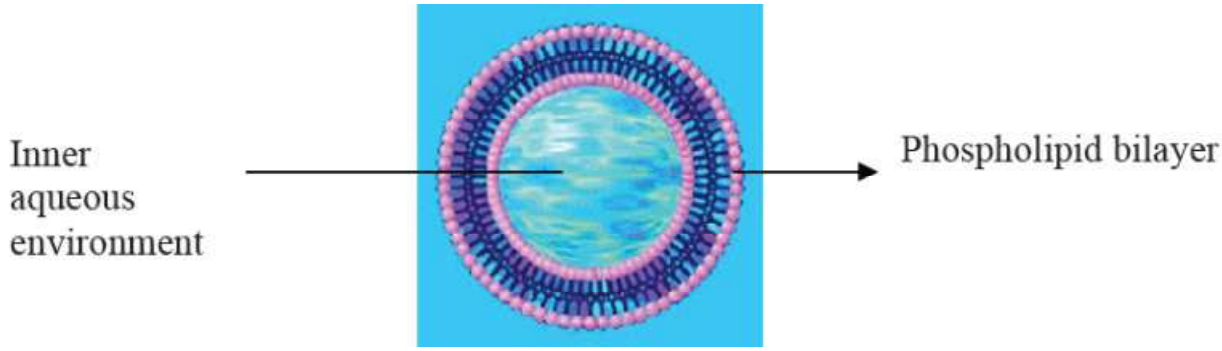

Figure 9 Structure of Liposomes

Drug molecules can be either entrapped in the aqueous space or intercalated into the lipid bilayer of liposomes, depending on the physicochemical characteristics of the drug. Liposomes can be prepared with enormous diversity in structure, composition, size, flexibility, and a variety of surface modification approaches proving most intelligent carrier system for both active and passive delivery of bioactives. They have been successfully exploited in cancer therapy, carrier for antigens, pulmonary delivery, leishmaniasis, ophthalmic drug delivery etc. Some of liposome-based formulations are already in market (Table I).

Table I Liposomal formulation in market

PRODUCT	STATUS	PAYLOAD	INDICATION
Daunoxome®	Market	Daunorubicin	Cancer
Doxil®/caelyx®	Market	Doxorubicin	Cancer
Moet®	Market	Doxorubicin	Cancer
Ambisome®	Market	Amphotericin B	Fungal infections

1.4.4.7 Polymeric micelles: Amphiphilic block copolymers assemble into nanoscopic supramolecular core-shell structures known as 'polymeric micelles'. Polymeric micelles are usually of <100 nm and their hydrophilic surface protects their nonspecific uptake by reticuloendothelial system. Micelles are formed in solution as aggregates in which the component molecules (e.g., amphiphilic AB-type or ABA-type block copolymers, where A and B are hydrophobic and hydrophilic components, respectively) are generally arranged in a spheroidal structure with hydrophobic cores shielded from water by a mantle of hydrophilic groups (Figure 10).

Figure 10 Structure of block copolymer micelles

These dynamic systems are used for the systemic delivery of water-insoluble drugs.

1.4.4.8 Polymer drug conjugate: The conjugation of low molecular weight drugs with polymer causes drastic change in pharmacokinetic disposition of drug in whole body and at cellular level. Polymer-drug conjugates are thus designed to increase the overall molecular weight, which facilitates their retention in cancer cells through enhanced permeation and retention (EPR) effect using passive delivery approach.

1.4.4.9 Polyplexes/Lipopolyplexes: These are assemblies, which form spontaneously between nucleic acids and polycations or cationic liposomes (or polycations conjugated to

targeting ligands or hydrophilic polymers), and are used in transfection protocols. The shape, size distribution, and transfection capability of these complexes depends on their composition and charge ratio of nucleic acid to that of cationic lipid/polymer. Examples of polycations that have been used in gene transfer/therapy protocols include poly-L-lysine, linear- and branched-poly (ethyleneimine), poly (amidoamine), poly-amino esters, and cationic cyclodextrin.

Table II Brief descriptions of nanosystems (Nahar et al., 2006)

Types of Nanosystems	Size	Characteristics	Applications
Polymeric nanoparticles	10-1000 nm	Biocompatible, biodegradable, offer complete drug protection	Excellent carrier for controlled and sustained delivery of drugs. Stealth and surface modified nanoparticles can be used for active and passive delivery of bioactives
Nanocrystal Quantum dots	2–9.5 nm	Semi conducting material synthesized with II-VI and III-V column element; Size between 10-100 Å; Bright fluorescence, narrow emission, Broad UV excitation and high photo stability	Long term multiple color imaging of liver cell; DNA hybridization, immunoassay; receptor mediated endocytosis; labeling of breast cancer marker HeR_2 surface of cancer cells
Carbon nanotubes	0.5–3 nm diameter and 20–1000 nm length	Third allotropic crystalline form of carbon sheets either single layer (single walled nanotube, SWNT) or multiple layer (multi-walled nanotube, MWNT). These crystals have remarkable strength and unique electrical properties (conducting, semi conducting, or insulating)	Functionalization enhanced solubility, penetration to cell cytoplasm and to nucleus, as carrier for gene delivery, peptide delivery

Dendrimer	<10 nm	Highly branched, nearly monodisperse polymer system produced by controlled polymerization; three main parts core, branch and surface	Long circulatory, controlled delivery of bioactives, targeted delivery of bioactives to macrophages, liver targeting
Metallic nanoparticles	<100 nm	Gold and silver colloids, very small size resulting in high surface area available for functionalization, stable	Drug and gene delivery, highly sensitive diagnostic assays, thermal ablation and radiotherapy enhancement
Polymeric micelles	10-100nm	Block amphiphilic copolymer micelles, high drug entrapment, payload, biostability	Long circulatory, target specific active and passive drug delivery, diagnostic value
Liposome	50-100 nm	Phospholipid vesicles, biocompatible, versatile, good entrapment efficiency, offer easy surface functionalization	Long circulatory, offer passive and active delivery of gene, protein, peptide and various other bioactives
Silica Nanoparticles	10nm–50 μm	Silanised and coated with oligonucleotide. Observable by fluorescence method.	Efficient nucleic acid hybridization Detection of DNA Nanobiosensor for trace analysis
Nanoshells		Nanoshells typically have a silicon core that is sealed in an outer metallic core. By manipulating the ratio of wall to core, the shells can be precisely tuned to scatter or absorb very specific wavelengths of light	Gold encased nanoshells have been used to convert light into heat, enabling the destruction of tumors by selective binding to malignant cells.

1.5 Characterization of Pharmaceutical Nanotools

1.5.1 Structural characterization: Structural characterization is a parameter that plays important role in determining various attributes of a nanosystem like shape, size, surface morphology, structural arrangement spatial distribution, density, geometric feature etc. Development of electron microscopy tool improves accessibility and feasibility to determine these attributes at nanometer scale. Scanning electron microscopy (SEM) produces the image down to length scales of 10 nm and provides valuable information regarding structural arrangement, spatial distribution as well as surface morphology of nanoparticles. Transmission electron microscopy (TEM) and high resolution TEM are more powerful imaging tools than SEM and give more detailed geometrical features and information like crystal structure, quality, and orientation of nanoparticles. Moreover, scanning tunneling probe such as scanning tunneling microscope (STM), electrical field gradient microscopy (EFM), and scanning thermal microscopy, combined with atomic force microscopy(AFM) have been employed to illustrate structural, electronic, magnetic and thermal properties besides topographical properties of nanosystems.

1.5.2 Particle Size Distribution: Particle size distribution (also known as polydispersity index) being an important aspect during the formulations of nanosystems, efforts are made to achieve a system with lowest polydispersity index. Some techniques to determine the particle size distribution are dynamic light scattering, which is used to measure particles ranging from a few nanometers to about 3 μm, while laser diffraction is used to detect microparticles or possible aggregates of drug nanoparticles.

1.5.3 Particle Charge / Zeta Potential: Zeta potential is used to determine the charge at particle surface. Zeta potential measurement is made to optimize formulation parameters and to make predictions regarding the storage stability of the colloidal dispersion. Currently principal technique involved in zeta potential determination is laser Doppler anemometry.

1.5.4 Crystalline Status: Differential scanning Calorimetry, X ray diffraction and other analytical methods are used to assess any possible changes brought about in the physical form of the drug during processing.

1.5.5 Toxicity Evaluation: Some important types of acute toxicities caused by nanosystems are enhanced endocytosis (cause inflammation, granuloma formation); oxidative stress (cause cell death due to free radical generation) and alter/modify protein/gene structure (resulting immune response causes autoimmune effect) while long-term toxicities are bioaccumulation, poor biodistribution and ultimate fate of nanosystems in body. These toxicities of nanosystems are evaluated using well defined and established protocols available in literature. *Ex vivo* toxicity evaluation generally carried out in various cell lines and MTT assay is used to determine the cell viability. *In vivo* acute and chronic toxicities are determined in various animal models.

1.6 Engineering of Pharmaceutical Nanosystems

Most of the nanosystems discussed above are not very efficient in biomedical and pharmaceutical applications due to non-specific uptake by reticulo endothelial system (RES); opsonization, aggregation and poor biocompatibility associated with them. However, manipulations in their size and surface by biocompatible polymers, hydrophilic polymers and some site-specific ligands render them efficient delivery vehicle for various drugs and utilized for various biomedical applications. Some examples of such manipulations are discussed below.

1.6.1 Functional nanosystems: Modification in properties by incorporation, adsorption or covalent coupling by moieties like polymers and/or ligands to nanoparticles surface is known as surface functionalization. Some commonly used tools for surface modification are polymers, carbohydrates, endogenous substances/ligands, peptide, protein, nucleic acid and polysaccharides. These tools make the nanosystems an intelligent tool and confer a large

variety of properties like higher biostability, lower aggregation and high target specificity in comparison to conventional nanosystems. Various nanosystems like polymeric nanoparticles, liposomes, dendrimers, carbon nanotubes, quantum dots etc. have been successfully functionalized for efficient use in biomedical area. Functional polymer nanoparticles, their methods of surface modifications and their pharmaceutical applications have been excessively reviewed by our group (Nahar et al., 2006)

1.6.2 Multifunctional nanosystems: Multifunctional nanosystems could be developed in following ways:

a) Multifunctionality imparted to core:
   - Simultaneous delivery of two or more therapeutic active moieties,
   - Containing contrast enhancer; and
   - Containing permeation enhancer

b) Multifunctionality imparted to surface:
   - Steric stabilization by PEG(poly ethylene glycol) in order to modify circulation time, and
   - Use of targeting moiety

c) Multifunctionality imparted to material:
   - By use of thermal sensitive, pH and stimuli sensitive biomaterials.

1.7 Applications of Pharmaceutical Nanotools

Miniaturization is often beneficial in pharmaceutical technology. Although it has increased complexicity yet it imparts large number of benefits in drug delivery and diagnostic (Reisch et al., 2007). Miniaturization is helpful in overcoming various physiological, biochemical and pharmaceutical barriers. Pharmaceutical nanotechnology provides wide array of systems or device of nanosize, which offer numerous benefits. Some major advantages are (i) improved bioavailability (ii) reduced toxicity (iii) sustained and controlled release (iv) ability to target (v) do not occlude blood capillaries and traverse easily to most physiological biobarrier and provide effective delivery to brain and intracellular compartment (vi) protects fragile drugs/proteins from harsh biological environment (vii) faster, safer and more accurate disease diagnosis (viii) more accurate, less invasive surgery (ix) inexpensive and (x) large-scale production is feasible. However some shortcomings in pharmaceutical applications of nanotechnology are (i) high aggregation in biological system due to high surface energy (ii) poor solubility and poor biocompatibility in case of carbon nanotubes (iii) quickly scavenged by RES system of body resulting in low biological half life (iv) poor target and site specificity (v) high immunogenicity or foreignness (vi) undefined and unpredictable safety issue and (vii) acute and chronic toxicity.

In spite of the above shortcomings, there are various pharmaceutical and biomedical areas where pharmaceutical nanosystems have achieved remarkable breakthrough and realized their market applications. Some important applications areas are discussed here:

1.7.1 As nanomaterials for tissue engineering: Nanotechnology offered numerous smart materials that are used for tissue repair and replacement, implant coatings, tissue regeneration scaffolds, structural implant materials, bone repair, bioresorbable materials, some implantable devices (sensory aids, retina implants etc.), surgical aids, operating tools, and smart instruments.

Table III Applications of nanosystems in tissue regeneration, growth and repair

Nanosystems	Property	Applications
Nanoengineered prosthetics	Increased miniaturization; increased prosthetic strength & weight reduction; improved biocompatibility	Retinal, auditory, spinal and cranial implants
Cellular manipulation	Manipulation of cellular systems	Persuasion of lost nerve tissue to grow; growth of body parts

1.7.2 As drug carrier system: Conventional drug delivery systems or dosage forms suffer from many limitations such as lack of target specificity, high rate of drug metabolism, cytotoxicity, high dose requirement, poor patient compliance etc. Nanotechnology enabled drug delivery system with optimized physical, chemical and biological properties can serve as effective delivery tools for currently available bioactives. Some nanobased drug delivery tools are polymeric nanoparticles, liposome, dendrimers, polymeric micelles, polymer-drug conjugates, antibody- drug conjugates, which can broadly be classify as (i) sustained and controlled delivery system (ii) stimuli sensitive delivery system (iii) functional system for delivery of bioactives (iii) multifunctional system for combined delivery of therapeutics, biosensing and diagnostic and (iv) site specific targeting (intracellular, cellular, tissue) (Vasir et al., 2005).

1.7.2.1 Cancer treatment: Nanotechnology can have a revolutionary impact on cancer diagnosis and therapy. Available therapies commonly employed in cancer treatment include surgery, chemotherapy, immunotherapy and radiotherapy. Nanotechnology offers tremendous opportunities to aid and improve these conventional therapies by virtue of its nanotools. Some nanotools that have played key role in cancer therapy are listed below (Table IV).

Table IV Applications of various nanosystems in cancer therapy

Nanosystem	Applications in cancer therapeutics
Carbon nanotubes	DNA mutation detection, disease protein biomarker detection
Dendrimers	Controlled release drug delivery, image contrast agents
Nanocrystals	Improved formulation for poorly-soluble drugs
Nanoparticles	MRI and ultrasound image contrast agents, targeted drug delivery, permeation enhancers, reporters of apoptosis, angiogenesis, etc.
Nanoshells	Tumor-specific imaging, deep tissue thermal ablation
Nanowires	Disease protein biomarker detection, DNA mutation detection, gene expression detection
Quantum dots	Optical detection of genes and proteins in animal models and cell assays, tumor and lymph node visualization.

Targeting and localized delivery are the key challenges in cancer therapy. These challenges can be overcome by virtue of development of functional and multifunctional system for passive and active delivery. The approaches are basically attributed to the pathophysiology of diseased sites like leaky vasculature of the cancer tissues (Ferrari, 2005). The nanocarriers can alter the biodistribution and pharmacokinetic parameters of the anticancer drug significantly compared to free drug due to nano size of the carrier. These nanotools identify biomarker or detect mutation in cancer cell and treat the abnormal cells by (i) thermotherapy by photo-thermal ablation therapy using silica nanoshells, carbon nanotubes; magnetic field-induced thermotherapy using magnetic nanoparticles; photodynamic therapy by quantum dots

as photosensitizes and carriers, (ii) chemotherapy by nano-structured polymer nanoparticles, dendrimers and nanoshells and (iii) radiotherapy by carbon nanotubes, dendrimers for boron neutron capture therapy.

1.7.2.2 Implantable delivery systems: Nanotechnology is opening up new opportunities in implantable delivery systems by virtue of its size, controlled and approximately zero order release which otherwise may cause toxicity when compared to intravenous administration (due to first order drug kinetics). Some pharmaceutical novel nano drug vascular carriers like liposome, ethosome and transferosome and some implant chips have been envisaged recently, which may help in minimizing peak plasma levels and reduce the risk of adverse reactions, allow for more predictable and extended duration of action, reduce the frequency of re-dosing and improve patient acceptance and compliance.

1.7.2.3 Site specific drug delivery: Several approaches are now being tested for better site-specific delivery using liposomes, polymeric micelles, dendrimers, iron oxide, proteins using manipulation in passive and active uptake of drug. The tumor targeting of drugs with passive delivery using enhanced permeation and retention (EPR) effect is thought to be one intelligent approach using these carrier system taking the advantages of leaky vasculature of tumor. Some surface modification approaches using various site-specific ligands via covalent binding or adsorption with carrier system enhanced their site specificity and make them intelligent tools for active delivery. The conjugations of these carriers with ligands provide them site specificity at various levels. In the chemotherapy of tuberculosis with active delivery to lung cells is reported to have improved drug bioavailability, reduction in dose frequency and overcoming the non-adherence problem encountered in the control of TB.

1.7.2.4 Gene therapy: In gene therapy, a normal gene is inserted in place of an abnormal disease-causing gene using a carrier molecule. Conventional uses of viral vectors are associated with adverse immunologic, inflammatory reactions and diseases in the host. Nanotechnology enabled delivery systems have currently emerged as potential vector and are shown to be effective and promising tool in systemic gene treatment. Various polymer based nanoparticles like chitosan, gelatin and poly-l-lysine and modified silica nanoparticles have been reported to have increased transfection efficiency and decreased cytotoxicity. It is well established that nanotechnology provides viable option as ideal vector in gene delivery.

1.7.3 Molecular Diagnostics: Molecular imaging is the nanoscience of representing, characterizing, and quantifying sub cellular biological processes in intact organisms. These processes include gene expression, protein-protein interaction, signal transduction, cellular metabolism, and both intracellular and intercellular trafficking. Some nanoparticles, which have inherent diagnostic properties, are quantum dots, iron oxide nanocrystal and metallic nanoparticles. They have been successfully utilized in various magnetic resonance imaging, optical imaging, ultrasonic imaging and nuclear imaging (Wickline and Lanza, 2002). Some other applications of nanoparticles in diagnostics are as specific labeling of cells and tissues, useful for long-term imaging, useful for multi-color multiplexing, suitable for dynamic imaging of sub-cellular structures and may be used for fluorescence resonance energy transfer (FRET)-based analysis and magnetic resonance imaging (MRI). FRET-based analysis and MRI are two main diagnostic techniques developed for molecular level diagnostics. Traditional MRI contrast agents (paramagnetic and super paramagnetic materials) are now being replaced by various novel nanosystems like dendrimers, quantum dots, carbon nanotubes and magnetic nanoparticles. They are proved very efficient contrast agent in providing stable, intense, clearer image of object due to high intensity photo

stability, resolution, resistance to photo bleaching. Some approved nanoparticles used as imaging and as drug carriers are listed below (Table V).

Table V Approved nanoparticles as imaging agents and drug carriers

Modality	Compound	Status	Use
Imaging Agents			
Endorem®	Super paramagnetic iron oxide nanoparticle.	Market	MRI agent
Gadomer®	Dendrimers-based MRI agents	Phase III clinical trial	MRI agent-cardiovascular
Drug delivery			
Abraxane®	Albumin nanoparticle containing paclitaxel	Market	Breast cancer

1.7.4. Biosensor and biolabels: A number of analytical tools have been developed with application of this smart and potential technology. These tools are employed for determination of various pathological proteins and physiological-biochemical indicator associated with disease or disrupted metabolic conditions of body. Various nanoenabled technologies, techniques and their analytical applications are listed below (Table VI).

Table VI Nanoenabled technologies, techniques and their analytical applications

Technology	Technique	Application
Bioarrays and Biosensors	Nanofabrication	Nano-Objects Detection
DNA Chips	Lab on Chip Nanotubes	Electrochemical Detection
Protein-Chips	Pill on Chip Nanowires	Optical Detection
Glyco-Chips	Nanofluidics Nanoparticles	Mechanical Detection
Cell-Chips	Nanostructured Surfaces	Electrical Detection

A biosensor is generally defined as a measurement system that consists of a probe with a sensitive biological recognition element, or bioreceptor, a physicochemical detector component, and a transducer in between to amplify and transduce these signals in to measurable form. A nanobiosensor or nanosensor is a biosensor that has dimensions on the nanometre size scale. Applications of various nanosystems as biosensor and biolabels are given below (Table VII).

Table VII Applications of various nanosystems as biosensor and biolabels (Kubik et al., 2005)

Nanosystem	**Applications**
Gold Nanoparticles	For ssDNA detection; in immune histochemistry to identify protein-protein interaction
Iron oxide nanocrystal	Monitor gene expression; detect the pathogens such as cancer, brain inflammation, arthritis and atherosclerosis
Nanopores	Sensing single DNA molecules by nanopores

Cantilever array	Diagnosis of diabetes mellitus, for detection of bacteria, fungi, viruses; for cancer diagnosis
Carbon nanotube	Blood glucose monitoring; sensors for DNA detection
Nanowire	Electrical detection of single viruses and biomolecules
Nanoparticle-based biodetection	Detection of pathogenic biomarkers, Ultra-sensitive detection of single bacteria

Nanosensors could provide the tools to investigate important biological processes at the cellular level *in vivo*. The basic functions of nanosensors are to understand living cell, to monitor cell as biomarker, as sensor and fluorescent biological labels (Kubik et al., 2005). Biosensors are currently used in the areas of target identification, validation, assay development, and absorption, distribution, metabolism, excretion and toxicity determination (Jain, 2005).

1.7.5 Drug discovery: Pharmaceutical nanotechnology is playing crucial role in drug discovery that rely on better understanding of mechanism of the drug action and identification of biomarker associated with specific disease. Nanotechnology help identification and validation of target by identifying the protein present on the cell surface or target surface. Nanotechnology will enhance the drug discovery process, through miniaturization, automation, speed and reliability of assays. For example single walled nanotubes are successfully used to identity surface protein of pathogen. QDs are used to track individual glycine receptors and to analyze their dynamics in the neuronal membrane of living cells, for periods ranging from milliseconds to minutes. Similarly, gold nanoparticles, nanobodies (smallest, available, intact, antigen-binding fragments) produced by Ablynx (Ghent, Belgium,) are some commonly used nanomaterials in diagnostics (Jain, 2005).

1.7.6 Miscellaneous Applications: Various other applications of nanosystems in biomedical and pharmaceutical fields are (i) biodetection of pathogens in humans, (ii) separation and purification of molecules and cells, (iii) detoxifying agents etc. One of future proposed nanomachine known as respirocytes is the nano-on-board minicomputer which can be used to simultaneous detection of disease causing marker/antigen/marker, to view the diseased site and to deliver the therapeutic agent to that site.

1.8 Challenges to Pharmaceutical Nanotechnology

Pharmaceutical nanotechnology has provided fine-tuned diagnosis and focused treatment of disease. However some ethical, scientific, social and regulatory issues posing various challenges in practical realization of pharmaceutical nanotechnology. Some major health risk associated with such devices includes cytotoxicity, translocation to undesired cells, acute and chronic toxicity; some unknown, unpredictable and undefined safety issues, environmental impacts of nanomaterials and non-biocompatibility. Some ethical issues are altered gene expression, ultimate fate and altered or permanent anomaly in cell behavior/ response on short/long term exposure. There are no specific FDA directives to regulate pharmaceutical nanotechnology based products and related issues. Altogether these challenges cause urgent need to regulate these nanotechnology based products and delivery devices. The characterization, safety and environment impact are three main elements that need to be regulated. Though regulatory agencies like FDA, EPA (Environment Protection Agency) and nuclear protection agency etc. are regulating the major health risk associated with nanomaterials, yet lack of adequate and conclusive research on the health risks of nano-based substances demand the need for a dialogue on regulatory adequacy, inadequacy, or possible alternatives more urgent. US-FDA kept nanotechnology as an element under evaluation in its critical path initiative.

FDA regulates most pharmaceutical nanotechnology based products as "combination products" (i.e., drug-device, drug-biologic, and device-biologic products). Some FDA approved nanotechnology based products, which have entered the market are liposome, nanoparticles, monoclonal antibody based product, polymer drug conjugate, polymer–protein conjugate and some polymeric drugs. Well-tuned, coordinated and sincere effort of government, industries, academia and researchers over guidelines for regulation must be drawn in order to utilize the benefit of nano-based technology without hampering its development.

1.8.1 Future Prospects of Pharmaceutical Nanotechnology

Pharmaceutical nanotechnology is an emerging field that could potentially make a major impact on human health. Nanomaterials promise to revolutionize medicine and are increasingly used in drug delivery or tissue engineering applications. Newly developed hybrid systems seem promising for future applications in human. Functional and multifunctional approaches have tremendous potential in temporal and spatial controlled delivery of bioactives. A modular approach to construct delivery systems that combine targeting, imaging and therapeutic functionalities into nanoplate forms is emerging as intelligent concept. These multifunctional nanoplate forms would localize to target cells, enable diagnostics and subsequently deliver therapeutics with great precision. But such approaches to nano devices construction are inherently complex. One very interesting and novel future strategy is to devise a nano machine, which can detect and attack pathogen simultaneously, detect the change in molecular event during diseased state, and also monitor the efficacy of treatment. However such intelligent machine (also known as nanorobots which can serves as mini onboard computer in human body) is very far reaching concept.

In short, recent development, market realization of various pharmaceutical nanotools and global interest shown by scientists, governments and industries ensure that there is tremendous potential and scope of nanobased drug delivery system in near future. There is no doubt to presume that in next ten years market will be flooded with nano-enabled delivery devices and materials.

CHAPTER-II

A REVIEW ON POLYMERIC NANOPARTICLES

2.1. Introduction

Nanoparticles have become one of the most active areas of research in the field of drug delivery due to their ability to deliver drugs to the right place, at appropriate times and in the right dosage (Desai et al., 1997). They have received considerable attention over the past 20 years due to their advantages compared to other drug delivery systems. These advantages include: targeted delivery of drugs to the specific site to minimize toxicity; improved bioavailability by reducing fluctuations in therapeutic ranges; improved stability of drugs against enzymatic degradation; sustained and controlled release effect that reduces dosing frequency with improved patience compliance; and the ease of administering through various routes including oral, nasal, pulmonary, intraocular, parenteral and transdermal (Kreuter J et al., 1994).

Nanotechnology focuses on synthesizing biocompatible nanocomposites such as nanoparticles, nanocapsule, micellar systems (Bae Y et al., 2007) and nanoconjugates (Ljubimova J.Y et al., 2008) for delivering small molecular weight drug as well as macromolecular therapeutic agents. Nanoparticles can be defined as solid, sub-micron, colloidal particles ranging in size from 10 nm to 1000 nm in diameter, generally but not necessarily made of natural or synthetic polymers, in which drugs can be adsorbed, entrapped, encapsulated or covalently attached and are produced by mechanical or chemical means (Kreuter J et al., 1983). The term "Nanoparticles" includes –Nanocapsule (Reservoir device) in which the drug is confined to an aqueous or oily core surrounded by a shell-like wall and Nanospheres (Monolithic/matrix device) in which the drug is adsorbed, dissolved, or dispersed throughout the matrix (Kreuter J et al., 2004) as seen in Figure 11.

Depending on the type of material or carrier used, four broad classes of nanoparticles are recognized: Polymeric nanoparticles, Lipid based nanoparticles (Wissing S.A et al., 2004), Metal based nanoparticles (Bhattacharya R et al., 2008) and Biological nanoparticles (Manchester M et al., 2006)

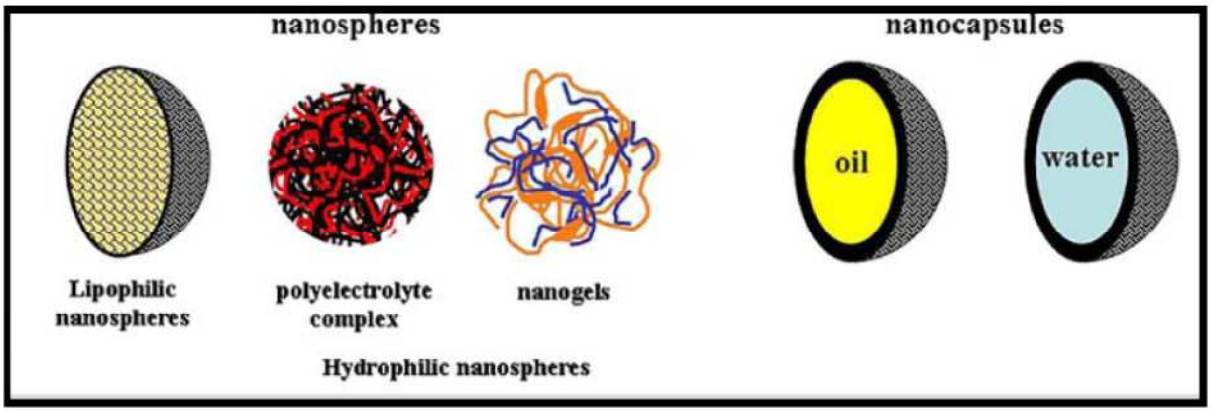

Figure 11 Structure of the polymeric nanospheres and nanocapsules (Vauthier et al., 2009)

2.1.1 Advantages over Microparticles

- They have higher intracellular uptake compared to micro particles (Desai et al., 1996)
- They are better suited for I.V. delivery since the smallest blood capillaries in the body is about 5-6 μm.

*2.1.2 Advantages over Liposomes (*Soppimath K.S et al., 2001)

They have better stability in biological fluids and during storage.

- Their preparation is more amenable to scale up.
- They have the unique ability to create a controlled release product.

2.1.3 Materials used for preparation of nanoparticles

Nanoparticles can be prepared from a variety of materials such as metals (silver, gold, platinum, silicon) as well as polymers and lipids. Researchers have developed virus based nanoparticles for tissue-specific targeting and imaging agents *in vivo.* Potential improvements in the field of polymer chemistry have made polymers the most suitable carrier for delivering small and macromolecules. Polymeric materials can be classified broadly as natural polymers and synthetic polymers (Table VIII).

The selection of materials for preparing nanoparticles depends upon consideration of the following factors:

- Size and surface characteristics of the particle desired.
- Aqueous solubility and stability of drugs or active ingredients.
- Degree of biodegradability, biocompatibility and toxicity.
- Drug release profile desired.
- Antigenicity of the polymers.

Table VIII Most widely used polymers for preparing nanoparticles in drug delivery *(Vauthier et al., 2009)*

MATERIAL	*FULL NAME*	*ABBREVIATION OR COMMERCIAL NAMES**
Synthetic homopolymers	Poly (lactide) Poly (lactide-co-glycolide) Poly (epsilon-caprolactone) Poly (isobutylcyanoacrylate) Poly (isohexylcyanoacrylate) Poly (n-butylcyanoacrylate) Poly (acrylate) and Poly(methacrylate)	PLA PLGA PCL PICBA PIHCA PBCA Eudragit*
Natural polymers	Chitosan Alginate Gelatin Albumin	
Copolymers	Poly (lactide)- poly (ethylene glycol) Poly (lactide-co-glycolide)-poly (ethylene glycol) Poly (epsilon-caprolactone)-poly (ethylene glycol) Poly (hexadecylcyanoacrylate-co-poly (ethylene glycol) cyanoacrylate)	PLA- PEG PLGA-PEG PCL-PEG Poly (HDCA-PEGCA)
Colloid stabilizers	Dextran Pluronic F68 Poly (vinyl alcohol) Co polymers (see above) Tween®20 and Tween® 80	F68 PVA

2.2. Methods for the preparation of nanoparticles

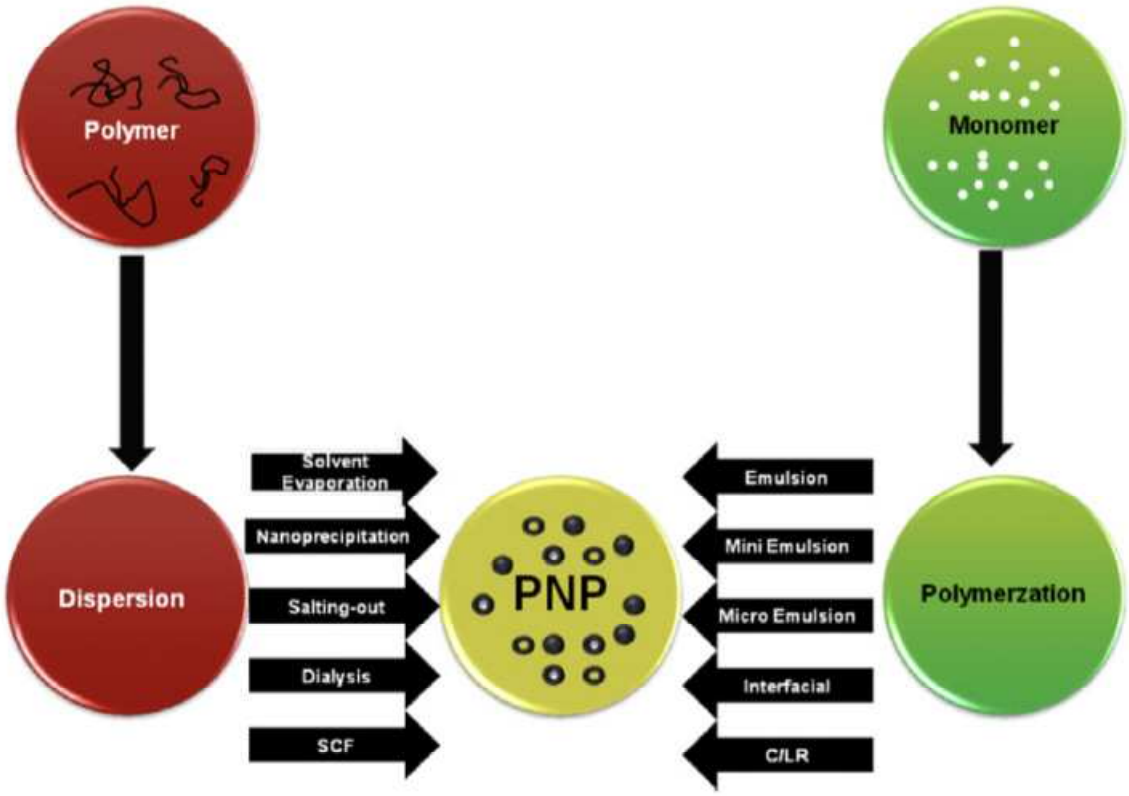

Figure 12 Schematic representation of various techniques for the preparation of polymer nanoparticles. SCF: supercritical fluid technology, C/LR: controlled/living radical

2.2.1 Dispersion of preformed polymers

2.2.1.1. Emulsification-solvent evaporation

The emulsification-solvent evaporation method was the first method used to prepare biodegradable and injectable lattices by Gurny et al., 1981. Briefly, both the drug and polymer are dissolved in a volatile, water immiscible organic solvent such as dichloromethane, chloroform or ethyl acetate. The organic phase is then emulsified as nanodroplets in an aqueous surfactant (such as Polyvinyl alcohol, Pluronic etc.) solution using high energy homogenizer or sonicator (Tice et al., 1985). The polymer precipitates as

nanospheres and subsequently the organic phase is evaporated using a rotary evaporator or by continuous stirring (Soppinath et al., 2001) as represented in Figure13.

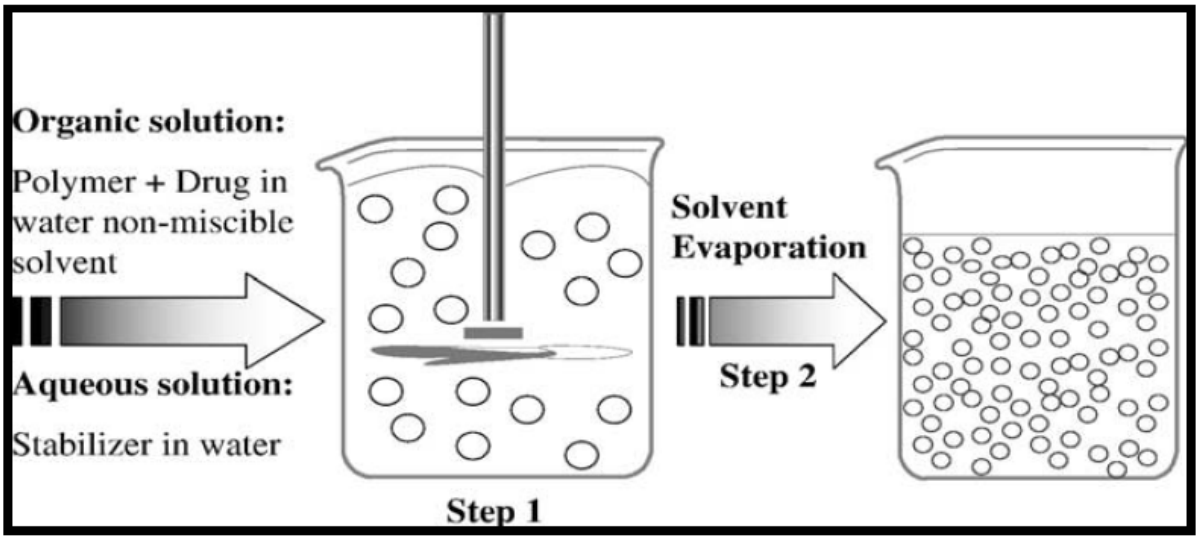

Figure 13 Schematic representation of the emulsification-solvent evaporation method

The parameters which affect particle size are the stirring rate, type and amount of dispersing agent, viscosity of the organic and aqueous phases, and temperature. The method can also be applied to prepare amphiphilic copolymers including PEG-PLA, PEG-PLGA, PEG-PCL, PEGPACA and polysaccharide-PCL without the need of any surfactant (Avgoustakis K et al., 2004; Brigger et al., 2004). Various lipophilic and hydrophilic drugs such as indomethacin (Bodmeier R et al., 1990), cyclosporine A (san chez et al., 1993), loperamide (Ueda H et al., 1997), praziquantel (Mainardes R.M et al., 2005) tetanus toxoid (Ya-Ping L et al., 2001) and testosterone (Gurny R et al., 1981) have been encapsulated in polymeric nanoparticles using this method.

2.2.1.2 Solvent displacement and interfacial deposition method

One of the easiest and reproducible techniques for preparing nanospheres was the solvent displacement (also called **nanoprecipitation**) method developed by Fessi et al., 1989 and has been widely used to prepare nanoparticles (Molpeceres J et al., 1996; Guterres S.S et al., 1995; Chacon M et al., 1996). The method is based on the precipitation of reformed polymer following displacement of a semipolar solvent miscible with water in the presence or absence of surfactant . The basic principle of this technique is similar to spontaneous emulsification of the organic phase containing drug and polymer into the external aqueous phase. Three basic ingredients are needed for this method: polymer, polymer solvent and non-solvent for the polymer. In brief, both the polymer and drug are dissolved in a water miscible organic solvent (polymer solvent phase) of intermediate polarity (e.g. acetone and ethanol). The resulting organic phase is injected into a stirred aqueous phase (non-solvent phase) containing a surfactant as stabilizer. The nanoparticles are formed instantaneously during the rapid diffusion of the organic phase into the aqueous phase as shown in Figure 14. Two important parameters affecting the physicochemical properties of the prepared nanoparticles include (Legrand P et al., 2007)

- Miscibility of the organic solvent with the nonsolvent.
- Nature of the polymer solvent interactions.
- Concentration of the polymer in the organic phase.

Interfacial deposition is an emulsification/solidification technique which allows production of nanocapsule when nontoxic oil (such as benzyl benzoate) is incorporated into the organic phase (Quintanar-Guerrero D et al., 1998). The polymer deposition occurs at the interface between the water and finely dispersed oil phase forming nanocapsule with a shell-like wall (Ammoury N et al., 1991; Seijo B et al., 1990) The method has been adapted to various polymeric materials such as PLA (Ugo Bilati et al., 2005), PLGA (Barichello J. M et al.,

1999), PCL (Molpeceres J et al., 1996), peptides (Duclairoir C et al., 1998), cyclodextrins (Skiba M et al., 1996) and various drugs (Skiba M et al., 1995; Némati F et al., 1996).

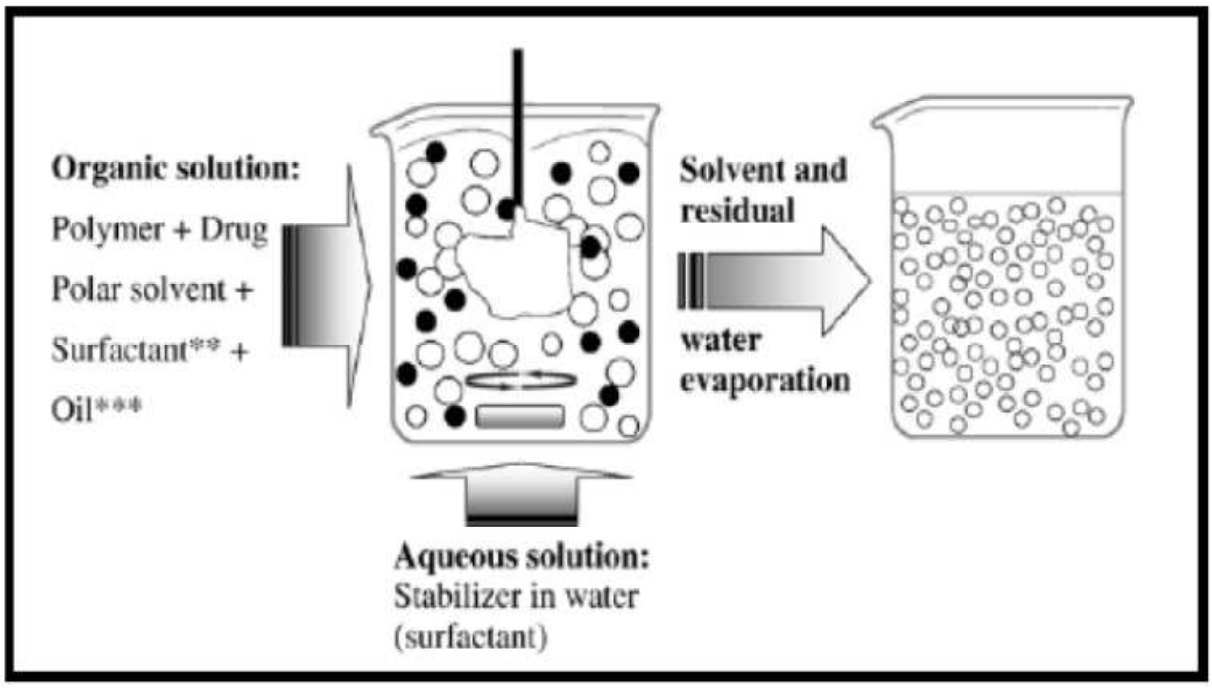

Figure 14 Schematic representation of the solvent displacement technique

2.2.1.3 Emulsification–solvent diffusion

The emulsification solvent diffusion or emulsification-solvent displacement method is the widely used method for preparing nanoparticles due to several advantages. These include high drug entrapment efficiency for poorly water soluble drugs, narrow particle size distribution, high batch-to-batch reproducibility, no homogenization required, simplicity, ease of scale up and rapid organic solvent extraction (Moinard-Chécot D et al., 2006). The drug and polymer usually PLA, PLGA, PCL or Eudragit are dissolved in a partially water soluble solvent. Commonly used solvents are propylene carbonate, benzyl alcohol, ethyl acetate, isopropyl acetate, methyl acetate, methyl ethyl ketone, butyl lactate or isovaleric acid (Battaglia L et al., 2007). The organic phase is saturated with water to ensure the initial thermodynamic equilibrium. It is then diluted with an extensive amount of pure water to facilitate diffusion of the organic solvent from the organic phase droplets leading to the

precipitation of the polymer as presented in Figure 15. The aqueous phase may contain surfactants such as Pluronic, PVA and sodium taurocholate while the organic phase sometimes contains soy lecithin as the emulsifier. Finally, the solvent is eliminated by evaporation or filtration, depending upon the boiling point. Several parameters can affect the size of the nanoparticles such as miscibility of the water with the organic solvent (Quintanar-Guerrero D et al., 1996) stirring rate, concentration of the surfactant(s) and concentration of the polymer is the organic phase (Quintanar-Guerrero D et al., 1998). Nanocapsules are successfully prepared by this method when a small amount of oil is incorporated into the organic phase (Quintanar-Guerrero D et al., 1998). The disadvantages of this method include: long time required to remove the high volume of water and leakage of water soluble drugs during processing.

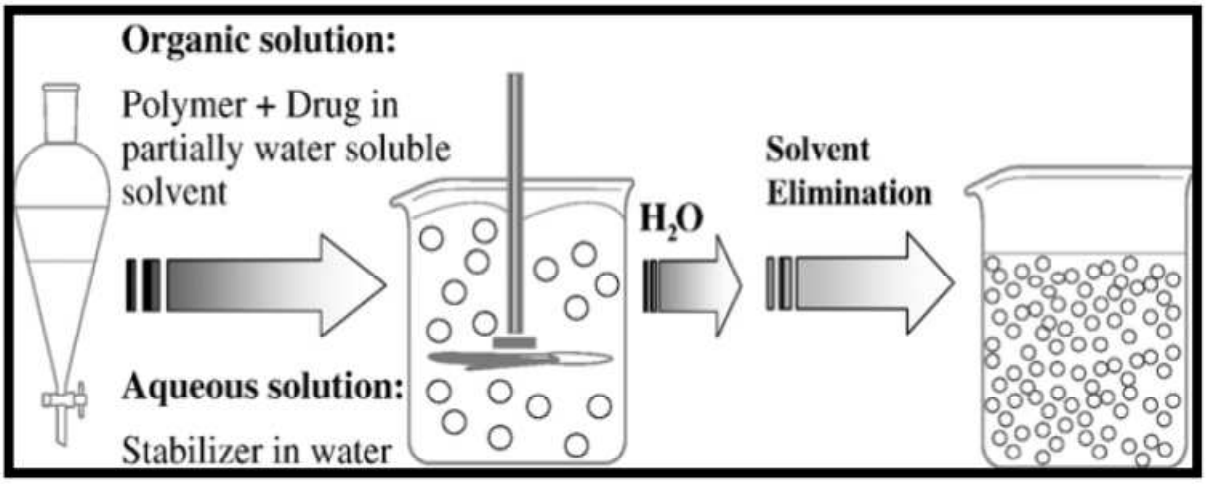

Figure 15 Schematic representation of the emulsification-solvent diffusion method

2.2.1.4 Salting out method

The salting-out procedure can be considered as a modification of the emulsification/solvent diffusion method. The separation of a water miscible solvent from aqueous solution is achieved via a salting-out effect (Figure 16). Briefly, a water miscible organic solvent, usually acetone, containing polymer and drug is added drop wise to an aqueous phase

saturated with an electrolyte or non-electrolyte (such as magnesium chloride, calcium chloride or sucrose) with a colloidal stabilizer (such as polyvinyl pyrrolidone) under agitation to form an o/w emulsion. A sufficient volume of water is added to enhance the diffusion of acetone to the water phase and nanospheres are thus obtained. The technique offers advantages such as the avoidance of chlorinated solvents and surfactants, minimization of stress for protein encapsulates (Jung T et al., 2005) useful for heat-sensitive substances (Lambert G et al., 2001), high encapsulation efficiency and easy scaling up. The method is not popular because of the extensive washing steps required to achieve purity of the nanoparticles (Couvreur P et al., 1995) and the possibility of incompatibility between drugs and salts.

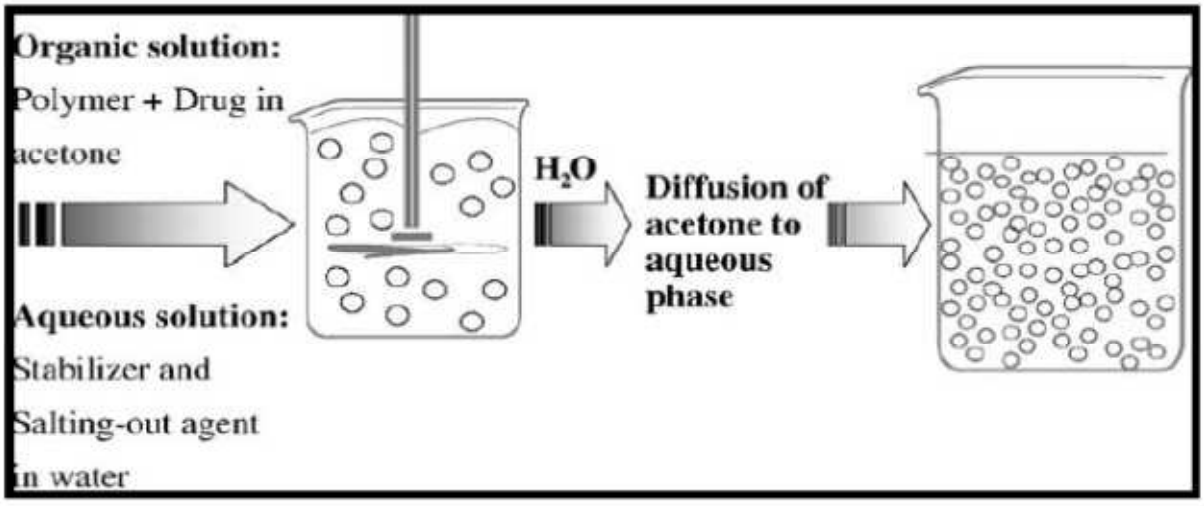

Figure 16 Schematic presentation of salting out method of preparing nanospheres

2.2.2 Polymerization method

In the polymerization method, monomers are polymerized to form nanoparticles in aqueous solution. The polymerization method can be classified into emulsion and interfacial polymerization. The emulsion polymerization method is the fastest and scalable method of producing nanoparticles (Kreuter J et al., 1990). It can be classified into two categories; continuous organic phase or continuous aqueous phase methodology depending on the use of

the continuous phase. In general, the monomer is dissolved into an organic or aqueous continuous phase. Additional monomer molecules are then emulsified into the emulsion droplets that are stabilized by surfactant. The polymerization is started by chemical initiation, pH shift or by irradiation of gamma, ultraviolet or visible rays. In the continuous phase, chain growth starts when the initiated monomer ion or monomer radical collide with each other and forms aggregates which are stabilized by polymeric emulsifier particles. This mechanism is known as anionic polymerization (Vauthier C et al., 2003). Several materials are used to produce nanoparticles such as polyacrylamide (Ekman B et al., 1978), poly (methylmethacrylate), polybutylcyanoacrylate (Li V.H.K et al., 1986), poly (hexylcyanoacrylate) (Maincent P et al., 1986) and poly (dialkylmethylidene melonate) (Mbela T.K.M et al., 1992). The interfacial polymerization method is generally used to prepare nanocapsule using oily components such as benzyl benzoate or migliol (Alle´mann E et al., 1998) along with an organic solvent. In this case, polymerization occurs at the interface between the oily and aqueous phase to produce nanocapsule spontaneously. The nanocapsules are stabilized with the help of surfactant added in the aqueous phase. The technique is advantageous from the standpoint of producing nanocapsule with high drug entrapment efficiency with hydrophilic insulin (Couvreur P et al., 2002). This process was used to produce nanoparticles of polyethylcyanoacrylate (Watnasirichaikul S et al., 2000), poly (isobutylcyanoacrylate) (Lambert G et al., 2000) and poly (isohexylcyanoacrylate) (Lenaerts V et al., 1995).

Interfacial polycondensation is another method by which lipophilic monomer, such as phtaloyldichloride, and hydrophilic monomer, such as diethylenetriamine, is condensed to prepare nanocapsule in the presence or absence of surfactant. It is a spontaneous emulsification technique in which the organic phase contains a water miscible solvent, lipophilic polymer and the oil, whereas the aqueous phase contains hydrophilic monomer and

surfactant. The polycondensation reaction occurs at the interface of the oil droplets to form an oil-in water emulsion and subsequently nanocapsule (Bouchemal K et al., 2006). By using the modified interfacial polycondensation method, encapsulation and stability of an oily drug, alpha-tocopherol, was improved by the use of polyurethane and poly (ether urethane) (Bouchemal K et al., 2004).

2.2.3 Coacervation and ionic gelation method

Much research has been focused on preparing nanoparticles from natural hydrophilic polymers such as chitosan (Mansouri S et al., 2004: Mao H-Q et al., 2001; Illum L et al., 1994), albumin (Kreuter J et al., 2007), gelatin (Yoshioka T et al., 1981), sodium alginate (Aslani P et al., 1996), agarose (Wang N et al., 1995) and gliadin (Duclairoir C et al., 2002). Coacervation is a process during which is a homogenous solution of charged macromolecules undergo liquid-liquid phase separation producing a separated phase of polymer rich particles (Mohantya B et al., 2005). In the ionic gelation method, the positive or negative charge of the hydrophilic polymer is complexed with a multivalent cationic (calcium chloride) or polyanionic (sodium tripolyphosphate) to form highly viscous gel particles with a size in the range of a nanometer. Calvo et al developed a method for preparing chitosan nanoparticles by this method (Calvo P et al., 1998).

2.2.4 Production of nanoparticles using supercritical fluid technology

Recently, supercritical or compressed fluids have been utilized as an alternative way to prepare biodegradable nanoparticles (Wang Y et al., 2004). This new technique obviates the use of toxic organic solvents associated with conventional methods. Two techniques are most commonly used for preparing nanoparticles – Supercritical anti-solvent (SAS) and Rapid Expansion of Critical Solution (RESS). In the SAS method, solutes are dissolved in methanol which is completely miscible with supercritical fluids. The extraction of methanol by the supercritical fluids leads to an instantaneous precipitation of the nanoparticles

(Thote A J et al., 2005). Dexamethasone phosphate nanoparticles were prepared by this method. In the RESS method, solutes are dissolved in the supercritical fluid and the solution is expanded through a small nozzle into a region of lower pressure. The solutes eventually precipitate as nanoparticles. Insulin loaded PEG/PLA nanoparticles were prepared by this method (Elvassore N et al., 2001). The technique is very expensive and requires elaborate recycling measures.

2.3. Separation and purification techniques of nanoparticles

Depending on the method of preparation, potentially toxic impurities can be present in the nanoparticulate suspensions. These impurities are organic solvents, surfactants, residual monomers, polymerization initiators and large polymer aggregates (Limayem I et al., 2004). Separation of the drug entrapped nanoparticles from free polymer and unentrapped drugs is a very critical step in producing pure nanoparticles. The separation can be achieved by using Ultracentrifugation, crossflow microfiltration (Allémann E et al., 1993), Gel filtration, Dialysis and Diafiltration.

2.4. Stability of nanoparticles

There are several physical and chemical factors that play a major role in the instability of prepared nanoparticles. The overall stability can be classified into two types: Physical and chemical stability.

2.4.1. Physical Stability

The colloidal submicron particles in homogenous suspension do not sediment due to the continuous thermal motion of the particles known as Brownian motion. Gravitational forces which cause the particles to sediment are opposed by Brownian motion. At colloidal size range, the particles tend to remain suspended since Brownian motion dominates over gravitational forces. Random collision of suspended particles of various surface charge

content and shape often lead to agglomeration and subsequent settling of the particles. In order to avoid this phenomenon, a suitable stabilizer such as PVA, DMAB, Pluronic or phospholipids is used. Magneheim et al investigated the PLA particle aggregation due to the absorption of nifedipine molecules which displaces a part of the steric stabilized surface layer (Magneheim B., Benita S 1991). Charged stabilized particles are often reported to coagulate when counter ions are absorbed within the electrical double layer (Jiang J et al., 2009).

2.4.2. Chemical Stability

There are several factors which contribute to chemical instability of nanoparticles such as storage conditions including temperature and pH, chemical stability of entrapped drugs as well as the type and molecular weight of the polymer used. Biodegradable polymeric nanoparticles are generally stored at 4-50C for improving stability (Coffin M.D., McGinity J.W 1992). Polymer degradation by hydrolysis was observed at extreme conditions of pH and temperature which the best stability was observed when the aqueous medium pH was adjusted to physiological pH (Belbella A et al., 1996). The overall stability of a nanoparticle formulation also depends on the chemical stability of the entrapped drugs. Most of the drugs have a pH dependent degradation profile and sometimes show photo degradation. Therefore, to reduce drug degradation and improve the stability of the nanoparticle formulation, freeze drying is most commonly used.

2.5. Freeze drying of nanoparticles

In order to remove the water from the nanoparticle system, freeze drying, also known as lyophilization is most commonly used. The basic principle of freeze drying is to remove water from a frozen sample by sublimation and desorption under vacuum (Williams N.A., Polli G.P 1984; Pikal M.J et al., 1990). However, the process could generate various stresses which could cause instability of particles. In order to protect the particles from freezing and dessication stresses, cryoprotectants and lyoprotectants are incorporated into the formulation

before freeze drying. Besides using these agents, other several excipients are commonly incorporated into the formulation for various purposes, as shown in Table IX.

Most commonly used cryoprotectants include sugars such as trehalose, sucrose, glucose, fructose, lactose and maltose (Abdelwahed W et al., 2006; Auvillain M et al., 1989; Zimmermann E et al., 2000). These saccharides act as a spacing matrix to prevent particle agglomeration. Freeze drying is generally carried out below the Tg´ temperature or T_{eu} temperature (eutectic crystallization temperature) so that nanoparticles can be immobilized within the glassy matrix of the cryoprotectants (Tang X et al., 2004).

Table IX Excipients used in freeze drying of nanoparticle suspension

TYPE	*FUNCTION*	*SUBSTANCE*
Bulking agents	Provide bulk to the formulation especially when the concentration of the product to freeze dry is very low.	Hydroxymethyl starch, trehalose, mannitol, lactose and glycine.
Buffers	Adjust pH changes during freezing.	Phosphate, Tris HCl, citrate and histidine.
Stabilizers	Protect the product during freeze drying against the freezing and the drying stresses.	Sucrose, lactose, glucose, trehalose, glycerol, mannitol, sorbitol, glycine, alanine, lysine, poly ethylene glycol, dextran and PVP.
Tonicity adjusters	Yield an isotonic solution and control osmotic pressure.	Mannitol, sucrose, glycine, glycerol and sodium chloride.
Collapse temperature modifiers	Increase collapse temperature of the product to get higher drying temperature	Dextran, hydroxypropyl-β-cyclodextrins, PEG, poly (vinyl pyrrolidone).

2.6. Physicochemical properties of nanoparticles

2.6.1. Particle size

Nanoparticles have relatively higher intracellular uptake as compared to microparticles (Desai M.P et al., 1997). They were able to penetrate throughout the sub mucosal layers while the larger size microparticles localized in the epithelial lining (Desai M.P et al., 1996). Nanoparticles are also reported to cross the blood brain barrier following the opening of the tight junctions by hyper osmotic barrier (Kreuter J et al., 2003). Drug release and polymer degradation are also affected by the size distribution of nanoparticles. Larger particles allow more drugs to encapsulate inside the hyper osmotic mannitol for sustained delivery of drugs to brain tumors. Polysorbate 80 coated nanoparticles were also reported to enhance drug delivery across blood-brain core and slowly diffuse the drug molecules (Redhead H.M et al., 2001). The rate of polymer degradation of PLGA nanoparticles was increased with increasing the particles size (Dunne M et al., 2000).

2.6.2. Surface charge

An important characteristic of nanoparticles is the surface charge which determines the physical stability in the formulation, in vivo distribution and targeting ability of nanoparticles. The zeta potential is the measure of the amount of charge on the particle and represents an index of particle stability. A physically stable nanosuspension stabilized by electrostatic repulsion should have a minimum zeta potential value of ± 30 Mv (Muller R.H et al., 2001). The stability is increased when negative zeta potential is lowered by the addition of PEG (Vila A., Sanchez A et al., 2002). The zeta potential also indicates whether the charged active material is encapsulated within the center or adsorbed onto the surface of the nanoparticles. Thus consideration of the zeta potential is important in preventing aggregation of the particles.

2.6.3. Surface hydrophobicity

Following intravenous administration, hydrophobic nanoparticles are easily recognized by the mononuclear phagocytic system. Thus, they are rapidly opsonized and massively cleared by macrophages of the liver, spleen, lungs and bone marrow (Grislain L et al., 1983). Thus in order to minimize opsonization and prolong blood circulation of nanoparticles in vivo, the surface of the hydrophilic nanoparticles must be modified. There are two general approaches employed for this purpose. One is the surface coating of nanoparticles with hydrophilic polymers such as polyethylene glycol (PEG), chitosan (Janes K.A et al., 2001) or surfactants such as Poloxamer or poloxamines. The second approach is the use of biodegradable copolymers having hydrophilic segments such as PLA-PEG (Avgoustakis K et al., 2002). PEG functionalized nanoparticles are not taken up by the body and often called as "stealth nanoparticles" (Peracchia M.T et al., 1999).

2.6.4. Drug loading

Loading of the drug inside nanoparticles can be achieved by two methods: the incorporation method and the adsorption/absorption method. There are several factors which can affect drug loading and entrapment efficiency of nanoparticles such as drug solubility in the polymer matrix, molecular weight, drug polymer interaction and presence of end carboxylic groups. Ideally a nanoparticulate system should have high drug loading capacity in order to reduce the quantity of polymer required.

2.6.5. Drug release

One of the most important applications of polymeric nanoparticles is the sustained and controlled delivery of drugs. Various factors such as solubility of drug, desorption, drug diffusion, particle matrix degradation or erosion can affect drug release. Smaller particles have higher initial burst release caused by poorly entrapped drug or drug adsorbed onto the surface of the nanoparticles. Larger particles have longer sustained release with smaller initial

burst release. It is also possible to alter the release rate from PLA-PEGPLA copolymer by changing the amount of PEG or the molecular weight of the polymer (Matsumoto J et al., 1999). Various methods can be used to study the in vitro release of drug from nanoparticles such as diffusion cell, dialysis bag diffusion, agitation followed by ultracentrifugation or ultra filtration.

2.7. Application of Nanoparticles in Drug Delivery Systems

i) Tumor targeting using nanoparticulate delivery systems

The rationale of using nanoparticles for tumor targeting is based on 1) nanoparticles will be able to deliver a concentrate dose of drug in the vicinity of the tumor targets via the enhanced permeability and retention effect or active targeting by ligands on the surface of nanoparticles; 2) nanoparticles will reduce the drug exposure of health tissues by limiting drug distribution to target organ. Verdun et al demonstrated in mice treated with doxorubicin incorporated into poly (Isohexylcyanoacrylate) nanospheres that higher concentrations of doxorubicin manifested in the liver, spleen and lungs than in mice treated with free doxorubicin. Studies show that the polymeric composition of nanoparticles such as type, hydrophobicity and biodegradation profile of the polymer along with the associated drug's molecular weight, its localization in the nanospheres and mode of incorporation technique, adsorption or incorporation, have a great influence on the drug distribution pattern in vivo. The exact underlying mechanism is not fully understood but the biodistribution of nanoparticles is rapid, within ½ hour to 3 hours, and it likely involves MPS and endocytosis/phagocytosis process. Recently Bibby et al reported the biodistribution and pharmacokinetics (PK) of a cyclic RGD doxorubicin- nanoparticle formulation in tumor bearing mice. Their biodistribution studies revealed decreasing drug concentrations over time in the heart, lung, kidney and plasma and accumulating drug concentrations in the liver, spleen and tumor. The majority injected dose appeared in the liver (56%) and only 1.6% in

the tumor at 48 hrs post injection, confirming that nanoparticles have a great tendency to be captured by liver. This indicates the greatest challenge of using nanoparticles for tumor targeting is to avoid particle uptake by mononuclear phagocytic system (MPS) in liver and spleen. Such propensity of MPS for endocytosis/phagocytosis of nanoparticles provides an opportunity to effectively deliver therapeutic agents to these cells. This biodistribution can be of benefit for the chemotherapeutic treatment of MPS- rich organs/tissues localized tumors like hepatocarcinoma, hepatic metastasis arising from digestive tract or gynecological cancers, brochopulmonary tumors, primitive tumors and metastasis, small cell tumors, myeloma and leukemia. It has been proved that using doxorubicin loaded conventional nanoparticles was effective against hepatic metastasis model in mice. It was found there was greater reduction in the degree of metastasis than when free drug was used. The underlying mechanism responsible for the increased therapeutic efficacy of the formulation was transfer of Doxorubicin from healthy tissue, acting as a drug reservoir to the malignant tissues. Histological examination showed a considerable accumulation of nanoparticles in the lysosomal vesicles of Kupffer cells, whereas nanoparticles could not be clearly identified in tumoral cells. Thus Kupffer cells, after a massive uptake of nanoparticles by phagocytosis, were able to induce the release of doxorubicin, leading to a gradient of drug concentration, favorable for a prolonged diffusion of the free and still active drug towards the neighboring metastatic cells. When conventional nanoparticles are used as carriers in chemotherapy, some cytotoxicity against the Kupffer cells can be expected, which would result in deficiency of Kupffer cells and naturally lead to reduced liver uptake and decreased therapeutic effect with intervals of less than 2 weeks administration. Moreover, conventional nanoparticles can also target bone marrow (MPS tissue), which is an important but unfavorable site of action for most anticancer drugs because chemotherapy with such carriers may increase myelosuppresive effect. Therefore, the ability of conventional nanoparticles to enhance

anticancer drugs efficacy is limited to targeting tumors at the level of MPS-rich organs. Also, directing anticancer drug-loaded nanoparticles to other tumoral sites is not feasible if a rapid clearance of nanoparticles occurs shortly after intravenous administration.

ii) Long circulating nanoparticles

To be successful as a drug delivery system, nanoparticles must be able to target tumors which are localized outside MPS-rich organs. In the past decade, a great deal of work has been devoted to developing so-called "stealth" particles or PEGylated nanoparticles, which are invisible to macrophages or phagocytes. A major breakthrough in the field came when the use of hydrophilic polymers (such as polyethylene glycol, poloxamines, poloxamers, and polysaccharides) to efficiently coat conventional nanoparticle surface produced an opposing effect to the uptake by the MPS. These coatings provide a dynamic "cloud" of hydrophilic and neutral chains at the particle surface which repel plasma proteins. As a result, those coated nanoparticles become invisible to MPS, therefore, remained in the circulation for a longer period of time. Hydrophilic polymers can be introduced at the surface in two ways, either by adsorption of surfactants or by use of block or branched copolymers for production of nanoparticles. Studies show nanoparticles containing a coat of PEG not only have a prolonged half-life in the blood compartment but also be able to selectively extravasate in pathological sites such as tumors or inflamed regions with a leaky vasculature. As a result, such long-circulating nanoparticles have increased the potential to directly target tumors located outside MPS-rich regions. The size of the colloidal carriers as well as their surface characteristics are the critical to the biological fate of nanoparticles. A size less than 100 nm and a hydrophilic surface are essential in achieving the reduction of opsonization reactions and subsequent clearance by macrophages. Coating conventional nanoparticles with surfactants or PEG to obtain a long-circulating carrier has now been used as a standard strategy for drug targeting in vivo.

Extensive efforts have been devoted to achieving "active targeting" of nanoparticles in order to deliver drugs to the right targets, based on molecular recognition processes such as ligand-receptor or antigen-antibody interaction. Considering that fact that folate receptors are over expressed on the surface of some human malignant cells and the cell adhesion molecules such as selectins and integrins are involved in metastatic events, nanoparticles bearing specific ligands such as folate may be used to target ovarian carcinoma while specific peptides or carbohydrates may be used to target integrins and selectins. Oyewumi et al demonstrated that the benefits of folate ligand coating were to facilitate tumor cell internalization and retention of Gd-nanoparticles in the tumor tissue.

Targeting with small ligands appears more likely to succeed since they are easier to handle and manufacture. Furthermore, it could be advantageous when the active targeting ligands are used in combination with the long-circulating nanoparticles to maximize the likelihood of the success in active targeting of nanoparticles.

iii) Reversion of multidrug resistance in tumor cells

Anticancer drugs, even if they are located in the tumor interstitium, can turn out to be of limited efficacy against numerous solid tumor types, because cancer cells are able to develop mechanisms of resistance. These mechanisms allow tumors to evade chemotherapy. Multidrug resistance (MDR) is one of the most serious problems in chemotherapy. MDR occurs mainly due to the over expression of the plasma membrane p-glycoprotein (Pgp), which is capable of extruding various positively charged xenobiotics, including some anticancer drugs, out of cells. In order to restore the tumoral cells' sensitivity to anticancer drugs by circumventing Pgp-mediated MDR, several strategies including the use of colloidal carriers have been applied. The rationale behind the association of drugs with colloidal carriers, such as nanoparticles, against drug resistance derives from the fact that Pgp probably recognizes the drug to be effluxed out of the tumoral cells only when this drug is present in

the plasma membrane, and not when it is located in the cytoplasm or lysosomes after endocytosis one of the most serious problems in chemotherapy. MDR occurs mainly due to the over expression of the plasma membrane p-glycoprotein (Pgp), which is capable of extruding various positively charged xenobiotics, including some anticancer drugs, out of cells . In order to restore the tumoral cells' sensitivity to anticancer drugs by circumventing Pgp-mediated MDR, several strategies including the use of colloidal carriers have been applied. The rationale behind the association of drugs with colloidal carriers, such as nanoparticles, against drug resistance derives from the fact that Pgp probably recognizes the drug to be effluxed out of the tumoral cells only when this drug is present in the plasma membrane, and not when it is located in the cytoplasm or lysosomes after endocytosis.

iv) Nanoparticles for oral delivery of peptides and proteins

Significant advances in biotechnology and biochemistry have led to the discovery of a large number of bioactive molecules and vaccines based on peptides and proteins. Development of suitable carriers remains a challenge due to the fact that bioavailability of these molecules is limited by the epithelial barriers of the gastrointestinal tract and their susceptibility to gastrointestinal degradation by digestive enzymes. Polymeric nanoparticles allow encapsulation of bioactive molecules and protect them against enzymatic and hydrolytic degradation. For instance, it has been found that insulin-loaded nanoparticles have preserved insulin activity and produced blood glucose reduction in diabetic rats for up to 14 days following the oral administration.

The surface area of human mucosa extends to 200 times that of skin. The gastrointestinal tract provides a variety of physiological and morphological barriers against protein or peptide delivery, e.g., (a) proteolytic enzymes in the gut lumen like pepsin, trypsin and chymotrypsin; (b) proteolytic enzymes at the brush border membrane (endopeptidases); (c) bacterial gut flora; and (d) mucus layer and epithelial cell lining itself. The histological architecture of the

mucosa is designed to efficiently prevent uptake of particulate matter from the environment. One important strategy to overcome the gastrointestinal barrier is to deliver the drug in a colloidal carrier system, such as nanoparticles, which is capable of enhancing the interaction mechanisms of the drug delivery system and the epithelia cells in the GI tract.

v) Targeting of nanoparticles to epithelial cells in the GI tract using ligands

Targeting strategies to improve the interaction of nanoparticles with adsorptive enterocytes and M-cells of Peyer's patches in the GI tract can be classified into those utilizing specific binding to ligands or receptors and those based on nonspecific adsorptive mechanism. The surface of enterocytes and M cells display cell-specific carbohydrates, which may serve as binding sites to colloidal drug carriers containing appropriate ligands. Certain glycoprotein's and lectins bind selectively to this type of surface structure by specific receptor-mediated mechanism. Different lectins, such as bean lectin and tomato lectin, have been studied to enhance oral peptide adsorption. Vitamin B-12 absorption from the gut under physiological conditions occurs via receptor-mediated endocytosis. The ability to increase oral bioavailability of various peptides (e.g., granulocyte colony stimulating factor, erythropoietin) and particles by covalent coupling to vitamin B-12 has been studied. For this intrinsic process, mucoprotein is required, which is prepared by the mucus membrane in the stomach and binds specifically to cobalamin. The mucoprotein completely reaches the ileum where resorption is mediated by specific receptors.

vi)Absorption enhancement using non-specific interactions

In general, the gastrointestinal absorption of macromolecules and particulate materials involves either paracellular route or endocytotic pathway. The paracellular route of absorption of nanoparticles utilizes less than 1% of mucosal surface area. Using polymers such as chitosan, starch or poly (acrylate) can increase the paracellular permeability of macromolecules. Endocytotic pathway for absorption of nanoparticles is either by receptor-

mediated endocytosis, that is, active targeting, or adsorptive endocytosis which does not need any ligands. This process is initiated by an unspecific physical adsorption of material to the cell surface by electrostatic forces such as hydrogen bonding or hydrophobic interactions. Adsorptive endocytosis depends primarily on the size and surface properties of the material. If the surface charge of the nanoparticles is positive or uncharged, it will provide an affinity to adsorptive enterocytes though hydrophobic, whereas if it is negatively charged and hydrophilic, it shows greater affinity to adsorptive enterocytes and M cells. This shows that a combination of size, surface charge and hydrophilicity play a major role in affinity. This is demonstrated with poly (styrene) nanoparticles and when it is carboxylated. Nanoparticles for gene delivery polynucleotide vaccines work by delivering genes encoding relevant antigens to host cells where they are expressed, producing the antigenic protein within the vicinity of professional antigen presenting cells to initiate immune response. Such vaccines produce both humoral and cell-mediated immunity because intracellular production of protein, as opposed to extracellular deposition, stimulates both arms of the immune system. The key ingredient of polynucleotide vaccines, DNA, can be produced cheaply and has much better storage and handling properties than the ingredients of the majority of protein-based vaccines. Hence, polynucleotide vaccines are set to supersede many conventional vaccines particularly for immunotherapy. However, there are several issues related to the delivery of polynucleotides which limit their application. These issues include efficient delivery of the polynucleotide to the target cell population and its localization to the nucleus of these cells, and ensuring that the integrity of the polynucleotide is maintained during delivery to the target site. Nanoparticles loaded with plasmid DNA could also serve as an efficient sustained release gene delivery system due to their rapid escape from the degradative endo-lysosomal compartment to the cytoplasmic compartment. Hedley et al. reported that following their intracellular uptake and endolysosomal escape, nanoparticles could release DNA at a

sustained rate resulting in sustained gene expression. This gene delivery strategy could be applied to facilitate bone healing by using PLGA nanoparticles containing therapeutic genes such as bone morphogenic protein.

vii) Nanoparticles for drug delivery into the brain

The blood-brain barrier (BBB) is the most important factor limiting the development of new drugs for the central nervous system. The BBB is characterized by relatively impermeable endothelial cells with tight junctions, enzymatic activity and active efflux transport systems. It effectively prevents the passage of water-soluble molecules from the blood circulation into the CNS, and can also reduce the brain concentration of lipid-soluble molecules by the function of enzymes or efflux pumps. Consequently, the BBB only permits selective transport of molecules that are essential for brain function. Strategies for nanoparticle targeting to the brain rely on the presence of and nanoparticle interaction with specific receptor-mediated transport systems in the BBB. For example polysorbate 80/LDL, transferrin receptor binding antibody (such as OX26), lactoferrin, cell penetrating peptides and melanotransferrin have been shown capable of delivery of a self non transportable drug into the brain via the chimeric construct that can undergo receptor-mediated transcytosis . It has been reported poly (butylcyanoacrylate) nanoparticles was able to deliver hexapeptide dalargin, doxorubicin and other agents into the brain which is significant because of the great difficulty for drugs to cross the BBB. Despite some reported success with polysorbate 80 coated NPs, this system does have many shortcomings including desorption of polysorbate coating, rapid NP degradation and toxicity caused by presence of high concentration of polysorbate. OX26 MAbs (anti-transferrin receptor MAbs), the most studied BBB targeting antibody, have been used to enhance the BBB penetration of liposomes.

CHAPTER-III

LITERATURE REVIEW

Mukesh S Patil et al., 2011, reported on preparation and optimization of simvastatin nanoparticle for solubility enhancement and in- vivo study. Simvastatin nanoparticles prepared by nanoprecipitation method using a partially water-miscible solvents and the mutual saturation of the aqueous and organic phases prior to form a nano suspension in order to reduce the initial thermodynamic instability of the nanoparticles. Because of the self-emulsifying properties of the methacrylic acid co-polymers, it was possible to prepare aqueous dispersions of colloidal size containing up to 30% w/v of Eudragit L100 using methanol as a water-miscible solvent with surfactant. Nanoparticles have become an important area of research in the field of drug delivery, because they have the ability to deliver a wide range of drugs to varying areas of the body for sustained periods of time. The nanoparticles have a higher surface-to-volume ratio as compared with bulk material, and therefore the dose and frequency of administration would be reduced hence increasing patient compliance.

Ji Jingou et al., 2011, reported on preparation, characterization of hydrophilic and hydrophobic drug in combine loaded chitosan/cyclodextrin nanoparticles and in vitro release study. The prepared nanoparticles were characterized by FT-IR spectroscopy to confirm the cross-linking reaction between CS and cross-linking agent. X-ray diffraction (XRD) was performed to reveal the form of the drug after encapsulation. The average size of nanoparticles ranged from 308.4±15.22 to 369.3±30.01 nm. The nanoparticles formed were spherical in shape with high zeta potentials (higher than +30 mV). In vitro release studies in phosphate buffer saline (pH 7.4) showed an initial burst effect and followed by a slow drug release. Cumulative release data were fitted to an empirical equation to compute diffusional exponent (n), which indicated the non-Fickian trend for drug release.

Akbari et al., 2011, reported on development and evaluation of orodispersible tablets of Rosuvastatin calcium-HP-β-CD inclusion complex by using different superdisintegrants rosuvastatin Calcium (RST), a poorly water-soluble 3-hydroxy3-methyl glut aryl CoA (HMG-CoA) Reductase inhibitor through inclusion complexation with hydroxy propyl β-cyclodextrin (HP-β-CD). The aim of this work was to develop Rosuvastatin Orodispersible tablets by exploiting the solubilizing effect of hydroxy propyl β-cyclodextrin (HP-β-CD). Drug–CD complex systems, prepared by different techniques, were characterized by differential scanning Calorimetry (DSC), X-ray diffractometry, and Fourier transform infrared (FT-IR) spectroscopy. The inclusion complex containing RST: HP-β-CD (1:1) was formulated into tablets using super disintegrants like sodium starch glycolate, crospovidone and croscarmellose. Tablets containing RST-HP- β-CD inclusion complex were prepared by direct compression and evaluated for various post compression parameters like hardness, friability, weight variation, thickness, drug content and in-vitro dissolution. A significant improvement of the drug dissolution profile was achieved from tablets containing drug-CD systems (Kneaded products showed the best dissolution profiles, reaching more than 97.46% drug release in 20 min.). The stability of tablets was studied and no significant changes were detected in the dissolution profile of tablets after 1 month.

Peng Lium et al., 2011, studied the nanosuspensions of poorly soluble drugs: Preparation and development by wet milling. Nanosizing techniques are important tools for improving the bioavailability of water insoluble drugs. Here, a rapid wet milling method was employed to prepare nanosuspensions: 4 types of stabilizers at 4 different concentrations were tested on 2 structurally different drug compounds: indomethacin and itraconazole. Photon correlation spectroscopy (PCS) results showed that the finest nanosuspensions were obtained when 80 wt% (to drug amount) pluronic F68 was the stabilizer for indomethacin and 60 wt% pluronic F127 for itraconazole. Compared to physical mixtures, dissolution rates of the

nanosuspensions showed significant increases. The morphology of nanoparticles was observed by transmission electron microscopy (TEM). Crystalline state of the drugs before and after milling was confirmed using differential scanning calorimetry (DSC) and X-ray powder diffraction (XRPD). The physical and chemical stabilities of the nanosuspensions after storage for 2 months at room temperature and at 4°C were investigated using PCS, TEM and HPLC. No obvious changes in particle size and morphology and no chemical degradation of the drug ingredients were seen.

Liang Fang et al., 2011, reported on preparation and in vitro/in vivo evaluation of revaprazan hydrochloride nanosuspension. To investigate the particle size reduction effect of RH on dissolution and absorption, three suspensions that containing different sized particles were prepared by high pressure homogenization and in vitro/in vivo evaluations were carried out. DSC and powder X-ray diffraction were used to study crystalline state of freeze dried powder of RH suspensions and the results showed that particles of RH micro suspension and nanosuspension remained in the same crystalline state as coarse suspension, but had lower lattice energy. In the in vitro dissolution test, both micro suspension and nanosuspension showed increased dissolution rate. In the in vivo evaluation, compared to coarse suspension, RH nanosuspension exhibited significant increase in AUC0–t, Cmax and decrease in Tmax, MRT. Nevertheless, RH micro suspension did not display any significant differences in these pharmacokinetic parameters compared to the coarse suspension. The findings revealed that particle size reduction can influence RH absorption in gastrointestinal tract and nanosuspension can enhance oral bioavailability of RH in rats.

Khosro Adibkia et al., 2011, developed the naproxen–Eudragit® RS100 nanoparticles and characterized. The nanoparticles of naproxen with Eudragit® RS100 were formulated using the solvent evaporation/extraction technique (the single emulsion technique). The effect of several process parameters, i.e., drug/polymer ratio, aqueous phase volume and speed of

homogenization were considered on the size of the nano formulations. The physicochemical characteristics of nanoparticles were studied applying particle size analysis, differential scanning calorimetry, X-ray crystallography, Fourier transform infrared spectroscopy and scanning electron microscopy. The release rate of naproxen from various drug/polymer nanoparticles was investigated as well. All the prepared formulations using Eudragit® RS100 resulted in nano-range size particles with relative spherical smooth morphology. The nanoparticles of naproxen–Eudragit® RS100 displayed lower crystallinity. The intermolecular interaction between naproxen and Eudragit® RS100 was detected in the FT-IR spectrum of the nanoparticles. All the nanoparticles displayed a slow release pattern with the reduced burst release in comparison with the intact drug powder and physical mixtures of drug and polymer. According of these findings, formulation of the naproxen–Eudragit® RS100 nanoparticles was able to improve the physicochemical characteristics of the drug and possibly will increase the anti-inflammatory effects of drug following its ocular or intra-joint administration.

Mohammed Anwar et al., 2011, evaluated the bioavailability of nano-sized chitosan-atorvastatin conjugate after oral administration to rats. Nano-sized conjugate with a mean size of 215.3 ± 14.2 nm was prepared by the process of high pressure homogenization (HPH). Scanning electron microscopy (SEM) revealed that CH-AT nano-conjugate possess smooth surface whereas X-ray diffraction (XRD) spectra demonstrated amorphous nature of nano-conjugate. Further, CH-AT nano-conjugate showed solubility enhancement of nearly 4-fold and 100-fold compared to CH-AT conjugate and pure AT, respectively. In vitro drug release studies in simulated gastric fluid and simulated intestinal fluid suggested sustained release of AT from the conjugate. Additionally, the nano-conjugate significantly reduced the acidic degradation of AT. The plasma-concentration time profile of AT after oral administration of CH-AT nano-conjugate (2574 ± 95.4 ng/mL) to rat exhibited nearly 5-fold increase in

bioavailability compared with AT suspension (583 ± 55.5 ng/mL). Finally, variable bioavailability, as observed for AT suspension was also reduced when AT was administered in form of CH-AT nano-conjugate. Taken together these data demonstrate that chitosan conjugate nano-prodrugs may be used as sustained polymeric prodrugs for enhancing bioavailability.

Avadi et al., 2011, performed the ex vivo studies for insulin nanoparticles using chitosan and arabic gum. The nanoparticles were prepared by the ion gelation method. Particle size distribution, zeta potential, and polydispersity index of the nanoparticles were determined. It was found that the nanoparticles carried positive charges and showed a size distribution in the range of 170–200 nm. The electrostatic interactions between the positively charged group of chitosan and negatively charged groups of Arabic gum play an important role in the association efficiency of insulin in nanoparticles. In vitro insulin release studies showed an initial burst followed by a slow release of insulin. The muco adhesion of the nanosystem was evaluated using excised rat jejunum. Ex vivo studies have shown a significant increase in absorption of insulin in the presence of chitosan nanoparticles in comparison with free insulin.

Chi H. Lee et al., 2011, developed the pH-sensitive Eudragit nanoparticles for mucosal drug delivery. The biocompatible pH-sensitive nanoparticles composed of Eudragit S-100 (ES) were developed to protect loaded compounds from being degraded under the rigorous vaginal conditions and achieve their therapeutically effective concentrations in the mucosal epithelium. ES nanoparticles containing a model compound (sodium fluorescein (FNa) or nile red (NR)) were prepared by the modified quasi-emulsion solvent diffusion method. Loading efficiencies were found to be 26% and 71% for a hydrophilic and a hydrophobic compound, respectively. Both hydrophilic and hydrophobic model drugs remained stable in nanoparticles at acidic pH, whereas they are quickly released from nanoparticles upon exposure at

physiological pH. The confocal study revealed that ES nanoparticles were taken up by vaginal cells, followed by pH-responsive drug release, with no cytotoxic activities. The pH-sensitive nanoparticles would be a promising carrier for the vaginal-specific delivery of various therapeutic drugs including microbicides and peptides/proteins.

Qiang Zhang et al., 2011, studied the bioavailability and pharmacokinetics of sorafenib suspension, nanoparticles and nanomatrix for oral administration to rat. The formulations were optimized by orthogonal design (L9 (34)) and their bioavailability were evaluated in rat and compared to pH-sensitive Eudragit nanoparticles and suspension of sorafenib. In the formulations, the ratio of sorafenib to Eudragit® S100 was found to be more important determinant of the sorafenib bioavailability than the ratio of sorafenib to Sylysia® 350. As for the bioavailability, the AUC0–36 h of sorafenib nanomatrix was 13–33 times to that of sorafenib suspension, but only 16.8% to 40.8% that of Eudragit® S100 nanoparticles. This may be resulted from the different drug dispersion degree, release character and bioadhesion activity. However, because all the materials used in the nanomatrix formulation are commonly adjuvant, safe, easy to get and cheap, above all, the nanomatrix formulation can solve the stability and scaling up problems in the nanoparticles, it had potential to develop into a product in the future.

Javed Ali et al., 2011, developed the nanocarrier for the enhancement of bioavailability of a cardiovascular agent: In vitro, pharmacodynamic, pharmacokinetic and stability assessment. The goals of the current study were to develop and characterize a nanoemulsion of ezetimibe, evaluate its stability, lipid lowering and pharmacokinetic profile. Solubility of the drug was estimated in various oils and surfactants. Existence of nanoemulsion region was confirmed by plotting phase diagrams. Various thermodynamic stability and dispersibility tests were performed on the formulations chosen from phase diagram. Percentage transmittance, refractive index, viscosity, droplet size and zeta potential of the optimized formulations were

determined. Dialysis bag method was employed to study the release rate. The formulation selected for bioavailability estimation contained Capryol 90 (10%, v/v), Crempophor EL (11.25%, v/v), Transcutol® P (33.75%, v/v), and double distilled water (45%, v/v). The release rate from the nanoemulsion was highly significant ($p < 0.001$) in contrast to the drug suspension. The level of total cholesterol in the group receiving nanoemulsion CF1 was found to be highly significant ($p < 0.001$) in comparison to the group receiving drug suspension. Bioavailability studies in rats revealed superior absorption of ezetimibe from nanoemulsion as compared to the marketed formulation and drug suspension. The shelf life of the nanoemulsion was estimated to be 18.53 months. The present study corroborated nanoemulsion to be a promising choice to improve the bioavailability of ezetimibe.

Xuenong Zhang et al., 2011, studied the pharmacokinetic profile of freeze-dried cyclosporine A- Eudragit S100 nanoparticle formulation in dogs. The pharmacokinetic profile of freeze-dried cyclosporine A-Eudragit S100 nanoparticles (CyA-S100-NP) was studied with a random two-way crossover study in dogs. The drug blood concentration was determined by internal standard HPLC method after oral administration of CyA-S100- NP and Neoral. Pharmacokinetics parameters were calculated by 3P97 program. The concentration-time data were fitted as a two-compartment open model. The AUC of CyA-S100-NP was higher than that of neoral ($P<0.05$), while the CL significantly decreased ($P<0.05$). The relative bioavailability of CyA-S100-NP was 135.9% compared with Neoral. The bioavailability of CyA was significantly improved. CyA-S100-NP was a potential drug for developing a new CyA nanoparticles solid formulation.

Vijaykumar et al., 2010, developed oral tablet dosage form incorporating drug nanoparticles. To enhance oral bioavailability and reduce variability in systemic exposure, nanoparticle formulation of these drugs were developed using a wet bead milling technique. The solid-state transitions of drug nanoparticles were evaluated before and after milling using

differential scanning calorimetry (DSC) and powder X-ray diffraction (XRPD). The nanosuspensions were converted into solid intermediate or granules by layering on to a water-soluble carrier lactose using a spray granulation processes. The granules were blended with excipients for tabletting. The saturation solubility and dissolution characteristics of nanoparticle formulations were investigated and compared with commercial tablet formulations in a discriminating dissolution media. The result indicated that there was no solid-state transition upon milling. A significant enhancement in dissolution rate for tablet dosage form incorporating drug nanoparticles was observed compared to the marketed products. The manufacturing process used is relatively simple and scalable indicating viability of the approach for commercial manufacture of drug product.

Pieter Annaert et al., 2010, performed the ex vivo permeability experiments in excised rat intestinal tissue and in vitro solubility measurements in aspirated human intestinal fluids support age-dependent oral drug absorption. The possible influence of advanced age on intestinal drug absorption was investigated by determining the effects of aging on (i) solubility of model drugs in human intestinal fluids (HIF) obtained from two age groups (18–25 years; 62–72 years); and (ii) transepithelial permeation of model drugs across intestinal tissue excised from young, adult and old rats. Average equilibrium solubility values for 10 poorly soluble compounds in HIF aspirated from both age groups showed high inter individual variability, but did not reveal significant differences. Characterization of the HIF from both age groups demonstrated comparable pH profiles, while concentrations of individual bile salts showed pronounced variability between individuals, however without statistical differences between age groups. Trans epithelial permeation of the transcellular probe metoprolol was significantly increased in old rats (38 weeks) compared to the younger age groups, while the modulatory role of P-glycoprotein in transepithelial talinolol transport was observed in adult and old rats but not in young rats. In conclusion, age-dependent

permeability of intestinal tissue (rather than age-dependent luminal drug solubility) may contribute to altered intestinal drug absorption in older patients compared to young adults.

Bivash Mandal et al., 2010, developed sulfacetamide loaded Eudragit L100 nanosuspension with potential for ocular delivery. Nanosuspensions were prepared by the solvent displacement method using acetone and Pluronic F108 solution. Drug to polymer ratio was selected as formulation variable. Characterization of the nanosupension was performed by measuring particle size, zeta potential, Fourier Transform infrared spectroscopy (FTIR), Differential Scanning Calorimetry (DSC), Powder X-Ray Diffraction (PXRD), drug entrapment efficiency and in vitro release. In addition, freeze drying, redispersibility and short term stability study at room temperature and at 40°C were performed. Spherical, uniform particles (size range below 500 nm) with positive zeta potential were obtained. No significant chemical interaction between drug and polymer were observed in the solid state characterization of the freeze dried nanosuspension (FDN). Drug entrapment efficiency of the selected batch was increased by pH alteration and addition of polymethyl methacrylate in the formulation. The prepared nanosuspension exhibited good stability after storage at room temperature and at 40°C. Sucrose and mannitol were used as cryoprotectants and exhibited good water redispersibility of the FDN. The results indicate that the formulation of sulfacetamide in Eudragit RL100 nanosuspension could be utilized as potential delivery system for treating ocular bacterial infections.

Syam Potnuru et al., 2010, designed biodegradable polymer nanoparticles for oral drug delivery of stavudine: in- vitro dissolution studies and characterization. The aim of present investigation was to describe formulation and characterization of novel biodegradable nanoparticles based on chitosan for encapsulation of Stavudine. To achieve this objective solvent evaporation method, in- situ nanoemulsion polymer cross linking method were used. Drug containing nanoparticles were prepared with different drug polymer ratio at ambient

temperature and freeze dried. The resulting nanoparticles loading efficiency is 55.19% to 90.60% , loading capacity is 25.16% to 42.27%, particle size of nanoparticles is 65.5-176nm and dissolution studies were done by dialysis bag method with ph 7.4 (phosphate buffer)as a dissolution medium. It followed zero order release kinetics.

Mishra et al., 2010, investigated the formulation variables affecting the properties of lamotrigine nanosuspension using fractional factorial design. Nanosuspension was prepared using emulsification-solvent diffusion method. All the formulations were subjected to in-vitro evaluation and the statistically optimized one was used for stability, scanning electron microscopic and differential scanning calorimetric studies. Nanoparticles were spherical with little surface adsorbed drug. Formulation characteristics in terms of size, zeta potential, polydispersity index (PDI), entrapment efficiency (EE), drug content and in vitro drug release were consistent and within their acceptable range. All the batches provided a burst release profile during first 1 hr, followed by a controlled release extending up to 24 hrs. The values of n in Peppas model ranged between 0.2-0.4 for all the formulations indicative of Fickian release mechanism. The formulation remained reasonably stable up to 3 months. No interaction was observed among the drug and polymers. Results of in vitro drug release studies suggested that nanosuspension might be used as a sustained delivery vehicle for LMG. Statistical analysis revealed that size of the nanoparticles was most strongly affected by stabilizer type while EE was influenced by the drug-to-polymer ratio.

Shishu et al., 2010, reported on comparative bioavailability of curcumin, turmeric and Biocurcumax in traditional vehicles using non-everted rat intestinal sac model. The bioavailability of curcumin from turmeric, Biocurcumax and as plain curcumin was investigated using conventional vehicles by a non-everted rat intestinal model. Results of ex vivo intestinal permeability studies showed an enhancement in the permeability of curcumin with increase in lipophilicity of the vehicle used. Maximum permeability of curcumin was

obtained from corn oil (13.4%) followed by clarified butter (9.82%), milk (4.24%) and aqueous suspension (1.66%) in 8 h. Another very interesting and important observation was that the permeation of curcumin was more from turmeric and Biocurcumax than from plain curcumin. These studies strongly suggest that curcumin may be consumed as turmeric/Biocurcumax in lipophilic vehicles instead of plain curcumin for maximum beneficial effects.

Swarnali Das et al., 2010, designed Eudragit RL 100 nanoparticles by nanoprecipitation method for ocular drug delivery. The particles were prepared by solvent displacement or nanoprecipitation method. The non-biodegradable positively charged polymer Eudragit RL 100 was used to prepare the different formulations with varying ratios of drug and polymer. The formulations were evaluated in terms of particle size, zeta potential, and differential scanning calorimetry measurements. Drug entrapment and release properties were also examined. The antimicrobial activity against Fusarium solani was determined. In vivo eye irritation study was carried out by a modified Draize test. All the formulations remained within a size range of 130 to 300 nm in fresh preparation as well as after 2 months. The zeta potential was positive (+22 to +42 mV) for all the formulations and was suitable for ophthalmic application. A prolonged drug release was shown by all the formulations. The formulation possesses a good antifungal activity against Fusarium solani when tested by disk diffusion method, and no eye irritation on in vivo testing was found.

Rezaei Mokarram et al., 2010, prepared and evaluated indomethacin nanoparticles. Nano-solid suspension of indomethacin in polyvinyl pyrrolidine (PVP) was prepared by controlled precipitation technique, characterized by differential scanning calorimetry (DSC), X-ray diffraction (XRD), Fourier Transform Infrared Spectroscopy (FTIR) and evaluated for in vitro solubility and dissolution rate. Absence of thermal and diffractional peaks in DSC and XRD studies indicated that indomethacin interacts with PVP in solid phase. The solubility of

indomethacin in nano-solid suspension compared to crystalline form was increased to about four-fold. It was found that particle size distribution depend to the polymer MW and drug: polymer ratios. Spectroscopy methods and Transmission Electron Microscopy (TEM) images showed that indomethacin dispersed as amorphous nanosized particles in freeze dried powder. Enhanced solubility and dissolution rate of indomethacin compared to physical mixtures and crystalline form of indomethacin (polymorph I), demonstrated that it interacts with PVP via hydrogen bond and probably forming eutectic mixture.

Yadav et al., 2009, formulated and evaluated carvedilol loaded Eudragit E 100 nanoparticles. Nanoparticles of Carvedilol with Eudragit E 100 were prepared by the nanoprecipitation method using polymeric stabilizer poloxamer 407. Nanoparticles of Carvedilol were obtained with high encapsulation efficiency. The particles were characterized for particle size by photon correlation spectroscopy and transmission electron microscopy. The in vitro release studies were carried out by USP type II apparatus in SGF without enzyme (pH 1.2).The particle size of the prepared nanoparticles ranged from 190 nm – 270 nm. Nanoparticles of Carvedilol were obtained with high encapsulation efficiency (85-91%). The drug release from the carvedilol nanoparticles showed within 5 minutes. These studies suggest that the feasibility of formulating carvedilol – loaded Eudragit E 100 nanoparticles for the treatment of hypertension.

Giuseppe Trapani et al., 2009, developed and characterized new nanoparticle systems based on Eudragit RS 100 and cyclodextrins (CDs) for the transmucosal administration of glutathione (GSH). For this purpose, nanoparticles (NPs) with the mucoadhesive properties of Eudragit RS 100 and the penetration enhancing and peptide protective properties of CDs were prepared and evaluated. The quasi-emulsion solvent diffusion technique was used to prepare the NPs with natural and chemically modified (HP-b-CD and Me-b-CD) CDs. The NPs prepared showed homogeneous size distribution, mean diameters between 99 and

156 nm, a positive net charge and spherical morphology. Solid state FT-IR, thermal analysis (DSC), and X-ray diffraction studies suggest that the nanoencapsulation process produces a marked decrease in crystallinity of GSH. The encapsulation efficiency of the peptide was found to be between 14.8% and 24%. The results indicate that mean diameters, surface charges and drug-loaded NPs were not markedly affected by the CD, whereas the presence of the latter influences drug release and to some extent peptide stability and absorption. Finally, it has been shown that CD/Eudragit RS 100 NPs may be used for transmucosal absorption of GSH without any cytotoxicity using the epithelial human HaCaT and murine monocytes macrophage RAW264.7 cell lines.

Singh et al., 2009, developed the Poly (d, l-lactide) nanosuspensions of risperidone for parenteral delivery: Formulation and In-Vitro Evaluation. Polymeric nanoparticles suspensions containing risperidone made of poly (D, Lactide) were designed by nanoprecipitation method using polymeric stabilizer (Pluronic® F-68 or Pluronic® F-127). The prepared nanosuspensions were characterized for particle size by photon correlation spectroscopy and scanning electron microscopy. The free dissolved drug in the nanosuspension was determined by bulk equilibrium reverse dialysis bag technique. In vitro release studies were carried out using dialysis bag diffusion technique. The particle size of the prepared nanoparticles in the nanosuspensions ranged between 78-184 nm. Nanoparticles of risperidone in the nanosuspensions were obtained with high encapsulation efficiency (91 - 94 %). The drug release from the risperidone nanosuspension was sustained in some batches for more than 24 h with 75% drug release whereas release from risperidone solution showed release within 1.5 h. The release pattern of drug is analyzed and found to follow first order equation and Fickian diffusion kinetics. These studies suggest the feasibility of formulating risperidone loaded poly(D, L-Lactide) nanoparticles suspension for the treatment of psychotic disorders.

Jawahar et al., 2009, developed and characterized PLGA-nanoparticles containing carvedilol. Prepared nanoparticles were examined for physicochemical characteristics, in vitro release kinetics and invivo biodistribution studies. Average size of the nanoparticles were in range of 132-234nm. The drug encapsulation efficiency was 77.6% at 33% drug loading. In vitro cumulative release from the nanoparticles was 72% at 24hr. In vivo biodistribution studies in rats revealed that these particles are distributed in heart, liver and kidney at higher concentration may allow their delivery to target sites.

Manish K Gupta et al., 2009, developed the nanoparticulate drug delivery system of cyclosporine .Cyclosporine (CYA) loaded Eudragit RL100 nanoparticles were prepared using solvent evaporation technique, with 2% PVA as stabilizer. Four batches of nanoparticles with varying drug concentrations (CYN-1, CYN-2, CYN-3 and CYN-4) were prepared. Cumulative % drug release of formulations CYN-1, CYN-2, CYN-3 and CYN-4 was 94.35%, 93.89%, 88.28% and 85.36% respectively. Formulation CYN-2, which proved to be the best showed a mean particle size of 236 nm and entrapment efficiency of 58.27%. The in vivo result of formulation CYN-2 revealed that the drug loaded nanoparticles showed preferential drug targeting to liver followed by spleen, lungs and kidneys. Stability studies showed that maximum drug content and closest in vitro release to initial data was found in the sample (formulation CYN-2) stored at 4ºC. So, in the present study Cyclosporine loaded Eudragit Nanoparticles were prepared and targeted to various organs to a satisfactory level and the prepared nanoparticles were stable at 4ºC.

Adlin et al., 2009, formulated and evaluated the nanoparticles containing Flutamide. Nanoparticles of Flutamide were formulated using chitosan polymer by ionic gelation technique. Nanoparticles of different core: coat ratio were formulated and analyzed for total drug content, loading efficiency, particle size and in vitro drug release studies. From the drug

release studies it was observed that nanoparticles prepared with chitosan in the core: coat ratio 1:4 gives better sustained release for about 12 hrs as compared to other formulations.

Le Thi Mai Hoa et al., 2009, formulated the polymeric drug nanoparticles by emulsion solvent evaporation method. In this study, prepared polymeric drug nanoparticles consist of ketoprofen and Eudragit E 100. The morphological structure was investigated by scanning electron microscopy (SEM). The interactions between the drug and polymer were investigated by Fourier transform infrared spectroscopy (FTIR). The size distribution was measured by means of Dynamic Light Scattering. The nanoparticles have an average size of about 150 nm. The incorporation ability of drugs in the polymeric nanoparticles depended on the integration between polymer and drug as well as the glass transition temperature of the polymer.

Gershon Golomb et al., 2009, developed the new double emulsion solvent diffusion technique for encapsulating hydrophilic molecules in PLGA nanoparticles. The new NP preparation technique, double emulsion solvent diffusion (DES-D), resulted in improved formulation characteristics including smaller size, lower size distribution, higher encapsulation yield, and more biocompatible ingredients in comparison to classical methods. The utilization of partially water-miscible organic solvent (ethyl acetate) enabled rapid diffusion through the aqueous phase forming smaller NP. In addition, the formulated alendronate NP exhibited profound inhibition of raw 264 macrophages, depletion of rabbit's circulating monocytes, and inhibition of restenosis in the rat model. It is concluded that the new technique is advantageous in terms of smaller size, lower size distribution, higher encapsulation yield, and more biocompatible ingredients, with unaltered bioactivity.

Sanjay Singh et al., 2009, developed the PLGA nanoparticle formulations of risperidone: preparation and neuropharmacological evaluation. PLGA nanoparticles of risperidone were designed by nanoprecipitation method using polymeric stabilizer (Poloxamer 407). The prepared nanoparticles were characterized for particle size by photon correlation spectroscopy and atomic force microscopy. Poloxamer 407–based in situ gel containing PLGA nanoparticles of risperidone was prepared by modified cold method to control the initial rapid release from the nanoparticles. The in vivo efficacy (antipsychotic effect) of prepared formulations (nanoparticles and in situ gel containing nanoparticles) was studied by administering them subcutaneously to mice. Extra pyramidal side effects of the formulations were also studied. The particle size of the prepared nanoparticles ranged between 85 and 219 nm. About 89% to 95% drug encapsulation efficiency was achieved when risperidone was loaded at 1.7% to 8.3% by weight of the polymer. During in vivo studies prepared risperidone formulations showed an antipsychotic effect that was significantly prolonged over that of risperidone solution for up to 72 hours with fewer extra pyramidal side effects. The prolonged effect of risperidone was obtained from the risperidone formulations administered subcutaneously, and this may improve the treatment of psychotic disorders by dose reduction.

Mohammad Reza Siahi Shadbad et al., 2008, studied the kinetic analysis of drug release from nanoparticles. Ten conventional models and three models developed in our laboratory were applied to release data of 32 drugs from 106 nanoparticle formulations collected from literature. The accuracy of the models was assessed employing mean percent error (E) of each data set, overall mean percent error (OE) and number of Es less than 10 percent. Among the models the novel reciprocal powered time (RPT), Weibull (W) and log- probability (LP) ones produced OE values of 6.47, 6.39 and 6.77, respectively. The OEs of other models were higher than 10%. Also the number of errors less than 10% for the models was 84.9, 80.2 and 78.3 percents of total number of data sets. Considering the accuracy criteria the reciprocal

powered time model could be suggested as a general model for analysis of multi mechanistic drug release from nanoparticles. Also W and LP models were the closest to the suggested model.

Weigen Lu et al., 2008, reported on preparation and characterization of intravenously injectable nimodipine nanosuspension which was prepared by high-pressure homogenization (HPH). The effects of the production parameters such as pressure, cycle numbers and crushing principles on the mean particle size, 99% diameter and polydispersity of the nanosuspension were investigated. Characterization of the product was performed by scanning electron microscope (SEM) and differential scanning calorimeter (DSC). The safety of the nimodipine nanosuspension was discussed with special attention to contamination by microparticles and the increase in saturation solubility Cs. Irritability study in rabbits showed that this formulation provided less local irritation and phlebitis risks than the commercial ethanol product, which represented a promising new drug formulation for intravenous therapy of subarachnoid hemorrhage (SAH)-related vasospasm.

Christine Vauthier et al., 2007, studied the influence of polymer behaviour in organic solution on the production of polylactide nanoparticles by nanoprecipitation. Poly(d,l)-lactides (PLAs) from a homologous series of different molar masses were nanoprecipitated at different initial polymer concentrations from two organic solvents, acetone and tetrahydrofuran (THF), into water without surfactant according to a standardized procedure. Quasi-elastic light scattering and gel permeation chromatography with universal detection were used respectively to size the particles and to determine the molar mass distribution of the polymeric chains forming both nanoparticles and bulk aggregates. The intrinsic viscosity of the polymers as a function of molar mass and solvent were determined by kinematic viscosity measurements in organic solutions. High yields of small nanoparticles were obtained with polymers of lower molar mass (22 600 and 32 100 g/mol). For a given polymer

concentration in organic solution, the particle diameter was always lower from acetone than from THF. For initial molar masses higher than 32 100 g/mol, only dilute organic solutions gave significant yields of nanoparticles. Furthermore, polymer mass fractionation occurred with increasing initial molar mass and/or concentration: the nanoparticles were formed by polymeric chains of molar masses significantly lower than the average initial one. In general, nanoparticle production was satisfactory when the initial organic solution of polymer was in the dilute rather than the semi-dilute regime. Moreover, acetone, which acted as a theta solvent for PLA, always led to smaller particles and better yields than THF.

Bernadette D'Souza et al., 2007, performed everted gut sac technique an ex vivo screening method for new drugs. The ex vivo everted sac technique is useful for screening the permeability parameter of drug substances associated with their in vivo absorbability. In this method, the intestinal sac is everted to expose the mucosal surface. It is then incubated in mucosal fluids and oxygenated to keep the tissue viable. The drug to be tested is then introduced into mucosal fluid and absorption mechanism is studied and compared. The transport of the drug across the mucosal membrane into the serosal (absorption) as well as the movement of drug from the serosal to the mucosal side (secretion) can be studied. Reasons for poor oral bioavailability of drugs can be assessed and appropriate modifications made. The everted gut sac permeability screening, when coupled with dissolution studies, allows for systematic evaluation of the potential absorbability of a drug in its initial stages of development.

Ravi Kumar et al., 2007, developed the estradiol loaded PLGA nanoparticles for oral administration: Effect of polymer molecular weight and copolymer composition on release behavior in vitro and in vivo. Nanoparticles were prepared by emulsion–diffusion–evaporation method employing didodecyl dimethyl ammonium bromide (DMAB) as stabilizer. The effect of polymer molecular weight and copolymer composition on particle

properties and release behavior (in vitro and in vivo) has been reported. Drug release in vitro decreased with increase in molecular weight and lactide content of PLGA. Zero order release was obtained with low molecular weight (14,500 and 45,000 Da) PLGA, while high molecular weight (85,000 and 213,000 Da) and different copolymer compositions followed square root of time (Higuchi's pattern) dependent release. The bioavailability of estradiol from nanoparticles was assessed in male Sprague Dawley (SD) rats at a dose of 1 mg estradiol/rat. The in vivo performance of the nanoparticles was found to be dependent on the particle size, polymer molecular weight and copolymer composition. The Cmax of drug in the plasma was dependent on the polymer molecular weight and composition while particle size was found to influence the duration of release, suggesting smaller is better. The histopathological examination revealed absence of any inflammatory response with the formulations prepared of low/high molecular weight or high lactide content polymers for the studied period. Together, these results indicate that nanoparticulate formulations are ideal carriers for oral administration of estradiol having great potential to address the dose related issues of estradiol.

Annick Ludwig et al., 2006, studied on the evaluation of ciprofloxacin-loaded Eudragit® RS100 or RL100/PLGA nanoparticles. The particles were prepared by water-in-oil-in-water (w/o/w) emulsification and solvent evaporation, followed by high-pressure homogenization. Two non-biodegradable positively charged polymers, Eudragit® RS100 and RL100, and the biodegradable polymer poly (lactic-co-glycolic acid) or PLGA were used alone or in combination, with varying ratios. The formulations were evaluated in terms of particle size and zeta potential. Differential scanning calorimetry measurements were carried out on the nanoparticles and on the pure polymers Eudragit® and PLGA. Drug loading and release properties of the nanoparticles were examined. The antimicrobial activity against Pseudomonas aeruginosa and Staphylococcus aureus was determined. During solvent

evaporation, the size and zeta potential of the nanoparticles did not change significantly. The mean diameter was dependent on the presence of Eudragit® and on the viscosity of the organic phase. The zeta potential of all Eudragit® containing nanoparticles was positive in ultrapure water (around +21/+25 mV). No burst effect but a prolonged drug release was observed from all formulations. The particles activity against P. aeruginosa and S. aureus was comparable with an equally concentrated ciprofloxacin solution.

Ronald J. Neufeld et al., 2006, studied the nanoencapsulation methods for preparation of drug-loaded polymeric nanoparticles. Polymeric nanoparticles have been extensively studied as particulate carriers in the pharmaceutical and medical fields, because they show promise as drug delivery systems as a result of their controlled- and sustained-release properties, sub cellular size, and biocompatibility with tissue and cells. Several methods to prepare nanoparticles have been developed during the last two decades, classified according to whether the particle formation involves a polymerization reaction or arises from a macromolecule or preformed polymer. In this review the most important preparation methods are described, especially those that make use of natural polymers. Advantages and disadvantages will be presented so as to facilitate selection of an appropriate nanoencapsulation method according to a particular application.

Ugo Bilati et al., 2005, investigated on formulation and process modifications to improve the versatility of the nanoprecipitation technique, particularly with respect to the encapsulation of hydrophilic drugs (e.g. proteins). More specifically, the principal objective was to explore the influence of such modifications on nanoparticle size. Selected parameters of the nanoprecipitation method, such as the solvent and the non-solvent nature, the solvent/non-solvent volume ratio and the polymer concentration, were varied so as to obtain polymeric nano-carriers. The feasibility of such a modified method was assessed and resulting unloaded nanoparticles were characterized with respect to their size and shape. It was shown that the

mean particle size was closely dependent on the type of non-solvent selected. When alcohols were used, the final mean size increased in the sequence: methanol < ethanol < propanol. Surfactants added to the dispersing medium were usually unnecessary for final suspension stabilization. Changing the solvent/non-solvent volume ratio was also not a determinant factor for nanoparticle formation and their final characteristics, provided that the final mixture itself did not become a solvent for the polymer. A too high polymer concentration in the solvent, however, prevented nanoparticle formation. Both poly (lactic acid) (PLA) and poly (DL lactic-co-glycolic acid) (PLGA) could be used by accurately choosing the polymer solvent and in this respect, some non-toxic solvents with different dielectric constants were selected. The nanoparticles obtained ranged from about 85–560 nm in size. The nanoparticle recovery step however needs further improvements, since bridges between particles which cause flocculation could be observed. Finally, the presented results demonstrate that the nanoprecipitation technique is more versatile and flexible than previously thought and that a wide range of parameters can be modified.

Ubrich et al., 2005, evaluated the cyclosporin-loaded Eudragit RS or RL nanoparticles in rabbits orally. The hydrophobic cyclic undecapeptide cyclosporin A (CyA) used in the prevention of graft rejection and in the treatment of autoimmune diseases was encapsulated by nanoprecipitation within non-biodegradable polymeric nanoparticles. The effect of polymers (Eudragit® RS or RL) and additives within the alcoholic phase (fatty acid esters and polyoxyethylated castor oil) on the size, zeta potential and the encapsulation efficiency of the nanoparticles was investigated. The mean diameter of the various CyA nanoparticles ranged from 170 to 310 nm. The size as well as the zeta potential increased by adding fatty acid ester and polyoxy ethylated castor oil within the organic phase. No significant differences in surface potential were observed for all formulations tested. Probably due to the very low water solubility of the drug, high encapsulation efficiencies were observed in a

range from 70 to 85%. The oral absorption of CyA from these polymeric nanoparticles was studied in rabbits and compared to that of Neoral® capsule. Based on comparison of the area under the blood concentration–time curve values, the relative bioavailability of CyA from each nanoparticulate formulation ranged from 20 to 35%.

Harivardhan Reddy et al., 2005, developed the etoposide-loaded nanoparticles made from glyceride lipids: characterization, in vitro drug release, and stability evaluation. The nanoparticles were prepared by melt emulsification and homogenization followed by spray drying of nano dispersion. Spray drying created powder nanoparticles with excellent redispersibility and a minimal increase in particle size (20-40 nm). Experimental variables, such as homogenization pressure, number of homogenization cycles, and surfactant concentration, showed a profound influence on the particle size and distribution. Spray drying of Poloxamer 407-stabilized nanodispersions lead to the formation of matrix-like structures surrounding the nanoparticles, resulting in particle growth. The in vitro steric stability test revealed that the lipid nanoparticles stabilized by sodium tauro glycocholate exhibit excellent steric stability compared with Poloxamer 407. All 3 glyceride nanoparticle formulations exhibited sustained release characteristics, and the release pattern followed the Higuchi equation. The spray-dried lipid nanoparticles stored in black polypropylene containers exhibited excellent long-term stability at 25ºC and room light conditions. Such stable lipid nanoparticles with in vitro steric stability can be a beneficial delivery system for intravenous administration as long circulating carriers for controlled and targeted drug delivery.

Qiang Zhang et al., 2004, developed the pH-sensitive nanoparticles for improving the oral bioavailability of cyclosporine A. The CyA-pH sensitive nanoparticles were prepared by using poly (methacrylic acid and methacrylate) copolymer. The characterization and the dispersion state of CyA at the surface or inside the polymeric matrices of the nanoparticles were investigated. The in vitro release studies were conducted by ultracentrifuge method. The

bioavailability of CyA from nanoparticles and neural micro emulsion was assessed in Sprague–Dawley (SD) rats at a dose of 15 mg/kg. The particle size of the nanoparticles was within the range from 37.4 ± 5.6 to 106.7 ± 14.8 nm. The drug entrapment efficiency was very high (from 90.9 to 99.9%) and in all cases the drug was amorphous or molecularly dispersed within the nanoparticles polymeric matrices. In vitro release experiments revealed that the nanoparticles exhibited perfect pH-dependant release profiles. The relative bioavailability of CyA was markedly increased by 32.5% for CyA-S100 nanoparticles ($P < 0.05$), and by 15.2% and 13.6% for CyA-L100-55 and CyA-L100 nanoparticles respectively, while it was decreased by 5.2% from CyA-E100 nanoparticles when compared with the neoral microemulsion. With these results, the potential of pH-sensitive nanoparticles for the oral delivery of CyA was confirmed.

Karen I. Winey et al., 2004, developed an emulsion-solvent evaporation method for producing haloperidol loaded PLGA nanoparticles with up to 2 % (wt/wt. of polymer) drug content, in-vitro release duration of over 13 days and less than 20% burst release. The free haloperidol is removed from the nanoparticle suspension using a novel solid phase extraction technique. This leads to a more accurate determination of drug incorporation efficiency than the typical washing methods. We have discovered that PLGA end groups have a strong influence on haloperidol incorporation efficiency and its release from PLGA nanoparticles. The hydroxyl terminated PLGA (uncapped) nanoparticles have a drug incorporation efficiency of more than 30% as compared to only 10% with methyl terminated PLGA (capped) nanoparticles. The in-vitro release profile of nanoparticles with uncapped PLGA has a longer release period and a lower initial burst as compared to capped PLGA. By varying other processing and materials parameters, we also controlled the size, haloperidol incorporation and haloperidol release of our haloperidol loaded PLGA nanoparticles.

Francesco Castelli et al., 2003, developed the eudragit as controlled release system for anti-inflammatory drugs. Nanosuspensions were prepared by a modification of the quasi-emulsion solvent diffusion technique (QESD), a particular approach to the general solvent-change method. This kind of system was planned for the ophthalmic release of non-steroidal anti-inflammatory drugs in ocular diseases associated with inflammatory processes (i.e. post-cataract surgery or uveitis). The drug release was monitored by differential scanning calorimetry (DSC), following the effects exerted by IBU on the thermotropic behaviour of DMPC multilamellar vesicles. IBU affects the main transition temperature (Tm) of phospholipid vesicles, causing a shift towards lower values, driven by the drug fraction entering the lipid bilayer. The obtained values have been used as a calibration curve. DSC was performed on suspensions of blank liposomes added to fixed amounts of unloaded and IBU-loaded Eudragit RS100® and RL100® nanosuspensions as well as to powdered free drug. The Tm shifts caused by the drug released from the polymer system or by the free drug, during incubation cycles at 37 ◦C, were compared to the calibration curve in order to obtain the fraction of drug released. The results were also compared with in vitro dialysis release experiments. The suitability of the two different techniques to follow the drug release as well as the differences between the RL and RS polymer systems was compared, confirming the efficacy of DSC for studying the release from polymer nanoparticulate systems.

Amarnath Maitra et al., 2003, studied the Cross-linked polyvinylpyrrolidone nanoparticles: a potential carrier for hydrophilic drugs. Injectable hydrogel polymeric nanoparticles of polyvinylpyrrolidone cross-linked with N, N- methylene bis-acrylamide and encapsulating water-soluble macromolecules such as FITC–dextran (FITC–Dx) have been prepared in the aqueous cores of reverse micellar droplets. These particles are 100 nm and below in diameter with a narrow size distribution. When dispersed in aqueous buffer these particles appear to be transparent and give an optically clear solution. Lyophilized powder of these nanoparticles is

redispersable in aqueous buffer without any change in the size and morphology of the particles. The efficiency of FITC–Dx entrapment by these nanoparticles is high (> 70%) and depends on the amount of cross-linking agent present in the polymeric material. The release of the entrapped molecules from these nanoparticles depends on the degree of cross-linking of the polymer, particle size, pH of the medium, and extent of loading, as well as temperature.

Ken-ichi nezasa et al., 2002, studied on liver-specific distribution of rosuvastatin in rats: The liver is the target organ for the lipid-regulating effect of rosuvastatin; therefore liver-selective uptake of this drug is a desirable property. The aim of this study was to investigate, and compare with pravastatin and simvastatin, the tissue specific distribution of rosuvastatin. Bolus intravenous doses (5 mg/kg) of radiolabeled rosuvastatin, pravastatin, and Simvastatin were administered to rats, and initial uptake clearance (CLuptake) in various tissues was calculated. Hepatic CLuptake of rosuvastatin (0.885 ml/min/g tissue) was significantly ($p < 0.001$) larger than that of pravastatin (0.703 ml/min/g tissue), and rosuvastatin was taken up by the hepatic cells more selectively and efficiently than pravastatin. Hepatic CLuptake of simvastatin (1.24 ml/min/g tissue) was significantly larger than that of rosuvastatin ($p < 0.01$) and pravastatin ($p < 0.001$). However, adrenal CLuptake of simvastatin (1.55 ml/min/g tissue) was larger than hepatic CLuptake, and Simvastatin was distributed to other tissues more easily than rosuvastatin. Microautoradiography of the liver, spleen, and adrenal was undertaken 5 min after administration of the study drugs; distribution was quantified by counting the number of silver grains. After administration of rosuvastatin and pravastatin, silver grains were distributed selectively in the intracellular space of the liver, but more rosuvastatin (3.3- 1.0 - 105 particles/mm2) than pravastatin (2.0 - 0.3 - 105 particles/mm2) tended to distribute to the liver. Simvastatin was less liver-specific (it also distributed to the

spleen and adrenal). The results of this study indicated that rosuvastatin was taken up by hepatic cells more selectively and more efficiently than pravastatin and simvastatin.

Kristl et al., 2002, Investigated the polymeric nanoparticles as carriers of enalaprilat for oral administration. Nanoparticle dispersions were prepared by the emulsification–diffusion method and characterized according to particle size, zeta potential, entrapment efficiency and physical stability. Effective permeabilities through rat jejunum of enalaprilat in solution and in enalaprilat-loaded nanoparticles were compared using side-by-side diffusion chambers. The solubility of enalaprilat is very low in many acceptable organic solvents, but in benzyl alcohol is sufficient to enable the production of nanoparticles by the emulsification–diffusion process. The diameters of drug-loaded PMMA and PLGA nanoparticles were 297 and 204 nm, respectively. The concentration of the stabilizer polyvinyl alcohol (PVA) in dispersion had an influence on particle size but not on drug entrapment. The type of polymer had a decisive influence on drug content- 7 and 13% for PMMA and PLGA nanoparticles, respectively. In vitro release studies show a biphasic release of enalaprilat from nanoparticle dispersions—fast in the first step and very slow in the second. The apparent permeability coefficient across rat jejunum of enalaprilat entrapped in PLGA nanoparticles is not significantly improved compared with enalaprilat in solution.

Snjezana Stolnik et al., 1999, formulated the PLGA nanoparticles by nanoprecipitation method: Approaches investigated for drug incorporation efficiency enhancement included the influence of aqueous phase pH, replacement of procaine hydrochloride with procaine dihydrate and the inclusion of excipients: poly (DL-lactide) (PLA) oligomers, poly(methyl methacrylate-co-methacrylic acid) (PMMA–MA) or fatty acids into the formulation. The nanoparticles produced were submicron size (210 nm) and of low polydispersity. It was found that an aqueous phase pH of 9.3, replacement of procaine hydrochloride with procaine dihydrate and the incorporation of PMMA–MA, lauric and caprylic acid into the formulation

could enhance drug incorporation efficiency without the size, morphology and nanoparticle recovery being adversely influenced. For instance changing the aqueous phase pH from 5.8 to 9.3 increased nanoparticle recovery from 65.1 to 93.4%, drug content from 0.3 to 1.3% w/w and drug entrapment from 11.0 to 58.2%. However, the presence of high ratios of lauric acid and procaine dihydrate in the formulation adversely affected the morphology and size of the nanoparticles. Also, PLA oligomers were not considered a feasible approach since it decreased drug entrapment from 11.0 to 8.4% and nanoparticle recovery from 65.1 to 19.6%. Drug release from nanoparticles appears to consist of two components with an initial rapid release followed by a slower exponential stage. This study has demonstrated that formulation variables can be exploited in order to enhance the incorporation of a water soluble drug into PLGA nanoparticles by the nanoprecipitation technique.

Philippe Maincent et al., 1997, reported on preparation and characterization of nanoparticles containing an antihypertensive agent.PCL nanoparticles were larger than nanoparticles prepared with the other polymers. The zeta potential of the nanoparticles was negative, with values of about -25 mV which promoted good stabilization of the particles. The amorphous state of PLA and PLAGA non-loaded nanoparticles and the semi-crystalline state of PCL were demonstrated with X-ray diffraction and differential scanning calorimetry. For all nanoparticles, isradipine was found to be totally amorphous in the polymer which suggested that the drug was molecularly dispersed in the matrix. The colloidal suspensions displayed a sustained release profile in comparison with the drug release profile of isradipine in a PEG solution. Results from this investigation suggest that these nanospheres will be a good candidate delivery system for oral administration, to reduce the initial hypotensive peak and to prolong the antihypertensive effect of the drug.

Quaroni et al., 1996, developed the intestinal cell culture models for drug transport and metabolism studies. From a drug discovery perspective, cell culture models can be used to expedite identification of compounds with favorable pharmacokinetic properties, and to evaluate structure-absorption/metabolism relationships. In this review, we will use the intestinal epithelium as an example for discussing issues associated with the development of new cell culture models for evaluating drug metabolism. Specifically, we will discuss biological properties of the intestinal epithelium and address biological and practical consideration in the application of tumor cell lines, short-term primary cultures, and stem-like cell cultures. And oncogene immortalized cells as approaches to establishing models for the intestinal epithelium.

CHAPTER-IV

SCOPE OF WORK

The aim of this study is to formulate and evaluate oral nanoparticulate drug delivery of rosuvastatin calcium used in the treatment of hypercholesterolemia.

Management of hypercholesterolemia continues to be challenging with the currently available drugs due to poor bioavailability by the oral route and due to toxicity which occur at higher doses. Since, the preferred route of oral administration is limited to those drug molecules due to its poor solubility and/or poor permeability across the gastric mucosa. A large majority of the new chemical entities (NCE) and many existing drug molecules are poorly soluble and/or poorly permeable, thereby limiting their potential uses and increasing the difficulty of formulating bioavailable drug products. These limitations necessitate urgent requirement of novel drug delivery which do not suffer from such problems.

Rosuvastatin calcium is a potent inhibitor of HMG CoA reductase, which is widely used in the treatment of hypercholesterolemia and may decrease the relative risk of heart attack and stroke. Currently this drug is administered orally as tablets. Since the drug is sparingly soluble and poorly permeable (partition coefficient (octanol/water) – 0.13 at pH 7.0) across the gastric mucosa, the drug displays oral bioavailability (absolute bioavailability-20%) problems in conventional dosage forms. Reported side effects are myopathy, rhabdomyolysis which occur at higher doses. Thus it could be a promising candidate in nanoparticulate drug delivery taking into accounts its poor solubility and poor permeability.

Nanoparticulate drug delivery systems appear to be promising for improving bioavailability of drugs. These nanoparticulate systems are a type of colloidal drug delivery systems where the particle size varies from 10nm – 1000 nm in diameter. Nanoparticles have important potential application for the administration of therapeutic, diagnostic agents and represent very promising drug delivery system of controlled and targeted drug release. Though a wide range of polymers are being used for the development of nanoparticles, the present study included Eudragit L-100 and Eudragit S-100 as polymers and Pluronic F68 and PVA as stabilizers.

CHAPTER- V

PLAN OF WORK

PART –I

STANDARD CURVES FOR ROSUVASTATIN CALCIUM

- Preparation of calibration medium.
- Estimation of absorption maximum (λ_{max}).
- Preparation of standard curves for rosuvastatin calcium in distilled water, hydrochloric acid buffer pH 1.2, phosphate buffer pH 6.8 and phosphate buffer saline pH 7.4.

PART-II

- Drug- polymer interaction studies using Fourier Transform- Infra Red spectroscopy (FT-IR) and Differential Scanning Caloimetry (DSC).

PART-III

- Formulation of rosuvastatin calcium loaded polymeric nanoparticles using different polymers (Eudragit L100 and Eudragit S100) at different ratios and different stabilizers (Pluronic F68 and PVA) at different concentrations by nanoprecipitation method.

PART-IV

CHARACTERIZATION OF ROSUVASTATIN CALCIUM LOADED POLYMERIC NANOPARTICLES

- Determination of particle size and polydispersity index using Malvern particle size analyzer.
- Determination of zeta potential.

- Determination of drug content.
- Determination of drug entrapment efficiency by centrifugation method.
- *Invitro* release studies of rosuvastatin calcium loaded polymeric nanoparticle formulations using dialysis membrane.
- Kinetics of drug release.

PART-V

- Selection of best formulation.

PART-VI

EVALUATION OF SELECTED BEST FORMULATION

- Solubility studies.
- *Ex vivo* intestinal permeability studies using Albino rats.
- Morphological studies of rosuvastatin calcium loaded polymeric nanoparticles by using Transmission electron microscopy (TEM).
- Stability studies.

CHAPTER-VI

MATERIALS AND EQUIPMENTS

MATERIALS USED

1. Rosuvastatin calcium	-	Gift sample from Safe tab Life Science, Pondicherry.
2. Eudragit L100	-	Gift sample from Orchid Pharmaceuticals, Chennai.
3. Eudragit S100	-	Gift sample from Orchid Pharmaceuticals, Chennai.
4. Pluronic F68	-	Gift sample from Orchid Pharmaceuticals, Chennai.
5. PVA	-	Gift sample from Orchid Pharmaceuticals, Chennai.
6. Methanol	-	Changshu Yangyuah chemicals, China.
7. Acetone	-	High purity laboratory chemicals, Mumbai.
8. Potassium dihydrogen phosphate	-	High purity laboratory chemicals, Mumbai.

9. Disodium hydrogen phosphate	-	Nice chemicals Pvt Ltd, Kerala.
10. Sodium chloride	-	Central Drug House (P) Ltd, New Delhi.
11. Hydrochloric acid	-	Universal Scientifics, Madurai.
12. Sodium hydroxide	-	Universal Scientifics, Madurai.
13. Dialysis membrane 50 – LA 387	-	Himedia Lab, Mumbai.

EQUIPMENTS USED

1. Electronic weighing balance	-	A & D Company, Japan.
2. UV-Visible spectrophotometer	-	Shimadzu Corporation, Japan.
3. FT-IR	-	Shimadzu, Japan.
4. Differential Scanning Calorimetry	-	DSC Q 200, Mumbai.
5. Homogenizer	-	M.S.E Ltd, England.
6. Refrigerator	-	Kelvinator, India.
7. Cooling Centrifuge Apparatus	-	Eppendorf Centrifuge 5417R, Germany.
8. Transmission electron microscope	-	Hitachi, Japan.
9. Particle size analyzer	-	Malvern, U.K.
10. Environmental chamber	-	Inlab equipments (Madras) Pvt. Ltd.
11. Rotary shaker	-	Secor, India.

CHAPTER-VII

DRUG PROFILE

ROSUVASTATIN CALCIUM

STRUCTURAL FORMULA

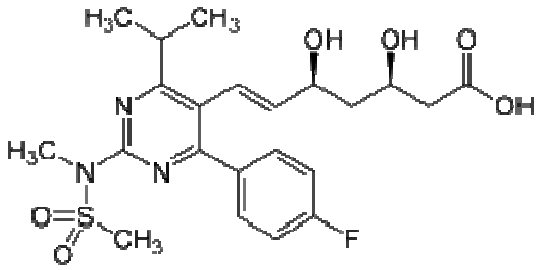

SYNONYMS

- Rosuvastatin calcium
- ZD-4522

EMPIRICAL FORMULA

- $C_{22}H_{28}FN_3O_6S$

CHEMICAL NAME

- (3R,5R,6E)-7-[4-(4-fluorophenyl)-2-(N-methylmethanesulfonamido)-6-(propan-2-yl) pyrimidin-5-yl]-3, 5-dihydroxyhept-6-enoic acid.

DESCRIPTION

- Nature : White crystalline powder
- Molecular weight : 1001.14
- Solubility : Sparingly soluble in water
- partition coefficient (octanol/water) : 0.13 at pH 7.0
- pKa : 14.65

MECHANISM OF ACTION

Rosuvastatin is a competitive inhibitor of HMG-CoA reductase. HMG-CoA reductase catalyzes the conversion of HMG-CoA to mevalonate, an early rate-limiting step in cholesterol biosynthesis. Rosuvastatin acts primarily in the liver. Decreased hepatic cholesterol concentrations stimulate the upregulation of hepatic low density lipoprotein (LDL) receptors which increases hepatic uptake of LDL. Rosuvastatin also inhibits hepatic synthesis of very low density lipoprotein (VLDL). The overall effect is a decrease in plasma LDL and VLDL. In vitro and in vivo animal studies also demonstrate that rosuvastatin exerts vasculoprotective effects independent of its lipid-lowering properties. Rosuvastatin exerts an anti-inflammatory effect on rat mesenteric microvascular endothelium by attenuating leukocyte rolling, adherence and transmigration. The drug also modulates nitric oxide synthase (NOS) expression and reduces ischemic-reperfusion injuries in rat hearts. Rosuvastatin increases the bioavailability of nitric oxide upregulating NOS and by increasing the stability of NOS through post-transcriptional polyadenylation. It is unclear as to how rosuvastatin brings about these effects though they may be due to decreased concentrations of mevalonic acid.

PHARMACOKINETICS

- **Absorption:** In clinical pharmacology studies in man, peak plasma concentrations of rosuvastatin were reached 3 to 5 hours following oral dosing. Both Cmax and AUC increased in approximate proportion to rosuvastatin dose. The absolute bioavailability of rosuvastatin is approximately 20%. The AUC of rosuvastatin does not differ following evening or morning drug administration.
- **Distribution:** Mean volume of distribution at steady-state of rosuvastatin is approximately 134 liters. Rosuvastatin is 88% bound to plasma proteins, mostly albumin. This binding is reversible and independent of plasma concentrations.
- **Metabolism:** Rosuvastatin is not extensively metabolized; approximately 10% of a radiolabeled dose is recovered as metabolite. The major metabolite is N-desmethyl rosuvastatin, which is formed principally by cytochrome P450 2C9, and in vitro studies have demonstrated that N-desmethyl rosuvastatin has approximately one-sixth to one-half the HMG-CoA reductase inhibitory activity of the parent compound. Overall, greater than 90% of active plasma HMG-CoA reductase inhibitory activity is accounted for by the parent compound.
- **Excretion:** Following oral administration, rosuvastatin and its metabolites are primarily excreted in the feces (90%). The elimination half-life (t1/2) of rosuvastatin is approximately 19 hours.

INDICATIONS AND USAGE

- Used as an adjunct to dietary therapy to treat primary hypercholesterolemia (heterozygous familial and nonfamilial), mixed dyslipidemia and hypertriglyceridemia. Also indicated for homozygous familial hypercholesterolemia as an adjunct to other lipid-lowering therapies or when other such therapies are not available.

DOSE

- 5-40 mg orally once daily
- The effects of rosuvastatin on LDL cholesterol are dose-related. At the 10 mg dose, the average LDL cholesterol reduction was found to be 46% in one trial. Increasing the dose from 10 mg to 40 mg gave a modest additional 9% absolute reduction in LDL levels (55% below baseline levels).

DOSAGE FORMS

Tablet- Oral 10 mg

Tablet -Oral 20 mg

Tablet -Oral 40 mg

Tablet -Oral 5 mg

ADVERSE EFFECTS

- Rhabdomyolysis with myoglobinuria and acute renal failure and myopathy (including myositis).
- headache
- myalgia
- abdominal pain
- asthenia
- nausea

OVERDOSAGE

- There is no specific treatment in the event of overdose. In the event of overdose, the patient should be treated symptomatically and supportive measures instituted as required. Hemodialysis does not significantly enhance clearance of rosuvastatin (Drug bank: rosuvastatin calcium).

CHAPTER-VIII

EXCIPIENTS PROFILE

EUDRAGIT L100 (POLYMETHACRYLATE)

Synonyms	:	Acryl-EZE; Acryl-EZE MP; Eastacryl 30D; Eudragit KollicoatMAE 30 D; Kollicoat MAE 30 DP; Polymeric methacrylates.
Nonproprietary names	:	BP: Methacrylic acid–ethyl acrylate copolymer (1: 1) PhEur: Acidum methacrylicum et ethylis acrylas polymerisatum (1: 1) Acidum methacrylicum et ethylis acrylas polymerisatum (1: 1) dispersion 30 per centum Acidum methacrylicum et methylis methacrylas (1: 1) Acidum methacrylicum et methylis methacrylas Polymerisatum (1: 2) Copolymerum methacrylatis butylati basicum Polyacrylatis dispersion 30 per centum USPNF: Ammonio methacrylate copolymer Methacrylic acid copolymer d copolymer dispersion
Chemical name	:	Poly (methacrylic acid, methyl methacrylate) 1 : 1

Empirical formula : $(C5\,H_8\,O_2)_n$

Structural formula

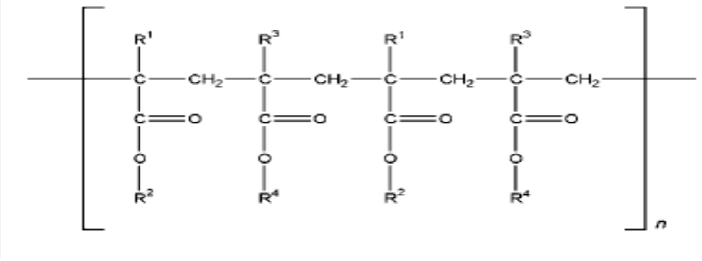

$R^1, R^3, R^4 = CH3,\ R^2 = H$

Description

- Nature : White free flowing powder
- Solubility : Soluble in acetone and alcohol
- Molecular weight : ≥100 000

Functional categories : Film former

Tablet binder

Tablet diluents

Properties

Loss on drying : ≤ 5.0%

Methyl methacrylate and

methacrylic acid : ≤ 0.1%

Sulfated ash : ≤ 0.1%

Apparent viscosity : 50–200 mPa s

Stability and storage : Dry powders are stable for at least 3 years if stored in a tightly closed container at less than 30ºC.

EUDRAGIT S100 (POLYMETHACRYLATE)

Synonyms	:	Acryl-EZE; Acryl-EZE MP; Eastacryl 30D; Eudragit; KollicoatMAE 30 D; Kollicoat MAE 30 DP; polymeric methacrylates.
Nonproprietary names	:	BP: Methacrylic acid–ethyl acrylate copolymer (1 : 1) PhEur: Acidum methacrylicum et ethylis acrylas polymerisatum (1 : 1) Acidum methacrylicum et ethylis acrylas polymerisatum (1 : 1) dispersio 30 per centum Acidum methacrylicum et methylis methacrylas Polymerisatum (1 : 1) Acidum methacrylicum et methylis methacrylas Polymerisatum (1 : 2) Copolymerum methacrylatis butylati basicum Polyacrylatis dispersion 30 per centum USPNF: Ammonio methacrylate copolymer Methacrylic acid copolymer Methacrylic acid copolymer dispersion
Chemical name	:	Poly(methacrylic acid, methyl methacrylate) 1 : 2

Empirical formula : $(C5\ H_8\ O_{2)\ n}$

Structural formula

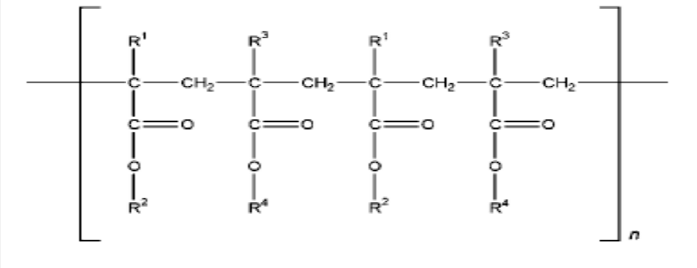

$R^1, R^3, R^4 = CH3, R^2 = H$

Description

- Nature : White free flowing powder
- Solubility : Soluble in acetone and alcohol
- Molecular weight : ≥100 000

Functional categories : Film former

Tablet binder

Tablet diluents

Properties

Loss on drying : ≤ 5.0%

Methyl methacrylate and

methacrylic acid : ≤ 0.1%

Sulfated ash : ≤ 0.1%

Apparent viscosity : 50–200 mPa s

Stablility and storage : Dry powders are stable for at least 3 years if

stored in a tightly closed container at less than 30ºC.

PLURONIC F68 (POLOXAMER)

Nonproprietary Names	:	BP: Poloxamers
		PhEur: Poloxamera
		USPNF: Poloxamer
Synonyms	:	Lutrol
		Monolan
		Pluronic
		Poloxalkol
		Polyethylene–propylene glycol copolymer
		Polyoxyethylene–polyoxypropylene
		Supronic
		Synperonic
Chemical Name	:	α-Hydro-ω-hydroxypoly(oxyethylene)-poly(oxypropylene) poly(oxyethylene)-block copolymer.
Empirical formula	:	$HO\,(C_2H_4O)_a\,(C_3H_6O)_b\,(C_2H_4O)_a\,H$

Structural Formula

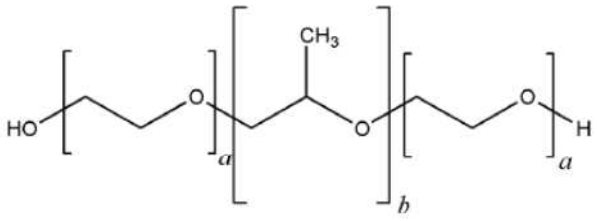

Description

Poloxamers generally occur as white, waxy, free-flowing prilled granules, or as cast solids. They are practically odorless and tasteless.

Functional Category

- Dispersing agent
- Emulsifying agent
- Co emulsifying agent
- Solubilizing agent
- Tablet lubricant
- Wetting agent

Properties

Density	:	1.06 g/cm^3 at 25°C
Flash point	:	260°C
Flowability	:	Free flowing.
HLB value	:	29
Melting point	:	52–57°C
Solubility	:	Freely soluble in water and ethanol.

8.4 POLYVINYL ALCOHOL

Nonproprietary Names	:	PhEur: Poly(vinylis acetas)
		USP: Polyvinyl alcohol
Synonyms	:	Airvol
		Alcotex
		Elvanol
		Gelvatol
		Gohsenol
		Lemol
		Mowiol
		Polyvinol
		PVA
		Vinyl alcohol polymer
Chemical Name	:	Ethenol
Empirical formula	:	$(C_2H_4O)_n$

Structural Formula

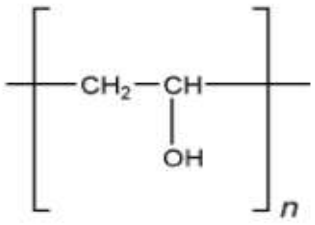

Description

Polyvinyl alcohol occurs as an odorless, white to cream-colored granular powder.

Functional Category

- Coating agent
- Lubricant
- Stabilizing agent
- Viscosity-increasing agent

Properties

Melting point	:	228°C for fully hydrolyzed grades; 180–190°C for partially hydrolyzed grades.
Solubility	:	soluble in water; slightly soluble in ethanol (95%); Insoluble in organic solvents
Specific gravity	:	1.19–1.31 for solid at 25°C
Specific heat	:	1.67 J/g (0.4 cal/g) (Raymond C. Rowe., 2006)

CHAPTER-IX

EXPERIMENTAL PROTOCOL

9.1 STANDARD CURVES FOR ROSUVASTATIN CALCIUM

Preparation of calibration medium

Hydrochloric Acid Buffer pH 1.2

50ml of 0.2 M potassium chloride solution is placed in a 200ml volumetric flask.85ml of 0.2M hydrochloric acid is added and makeup to the volume with distilled water.

- ***0.2M potassium chloride***

14.911 g of potassium chloride is dissolved in distilled water and the volume is makeup to 1000ml.

- ***0.2M Hydrochloric acid***

7.292 g of hydrochloric acid is diluted to 1000ml with distilled water.

Phosphate Buffer pH 6.8

50ml of 0.2M potassium dihydrogen phosphate is placed in a 200ml volumetric flask. 22.4ml of 0.2M sodium hydroxide is added and makeup to the volume with distilled water.

- ***0.2 M potassium dihydrogen phosphate***

27.218 g of potassium dihydrogen phosphate is dissolved and diluted to 1000ml with water.

- ***0.2 M sodium hydroxide***

8 g of sodium hydroxide is dissolved and makeup to 1000ml with water.

Phosphate Buffer Saline (PBS) pH 7.4

2.38 g of disodium hydrogen phosphate, 0.19 g of potassium dihydrogen phosphate and 8.0 g of sodium chloride are dissolved in sufficient quantity of distilled water and made up to 1000 ml (IP 1996).

9.1.1 Estimation of absorption maximum (λmax)

- ***Stock solution:***

Rosuvastatin calcium (100mg) is accurately weighed and dissolved in 100ml methanol to form a stock solution (1000µg/ml).

- ***Working standard solution:***

The stock solution is further diluted suitably with pH 6.8 phosphate buffer to get a working standard solution of concentration 100µg/ml.

This working standard solution is suitably diluted to get a concentration of 10µg/ml and the resultant solution is scanned in the range of 200-400 nm in UV Spectrophotometer to get absorption maximum(Alka Gupta et al., 2009).

9.1.2 Preparation of standard curves

From the working standard solution**,** 2ml, 4ml, 6ml, 8ml, 10ml, 12ml, 14ml, 16ml, 18ml and 20ml are taken separately and diluted to 100ml with the same pH 6.8 phosphate buffer, so that the final concentrations of 2-20 µg/ml solutions are obtained. The above solutions are analyzed by Ultraviolet (UV) spectrophotometer at λ_{max}.

Calibration curve is plotted by taking the concentration in X-axis and respective absorbance in Y-axis.

Calibration curves are also prepared similarly in hydrochloric acid buffer pH 1.2, PBS pH 7.4, and Distilled water.

9.2 DRUG-POLYMER INTERACTION STUDIES

Preformulation testing is the first step in rational development of dosage forms of a drug substance. It gives the information needed to define the nature of the drug substance and provide a framework for the drug combination with pharmaceutical excipients in the dosage forms. Hence, preformulation studies are performed for the obtained sample of drug for compatibility studies (Wadke PA et al., 1980).

- **Compatibility studies**

FT-IR Spectroscopy and DSC studies are carried out to check the compatibility between drug and polymer.

9.2.1 Fourier Transform- Infra Red spectroscopy (FT-IR)

FT-IR spectroscopy is carried out to find out the compatibility between the drug (Rosuvastatin calcium) and the polymers (EL 100, ES 100). 10mg of the sample and 400mg of kBr are taken in a mortar and triturated (Bivash Mandal et al., 2010). A small amount of the triturated sample is taken into a pellet maker and it is compressed at 10 kg/cm^2 using a hydraulic press. The pellet is kept onto the sample holder and scanned from 4000 cm^{-1} to 400 cm^{-1} in FT-IR spectrophotometer, Shimadzu, Japan. Samples are prepared for drug, polymers and physical mixture of drug and polymers. The spectra obtained are compared and interpreted for the shifting of functional peaks and disappearance or appearance of new functional peaks (Poovi G et al., 2011).

9.2.2 *Differential Scanning Calorimetry (DSC)*

DSC is a useful tool to monitor the effect of additives on the thermal behavior of material (Sivabalan M et al., 2011). Accurately weighed samples, equivalent to 5mg of drug (Rosuvastatin Calcium) are placed into the sealed standard aluminum pans with lids. Subsequently, the polymers (EL 100, ES 100) and physical mixtures of drug and polymers are ascertained using the differential scanning calorimetry thermogram analysis, DSC Q200, Shimadzu, Japan. The heating rate is 20°C/min and the heat flow is recorded from 20°C to 180°C. The aluminum oxide and indium powders are employed as reference and standard, respectively. DSC analysis of pure rosuvastatin calcium, Eudragit L 100 and Eudragit S100 is performed to identify the drug melting point peak and polymer glass transition temperature (TG) respectively. As a control the physical mixtures of rosuvastatin calcium- Eudragit L100, Eudragit S 100 are analyzed to observe the changes of the melting endotherm of rosuvastatin calcium (Khosro Adibkia et al., 2011).

9.3 FORMULATION OF ROSUVASTATIN CALCIUM LOADED POLYMERIC NANOPARTICLES

Nanoparticles containing rosuvastatin calcium are prepared by Nanoprecipitation according to the method developed by Fessi et al., 1992; Ugo Bilati et al., 2005.

Briefly, a 20mg of rosuvastatin calcium and 200mg of Eudragit L100/ Eudragit S 100 are dissolved in 20 mL of acetone (Swarnali Das et al., 2010). This organic phase is quickly injected into the aqueous phase containing 40 mL of an either 1% or 2% w/v of Pluronic F68/PVA solution with moderate magnetic stirring at room temperature (Manish K Gupta et al., 2009; Kurt E. Geckeler et al., 2011).

The organic phase to aqueous phase ratio is 1:2 (Christine Vauthier et al., 2007). Nanoparticles are spontaneously formed and turned the solution slightly turbid. Then, acetone is removed by continuous stirring for 3-4 hrs.

Drug free nanoparticles are prepared by the same procedure omitting the drug (Snjezana Stolnik et al., 1999).

The process variables involved in NPs preparation is presented in Table XVI –XIX.

In this study, the effects of various process parameters on nanoparticles mean diameter and drug entrapment efficiencies are assessed, including different drug-to-polymer ratios (1:10,1:20,1:30,1:40,1:50) , Pluronic F68 concentration(1%,2%) in the aqueous phase, PVA concentration (1%,2%) in the aqueous phase (Xiangrong Song et al., 2008).

9.4 CHARACTERIZATION OF ROSUVASTATIN CALCIUM LOADED POLYMERIC NANOPARTICLES

All the formulations are evaluated for its particle size, polydispersity index, zeta potential, drug content, entrapment efficiency, *in vitro* drug release studies, and kinetics of drug release.

9.4.1 Particle size and poly dispersity index

Particle size and size distribution are the most important characteristics to be evaluated for nanoparticles systems (Mohanraj VJ et al., 2006). The particle size distribution is reported as Poly Dispersity Index (PDI).

The particle size and Polydispersity index (PDI) of rosuvastatin calcium loaded polymeric nanosuspension are measured using a Zeta sizer nano ZS (Malvern Instruments Ltd., Malvern, UK) (Angela Lopedota et al., 2009).The samples are placed in the analyzer chamber and the readings are carried out at a 90° angle with respect to the incident beam. Disposable cuvettes of 0.75ml capacity are used for all measurements (Bivash Mandal et al., 2010).

9.4.2 Zeta potential

The zeta potential of nanoparticles is commonly used to characterize the surface charge property of nanoparticles (Mohanraj VJ et al., 2006). The zeta potential of rosuvastatin calcium loaded polymeric nanosuspension are measured using a Zeta sizer Nano ZS

(Malvern Instruments Ltd., Malvern, UK) at 25 ± 0.5°C (Dhananjay S. Singare et al., 2010 ; Xiangrong Song et al., 2008). A potential of ±150 mV is set in the instrument. Disposable cuvettes of 0.75ml capacity are used for all measurements (Bivash Mandal et al., 2010).

9.4.3 Drug content

The total drug content in nanosuspension is quantified by Spectrophotometric analysis (Angela Lopedota et al., 2009; Sanjay Singh et al., 2009).

1 mg equivalent of rosuvastatin calcium polymeric nanosuspension is dissolved in 1 ml of acetone and the volume is made up to 100 ml to make 10 µg / ml concentration and the absorbance is measured at 241 nm (λ_{max}) using UV spectrophotometer.

The calculation is performed as follows:

$$\text{Total drug content} = \frac{\text{Vol. Total}}{\text{Vol. Aliquot}} \text{ x Drug amount in aliquot}$$

9.4.4 Entrapment efficiency

The amount of rosuvastatin calcium embedded in the NPs is calculated from the difference between the total amount incorporated in the NP formation medium and the amount of non-embedded rosuvastatin calcium remaining in the aqueous suspending medium (Angela Lopedota et al., 2009). The latter amount is determined by the separation of rosuvastatin calcium loaded NPs from the aqueous medium by centrifugation using refrigerated centrifuge (Eppendorf, 5417R, Germany) at 14,000 rpm for 2 hrs at 4°C. After centrifugation, the supernatant solution is made up to desired volume with buffer and the amount of free drug is determined by measuring the absorbance of samples at 241 nm using UV spectrophotometer.

The % entrapment efficiency is calculated by following formula:

$$\% \text{ drug entrapment} = \frac{\text{(Total drug – Drug in supernatant liquid)}}{\text{Total drug}} \times 100.$$

9.4.5 In vitro release studies

Dialysis bag diffusion technique is used to study *in vitro* release of drug from the prepared nanosuspension (Mishra B et al., 2010).

Dialysis membrane having pore size 2.4 nm, molecular weight cut off 14,000 is used. The nanosuspension equivalent to 1 mg of rosuvastatin calcium (2 ml) is placed in the dialysis bag, hermetically sealed and immersed into a 250ml beaker containing 100ml of the release media maintained at 37±0.5° C.

Aliquots of samples (5 ml) are withdrawn at pre determined intervals and immediately restored with the same volume of fresh media maintained at the same temperature (Mishra B et al., 2010).

The study is carried out by buffer change method using acidic buffer (pH 1.2) for the first 2 hrs and phosphate buffer (pH 6.8) for the rest of the study period, i.e. 10 hrs (Mishra B et al., 2010; Martine Leroueil-Le Verger et al., 1998; Angela Lopedota et al., 2009).

The amount of rosuvastatin calcium dissolved is determined with UV spectrophotometer at 241nm. All the experiments were repeated three times and the average values were taken.

9.4.6 Kinetics of drug release

In order to analyze the drug release mechanism, *in vitro* release data are fitted into a

- Zero-order
- First order
- Higuchi
- Hixon-Crowell cube root law
- Korsmeyer-peppas model.

- The zero order rate Eq. (1) describes the systems where the drug release rate is Independent of its concentration.

$$C = k_0 t \longrightarrow (1)$$

Where C is the concentration of the drug at time (t) and k_0 is the zero-order release rate constant.

- The first order Equation Eq. (2) describes the release from a system where the release rate is concentration dependent.

$$\log C = \log C_0 - kt / 2.303 \longrightarrow (2)$$

Where C is the concentration of the drug at time (t), C_0 is the initial concentration of the drug and k is the first-order release rate constant.

- Higuchi described the release of drugs from porous, insoluble matrix as a square root of time dependent process based on Fickian diffusion as shown in Eq .(3).

$$Q = kt^{1/2} \longrightarrow (3)$$

Where Q is the amount of drug released in time t.

- The Hixson-Crowell cube root law Eq. (4) describes the release from systems where there is a change in surface area and diameter of particles.

$$W_0^{1/3} - W_t^{1/3} = \kappa t \longrightarrow (4)$$

Where W_0 is the initial amount of drug in the pharmaceutical dosage form, W_t is the remaining amount of drug in the pharmaceutical dosage form at time t, and κ is the constant incorporating the surface-volume relationship (Suvakanta Dash et al., 2010; Mohammad Barzegar-Jalali et al., 2008).

9.5 SELECTION OF BEST FORMULATION

The best formulation is selected depending on the results obtained from particle size, entrapment efficiency, *in vitro* drug release studies, and kinetics of drug release.

9.6 EVALUATION OF SELECTED BEST FORMULATION

9.6.1 Solubility studies

The solubility of the best formulation is compared with the solubility of the pure drug solution. For this purpose, saturation solubility measurement is carried out. Accurately weighed amount of pure drug and rosuvastatin calcium loaded polymeric nanoparticles are introduced into separate 25 ml stoppered conical flask containing 10 ml of distilled water. The sealed flask is agitated on a rotary shaker for 24 hr. An aliquot is filtered and the filtrate is suitably diluted and analyzed on a UV spectrophotometer (Arunkumar N et al., 2009; Rezaei Mokkarram et al., 2010; Akbari B.V et al., 2011; Yasushi Shono et al., 2010).

9.6.2 Ex vivo intestinal permeability studies

Ex vivo intestinal permeability studies are useful for screening the permeability of drug substances associated with their *in vivo* absorbability. The *in vitro* rat intestinal model is useful for screening passive drug absorption in humans than the drug absorbed by carrier-mediated mechanism (Lennernas et al., 1997).

The *ex vivo* intestinal permeability studies was approved by the institutional ethical committee (Ref. No: 14024/ E1/ 4/ 2011) using 9 albino male rat. Male Albino rats weighing 150-200 g are used for the study. After overnight fasting, rats are anesthetized by some ether sprinkled to a piece of cotton wool in a glass container equipped with a lid (Hussain Kooshapur et al., 1999). After making a midline incision in the abdomen, the intestinal segments are isolated as follows: duodenum segment of 8 cm is isolated starting from the pylorus; jejunum segment of 10-15 cm is isolated 25 cm from the pylorus; an ileum segment of 10-15 cm is isolated 20 cm upward from caecum (Mallikarjun Chitneni et al., 2011).

The isolated segments are washed with pH 7.4 phosphate buffer saline (USP 30) to remove any mucous and lumen contents. These segments are tied at one end with suture thread and the selected formulations of rosuvastatin calcium Nanosuspension (equivalent to 1mg of drug) and pure drug solution (drug in PBS pH7.4 equivalent to 1 mg) are injected separately into the different parts of intestine using a syringe and the other end of intestine are tied with the help of suture thread. Then the tied segments are placed separately in a beaker containing 100ml of PBS (pH7.4) continuously bubbled with 95% O_2 and 5 % CO_2 with constant stirring at 37ºC.

The studies are completed in triplicates and aliquots of samples (5ml) are withdrawn at 15,30,60,90 and 120 min. The samples are measured using a UV-Visible spectrophotometer at a wave length of 241 nm. The cumulative amount of drug permeated is plotted against time to calculate apparent permeability coefficient (P_{app}) (Shishu et al., 2010; Arpan Chudasama et al., 2011; Ibrahim A. Alsarra et al., 2005).

The apparent permeability coefficient (P_{app}) (cm/s) is calculated as follows:

$$\text{Papp} = \frac{\frac{dQ}{dT}}{AC}$$

where dQ/dt is the rate of drug appearance in the receptor (µg/s), A is the surface area of the intestinal sac (cm^2) and C is the initial concentration of the drug in the sac (µg/ml) (Qiu S X et al., 2006; Albert H. L. Chow et al., 2005; Abdullah M. Al-Mohizea et al., 2010).

Statistical analysis

Statistical analysis for the determination of differences in permeability profiles of rosuvastatin calcium loaded polymeric nanosuspensions and rosuvastatin calcium pure drug solution was assessed by the use of Student's t-test (Graph pad Instat Version 3.0 software). Statistical probability (p) values less than 0.05 were considered significantly different (Arpan Chudasama et al., 2011).

9.6.3 Transmission electron microscopy (TEM)

The morphology of the prepared nanosuspension formulations is determined by TEM: (Hitachi, Japan). Before analysis, the samples were diluted 1:5 and stained with 2% (w/v) phosphotungstic acid for 30 s and placed on copper grids with films for observation (Xiangrong Song et al., 2008).

9.6.4 Stability Studies

Stability is defined as the ability of particular drug or dosage form in a specific container to remain with its physical, chemical and therapeutic specifications. Stability tests are the series of tests designed to obtain information on the stability of the pharmaceutical product in order to define its shelf life and utilization period under specified packaging and storage conditions. The purpose of stability testing is to provide information on how the quality of a drug product varies with time under the influence of variety of environmental factors such as temperature, humidity and light, and to establish a shelf life for the drug product at recommended storage conditions.

Stability testing of pharmaceutical product is done for the following purposes:

- To ensure the efficacy, safety and quality of active drug substance and dosage forms.
- To establish shelf life or expiration period.

Procedure:

The selected best formulation is tested for stability studies. Stability studies are done according to ICH and WHO guidelines. The formulation is divided into 2 sample sets and stored at:

- $4 \pm 1^{o}C$
- $25 \pm 2^{o}C$ and $60 \pm 5\%$ RH.

The entrapment efficiency of the best formulation is determined for a period of 3 months.

CHAPTER-X

RESULTS AND DISCUSSION

10.1 STANDARD CURVES FOR ROSUVASTATIN CALCIUM

10.1.1 Estimation of absorption maximum (λmax)

The λ max of rosuvastatin calcium was estimated by scanning the 10µg/ml concentration of the drug solution in UV region (200-400 nm). It showed the λ max of 241nm (Vishal V. Rajkondwar et al., 2009) which were shown in the Figure 17.

10.1.2 Preparation of standard curves

The standard curves of rosuvastatin calcium prepared using distilled water, hydrochloric acid buffer pH 1.2; phosphate buffer pH 6.8 and phosphate buffer saline pH 7.4 were shown in Figure 18- 21 and Table X-XIII. The linear correlation coefficient was obtained for calibration of rosuvastatin calcium in each medium. Rosuvastatin calcium obeys the Beer's law within the concentration range of 2 to 20µg/ml (Alka Gupta et al., 2009).

10.2 DRUG-POLYMER INTERACTION STUDIES

- **Compatibility studies**

10.2.1 Fourier Transform- Infra Red spectroscopy (FT-IR)

FT- IR spectroscopy was carried out separately to check the compatibility between drug (rosuvastatin calcium) and the polymers (Eudragit L 100, Eudragit S 100) used for the preparation of nanoparticles.

The FT- IR was performed for pure drug, polymers and physical mixture of drug and polymers. The spectra studied at 4000cm^{-1} to 400 cm^{-1} were shown in Figure 22 a,b,c,d,e and Table XIV. It was found from the spectra that there was no major shifting as well as any loss of functional peaks in the spectra of drug, polymers and physical mixture of drug and polymers. The results indicate that the selected polymers (Eudragit L 100, Eudragit S 100) were found to be compatible with the chosen drug rosuvastatin calcium.

10.2.2 Differential Scanning Calorimetry (DSC)

DSC is a useful tool to monitor the effect of additives on the thermal behavior of materials.DSC thermograms of pure drug (rosuvastatin calcium), polymers (Eudragit L100 and Eudragit S100) and the physical mixtures of drug and polymers were shown in the Figure 23 a,b,c,d,e and Table XV. Pure rosuvastatin calcium showed a sharp endothermic peak at 88.12°C, Eudragit L 100 showed a melting endothermic peak at 83.02°C, Eudragit S 100 at 91.50°C. The physical mixture of drug (rosuvastatin calcium) and polymer (Eudragit L100) exhibited an endothermic peak at 85.36°C and the physical mixture of drug (rosuvastatin calcium) and polymer (Eudragit S 100) exhibited an endothermic peak at 88.93°C. Thus, an endothermic peak corresponding to the melting point of pure drug (88°C) was prominent in all the drug polymer mixtures, which suggested clearly that there was no interaction between the drug and the polymers and thus the drug found to be existed in its unchanged form.

10.3 FORMULATION OF ROSUVASTATIN CALCIUM LOADED POLYMERIC NANOPARTICLES

Eudragit L 100 and Eudragit S 100 nanosuspensions were successfully prepared by the Nanoprecipitation technique (Fessi et al., 1992). The method was simple, reproducible, fast, economic and one of the easiest procedure for the preparation of nanospheres (Ugo Bilati et al., 2004). The nanoparticle formation was instantaneous and entire procedure was carried out in only one step. Briefly it required two solvents that were miscible. Ideally, both the polymers and the drug must dissolve in the first one (the organic solvent- acetone), but not in the second system (the non-solvent-water). Indeed, as soon as the polymer containing solvent had diffused into the dispersing medium, the polymers precipitates, involving immediate drug entrapment.

Thus, nanoparticles were spontaneously formed when the organic phase (acetone) containing Eudragit L100 (EL 100) and Eudragit S100 (ES 100) with or without Rosuvastatin calcium was added dropwise into stirred aqueous surfactant solution (1%w/v, 2%w/v Pluronic F68/PVA) resulting in a colloidal suspension.

Instantaneous formation of a colloidal suspension occurred as a result of the polymer deposition on the interface between the organic phase and water, when partially water miscible organic solvent (acetone) diffused out quickly into the aqueous phase from each transient particle intermediate. According to the "Marangoni effect" the transient particle intermediate causes a size reduction to the nano range (Quintanar – Guerrero et al., 1998).

Various formulations of Rosuvastatin calcium (F1-F40) were prepared using different polymers (EL 100/ES 100) at different ratios (1:10,1:20,1:30,1:40,1:50) and different stabilizers (Pluronic F68/PVA) at different concentrations (1%,2%).

The polymer ratios and stabilizer concentrations were selected arbitrarily as shown in Table XVI-XIX with a view to study the effect on physicochemical and release of the polymeric nanoparticles.

10.4 CHARACTERIZATION OF ROSUVASTATIN CALCIUM LOADED POLYMERIC NANOPARTICLES

10.4.1 Particle size and polydispersity index

Particle size plays a critical role in influencing the physico chemical and biological characteristics of the nanoparticles. Nanoparticles were charactized by mean particle diameter and their distribution. The average diameters, polydispersity index of rosuvastatin calcium loaded nanoparticles were listed in Table XX a,b,c,d,e,f,g,h and Figure 24; smaller particles less than 400nm were most preferred in pharmaceutical process development.

In the present study the particle size of nanoparticles ranged between 125.9 nm - 191.9 nm with respect to nanoparticles prepared with EL100 containing Pluronic F68 (1%) as stabilizer (F1-F5), 110.5 nm-182.8 nm with respect to nanoparticles prepared with EL100 containing Pluronic F68 (2%) as stabilizer (F6-F10), 135.9 nm-209.3 nm with respect to nanoparticles prepared with EL 100 containing PVA (1%) as stabilizer (F11-F15), 127.0 nm-190.1 nm with respect to nanoparticles prepared with EL100 containing PVA (2%) as stabilizer (F16-F20), 139.2 nm-229.3 nm with respect to nanoparticles prepared with ES100 containing Pluronic F68 (1%) as stabilizer (F21-F25), 131.0 nm-210.1 nm with respect to nanoparticles prepared with ES100 containing Pluronic F68 (2%) as stabilizer (F26-F30), 149 nm-231.0 nm with respect to nanoparticles prepared with ES100 containing PVA (1%) as stabilizer (F31-F35), 137.0 nm-229.5 nm with respect to nanoparticles prepared with ES100 containing PVA (2%) as stabilizer (F36-F40).

EFFECT OF PREPARATION VARIABLES ON PARTICLE SIZE:

1. ***Effect of drug –polymer ratio:***

The influence of different drug- polymer ratios of Rosuvastatin calcium loaded EL100 and ES100 nanoparticles on the particle size was investigated. The results were presented in Table XX a,b,c,d,e,f,g,h and Figure 24.

Formulations F1-F5 prepared using different ratios of polymer (EL 100) (1:10, 1:20, 1:30, 1:40 and 1:50) containing Pluronic F68 (1%) as stabilizer showed the particle size of 125.9 nm, 142.2 nm, 166.2 nm, 178.5 nm and 191.9 nm respectively.

Formulations F6-F10 prepared using different ratios of polymer (EL 100) (1:10, 1:20, 1:30, 1:40 and 1:50) containing Pluronic F68 (2%) as stabilizer showed the particle size of 110.5 nm, 133.9 nm, 152.2 nm, 168.3 nm and 182.8 nm respectively.

Formulations F11-F15 prepared using different ratios of polymer (EL 100) (1:10, 1:20, 1:30, 1:40 and 1:50) containing PVA (1%) as stabilizer showed the particle size of 135.9 nm, 151.0 nm, 174.1 nm, 187.0 nm and 209.3 nm respectively.

Formulations F16-F20 prepared using different ratios of polymer (EL 100) (1:10, 1:20, 1:30, 1:40 and 1:50) containing PVA (2%) as stabilizer showed the particle size of 127.0 nm, 145.0 nm, 168.0 nm, 174.0 nm and 190.1 nm respectively.

Formulations F21-F25 prepared using different ratios of polymer (ES 100) (1:10, 1:20, 1:30, 1:40 and 1:50) containing Pluronic F68 (1%) as stabilizer showed the particle size of 139.2 nm, 157.1 nm, 174.1 nm, 192.0 nm and 229.3 nm respectively.

Formulations F26-F30 prepared using different ratios of polymer (ES 100) (1:10, 1:20, 1:30, 1:40 and 1:50) containing Pluronic F68 (2%) as stabilizer showed the particle size of 131.0 nm, 145.0 nm, 164.0 nm, 179.0 nm and 210.1 nm respectively.

Formulations F31-F35 prepared using different ratios of polymer (ES 100) (1:10, 1:20, 1:30, 1:40 and 1:50) containing PVA (1%) as stabilizer showed the particle size of 149.0 nm, 161.0 nm, 178.0 nm, 199.0 nm and 231.0 nm respectively.

Formulations F36-F40 prepared using different ratios of polymer (ES 100) (1:10, 1:20, 1:30, 1:40 and 1:50) containing PVA (2%) as stabilizer showed the particle size of 137.0 nm, 159.0 nm, 165.0 nm, 192.1 nm and 229.5 nm respectively.

It could be seen that the particle size was affected by increasing the polymer concentration. The particle size of rosuvastatin calcium loaded polymeric nanoparticles showed a positive relationship with polymer (EL100/ ES100) concentration.

This is because, increasing EL100 and ES100 concentration led to increase in the viscosity of the organic phase. A more viscous organic phase provides a higher mass transfer resistance, the diffusion of polymer – solvent phase into the external aqueous phase is reduced and larger nanoparticles are formed (Xiangrong Song et al., 2008, Annick Ludwig et al., 2006). A decrease in viscosity of the organic phase increase the distribution effect of the polymer – solvent phase into the external phase leading to formation of smaller nanoparticles (Hatem Fessi et al., 2005).

2. ***Effect of stabilizers:***

The effect of stabilizers (Pluronic F68 and PVA) on the particle size of rosuvastatin calcium loaded EL 100 and ES 100 nanoparticles were investigated. The results were shown in Table XX a,b,c,d,e,f,g,h and Figure 24. Rosuvastatin calcium loaded polymeric

nanoparticles prepared with Pluronic F68 were smaller than those prepared with PVA. This result is in accord with the earlier studies of Gershon Golomb et al., 2009.

3. ***Effect of Pluronic F68 concentration in the aqueous phase:***

The influence of Pluronic F68 concentration (1%, 2%) in the aqueous phase of rosuvastatin calcium loaded EL 100/ES 100 nanoparticles on the particle size was investigated. The results were shown in Table XX a,b,c,d,e,f,g,h and Figure 24.

It could be seen that the particle size of rosuvastatin calcium loaded polymeric nanoparticles showed a negative relationship with Pluronic F68 concentration.

The mean diameter of polymeric nanoparticles decreased with the increase of Pluronic F68 concentration. At high concentration, more Pluronic F68 could be oriented at organic solvent/water interface to reduce efficiently the interfacial tension, which resulted in significant increase in the net shear stress at a constant energy density during emulsification and promoted the formation of smaller emulsion droplets (Xiangrong Song et al., 2008).

4. ***Effect of PVA concentration in the aqueous phase*** **:**

Table XX a,b,c,d,e,f,g,h and Figure 24 showed that the mean diameter decreased with increasing concentration of PVA. This is because, at high concentration, more PVA could be oriented at organic solvent/water interface to reduce efficiently the interfacial tension, which resulted in significant increase in the net shear stress at a constant energy density during emulsification and promoted the formation of smaller emulsion droplets (Xiangrong Song al., 2008).

Polydispersity index (PDI):

PDI is another factor that represents the dispersion homogenicity, the range for the PDI is from 0 to 1. Values close to 0 indicate the homogeneous dispersion, and those greater than 0.5 indicate high homogenicity. The PDI for all the formulations as shown in Table XX a,b,c,d,e,f,g,h and Figure 24 is smaller than 0.5, which indicates a relative homogenous dispersion (Mohammed Reza Avadi et al., 2010).

10.4.2 Zeta potential

The rosuvastatin calcium loaded polymeric nanoparticles were characterized to evaluate the effect of different polymers and stabilizers at different concentrations on surface charge of nanoparticles. The results were presented in Table XXI a,b.

Zeta potential of formulations F1-F20 prepared with EL 100 showed negative zeta potential (-25mV to -29mV).

Zeta potential of formulations F21-F40 prepared with ES 100 showed negative zeta potential (-26mV to -30mV).

All the formulations showed negative surface charge possibly due to the presence of terminal carboxylic acid groups in the polymers (EL 100 and ES 100) (Mora CE-Huertas et al.,2010).

Commonly, zeta potential is an index of the stability of the nanoparticles. Muller considered that a zeta potential of about -25mV allows an ideal stabilization of nanoparticles because the repulsive forces prevent aggregation upon ageing (Martine Leroueil-Le Verger.M et al., 1998).

However, zeta potential values between -25mV and -30mV allow predicting good colloidal stability due to high energy barrier between particles (Mora CE-Huertas et al., 2010).

10.4.3 Drug content

Table XXII a,b showed the percentage drug content of all formulations F1-F40. The drug content was found to be in the range of 90.75% to 96.86 %, indicating uniform distribution of drug.

10.4.4 Entrapment efficiency

The entrapment efficiencies of rosuvastatin calcium loaded nanosuspension were listed in the Table XXIII a,b,c,d,e,f,g,h and Figure 25 a,b,c,d.The entrapment efficiencies ranged between 42.1% - 78.59% with respect to nanoparticles prepared with EL 100 containing Pluronic F68 (1%) as stabilizer (F1-F5),38.35% - 74.25% with respect to nanoparticles prepared with EL 100 containing Pluronic F68 (2%) as stabilizer (F6-F10), 47.5% - 75.25% with respect to nanoparticles prepared with EL 100 containing PVA (1%) as stabilizer (F11-F15), 36.06% - 70.35% with respect to nanoparticles prepared with EL 100 containing PVA (2%) as stabilizer (F16-F20), 33% - 70.5% with respect to nanoparticles prepared with ES 100 containing PluronicF68 (1%) as stabilizer (F21-F25),28% - 62% with respect to nanoparticles prepared with ES 100 containing Pluronic F68 (2%) as stabilizer (F26-F30), 29.5% - 60.4% with respect to nanoparticles prepared with ES 100 containing PVA (1%) as stabilizer (F31-F35), 28% - 55.5% with respect to nanoparticles prepared with ES 100 containing PVA (2%) as stabilizer (F36-F40).

The fabrication parameters such as different drug-polymer ratios and different stabilizers at different concentrations were used to achieve the highest entrapment of rosuvastatin calcium.

EFFECT OF PREPARATION VARIABLES ON ENTRAPMENT EFFICIENCY:

1. *Effect of drug-polymer ratio*

The effect of different drug- polymer ratios of rosuvastatin calcium loaded EL100/ ES100 nanoparticles on the entrapment was investigated. The results were shown in Table XXIII a,b,c,d,e,f,g,h and Figure 25 a,b,c,d.

Formulations F1-F5 prepared using different ratios of polymer (EL 100) (1:10, 1:20, 1:30, 1:40 and 1:50) containing Pluronic F68 (1%) as stabilizer showed the entrapment efficiency of 42.1%, 54.42%, 69.95%, 75.81% and 78.59% respectively.

Formulations F6-F10 prepared using different ratios of polymer (EL 100) (1:10, 1:20, 1:30, 1:40 and 1:50) containing Pluronic F68 (2%) as stabilizer showed the entrapment efficiency of 38.35%, 50.84%, 63.97%, 69.25 and 74.25% respectively.

Formulations F11-F15 prepared using different ratios of polymer (EL 100) (1:10, 1:20, 1:30, 1:40 and 1:50) containing PVA (1%) as stabilizer showed the entrapment efficiency of 47.5%, 55.5%, 65.09%, 71.45% and 75.25% respectively.

Formulations F16-F20 prepared using different ratios of polymer (EL 100) (1:10, 1:20, 1:30, 1:40 and 1:50) containing PVA (2%) as stabilizer showed the entrapment efficiency of 36.06%, 47.65%, 54.9%, 66.6% and70.35% respectively.

Formulations F21-F25 prepared using different ratios of polymer (ES 100) (1:10, 1:20, 1:30, 1:40 and 1:50) containing Pluronic F68 (1%) as stabilizer showed the entrapment efficiency of 33.0%, 42.0%, 52.6%, 60.2% and 70.5% respectively.

Formulations F26-F30 prepared using different ratios of polymer (ES 100) (1:10, 1:20, 1:30, 1:40 and 1:50) containing Pluronic F68 (2%) as stabilizer showed the entrapment efficiency of 28.0%, 39.8%, 49.0%, 54.35% and 62.0% respectively.

Formulations F31-F35 prepared using different ratios of polymer (ES 100) (1:10, 1:20, 1:30, 1:40 and 1:50) containing PVA (1%) as stabilizer showed the entrapment efficiency of 29.5%, 34.6%,47.0%,54.9% and 60.4% respectively.

Formulations F36-F40 prepared using different ratios of polymer (ES 100) (1:10, 1:20, 1:30, 1:40 and 1:50) containing PVA (2%) as stabilizer showed the entrapment efficiency of 28.0%, 32.0%, 41.7%,47.0% and 55.5% respectively.

It could be seen that the entrapment was affected by increasing the polymer concentration.

The entrapment efficiency of Rosuvastatin calcium loaded polymeric nanoparticles showed a positive relationship with polymer (EL100/ES100) concentration.

This is because, increase in polymer concentration in organic phase increases drug entrapment due to increase in organic phase viscosity, which increases the diffusional resistance to drug molecules from organic phase to aqueous phase, thereby entrapping more drug in the polymeric nanoparticles(Swarnali Das et al., 2010 ; Xiangrong Songet al., 2008).

2. *Effect of stabilizers:*

The effect of stabilizers (Pluronic F68 and PVA) on the entrapment efficiency of rosuvastatin calcium loaded EL 100 and ES 100 nanoparticles were investigated. The results were shown in Table XXIII a,b,c,d,e,f,g,h and Figure 25 a,b,c,d.

Rosuvastatin calcium loaded polymeric nanoparticles prepared with Pluronic F68 showed better entrapment than those prepared with PVA. This result was in accord with the earlier studies of Gershon Golomb et al., 2009.

3. ***Effect of Pluronic F68 concentration in the aqueous phase:***

The influence of Pluronic F68 concentration (1%, 2%) in the aqueous phase on the entrapment efficiency of rosuvastatin calcium polymeric nanoparticles was investigated. The results were shown in Table XXIII a,b,c,d,e,f,g,h and Figure 25 a,b,c,d.

It could be seen that the entrapment efficiencies of rosuvastatin calcium loaded polymeric nanoparticles showed a negative relationship with Pluronic F68 concentration.

The entrapment efficiencies of polymeric nanoparticles decreased with the increase of Pluronic F68 concentration. This was probably caused by the decrease in particle size. Moreover , with the increase of Pluronic F68 concentration ,more molecules of drug may partition out rapidly in to the aqueous phase during emulsification procedure and less drug molecules remained in emulsion droplets to interact with polymers(EL 100/ES100), hence decreasing the entrapment efficiencies (Xiangrong Song al., 2008).

4. ***Effect of PVA concentration in the aqueous phase*** **:**

Table XXIII a,b,c,d,e,f,g,h and Figure 25 a,b,c,d showed that the entrapment efficiencies decreased with increasing concentration of PVA. This was probably caused by the decrease in particle size. Moreover, with the increase of PVA concentration ,more molecules of drug may partition out rapidly in to the aqueous phase during emulsification procedure and less drug molecules remained in emulsion droplets to interact with polymers(EL 100/ES100), hence decreasing the entrapment efficiencies (Xiangrong Song al., 2008).

10.4.5 In vitro release studies

The suitability of EL 100/ES 100 nanoparticles for the release of rosuvastatin calcium was studied in vitro at pH 1.2 and 6.8 to mimic the in vivo condition eg: gastric pH and intestinal pH, since the aim of this study was to administer the nanoparticles by the oral route.

Rosuvastatin calcium loaded polymeric nanoparticles containing two different polymers (EL 100 and ES 100) displayed a similar biphasic drug release pattern with a burst release within 2 hours followed by sustained release. The values are shown in Table XXIV a,b,c,d,e,f,g,h and Figure 26a,b,c,d,e,f,g and h.

Formulations F1-F5 prepared using different ratios of polymer (EL 100) (1:10,1:20,1:30,1:40 and 1:50) containing Pluronic F68 (1%) as stabilizer showed a burst release of 33.3%, 37.7%, 26.2%, 23.1% and 20.7% at 2 hours followed by sustained release of 81.0%, 75.2%, 70.6%, 65.6% and 60.5% at 12 hours.

Formulations F6-F10 prepared using different ratios of polymer (EL 100) (1:10,1:20,1:30,1:40 and 1:50) containing Pluronic F68 (2%) as stabilizer showed a burst release of 38.9%, 33.1%, 32.4%, 31.3% and 28.5% at 2 hours followed by sustained release of 88.1%, 78.2%, 76.4%, 70.9% and 65.9% at 12 hours.

Formulations F11-F15 prepared using different ratios of polymer (EL 100) (1:10,1:20,1:30,1:40 and 1:50) containing PVA (1%) as stabilizer showed a burst release of 40.0%, 36.4%, 32.8%, 30.0% and 26.0% at 2 hours followed by sustained release of 86.1%, 81.1%, 75.8%, 69.1% and 65.6% at 12 hours.

Formulations F16-F20 prepared using different ratios of polymer (EL 100) (1:10,1:20,1:30,1:40 and 1:50) containing PVA (2%) as stabilizer showed a burst release of 41.3%, 39.4%, 36.0%, 33.0% and 31.7% at 2 hours followed by sustained release of 92.5%, 85.8%, 79.0%, 72.6% and 68.2% at 12 hours.

Formulations F21-F25 prepared using different ratios of polymer (ES 100) (1:10,1:20,1:30,1:40 and 1:50) containing Pluronic F68 (1%) as stabilizer showed a burst release of 38.6%, 34.2%, 31.6%, 29.4% and 27.1% at 2 hours followed by sustained release of 88.5%, 78.4%, 72.6%, 67.6% and 62.9%at 12 hours.

Formulations F26-F30 prepared using different ratios of polymer (ES 100) (1:10,1:20,1:30,1:40 and 1:50) containing Pluronic F68 (2%) as stabilizer showed a burst release of 40.1%, 35.8%, 33.2%, 30.6% and 29.3% at 2 hours followed by sustained release of 91.2%, 82.2%, 77.3%, 71.0% and 67.2% at 12 hours.

Formulations F31-F35 prepared using different ratios of polymer (ES 100) (1:10,1:20,1:30,1:40 and 1:50) containing PVA (1%) as stabilizer showed a burst release of 40.0%, 35.9%, 33.3%, 31.7% and 28.6% at 2 hours followed by sustained release of 91.2%, 81.8%, 76.9%, 71.8% and 66.2% at 12 hours.

Formulations F35-F40 prepared using different ratios of polymer (ES 100) (1:10,1:20,1:30,1:40 and 1:50) containing PVA (2%) as stabilizer showed a burst release of 41.3%, 39.0%, 35.1%, 32.5% and 30.4% at 2 hours followed by sustained release of 93.7%, 87.9%, 80.1%, 74.7% and 70.2% at 12 hours.

The reason for burst release is possibly due to the unentrapped drug adsorbed on the surface of nanoparticles (Swarnali Das et al., 2010). Burst phase was, however, followed by hydration and swelling of the nano-matrix which eventually led to a controlled release

profile. Hydration brings about an increment in the diffusional path length of molecules and consequently the rate of their diffusion becomes lower (Wong CF et al., 1999). Therefore, gaining of controlled release profile and its maintenance could be assumed to be dependent upon the relative hydration rate of the polymer and integrity of hydrated matrix (Mishra B et al., 2010).

Therefore, superiority of one formulation over the other could be established on the basis of avoidance of burst release, achievement of a controlled release profile and its maintenance in a time dependent manner.

Influence of particle size and entrapment efficiency on rosuvastatin calcium release was studied.

1. Influence of particle size on in vitro release studies

Among all formulations, F6 (EL 100 1:10, Pluronic F68 2%) showing lower particle size (110.5 nm) provided a higher burst effect when compared to formulation F35 (ES 100 1:50, Pluronic 1%) showing larger particle size (231nm).

Formulation provided burst effect in the order of

F6 (burst release-38.9% at 2 hours) > F35 (burst release-28.6% at 2 hours)

This is because decrease in the mean particle size in nanoparticles leads to an increase in the release rate which could be explained on the basis of surface area relationship (Lemos-Senna E et al.,1998, Hans and Lowman et al., 2002).

2. Influence of entrapment efficiency on in vitro release studies

Among all formulations, F5 (EL 100 1:50, Pluronic F68 1%) showing higher entrapment (78.59%) provided a better controlled release when compared to formulation F26 (ES 100 1:10, Pluronic 2%) showing lower entrapment (28.0%).

Formulation provided better controlled release in the order of

F5 (release-60.5% at 12 hours) > F26 (release-91.2% at 12 hours)

This is because, increase in entrapment efficiency leads to a better controlled release which could be explained on the basis of free drug concentration on the surface of nanoparticles (Wong CF et al., 1999).

10.4.6 Kinetics of drug release

The results obtained from the *in vitro* release studies were attempted to fit into various mathematical models as follows:

a) Cumulative percentage drug release Vs time (zero order rate kinetics)
b) Log cumulative percentage drug remaining Vs time (first order rate kinetics)
c) Cumulative percentage drug release Vs square root of time (Higuchi classical diffusion model)
d) Cube root of percentage drug remaining Vs time (Hixon Crowell erosion equation).
e) Log cumulative percentage drug release Vs log time (Korsmeyer Peppas exponential equation)

Plots of zero order, first order, Higuchi matrix, Korsmeyer - Peppas and Hixon - Crowell were depicted in Figure 27-31. The regression coefficient (r^2) and n values were tabulated in Table XXV a,b,c,d,e,f,g and h.

Among the models tested, the drug release profile of all formulations F1-F40 were best fitted with first order with r^2 values ranging from 0.943-0.994 and Higuchi model with r^2 values ranging from 0.966-0.999.

Thus Higuchi model describes drug release was purely diffusion controlled.

Fickian and non Fickian anomalous behaviors have been used for determining the mechanism of drug release of polymeric nanoparticles. Korsmeyer Peppas model was used, which plots the log cumulative percentage of drug release up to 60% Vs log time and the release exponent n which indicated the release mechanism was determined.

Different values of n for cylindrical, spherical and slab of geometrices are available in the literature. For spheres, values of 0.5, $0.5 < n < 1.0$, 1.0 and higher than 1.0 are related to Fickian diffusion, anomalous, case II transport and super case II transport respectively(Korsmeyer et al., 1983; Paulo Costa et al., 2001).

According to the data presented in the tables, the values of exponent n were within 0.5 which indicated that the drug release mechanism followed pure Fickian diffusion. This report was in accord with the earlier studies of Annick Ludwig et al., 2006.

10.5 SELECTION OF BEST FORMULATION

From the above results of characterization, F5 and F25 were selected as the best formulation showing,

F5:

Particle size	:	191.9nm
Entrapment efficiency	:	78.59%
In vitro drug release	:	60.5% in 12 hours.
Release kinetics	:	Closest linearity to first order kinetics (R^2 - 0.994) and Higuchi model (R^2- 0.999).

F25:

Particle size	:	229.3nm
Entrapment efficiency	:	70.5%
In vitro drug release	:	62.9% in 12 hours.
Release kinetics	:	Closest linearity to first order kinetics (R^2 - 0.992) and Higuchi model (R^2- 0.997).

10.6 EVALUATION OF SELECTED BEST FORMULATION

10.6.1 Solubility studies

The solubility of pure drug solution was about 357.60µg/ml and the rosuvastatin calcium loaded polymeric nanoparticles had the solubility of about 743.94µg/ml (F5) and 624.60 µg/ml (F25). The results were shown in Figure 32 and Table XXVI.

It has been reported that a progressive reduction in particle size increases the solubility. According to Thomson – Freundlich equation, solubility of low soluble drug is increased by decrease in particle size. So, reduction of particle size of poorly soluble drug rosuvastatin calcium had an influent effect on drug solubility (Rezaei Mokkarram et al., 2010).

In conclusion solubility of rosuvastatin calcium polymeric nanoparticles compared to pure drug form was increased to about two-fold.

10.6.2 Ex vivo intestinal permeability studies

The results were shown in Table XXVII a,b,c,d,e and Figure 33 a,b,c,d.

In the duodenum region, the cumulative amount of drug permeated for pure drug solution was about 0.32 mg and the nanoparticle formulations had the permeability of about 1.00 mg (F5) and 0.91 mg (F25) at the end of 2 hrs.

Similarly in the jejunum region also, the cumulative amount of drug permeated for pure drug solution was 0.35 mg and for the nanoparticle formulations had the permeability of 1.00 mg (F5) and 0.89 (F25) at the end of 2 hrs.

The same type of results was also obtained from the ileum region of rat intestine. The pure drug solution had the cumulative amount of drug permeability of 0.327 mg and the formulations had the permeability of 0.99 mg (F5) and 0.87 mg (F25) at the end of 2 hrs.

The intestinal permeability was found to be increase in the order of

F5 (EL 100 1:50, Pluronic F 68 1%) > F25 (ES 100 1:50, Pluronic F 68 1%) > Pure drug solution.

From the results, it was observed that all the nanoparticle formulations showed better permeability than the pure drug solution.

Effect of particle size on intestinal permeation

Polymeric nanoparticles showed particle size dependent permeation through intestinal segments. Maximum permeation was observed for F5 (191.9nm size). Increase in particle size of polymeric nanoparticles F25 (229.3nm size) revealed decrease in permeation through intestinal segments (Kimiko Makino et al., 2008).

The Anova analysis of apparent permeability (Papp) values in the duodenum region indicated that the best formulations F5 and F25 exhibited significant increase in rosuvastatin calcium permeability compared to pure drug ($p<0.001$), similarly in the jejunum and ileum region also, the apparent permeability values showed significant increase when compared to pure drug ($p<0.001$). Hence, from these results it was inferred that the, nanoparticle formulations showed significant improvement in the rosuvastatin calcium permeability compared to pure drug.

10.6.3 Transmission electron microscopy (TEM)

TEM was used to investigate the morphology of nanoparticles. The TEM micrograph of the best formulation F5 is presented in Figure 34.

TEM shows nanoparticles with mean diameter of 101 nm, spherical shape and smooth surface. The size of the formulation F5 (Rosuvastatin calcium: EL 100 (1:50) containing Pluronic F68 (1%) as stabilizer) determined by Photon correlation spectroscopy (PCS) was

not consistent with that determined by TEM, which was probably caused by the different mechanisms of the two methods. PCS and TEM were based on scattering (Hydrodynamic radius) and diffraction technique in particle size measurement, respectively.

The diameters detected by PCS were 'hydrated diameters', which are usually larger than their genuine diameters. In the case of TEM sample preparation, the formulation F5 were stained with 2% w/v phosphotungstic acid and all the free water and even some hydrated water were stained. This implied that the size of formulation F5 derived from TEM might be considerably smaller than their real diameters (Xiangrong Song et al., 2008).

10.6.4 Stability studies

The formulation F5 (EL 100 1:50, Pluronic F 68 1%) and F25 (ES 100 1:50, Pluronic F 68 1%) divided into two sample sets and stored at refrigeration temperature (4 ± 2°C) and 25ºC± 60% RH at the accelerated stability chamber were examined for entrapment efficiency for a period of 3 months.

The physical appearance of the F5 and F25 nanosuspensions did not change when samples were stored at 4°C for 3 months. A loose, thin layer of sediment were observed when the F5 and F25 nanosuspensions were stored in accelerated stability chamber at 25ºC± 60% RH. However, the sediment disappeared with slight hand shaking.

The entrapment efficiencies of formulation F5 and F25 stored at 4ºC and 25ºC± 60% RH were shown in Table XXVIII a,b. These findings thus indicate that the nanoparticles were stable over storage at 4ºC and 25ºC± 60% RH for the period of 3 months.

Based on the observations, it was concluded that the developed rosuvastatin calcium polymeric nanoparticles are physically and chemically stable and retain their pharmaceutical properties at various temperature and humidity conditions over a period of 3 months. This result was in accord with the earlier studies of Bivash Mandal et al., 2010.

Table X Calibration of Rosuvastatin Calcium in Distilled Water

S. NO	CONCENTRATION(µg/ml)	ABSORBANCE ± SD*
1	2	0.071 ± 0.005
2	4	0.142 ± 0.007
3	6	0.213 ± 0.003
4	8	0.284 ± 0.006
5	10	0.355 ± 0.008
6	12	0.426 ± 0.003
7	14	0.497 ± 0.002
8	16	0.568 ± 0.006
9	18	0.639 ± 0.004
10	20	0.709 ± 0.007

γ = 0.9999992

n=3*

Table XI Calibration of Rosuvastatin Calcium in pH 1.2

S. NO	CONCENTRATION(µg/ml)	ABSORBANCE ± SD*
1	2	0.079 ± 0.003
2	4	0.137 ± 0.006
3	6	0.206 ± 0.004
4	8	0.279 ± 0.004
5	10	0.353 ± 0.004
6	12	0.425 ± 0.004
7	14	0.488 ± 0.001
8	16	0.563 ± 0.001
9	18	0.634 ± 0.002
10	20	0.717 ± 0.006

$\gamma = 0.999650$

n=3*

Table XII Calibration of Rosuvastatin Calcium in pH 6.8

S. NO	CONCENTRATION(µg/ml)	ABSORBANCE ± SD*
1	2	0.073 ± 0.003
2	4	0.136 ± 0.002
3	6	0.216 ± 0.001
4	8	0.288 ± 0.001
5	10	0.360 ± 0.005
6	12	0.424 ± 0.003
7	14	0.496 ± 0.007
8	16	0.568 ± 0.001
9	18	0.638 ± 0.005
10	20	0.716 ± 0.006

$\gamma = 0.999858$

n=3*

Table XIII Calibration of Rosuvastatin Calcium in PBS of pH 7.4

S. NO	CONCENTRATION(µg/ml)	ABSORBANCE ± SD*
1	2	0.073 ± 0.0008
2	4	0.143 ± 0.0009
3	6	0.227 ± 0.0009
4	8	0.297 ± 0.001
5	10	0.370 ± 0.0004
6	12	0.445 ± 0.0009
7	14	0.520 ± 0.0004
8	16	0.593 ± 0.0009
9	18	0.669 ± 0.0004
10	20	0.744 ± 0.001

$\gamma = 0.999946$

n=3*

Table XIV FT-IR Peaks of Drug, Polymers and Physical Mixture of Drug and Polymers

S.NO	DESCRIPTION	CHARACTERISTIC PEAKS (cm^{-1}) OBTAINED
1	**Rosuvastatin calcium**	358.77, 516.94, 570.95, 636.53, 717.54, 775.41, 812.06, 844.85, 900.79, 964.44, 1070.53, 1153.47, 1195.91, 1228.7, 1334.78, 1381.08, 1437.02, 1510.31, 1545.03, 1600.97, 2933.83, 2968.55, 3375.54
2	**Eudragit L100**	360.7, 520.8, 759.98, 788.91, 850.64, 935.51, 1020.38, 1166.97, 1178.55, 1265.35, 1386.86, 1452.45, 1475.59, 1707.06,1735.99, 2615.56, 2937.68, 2985.91, 3545.28
3	**Eudragit S100**	484.15, 520.8, 754.19, 842.92, 968.3, 1066.67, 1157.33, 1193.98,1269.2, 1390.72, 1448.59, 1483.31, 1645.33, 1726.35, 2953.12, 2997.48, 3525.99
4	**Physical mixture of Rosuvastatin calcium and Eudragit L100**	516.94, 570.95, 632.67, 775.41, 812.06, 844.85, 900.79, 964.44, 1153.47, 1228.7, 1332.86, 1383.01,1438.94, 1510.31, 1546.96, 1600.97,1697.41, 1741.78, 2931.9, 2968.55, 3394.83
5	**Physical mixture of Rosuvastatin calcium and Eudragit S100**	516.94, 570.95, 632.67, 775.41, 844.85, 900.79, 964.44, 1068.60,1153.47, 1193.98, 1234.48, 1440.87, 1508.38, 1546.96, 1602.9, 1730.21, 2956.97, 3427.62

Table XV Endothermic Peak of Drug, Polymers and Physical Mixture of Drug and Polymers

S.NO	DESCRIPTION	ENDOTHERMIC PEAKS OBTAINED
1	**Rosuvastatin calcium**	88.12°C
2	**Eudragit L100**	83.02°C
3	**Eudragit S100**	91.50°C
4	**Physical mixture of Rosuvastatin calcium and Eudragit L100**	85.36°C
5	**Physical mixture of Rosuvastatin calcium and Eudragit S100**	88.93°C

Table XVI Composition of Rosuvastatin Calcium Loaded Eudragit L 100 Nanoparticles Containing Pluronic F68 as Stabilizer

FORMULATION CODE	AMOUNT OF DRUG (mg)	AMOUNT OF POLYMER	DRUG:POLYMER	STABILIZER CONCENTRATION
		EUDRAGIT L 100(mg)		PLURONIC F68 (%)
F1	20	200	1:10	1
F2	20	400	1:20	1
F3	20	600	1:30	1
F4	20	800	1:40	1
F5	20	1000	1:50	1
F6	20	200	1:10	2
F7	20	400	1:20	2
F8	20	600	1:30	2
F9	20	800	1:40	2
F10	20	1000	1:50	2

Table XVII Composition of Rosuvastatin Calcium Loaded Eudragit L 100 Nanoparticles Containing PVA as Stabilizer

FORMULATION CODE	AMOUNT OF DRUG (mg)	AMOUNT OF POLYMER	DRUG:POLYMER	STABILIZER CONCENTRATION
		EUDRAGIT L 100(mg)		PVA (%)
F11	20	200	1:10	1
F12	20	400	1:20	1
F13	20	600	1:30	1
F14	20	800	1:40	1
F15	20	1000	1:50	1
F16	20	200	1:10	2
F17	20	400	1:20	2
F18	20	600	1:30	2
F19	20	800	1:40	2
F20	20	1000	1:50	2

Table XVIII Composition of Rosuvastatin Calcium Loaded Eudragit S 100 Nanoparticles Containing Pluronic F68 as Stabilizer

FORMULATION CODE	AMOUNT OF DRUG (mg)	AMOUNT OF POLYMER	DRUG:POLYMER	STABILIZER CONCENTRATION
		EUDRAGIT S 100(mg)		PLURONIC F68 (%)
F21	20	200	1:10	1
F22	20	400	1:20	1
F23	20	600	1:30	1
F24	20	800	1:40	1
F25	20	1000	1:50	1
F26	20	200	1:10	2
F27	20	400	1:20	2
F28	20	600	1:30	2
F29	20	800	1:40	2
F30	20	1000	1:50	2

Table XIX Composition of Rosuvastatin Calcium Loaded Eudragit S 100 Nanoparticles Containing PVA as Stabilizer

FORMULATION CODE	AMOUNT OF DRUG (mg)	AMOUNT OF POLYMER	DRUG:POLYMER	STABILIZER CONCENTRATION
		EUDRAGIT S 100(mg)		PVA (%)
F31	20	200	1:10	1
F32	20	400	1:20	1
F33	20	600	1:30	1
F34	20	800	1:40	1
F35	20	1000	1:50	1
F36	20	200	1:10	2
F37	20	400	1:20	2
F38	20	600	1:30	2
F39	20	800	1:40	2
F40	20	1000	1:50	2

Table XX a Particle Size of Rosuvastatin Calcium Loaded EL 100 (Different Ratios) Nanoparticles Containing Pluronic F68 (1%) as Stabilizer

FORMULATION CODE	DRUG: POLYMER	MEAN DIAMETER(nm)	PDI
F1	1:10	125.9	0.095
F2	1:20	142.2	0.092
F3	1:30	166.2	0.162
F4	1:40	178.5	0.185
F5	1:50	191.9	0.109

Table XX b Particle Size of Rosuvastatin Calcium Loaded EL 100 (Different Ratios) Nanoparticles Containing Pluronic F68 (2 %) as Stabilizer

FORMULATION CODE	DRUG: POLYMER	MEAN DIAMETER(nm)	PDI
F6	1:10	110.5	0.095
F7	1:20	133.9	0.159
F8	1:30	152.2	0.132
F9	1:40	168.3	0.123
F10	1:50	182.8	0.192

Table XX c Particle Size of Rosuvastatin Calcium Loaded EL 100 (Different Ratios) Nanoparticles Containing PVA (1%) as Stabilizer

FORMULATION CODE	DRUG: POLYMER	MEAN DIAMETER(nm)	PDI
F11	1:10	135.9	0.159
F12	1:20	151.0	0.161
F13	1:30	174.1	0.173
F14	1:40	187.0	0.175
F15	1:50	209.3	0.192

Table XX d Particle Size of Rosuvastatin Calcium Loaded EL 100 (Different Ratios) Nanoparticles Containing PVA (2%) as Stabilizer

FORMULATION CODE	DRUG: POLYMER	MEAN DIAMETER(nm)	PDI
F16	1:10	127.0	0.167
F17	1:20	145.0	0.159
F18	1:30	168.0	0.123
F19	1:40	174.0	0.173
F20	1:50	190.1	0.175

Table XX e Particle Size of Rosuvastatin Calcium Loaded ES 100 (Different Ratios) Nanoparticles Containing Pluronic F68 (1%) as Stabilizer

FORMULATION CODE	DRUG: POLYMER	MEAN DIAMETER(nm)	PDI
F21	1:10	139.2	0.092
F22	1:20	157.1	0.174
F23	1:30	174.1	0.164
F24	1:40	192.0	0.175
F25	1:50	229.3	0.175

Table XX f Particle Size of Rosuvastatin Calcium Loaded ES 100 (Different Ratios) Nanoparticles Containing Pluronic F68 (2%) as Stabilizer

FORMULATION CODE	DRUG: POLYMER	MEAN DIAMETER(nm)	PDI
F26	1:10	131.0	0.159
F27	1:20	145.0	0.176
F28	1:30	164.0	0.182
F29	1:40	179.0	0.169
F30	1:50	210.1	0.109

Table XX g Particle Size of Rosuvastatin Calcium Loaded ES 100 (Different Ratios) Nanoparticles Containing PVA (1%) as Stabilizer

FORMULATION CODE	DRUG: POLYMER	MEAN DIAMETER(nm)	PDI
F31	1:10	149.0	0.161
F32	1:20	161.0	0.141
F33	1:30	178.0	0.094
F34	1:40	199.0	0.109
F35	1:50	231.0	0.175

Table XX h Particle Size of Rosuvastatin Calcium Loaded ES 100 (Different Ratios) Nanoparticles Containing PVA (2%) as Stabilizer

FORMULATION CODE	DRUG: POLYMER	MEAN DIAMETER(nm)	PDI
F36	1:10	137.0	0.163
F37	1:20	159.0	0.093
F38	1:30	165.0	0.135
F39	1:40	192.1	0.175
F40	1:50	229.5	0.175

Table XXI a Zeta Potential Values of Rosuvastatin Calcium Loaded EL 100 Nanoparticles

S.NO	FORMULATION CODE	ZETA POTENTIAL (mV)
1	F 1	-25.3
2	F 2	-26.4
3	F 3	-27.6
4	F 4	-25.9
5	F 5	-28.4
6	F 6	-26.5
7	F 7	-28.5
8	F 8	-25.8
9	F 9	-25.4
10	F 10	-26.9
11	F 11	-28.6
12	F 12	-28.1
13	F 13	-25.2
14	F 14	-26.7
15	F 15	-27.5
16	F 16	-28.3
17	F 17	-26.8
18	F 18	-27.3
19	F 19	-28.7
20	F 20	-25.8

Table XXI b Zeta Potential Values of Rosuvastatin Calcium Loaded ES 100 Nanoparticles

S.NO	FORMULATION CODE	ZETA POTENTIAL (mV)
1	F 21	-26.2
2	F 22	-26.1
3	F 23	-29.4
4	F 24	-28.9
5	F 25	-27.5
6	F 26	-26.4
7	F 27	-29.8
8	F 28	-26.1
9	F 29	-29.9
10	F 30	-27.4
11	F 31	-26.7
12	F 32	-26.1
13	F 33	-27.8
14	F 34	-28.9
15	F 35	-29.4
16	F 36	-29.5
17	F 37	-27.2
18	F 38	-28.5
19	F 39	-27.2
20	F 40	-26.2

Table XXII a Drug Content of Rosuvastatin Calcium Loaded

EL100 Nanoparticles

S.NO	FORMULATION CODE	DRUG CONTENT (%) ±SD*
1	F 1	91.45 % ±0.98
2	F 2	96.78 % ±0.66
3	F 3	92.48 % ±0.56
4	F 4	95.56 % ±0.45
5	F 5	92.34 % ±0.33
6	F 6	93.78 % ±0.24
7	F 7	91.58 % ±0.37
8	F 8	96.86 % ±0.67
9	F 9	95.87 % ±0.34
10	F 10	94.10 % ±0.42
11	F 11	95.50 % ±0.56
12	F 12	91.80 % ±0.56
13	F 13	93.90 % ±0.87
14	F 14	90.75 % ±0.45
15	F 15	95.90 % ±0.88
16	F 16	91.50 % ±0.72
17	F 17	93.70 % ±0.31
18	F 18	94.90 % ±0.56
19	F 19	92.79 % ±0.67
20	F 20	91.92 % ±0.34

n=3*

Table XXII b Drug Content of Rosuvastatin Calcium Loaded

ES 100 Nanoparticles

S.NO	FORMULATION CODE	DRUG CONTENT (%) ±SD*
1	F 21	94.55 % ±0.67
2	F 22	93.08 % ±0.34
3	F 23	95.48 % ±0.78
4	F 24	92.66 % ±0.98
5	F 25	96.34 % ±0.56
6	F 26	92.18 % ±0.45
7	F 27	91.46 % ±0.67
8	F 28	94.21 % ±0.56
9	F 29	93.37 % ±0.23
10	F 30	94.60 % ±0.33
11	F 31	94.70 % ±0.43
12	F 32	92.45 % ±0.45
13	F 33	92.56 % ±1.09
14	F 34	94.25 % ±0.34
15	F 35	93.40 % ±0.23
16	F 36	95.56 % ±0.94
17	F 37	95.76 % ±0.98
18	F 38	95.07 % ±0.66
19	F 39	95.71 % ±0.45
20	F 40	94.23 % ±0.78

n=3*

Table XXIII a Entrapment Efficiencies of Rosuvastatin Calcium Loaded EL 100 (Different Ratios) Nanoparticles Containing Pluronic F68 (1%) as Stabilizer

FORMULATION CODE	DRUG: POLYMER	ENTRAPMENT EFFICIENCY (%) ± S.D*
F1	1:10	42.1 ±0.78
F2	1:20	54.4 ±0.45
F3	1:30	69.9 ±0.67
F4	1:40	75.8 ±0.98
F5	1:50	78.5 ±0.12

Table XXIII b Entrapment Efficiencies of Rosuvastatin Calcium Loaded EL 100 (Different Ratios) Nanoparticles Containing Pluronic F68 (2 %) as Stabilizer

FORMULATION CODE	DRUG: POLYMER	ENTRAPMENT EFFICIENCY (%) ± S.D*
F6	1:10	38.3 ±0.45
F7	1:20	50.8 ±0.78
F8	1:30	63.9 ±0.98
F9	1:40	69.2 ±0.23
F10	1:50	74.2 ±0.56

Table XXIII c Entrapment Efficiencies of Rosuvastatin Calcium Loaded EL 100 (Different Ratios) Nanoparticles Containing PVA (1%) as Stabilizer

FORMULATION CODE	DRUG: POLYMER	ENTRAPMENT EFFICIENCY (%) ± S.D*
F11	1:10	47.5 ±0.66
F12	1:20	55.5 ±0.44
F13	1:30	65.0 ±0.34
F14	1:40	71.4 ±0.76
F15	1:50	75.2 ±0.45

Table XXIII d Entrapment Efficiencies of Rosuvastatin Calcium Loaded EL 100 (Different Ratios) Nanoparticles Containing PVA (2%) as Stabilizer

FORMULATION CODE	DRUG: POLYMER	ENTRAPMENT EFFICIENCY (%) ± S.D*
F16	1:10	36.0 ±0.45
F17	1:20	47.6 ±0.32
F18	1:30	54.9 ±0.65
F19	1:40	66.6 ±0.13
F20	1:50	70.3 ±0.98

Table XXIII e Entrapment Efficiencies of Rosuvastatin Calcium Loaded ES 100 (Different Ratios) Nanoparticles Containing Pluronic F68 (1%) as Stabilizer

FORMULATION CODE	DRUG: POLYMER	ENTRAPMENT EFFICIENCY (%) ± S.D*
F21	1:10	33.0 ±0.45
F22	1:20	42.0 ±0.43
F23	1:30	52.6 ±0.66
F24	1:40	60.2 ±0.32
F25	1:50	70.5 ±0.18

Table XXIII f Entrapment Efficiencies of Rosuvastatin Calcium Loaded ES 100 (Different Ratios) Nanoparticles Containing Pluronic F68 (2%) as Stabilizer

FORMULATION CODE	DRUG: POLYMER	ENTRAPMENT EFFICIENCY (%) ± S.D*
F26	1:10	28.0 ±0.99
F27	1:20	39.8 ±0.45
F28	1:30	49.0 ±0.23
F29	1:40	54.3 ±0.43
F30	1:50	62.0 ±0.15

Table XXIII g Entrapment Efficiencies of Rosuvastatin Calcium Loaded ES 100 (Different Ratios) Nanoparticles Containing PVA (1%) as Stabilizer

FORMULATION CODE	DRUG: POLYMER	ENTRAPMENT EFFICIENCY (%) ± S.D*
F31	1:10	29.5 ±0.45
F32	1:20	34.6 ±0.66
F33	1:30	47.0 ±0.12
F34	1:40	54.9 ±0.45
F35	1:50	60.4 ±0.76

Table XXIII h Entrapment Efficiencies Of Rosuvastatin Calcium Loaded ES 100 (Different Ratios) Nanoparticles Containing PVA (2%) as Stabilizer

FORMULATION CODE	DRUG: POLYMER	ENTRAPMENT EFFICIENCY (%) ± S.D*
F36	1:10	28.0 ±0.22
F37	1:20	32.0 ±1.02
F38	1:30	41.7 ±0.98
F39	1:40	47.0 ±0.45
F40	1:50	55.5 ±0.12

Table XXIV a Comparison of *Invitro* Release of Rosuvastatin Calcium Loaded EL 100 (Different Ratios) Nanoparticles Containing Pluronic F68 (1%) as Stabilizer

pH	TIME(HRS)	CUMULATIVE % DRUG RELEASE ± S.D*				
		F1 EL 100(1:10)	F2 EL 100(1:20)	F3 EL 100(1:30)	F4 EL 100(1:40)	F5 EL 100(1:50)
1.2	0.25	9.2 ± 0.72	7.1 ± 0.80	6.2 ± 0.70	5.1 ± 0.41	3.7 ± 0.41
	0.50	11.5 ± 0.23	10.3 ± 0.31	8.0 ± 0.70	7.3 ± 0.76	6.2 ± 0.43
	0.75	15.5 ± 0.90	13.0 ± 0.50	10.7 ± 0.75	9.6 ± 0.91	10.1 ± 0.70
	1.00	20.7 ± 0.34	20.0 ± 0.72	15.3 ± 0.34	13.8 ± 0.49	13.3 ±0.28
	1.50	27.5 ± 0.87	24.7 ± 0.38	21.5 ± 0.70	18.5 ± 0.47	16.9 ± 0.60
	2.00	33.3 ± 0.20	29.5 ± 0.89	26.2 ± 0.15	23.1 ± 0.29	20.7 ± 0.35
6.8	2.50	41.9 ± 0.36	36.6 ± 0.96	32.8 ± 0.88	28.7 ± 0.80	25.7 ± 0.25
	3.00	43.7 ± 0.90	37.7 ± 0.68	33.8 ± 0.27	29.7 ± 0.52	26.5 ± 0.60
	3.50	45.0 ± 0.86	39.2 ± 0.15	35.7 ± 0.95	31.5 ± 0.87	27.5 ± 0.89
	4.00	47.6 ± 0.23	41.2 ± 0.15	36.9 ± 0.91	33.1 ± 0.83	29.2 ± 0.51
	4.50	48.7 ± 0.89	42.4 ± 0.40	38.4 ± 0.83	34.2 ± 0.83	30.1 ± 0.52
	5.00	50.4 ± 0.45	44.6 ± 0.57	39.8 ± 0.83	35.3 ± 0.69	31.1 ± 0.49
	5.50	52.1 ± 0.54	46.2 ± 0.31	41.8 ± 0.22	37.1 ± 0.58	32.1 ± 0.51
	6.00	54.1 ± 0.33	48.1 ± 0.41	44.5 ± 0.53	39.8 ± 0.72	33.9 ± 0.28
	6.50	55.7 ± 0.67	49.9 ± 0.53	47.0 ± 0.59	41.6 ± 0.70	35.5 ± 0.47
	7.00	57.6 ± 0.45	51.9 ± 0.34	49.4 ± 0.90	44.0 ± 0.40	37.4 ± 0.37
	7.50	60.1 ± 0.87	54.1 ± 0.95	51.4 ± 0.82	46.6 ± 0.13	39.1 ± 0.75
	8.00	61.7 ± 0.39	56.0 ± 0.63	53.5 ± 0.85	48.6 ± 0.26	41.8 ± 0.24
	8.50	64.2 ± 0.56	58.8 ± 0.95	55.8 ± 0.76	51.0 ± 0.53	44.0 ± 0.81
	9.00	66.9 ± 0.67	60.9 ± 0.55	57.6 ± 0.82	53.0 ± 0.53	47.5 ± 0.36
	9.50	68.9 ± 0.93	62.9 ± 0.42	59.5 ± 0.73	55.1 ± 0.32	49.8 ± 0.92
	10.00	71.0 ± 0.78	65.4 ± 0.33	61.6 ± 0.56	57.4 ± 0.20	51.7 ± 0.81
	10.50	73.0 ± 0.45	67.7 ± 0.10	63.7 ± 0.82	59.3 ± 0.30	54.0 ± 0.91
	11.00	75.5 ± 0.63	70.0 ± 0.43	66.1 ± 0.67	61.4 ±0.57	55.9 ± 0.70
	11.50	77.8 ± 0.39	72.6 ± 0.65	68.2 ± 0.87	63.1 ± 0.59	57.9 ± 0.75
	12.00	81.0 ± 0.45	75.2 ± 0.72	70.6 ± 0.79	65.6 ± 0.51	60.5 ± 0.60

n=3*

Table XXIV b Comparison of *Invitro* Release of Rosuvastatin Calcium Loaded EL 100 (Different Ratios) Nanoparticles Containing Pluronic F68 (2%) as Stabilizer

pH	TIME(HRS)	CUMULATIVE % DRUG RELEASE ± S.D*				
		F6 EL 100(1:10)	F7 EL 100(1:20)	F8 EL 100(1:30)	F9 EL 100(1:40)	F10 EL 100(1:50)
1.2	0.25	9.1 ± 0.70	7.5 ± 0.50	7.1 ± 0.10	6.7 ± 0.41	5.3 ± 0.28
	0.50	16.3 ± 0.60	13.2 ± 0.47	12.7 ± 0.83	12.7 ± 0.52	9.7 ± 0.31
	0.75	19.7 ± 0.56	16.0 ± 0.49	15.8 ± 0.75	15.5 ± 0.60	14.1 ± 0.43
	1.00	24.9 ± 0.25	21.9 ± 0.75	88.0 ± 0.15	20.8 ± 0.37	17.5 ± 0.42
	1.50	32.7 ± 0.61	28.5 ± 0.80	28.2 ± 0.83	27.6 ± 0.20	24.3 ± 0.13
	2.00	38.9 ± 0.86	33.1 ± 0.85	32.4 ± 0.96	31.3 ± 0.32	28.5 ± 0.41
6.8	2.50	48.9 ± 0.56	41.5 ± 0.26	40.5 ± 0.15	38.8 ± 0.28	35.6 ± 0.40
	3.00	49.9 ± 0.60	42.5 ± 0.17	41.3 ± 0.27	39.6 ± 0.26	36.2 ± 0.40
	3.50	50.9 ± 0.90	43.5 ± 0.55	42.2 ± 0.22	40.8 ± 0.05	37.1 ± 0.45
	4.00	52.3 ± 0.80	44.4 ± 0.73	43.6 ± 0.84	41.7 ± 0.15	37.7 ± 0.40
	4.50	54.2 ± 0.70	45.8 ± 0.64	44.7 ± 0.18	42.8 ± 0.17	38.9 ± 0.56
	5.00	55.9 ± 0.74	47.1 ± 0.90	46.0 ± 0.20	44.4 ± 0.15	40.4 ± 0.41
	5.50	57.7 ± 0.87	49.3 ± 0.70	47.6 ± 0.73	46.1 ± 0.11	41.6 ± 0.41
	6.00	60.2 ± 0.17	51.0 ± 0.62	49.1 ± 0.76	47.5 ± 0.20	42.8 ± 0.41
	6.50	62.5 ± 0.25	52.8 ± 0.90	50.9 ± 0.22	49.1 ± 0.25	44.3 ± 0.41
	7.00	64.5 ± 0.32	55.0 ± 0.29	52.9 ± 0.57	50.7 ± 0.20	46.1 ± 0.49
	7.50	66.4 ± 0.95	57.1 ± 0.42	54.6 ± 0.66	52.5 ± 0.55	48.1 ± 0.42
	8.00	68.4 ± 0.24	59.1 ± 0.28	57.1 ± 0.32	53.9 ± 0.40	49.7 ± 0.51
	8.50	71.2 ± 0.44	61.2 ± 0.26	59.4 ± 0.26	56.1 ± 0.52	51.2 ± 0.52
	9.00	73.0 ± 0.27	63.6 ± 0.61	62.2 ± 0.44	58.0 ± 0.63	53.3 ± 0.53
	9.50	75.5 ± 0.80	65.7 ± 0.28	64.0 ± 0.28	59.8 ± 0.45	54.9 ± 0.38
	10.00	77.4 ± 0.15	67.5 ± 0.31	66.1 ± 0.33	62.1 ± 0.40	56.6 ± 0.77
	10.50	80.1 ± 0.52	69.9 ± 0.16	68.2 ± 0.75	64.3 ± 0.35	58.7 ± 0.47
	11.00	82.4 ± 0.95	72.5 ± 0.98	70.7 ± 0.57	66.2 ± 0.25	60.7 ± 0.47
	11.50	85.4 ± 0.44	75.2 ± 0.15	73.5 ± 0.86	68.4 ± 0.61	63.2 ± 0.64
	12.00	88.1 ± 0.12	78.2 ± 0.12	76.4 ± 0.72	70.9 ± 0.61	65.9 ± 0.70

n=3*

Table XXIV c Comparison of *Invitro* Release of Rosuvastatin Calcium Loaded EL 100 (Different Ratios) Nanoparticles Containing PVA (1%) as Stabilizer

pH	TIME(HRS)	CUMULATIVE % DRUG RELEASE ± S.D*				
		F11 EL 100(1:10)	F12 EL 100(1:20)	F13 EL 100(1:30)	F14 EL 100(1:40)	F15 EL 100(1:50)
1.2	0.25	10.8 ± 0.58	8.9 ± 0.42	7.6 ± 0.28	6.7 ± 0.28	5.9 ± 0.28
	0.50	17.5 ± 0.61	15.8 ± 0.41	14.0 ± 0.43	12.5 ± 0.41	12.3 ± 0.43
	0.75	23.9 ± 0.76	22.9 ± 0.30	18.7 ± 0.56	17.1 ± 0.42	15.8 ± 0.30
	1.00	30.2 ± 0.24	26.4 ± 0.32	24.1 ± 0.27	20.8 ± 0.28	18.6 ± 0.44
	1.50	33.3 ± 0.67	30.6 ±0.69	29.4 ± 0.46	25.2 ± 0.29	21.8 ± 0.45
	2.00	40.0 ± 0.48	36.4 ± 0.73	32.8 ± 0.47	30.0 ± 0.24	26.0 ± 0.37
6.8	2.50	51.8 ± 0.14	46.2 ± 0.21	41.3 ± 0.52	37.9 ± 0.13	33.2 ± 0.13
	3.00	53.4 ± 0.12	47.3 ± 0.09	42.5 ± 0.82	38.6 ± 0.06	34.4 ± 0.12
	3.50	54.6 ± 0.10	48.6 ± 0.98	43.7 ± 0.96	39.8 ± 0.08	35.3 ± 0.14
	4.00	55.6 ± 0.25	49.7 ± 0.72	45.0 ± 0.98	40.9 ± 0.35	36.4 ± 0.15
	4.50	57.4 ± 0.23	50.9 ± 0.54	46.3 ± 0.87	41.9 ± 0.44	37.8 ± 0.17
	5.00	58.6 ±0.22	52.5 ± 0.39	47.4 ± 0.89	43.0 ± 0.30	39.3 ± 0.12
	5.50	60.1 ± 0.88	53.8 ± 0.37	48.9 ± 0.75	44.2 ± 0.31	40.6 ± 0.13
	6.00	61.3 ± 0.12	55.1 ± 0.79	51.1 ± 0.76	45.3 ± 0.16	42.0 ± 0.22
	6.50	62.8 ± 0.16	57.0 ± 0.52	53.0 ± 0.77	47.0 ± 0.23	43.5 ± 0.11
	7.00	64.5 ± 0.15	58.6 ± 0.83	54.6 ± 0.77	48.6 ± 0.34	45.0 ±0.62
	7.50	66.7 ± 0.68	60.5 ± 0.68	56.5 ± 0.92	50.2 ± 0.16	46.8 ± 0.32
	8.00	68.5 ± 0.12	62.0 ± 0.76	58.5 ± 1.07	51.9 ± 0.17	48.6 ± 0.17
	8.50	70.3 ± 0.95	63.5 ± 0.84	60.4 ± 1.09	53.7 ± 0.32	50.4 ± 0.18
	9.00	71.9 ± 0.76	65.0 ± 0.94	62.4 ± 0.84	55.5 ± 0.41	52.5 ± 0.34
	9.50	73.7 ± 0.89	67.1 ± 0.34	64.4 ± 0.85	57.4 ± 0.43	54.2 ± 0.36
	10.00	75.3 ± 0.44	69.8 ± 0.14	66.4 ± 0.75	59.3 ± 0.44	56.4 ± 0.37
	10.50	77.6 ± 0.40	72.6 ± 0.47	69.0 ± 0.66	61.4 ± 0.53	58.6 ± 0.22
	11.00	80.2 ± 0.43	75.4 ± 0.25	71.4 ± 0.86	63.5 ± 0.55	60.9 ± 0.46
	11.50	83.1 ± 0.60	78.1 ± 0.36	73.4 ± 0.60	66.3 ± 0.76	63.1 ± 0.49
	12.00	86.1 ± 0.60	81.1 ± 0.31	75.8 ± 0.68	69.1 ± 0.51	65.6 ± 0.49

n=3*

Table XXIV d Comparison of *Invitro* Release of Rosuvastatin Calcium Loaded EL 100 (Different Ratios) Nanoparticles Containing PVA (2%) as Stabilizer.

pH	TIME(HRS)	CUMULATIVE % DRUG RELEASE ± S.D*				
		F16 EL 100(1:10)	F17 EL 100(1:20)	F18 EL 100(1:30)	F19 EL 100(1:40)	F20 EL 100(1:50)
1.2	0.25	10.9 ± 0.28	9.6 ± 0.16	8.5 ± 0.16	7.3 ± 0.28	6.5 ± 0.16
	0.50	17.7 ± 0.29	16.8 ± 0.28	14.7 ± 0.27	12.8 ± 0.44	11.8 ± 0.28
	0.75	24.6 ± 0.69	23.4 ± 0.14	21.3 ± 0.42	20.0 ± 0.44	18.5 ± 0.44
	1.00	29.9 ± 0.45	29.7 ± 0.41	27.0 ± 0.43	25.2 ± 0.29	24.2 ± 0.32
	1.50	33.4 ± 0.61	33.0 ± 0.28	31.1 ± 0.18	28.9 ± 0.31	27.95 ± 0.33
	2.00	41.3 ± 0.47	39.4 ± 0.44	36.0 ± 0.46	33.0 ± 0.24	31.7 ± 0.35
6.8	2.50	52.7 ± 0.48	49.9 ± 0.45	45.9 ±0.48	42.0 ± 0.16	40.2 ± 0.58
	3.00	54.1 ± 0.43	50.9 ± 0.59	46.7 ± 0.63	43.0 ± 0.17	41.2 ± 0.58
	3.50	55.5 ± 0.53	51.8 ± 0.61	47.6 ± 0.63	44.0 ± 0.49	42.0 ± 0.59
	4.00	56.8 ± 0.38	53.1 ± 0.68	48.7 ± 0.68	44.9 ± 0.36	43.1 ± 0.60
	4.50	58.7 ± 0.43	54.4 ± 0.63	50.0 ± 0.65	46.2 ± 0.22	44.0 ± 0.65
	5.00	60.0 ± 0.43	56.4 ± 0.64	51.4 ± 0.65	47.4 ± 0.23	45.1 ± 0.66
	5.50	61.9 ± 0.55	57.7 ± 0.77	52.8 ± 0.81	48.6 ± 0.24	46.3 ± 0.67
	6.00	63.4 ± 0.37	59.3 ± 0.78	54.0 ± 0.83	49.9 ± 0.25	47.5 ± 0.68
	6.50	65.9 ± 0.44	61.1 ± 0.67	55.9 ± 0.84	51.2 ± 0.26	48.8 ± 0.69
	7.00	68.3 ± 0.44	63.0 ± 0.57	57.3 ± 0.85	52.8 ± 0.27	50.3 ± 0.65
	7.50	69.8 ± 0.44	64.7 ± 0.73	58.9 ± 0.72	54.2 ± 0.29	52.0 ± 0.71
	8.00	71.9 ± 0.58	66.6 ± 0.50	60.7 ± 0.72	55.7 ± 0.22	53.4 ± 0.72
	8.50	73.9 ± 0.77	68.9 ± 0.67	62.3 ± 0.88	57.5 ± 0.42	55.2 ± 0.73
	9.00	76.4 ± 0.61	71.3 ± 0.52	64.8 ± 0.89	59.5 ± 0.19	56.7 ± 0.81
	9.50	79.0 ± 0.78	73.4 ± 0.59	66.8 ± 0.61	61.7 ± 0.64	58.3 ± 0.82
	10.00	81.5 ± 0.64	75.8 ± 0.59	68.8 ± 0.61	63.7 ± 0.45	60.0 ± 0.69
	10.50	84.5 ± 0.74	78.1 ± 0.69	71.1 ± 0.49	65.5 ± 0.12	61.7 ± 0.72
	11.00	86.9 ± 0.53	80.5 ± 0.54	73.6 ± 0.51	67.7 ± 0.28	63.8 ± 0.72
	11.50	89.5 ± 0.31	82.8 ± 0.55	76.3 ± 0.59	70.3 ± 0.42	65.9 ± 0.71
	12.00	92.5 ± 0.84	85.8 ± 0.60	79.0 ± 0.66	72.6 ± 0.22	68.2 ± 0.86

n=3*

Table XXIV e Comparison of *Invitro* Release of Rosuvastatin Calcium Loaded ES 100 (Different Ratios) Nanoparticles Containing Pluronic F68 (1%) as Stabilizer.

pH	TIME(HRS)	CUMULATIVE % DRUG RELEASE ± S.D*				
		F21 ES 100(1:10)	F22 ES 100(1:20)	F23 ES 100(1:30)	F24 ES 100(1:40)	F25 ES 100(1:50)
1.2	0.25	9.8 ± 0.28	9.3 ± 0.28	7.9 ± 0.28	7.0 ± 0.28	5.9 ± 0.28
	0.50	17.0 ± 0.15	14.9 ± 0.32	13.1 ± 0.16	12.5 ± 0.16	10.7 ± 0.29
	0.75	21.2 ± 0.27	18.4 ± 0.32	16.9 ± 0.17	15.9 ± 0.14	14.9 ± 0.18
	1.00	26.2 ± 0.28	24.1 ± 0.17	22.3 ± 0.30	21.6 ± 0.27	18.7 ± 0.19
	1.50	32.0 ± 0.16	28.9 ± 0.30	27.3 ± 0.31	26.0 ± 0.28	24.2 ± 0.19
	2.00	38.6 ± 0.30	34.2 ± 0.29	31.6 ± 0.33	29.4 ± 0.30	27.1 ± 0.31
6.8	2.50	48.8 ± 0.38	43.2 ± 0.48	40.1 ± 0.54	37.5 ± 0.48	34.7 ± 0.51
	3.00	50.1 ± 0.40	44.4 ± 0.47	41.1 ± 0.55	38.3 ± 0.37	35.7 ± 0.52
	3.50	51.3 ± 0.34	46.0 ± 0.65	42.6 ± 0.55	39.7 ± 0.54	36.9 ± 0.65
	4.00	53.0 ± 0.55	47.3 ± 0.57	43.5 ± 0.56	40.9 ± 0.50	38.0 ± 0.66
	4.50	54.7 ± 0.24	48.6 ± 0.74	44.4 ± 0.57	42.1 ± 0.50	39.0 ± 0.71
	5.00	56.5 ± 0.24	49.8 ± 0.53	45.3 ± 0.63	43.0 ± 0.50	39.8 ± 0.58
	5.50	58.3 ± 0.18	51.1 ± 0.54	46.4 ± 0.58	44.1 ± 0.66	40.7 ± 0.59
	6.00	60.0 ± 0.17	52.4 ± 0.55	47.9 ± 0.59	45.6 ± 0.57	41.5 ± 0.45
	6.50	62.2 ± 0.24	53.8 ± 0.56	49.3 ± 0.73	47.0 ± 0.67	42.7 ± 0.50
	7.00	64.3 ± 0.24	55.4 ± 0.68	50.9 ± 0.61	48.5 ± 0.60	44.0 ±0.47
	7.50	66.2 ± 0.15	56.8 ± 0.55	52.2 ± 0.62	49.8 ± 0.56	45.0 ± 0.48
	8.00	68.2 ± 0.15	58.5 ± 0.56	53.8 ± 0.76	51.0 ± 0.62	46.4 ± 0.48
	8.50	70.7 ± 0.25	60.6 ± 0.56	55.5 ± 0.77	52.7 ± 0.62	47.7 ± 0.51
	9.00	72.7 ± 0.29	62.7 ± 0.33	57.9 ± 0.78	54.5 ± 0.58	49.2 ± 0.52
	9.50	75.2 ± 0.13	65.0 ±0.56	59.8 ± 0.80	56.0 ± 0.44	51.1 ± 0.38
	10.00	77.9 ± 0.44	67.3 ± 0.57	62.6 ± 0.69	57.9 ± 0.44	53.5 ± 0.38
	10.50	80.0 ± 0.14	69.8 ± 0.45	65.0 ± 0.68	60.1 ± 0.57	55.3 ± 0.52
	11.00	83.2 ± 0.13	72.3 ± 0.45	67.6 ± 0.71	62.1 ± 0.30	57.5 ± 0.53
	11.50	85.6 ± 0.13	75.2 ± 0.36	69.9 ± 0.87	64.6 ± 0.35	60.2 ± 0.39
	12.00	88.5 ± 0.29	78.4 ± 0.29	72.6 ± 0.74	67.6 ± 0.60	62.9 ± 0.39

n=3*

Table XXIV f Comparison of *Invitro* Release of Rosuvastatin Calcium Loaded ES 100 (Different Ratios) Nanoparticles Containing Pluronic F68 (2%) as Stabilizer

pH	TIME(HRS)	CUMULATIVE % DRUG RELEASE ± S.D*				
		F26 ES 100(1:10)	**F27** ES 100(1:20)	**F28** ES 100(1:30)	**F29** ES 100(1:40)	**F30** ES 100(1:50)
1.2	0.25	10.9 ± 0.28	9.9 ± 0.16	9.1 ± 0.16	8.0 ± 0.16	6.9 ± 0.16
	0.50	17.7 ± 0.29	16.9 ± 0.17	14.3 ± 0.15	13.1 ± 0.15	11.3 ± 0.28
	0.75	23.6 ± 0.25	21.7 ± 0.17	18.8 ± 0.28	17.8 ± 0.16	16.4 ± 0.15
	1.00	29.0 ± 0.31	27.0 ± 0.30	23.7 ± 0.29	22.5 ± 0.15	21.4 ± 0.16
	1.50	34.8 ± 0.17	31.3 ± 0.13	28.2 ± 0.19	27.2 ± 0.16	25.8 ± 0.17
	2.00	40.1 ± 0.14	35.8 ± 0.13	33.2 ± 0.18	30.6 ± 0.15	29.3 ± 0.15
6.8	2.50	49.7 ± 0.78	45.5 ± 0.64	42.1 ± 0.38	39.1 ± 0.27	37.3 ± 0.30
	3.00	52.2 ± 0.40	46.8 ± 0.05	43.4 ± 0.19	40.2 ± 0.15	38.1 ± 0.33
	3.50	53.5 ± 0.28	48.2 ± 0.11	44.6 ± 0.08	41.5 ± 0.15	39.1 ± 0.33
	4.00	54.9 ± 0.29	49.7 ± 0.18	46.0 ± 0.14	42.8 ± 0.26	40.8 ± 0.13
	4.50	56.8 ± 0.21	51.4 ± 0.21	47.9 ± 0.30	43.9 ± 0.02	41.8 ± 0.30
	5.00	58.7 ± 0.21	52.8 ± 0.08	49.4 ± 0.10	44.9 ± 0.18	42.7 ± 0.31
	5.50	60.6 ± 0.30	54.1 ± 0.09	50.6 ± 0.15	45.9 ± 0.19	43.6 ± 0.31
	6.00	62.2 ± 0.26	55.7 ± 0.10	52.3 ± 0.12	47.0 ± 0.25	44.6 ± 0.32
	6.50	64.6 ± 0.23	57.0 ± 0.24	53.6 ± 0.15	48.5 ± 0.28	45.6 ± 0.35
	7.00	66.6 ± 0.40	58.4 ± 0.26	55.0 ± 0.15	50.1 ± 0.18	46.8 ± 0.33
	7.50	68.7 ± 0.11	59.9 ± 0.27	56.5 ± 0.15	51.4 ± 0.27	48.0 ± 0.36
	8.00	70.7 ± 0.44	61.9 ± 0.18	58.5 ± 0.89	52.6 ± 0.35	49.5 ± 0.35
	8.50	72.9 ± 0.33	64.2 ± 0.14	60.1 ± 0.27	54.2 ± 0.29	51.1 ± 0.41
	9.00	75.4 ± 0.46	66.2 ± 0.13	62.1 ± 0.16	56.0 ± 0.29	52.6 ± 0.42
	9.50	78.0 ± 0.35	68.2 ± 0.14	64.2 ± 0.21	57.8 ± 0.30	54.5 ± 0.38
	10.00	80.6 ± 0.36	70.2 ± 0.15	66.4 ± 0.16	59.8 ± 0.31	57.0 ± 0.28
	10.50	83.0 ± 0.45	73.0 ± 0.17	68.7 ± 0.14	61.8 ± 0.31	59.0 ± 0.27
	11.00	85.7 ± 0.31	75.4 ± 0.33	71.3 ± 0.24	64.5 ± 0.32	61.6 ± 0.13
	11.50	88.3 ± 0.32	78.4 ± 0.24	74.1 ± 0.04	67.7 ± 0.46	64.3 ± 0.37
	12.00	91.2 ± 0.32	82.2 ± 0.26	77.3 ± 0.23	71.0 ± 0.47	67.2 ± 0.28

n=3*

Table XXIV g Comparison of *Invitro* Release of Rosuvastatin Calcium Loaded ES 100 (Different Ratios) Nanoparticles Containing PVA (1%) as Stabilizer

pH	TIME(HRS)	CUMULATIVE % DRUG RELEASE ± S.D*				
		F31 ES 100(1:10)	F32 ES 100(1:20)	F33 ES 100(1:30)	F34 ES 100(1:40)	F35 ES 100(1:50)
1.2	0.25	11.0 ± 0.16	10.7 ± 0.28	9.7 ± 0.16	8.5 ± 0.16	7.4 ± 0.16
	0.50	17.9 ± 0.16	16.1 ± 0.16	14.8 ± 0.28	13.8 ± 0.15	11.5 ± 0.15
	0.75	22.5 ± 0.27	19.8 ± 0.29	19.5 ± 0.73	17.5 ± 0.16	15.2 ± 0.28
	1.00	26.9 ± 0.27	24.5 ± 0.18	23.5 ± 0.26	22.4 ± 0.28	19.0 ± 0.29
	1.50	33.5 ± 0.27	31.0 ± 0.19	29.0 ± 0.30	26.7 ± 0.16	24.8 ± 0.18
	2.00	40.0 ± 0.27	35.9 ± 0.30	33.3 ± 0.13	31.7 ± 0.26	28.6 ± 0.30
6.8	2.50	50.5 ± 0.31	45.1 ± 0.19	42.2 ± 0.28	40.4 ± 0.40	36.5 ± 0.24
	3.00	52.0 ± 0.33	46.4 ± 0.40	43.2 ± 0.29	41.2 ± 0.13	37.7 ± 0.23
	3.50	54.1 ± 0.99	48.0 ± 0.19	44.6 ± 0.06	42.9 ± 0.53	39.2 ± 0.07
	4.00	55.0 ± 0.19	49.4 ± 0.18	45.9 ± 0.07	43.8 ± 0.42	40.3 ± 0.16
	4.50	57.0 ± 0.27	50.4 ± 0.23	47.1 ± 0.28	45.0 ± 0.42	41.1 ± 0.16
	5.00	59.1 ± 0.19	52.1 ± 0.16	48.0 ± 0.29	46.1 ± 0.47	42.0 ± 0.15
	5.50	60.5 ± 0.26	53.4 ± 0.31	49.2 ± 0.30	47.2 ± 0.64	42.9 ± 0.15
	6.00	62.1 ± 0.39	54.7 ± 0.16	50.5 ± 0.21	48.4 ± 0.44	43.9 ± 0.14
	6.50	64.4 ± 0.40	56.1 ± 0.31	52.1 ± 0.22	49.8 ± 0.45	45.0 ± 0.23
	7.00	66.6 ± 0.28	57.9 ± 0.47	53.6 ± 0.30	51.4 ± 0.46	46.2 ± 0.13
	7.50	68.4 ± 0.40	59.4 ± 0.26	55.0 ± 0.31	52.9 ± 0.52	47.5 ± 0.13
	8.00	70.6 ± 0.23	61.1 ± 0.26	56.8 ± 0.32	54.0 ± 0.54	48.6 ± 0.12
	8.50	73.3 ± 0.40	63.5 ± 0.27	58.4 ± 0.24	55.8 ± 0.61	50.2 ± 0.14
	9.00	75.3 ± 0.40	65.9 ± 0.32	60.9 ± 0.33	57.5 ± 0.50	51.4 ± 0.14
	9.50	78.1 ± 0.13	67.7 ± 0.79	62.8 ± 0.27	59.4 ± 0.51	53.8 ± 0.10
	10.00	80.4 ± 0.28	69.8 ± 0.35	65.7 ± 0.33	61.3 ± 0.52	56.1 ± 0.13
	10.50	82.9 ± 0.03	72.2 ± 0.28	68.3 ± 0.34	63.2 ± 0.51	58.0 ± 0.13
	11.00	85.7 ± 0.27	74.9 ± 0.28	70.9 ± 0.33	65.7 ± 0.55	60.4 ± 0.08
	11.50	88.2 ± 0.28	78.4 ± 0.20	73.6 ± 0.36	68.4 ± 0.52	62.9 ± 0.12
	12.00	91.2 ± 0.28	81.8 ± 0.27	76.9 ± 0.06	71.8 ± 0.53	66.2 ± 0.12

n=3*

Table XXIV h Comparison of *Invitro* Release of Rosuvastatin Calcium Loaded ES 100 (Different Ratios) Nanoparticles Containing PVA (2%) as Stabilizer

pH	TIME(HRS)	CUMULATIVE % DRUG RELEASE ± S.D*				
		F36 ES 100(1:10)	F37 ES 100(1:20)	F38 ES 100(1:30)	F39 ES 100(1:40)	F40 ES 100(1:50)
1.2	0.25	11.7 ± 0.16	10.6 ± 0.16	9.5 ± 0.28	9.2 ± 0.16	8.0 ± 0.16
	0.50	18.6 ± 0.16	17.3 ± 0.16	15.9 ± 0.28	14.5 ± 0.28	13.9 ± 0.27
	0.75	24.6 ± 0.15	22.5 ± 0.14	21.2 ± 0.30	19.7 ± 0.28	17.7 ± 0.16
	1.00	30.0 ± 0.15	28.0 ± 0.27	25.8 ± 0.31	24.1 ± 0.14	22.8 ± 0.17
	1.50	36.6 ± 0.28	33.4 ± 0.17	30.6 ± 0.11	28.3 ± 0.18	26.7 ± 0.14
	2.00	41.3 ± 0.26	39.0 ± 0.17	35.1 ± 0.25	32.5 ± 0.30	30.4 ± 0.15
6.8	2.50	52.8 ± 0.41	49.6 ± 0.36	44.6 ± 0.25	41.7 ± 0.40	39.0 ± 0.30
	3.00	54.5 ± 0.41	50.8 ± 0.32	46.0 ± 0.37	42.7 ± 0.49	39.7 ± 0.31
	3.50	55.6 ± 0.15	52.1 ± 0.05	47.0 ± 0.26	43.9 ± 0.57	41.1 ± 0.15
	4.00	57.1 ± 0.15	53.5 ± 0.05	48.5 ± 0.11	45.6 ± 0.38	42.7 ± 0.16
	4.50	58.9 ± 0.31	55.2 ± 0.34	49.8 ± 0.15	46.5 ± 0.38	43.8 ± 0.15
	5.00	60.9 ± 0.15	57.0 ± 0.47	51.3 ± 0.15	47.5 ± 0.46	45.0 ± 0.14
	5.50	62.7 ± 0.47	58.3 ± 0.39	53.2 ± 0.15	48.6 ± 0.55	46.0 ± 0.30
	6.00	64.0 ± 0.42	59.7 ± 0.36	54.6 ± 0.08	49.7 ± 0.51	47.5 ± 0.32
	6.50	66.5 ± 0.49	62.0 ± 0.50	56.2 ± 0.26	51.4 ± 0.65	48.6 ± 0.33
	7.00	68.3 ± 0.51	63.3 ± 0.36	57.6 ± 0.37	53.0 ± 0.67	49.7 ± 0.34
	7.50	70.3 ± 0.45	65.6 ± 0.37	59.1 ± 0.37	54.5 ± 0.68	50.8 ± 0.36
	8.00	72.7 ± 0.53	68.1 ± 0.38	60.9 ± 0.25	55.6 ± 0.70	52.1 ± 0.21
	8.50	74.9 ± 0.46	70.0 ± 0.39	62.5 ± 0.38	57.3 ± 0.58	53.5 ± 0.22
	9.00	77.5 ± 0.47	72.0 ± 0.40	63.9 ± 0.37	59.2 ± 0.58	55.1 ± 0.38
	9.50	80.0 ±0.48	74.0 ± 0.45	66.1 ± 0.38	61.1 ± 0.64	57.1 ± 0.24
	10.00	82.5 ± 0.49	77.0 ± 0.47	68.2 ± 0.52	63.0 ± 0.60	59.7 ± 0.11
	10.50	84.8 ± 0.50	79.5 ± 0.48	71.2 ± 0.41	65.6 ± 0.74	61.8 ± 0.24
	11.00	87.5 ± 0.50	81.9 ± 0.33	73.9 ± 0.42	68.0 ± 0.75	64.3 ± 0.12
	11.50	90.0 ± 0.51	84.6 ± 0.17	76.6 ± 0.41	71.4 ± 0.51	67.2 ± 0.12
	12.00	93.7 ± 0.68	87.9 ± 0.55	80.1 ± 0.46	74.7 ± 0.35	70.2 ± 0.19

n=3*

Table XXV a Release Kinetics of Rosuvastatin Calcium Loaded

EL 100 Nanoparticles (Different Ratios) Containing Pluronic F68 (1%) as Stabilizer

Formulation code	Zero order		First order		Higuchi model		Korsmeyer peppas		Hixon-Crowell	
	R^2	K_0 (h^{-1})	R^2	K_1 (h^{-1})	R^2	K_H ($h^{-1/2}$)	R^2	n	R^2	K_{HC} ($h^{-1/3}$)
F1	0.936	5.439	0.975	-0.049	0.986	22.98	0.976	0.485	0.974	-0.135
F2	0.953	5.064	0.978	-0.042	0.988	21.58	0.985	0.495	0.979	-0.120
F3	0.961	4.988	0.986	-0.038	0.991	21.20	0.984	0.478	0.985	-0.112
F4	0.972	4.708	0.987	-0.034	0.989	19.88	0.985	0.497	0.987	-0.102
F5	0.972	4.248	0.994	-0.028	0.999	17.80	0.978	0.498	0.978	-0.088

Table XXV b Release Kinetics of Rosuvastatin Calcium Loaded

EL 100 Nanoparticles (Different Ratios) Containing Pluronic F68 (2%) as Stabilizer

Formulation code	Zero order		First order		Higuchi model		Korsmeyer peppas		Hixon-Crowell	
	R^2	K_0 (h^{-1})	R^2	K_1 (h^{-1})	R^2	K_H ($h^{-1/2}$)	R^2	n	R^2	K_{HC} ($h^{-1/3}$)
F6	0.926	5.632	0.963	-0.061	0.982	24.28	0.973	0.446	0.971	-0.158
F7	0.936	5.023	0.970	-0.044	0.981	21.53	0.974	0.453	0.969	-0.123
F8	0.935	4.891	0.967	-0.042	0.979	20.94	0.970	0.451	0.967	-0.118
F9	0.925	4.495	0.969	-0.036	0.979	19.34	0.973	0.431	0.962	-0.104
F10	0.923	4.207	0.964	-0.031	0.976	18.10	0.964	0.451	0.955	-0.092

Table XXV c Release Kinetics of Rosuvastatin Calcium Loaded

EL 100 Nanoparticles (Different Ratios) Containing PVA (1%) as Stabilizer

Formulation code	Zero order		First order		Higuchi model		Korsmeyer peppas		Hixon-Crowell	
	R^2	K_0 (h^{-1})	R^2	K_1 (h^{-1})	R^2	K_H ($h^{-1/2}$)	R^2	n	R^2	K_{HC} ($h^{-1/3}$)
F11	0.891	5.124	0.958	-0.054	0.967	22.33	0.963	0.384	0.953	-0.142
F12	0.912	4.866	0.956	-0.046	0.972	21.02	0.967	0.404	0.955	-0.125
F13	0.931	4.772	0.973	-0.041	0.982	20.51	0.979	0.423	0.968	-0.116
F14	0.924	4.267	0.963	-0.033	0.976	18.35	0.969	0.428	0.957	-0.096
F15	0.950	4.207	0.975	-0.031	0.984	17.92	0.978	0.471	0.972	-0.092

Table XXV d Release Kinetics of Rosuvastatin Calcium Loaded

EL 100 Nanoparticles (Different Ratios) Containing PVA (2%) as Stabilizer

Formulation code	Zero order		First order		Higuchi model		Korsmeyer peppas		Hixon-Crowell	
	R^2	K_0 (h^{-1})	R^2	K_1 (h^{-1})	R^2	K_H ($h^{-1/2}$)	R^2	n	R^2	K_{HC} ($h^{-1/3}$)
F16	0.919	5.790	0.943	-0.073	0.979	25.01	0.970	0.426	0.966	-0.177
F17	0.912	5.218	0.962	-0.055	0.974	22.57	0.971	0.396	0.962	-0.143
F18	0.907	4.764	0.960	-0.043	0.970	20.62	0.968	0.391	0.954	-0.120
F19	0.904	4.393	0.959	-0.036	0.969	19.03	0.970	0.387	0.948	-0.104
F20	0.895	4.132	0.955	-0.032	0.966	17.97	0.972	0.379	0.941	-0.094

Table XXV e Release Kinetics of Rosuvastatin Calcium Loaded

ES 100 Nanoparticles (Different Ratios) Containing Pluronic F68 (1%) as Stabilizer

Formulation code	Zero order		First order		Higuchi model		Korsmeyer peppas		Hixon-Crowell	
	R^2	K_0 (h^{-1})	R^2	K_1 (h^{-1})	R^2	K_H ($h^{-1/2}$)	R^2	n	R^2	K_{HC} ($h^{-1/3}$)
F21	0.929	5.590	0.958	-0.062	0.982	24.06	0.975	0.441	0.970	-0.158
F22	0.921	4.782	0.959	-0.042	0.975	20.59	0.968	0.420	0.957	-0.118
F23	0.920	4.456	0.957	-0.036	0.971	19.16	0.964	0.417	0.953	-0.104
F24	0.915	4.119	0.960	-0.031	0.974	17.79	0.973	0.408	0.951	-0.092
F25	0.908	3.814	0.992	-0.027	0.997	16.47	0.961	0.414	0.939	-0.082

Table XXV f Release Kinetics of Rosuvastatin Calcium Loaded

ES 100 Nanoparticles (Different Ratios) Containing Pluronic F68 (2%) as Stabilizer

Formulation code	Zero order		First order		Higuchi model		Korsmeyer peppas		Hixon-Crowell	
	R^2	K_0 (h^{-1})	R^2	K_1 (h^{-1})	R^2	K_H ($h^{-1/2}$)	R^2	n	R^2	K_{HC} ($h^{-1/3}$)
F26	0.930	5.685	0.950	-0.068	0.984	24.46	0.981	0.423	0.970	-0.169
F27	0.922	4.910	0.958	-0.047	0.977	21.15	0.973	0.405	0.960	-0.127
F28	0.925	4.752	0.965	-0.041	0.979	20.46	0.974	0.427	0.962	-0.116
F29	0.915	4.228	0.954	-0.033	0.971	18.23	0.967	0.405	0.948	-0.097
F30	0.908	4.032	0.948	-0.030	0.966	17.40	0.963	0.402	0.941	-0.090

Table XXV g Release Kinetics of Rosuvastatin Calcium Loaded

ES 100 Nanoparticles (Different Ratios) Containing PVA (1%) as Stabilizer

Formulation code	Zero order		First order		Higuchi model		Korsmeyer peppas		Hixon-Crowell	
	R^2	K_0 (h^{-1})	R^2	K_1 (h^{-1})	R^2	K_H ($h^{-1/2}$)	R^2	n	R^2	K_{HC} ($h^{-1/3}$)
F31	0.927	5.725	0.950	-0.068	0.982	24.66	0.974	0.438	0.969	-0.169
F32	0.919	4.904	0.951	-0.046	0.974	21.12	0.965	0.417	0.954	-0.126
F33	0.926	4.624	0.955	-0.040	0.973	19.84	0.965	0.416	0.956	-0.113
F34	0.912	4.314	0.957	-0.035	0.973	18.64	0.966	0.411	0.949	-0.100
F35	0.907	3.988	0.948	-0.029	0.967	17.23	0.956	0.420	0.940	-0.088

Table XXV h Release Kinetics of Rosuvastatin Calcium Loaded

ES 100 Nanoparticles (Different Ratios) Containing PVA (1%) as Stabilizer

Formulation code	Zero order		First order		Higuchi model		Korsmeyer peppas		Hixon-Crowell	
	R^2	K_0 (h^{-1})	R^2	K_1 (h^{-1})	R^2	K_H ($h^{-1/2}$)	R^2	n	R^2	K_{HC} ($h^{-1/3}$)
F36	0.923	5.739	0.933	-0.074	0.980	24.75	0.976	0.413	0.964	-0.178
F37	0.921	5.387	0.955	-0.059	0.978	23.23	0.973	0.415	0.965	-0.151
F38	0.919	4.800	0.959	-0.044	0.976	20.70	0.973	0.407	0.958	-0.121
F39	0.916	4.420	0.954	-0.037	0.972	19.05	0.966	0.403	0.950	-0.105
F40	0.915	4.175	0.954	-0.033	0.971	18.00	0.968	0.402	0.948	-0.095

Table XXVI Comparison of Solubility of Best Formulations (F5, F25) with Pure Drug

TIME(HRS)	SOLUBILITY (µg/ml) ± SD*		
	PURE DRUG	F 5 EL 100 (1:50), Pluronic F 68 1%	F25 ES 100 (1:50), Pluronic F 68 1%
24hrs	357.73 ± 0.86	743.94 ± 0.71	624.60 ± 0.63

n=3*

Table XXVII a Comparison of Cumulative Amount of Drug Permeated across Duodenum Segment

TIME(HRS)	CUMULATIVE AMOUNT OF DRUG PERMEATED(mg)± SD*		
	PURE DRUG SOLUTION	F 5 EL 100 (1:50), Pluronic F 68 1%	F25 ES 100 (1:50), Pluronic F 68 1%
0.25	0.1038± 0.50	0.2416± 0.10	0.1841± 0.63
0.50	0.1465± 0.67	0.2854 ± 0.19	0.2678 ± 0.70
1.00	0.1822± 0.89	0.5109 ± 0.18	0.4633 ± 0.83
1.50	0.2811± 0.73	0.7588 ± 0.12	0.6464 ± 0.62
2.00	0.3246± 0.52	1.0021 ± 0.36	0.9137 ± 0.76

n=3*

Table XXVII b Comparison of Cumulative Amount of Drug Permeated across Jejunum Segment

TIME(HRS)	CUMULATIVE AMOUNT OF DRUG PERMEATED(mg)± SD*		
	PURE DRUG SOLUTION	F 5 EL 100 (1:50), Pluronic F 68 1%	F25 ES 100 (1:50), Pluronic F 68 1%
0.25	0.1136± 0.51	0.2523 ± 0.15	0.1977 ± 0.91
0.50	0.1676± 0.82	0.2962 ± 0.83	0.2658 ± 0.24
1.00	0.1981± 0.11	0.5190 ± 0.16	0.4533 ± 0.98
1.50	0.2887± 0.33	0.7848 ± 0.14	0.6526 ± 0.65
2.00	0.3503± 0.81	1.0029 ± 0.44	0.8978 ± 0.53

n=3*

Table XXVII c Comparison of Cumulative Amount of Drug Permeated across ileum Segment

TIME(HRS)	CUMULATIVE AMOUNT OF DRUG PERMEATED(mg)± SD*		
	PURE DRUG SOLUTION	F 5 EL 100 (1:50), Pluronic F 68 1%	F25 ES 100 (1:50), Pluronic F 68 1%
0.25	0.1011± 0.11	0.2129 ± 0.12	0.1745 ± 0.11
0.50	0.1401± 0.82	0.2874 ± 0.12	0.2485 ± 0.34
1.00	0.1791± 0.63	0.5007 ± 0.16	0.4359 ± 0.43
1.50	0.2770 ± 0.69	0.7818 ± 0.18	0.6347 ± 0.82
2.00	0.3274± 0.93	0.9977 ± 0.71	0.8765 ± 0.76

n=3*

Table XXVII d Comparison of Cumulative Amount of Drug Permeated through small Intestinal Segments (At 2 Hour)

SMALL INTESTINAL SEGMENTS	CUMULATIVE AMOUNT OF DRUG PERMEATED(mg) ± SD*		
	PURE DRUG SOLUTION	F 5 EL 100 (1:50), Pluronic F 68 1%	F25 ES 100 (1:50), Pluronic F 68 1%
DUODENUM	0.3246± 0.52	1.0021 ± 0.36	0.9137 ± 0.76
JEJUNUM	0.3503± 0.81	1.0029 ± 0.44	0.8978 ± 0.53
ILEUM	0.3274± 0.93	0.9977 ± 0.71	0.8765 ± 0.76

n=3*

Table XXVII e Comparison of e*x vivo* Apparent Permeability Coefficient (P_{app}) of Formulations F5, F25 with Pure Drug Solution

SMALL INTESTINAL SEGMENTS OF RAT	APPARENT PERMEABILITY (Papp) x 10^{-6} cm/s ± SD*		
	PURE DRUG SOLUTION	F 5 EL 100 (1:50), Pluronic F 68 1%	F25 ES 100 (1:50), Pluronic F 68 1%
DUODENUM	3.300 ± 0.10	11.647 ± 0.22	10.680 ± 0.04
JEJUNUM	3.400 ± 0.17	11.617 ± 0.20	10.407 ± 0.18
ILEUM	3.367 ± 0.152	11.683 ± 0.40	10.410 ± 0.08

n=3*

DUODENUM	JEJUNUM	ILEUM
Pure drug Vs F5 p>0.001	Pure drug Vs F5 p>0.001	Pure drug Vs F5 p>0.001
Pure drug Vs F25 p>0.001	Pure drug Vs F25 p>0.001	Pure drug Vs F25 p>0.001
F5 Vs F25 p>0.001	F5 Vs F25 p>0.001	F5 Vs F25 p>0.01

Table XXVIII a Stability study of best formulation (F5) stored at 4°C and 25°C ± 60%RH

Evaluation parameter	Storing Temperature	0 month	1 month	2 month	3 month
% Entrapment Efficiency	4°C	79.0±0.87%	79.0±0.56%	78.6±0.57%	78.3±0.44%
	25°C ± 60% RH	79.0±0.87%	78.5±0.77%	78.2±0.88%	77.9±0.89%

Table XXVIII b Stability study of best formulation (F25) stored at 4°C and 25°C ± 60%RH

Evaluation parameter	Storing Temperature	0 month	1 month	2 month	3 month
% Entrapment Efficiency	4°C	72.0±0.88%	71.5±0.59%	71.3±0.66%	71.3±0.97%
	25°C ± 60% RH	72.0±0.88%	71.2±0.73%	71.0±0.82%	70.8±0.19%

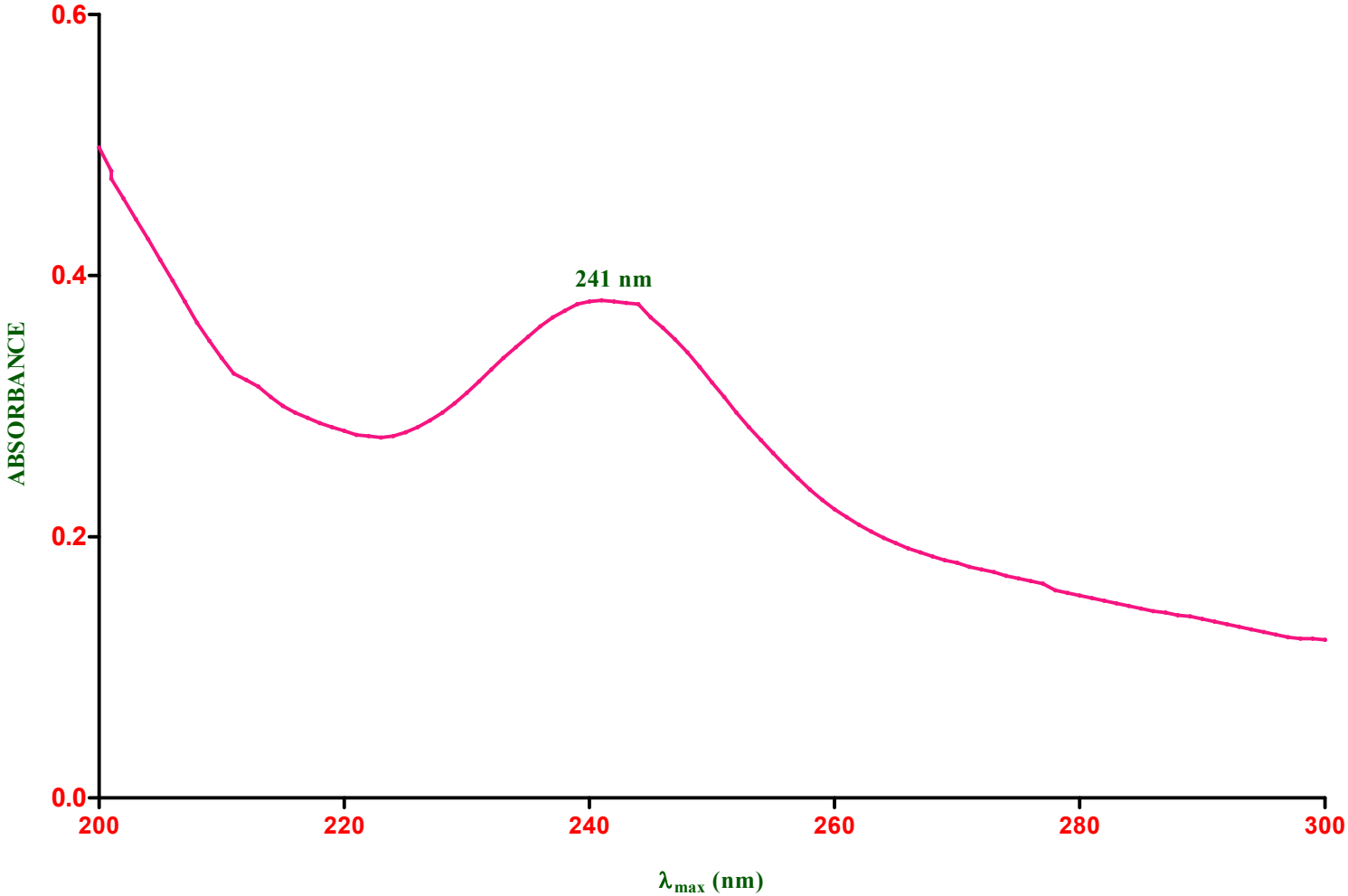

Figure 17 Determination of Absorption Maximum (λ_{max}) of Rosuvastatin Calcium in pH 6.8.

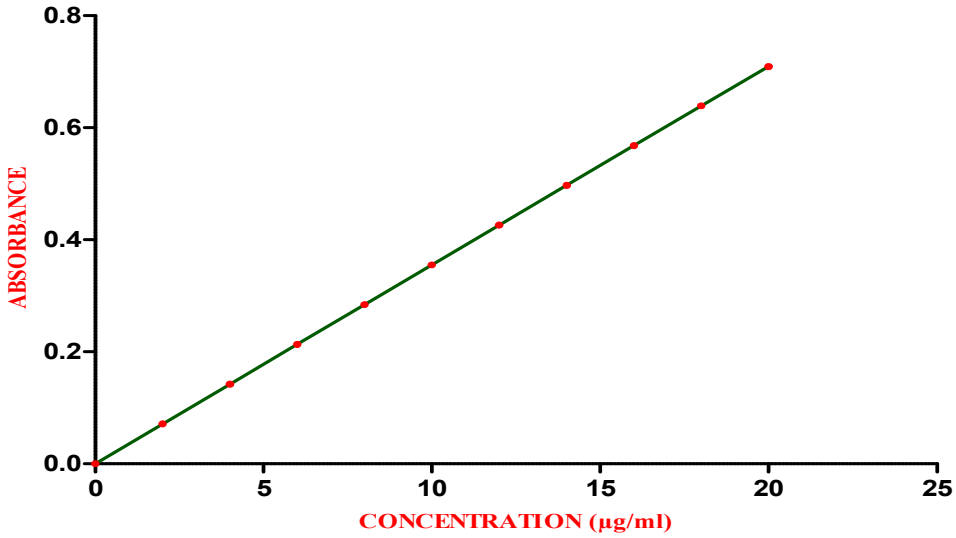

Figure 18 Calibration Curve of Rosuvastatin Calcium in Distilled Water

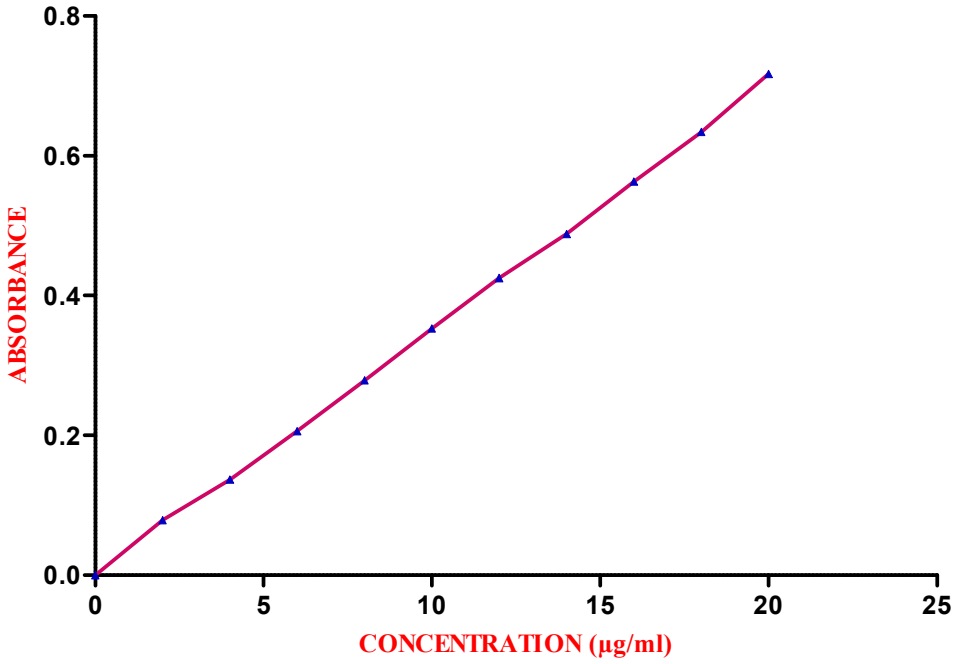

Figure 19 Calibration Curve of Rosuvastatin Calcium in pH 1.2

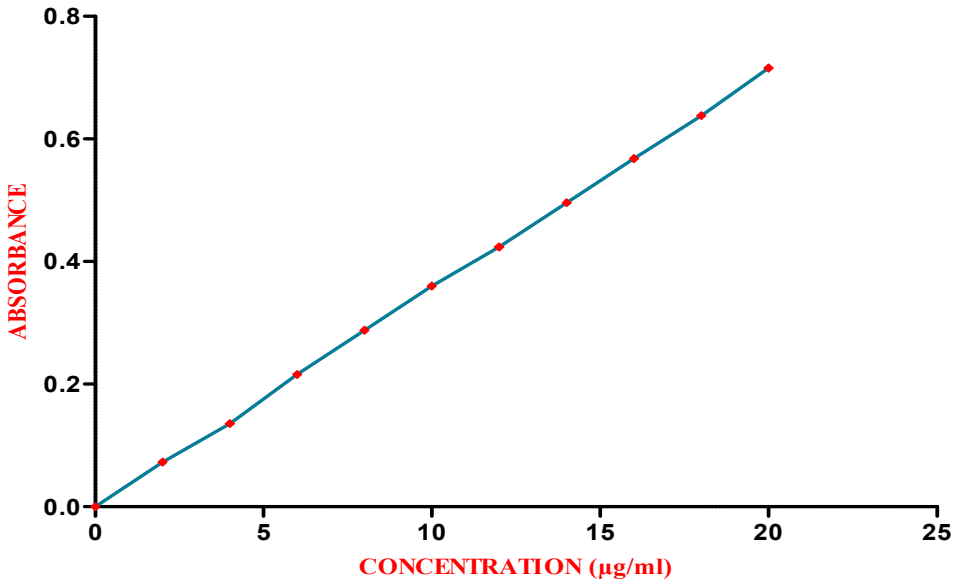

Figure 20 Calibration Curve of Rosuvastatin Calcium in pH 6.8

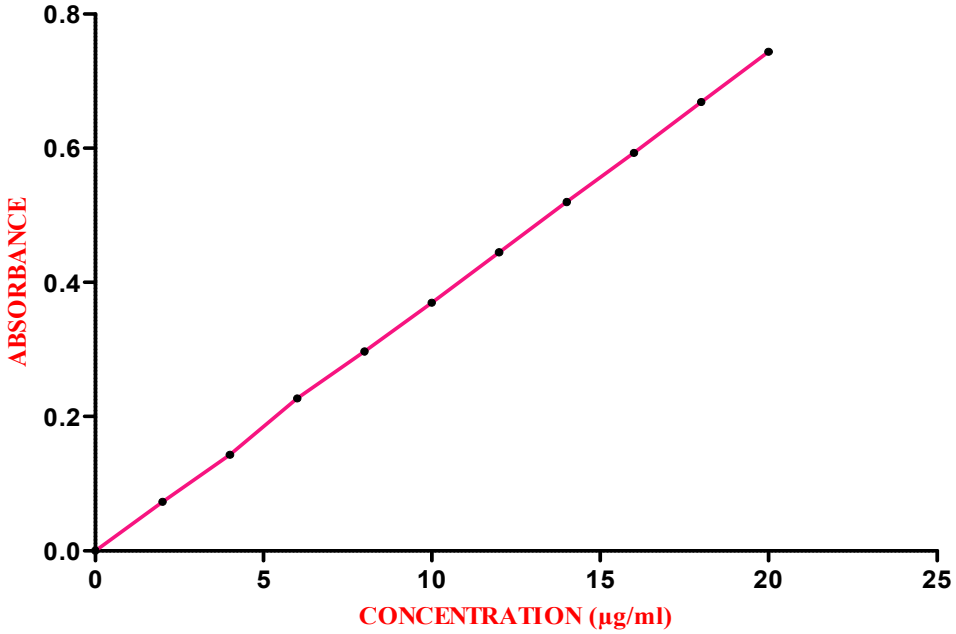

Figure 21 Calibration Curve of Rosuvastatin Calcium in PBS of pH 7.4

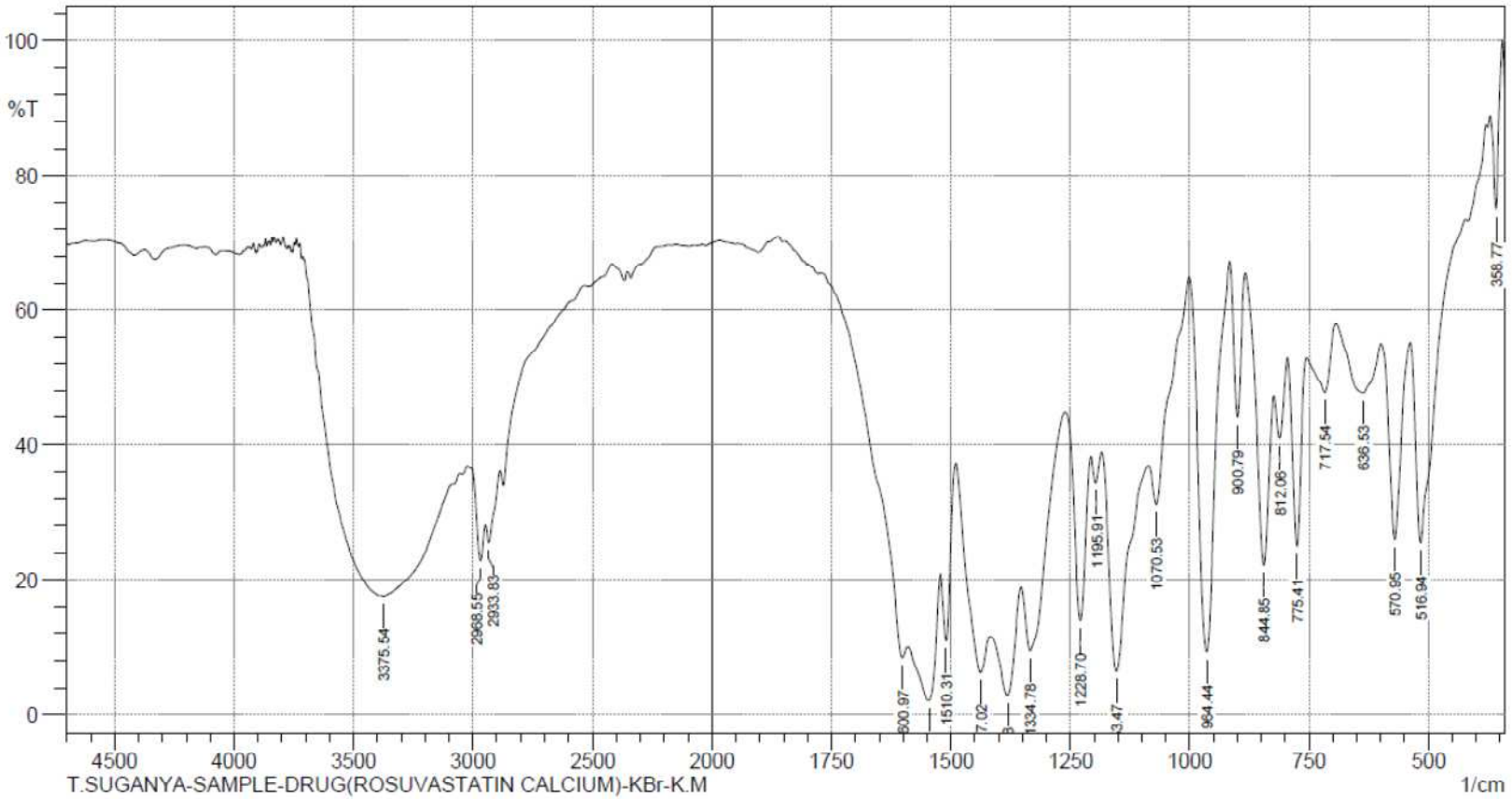

Figure 22 a FT-IR Spectra of Rosuvastatin Calcium

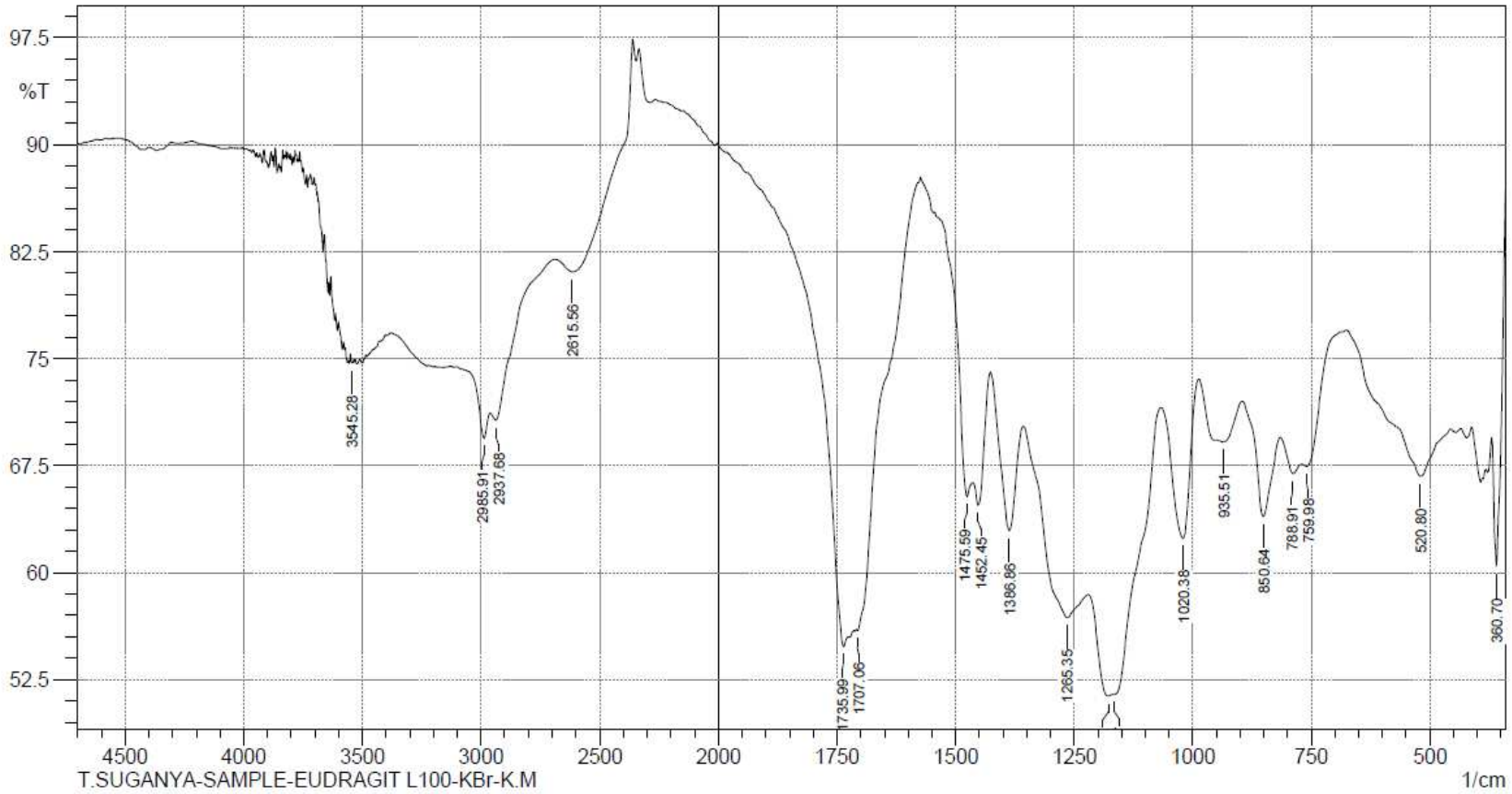

Figure 22 b FT-IR Spectra of Eudragit L 100

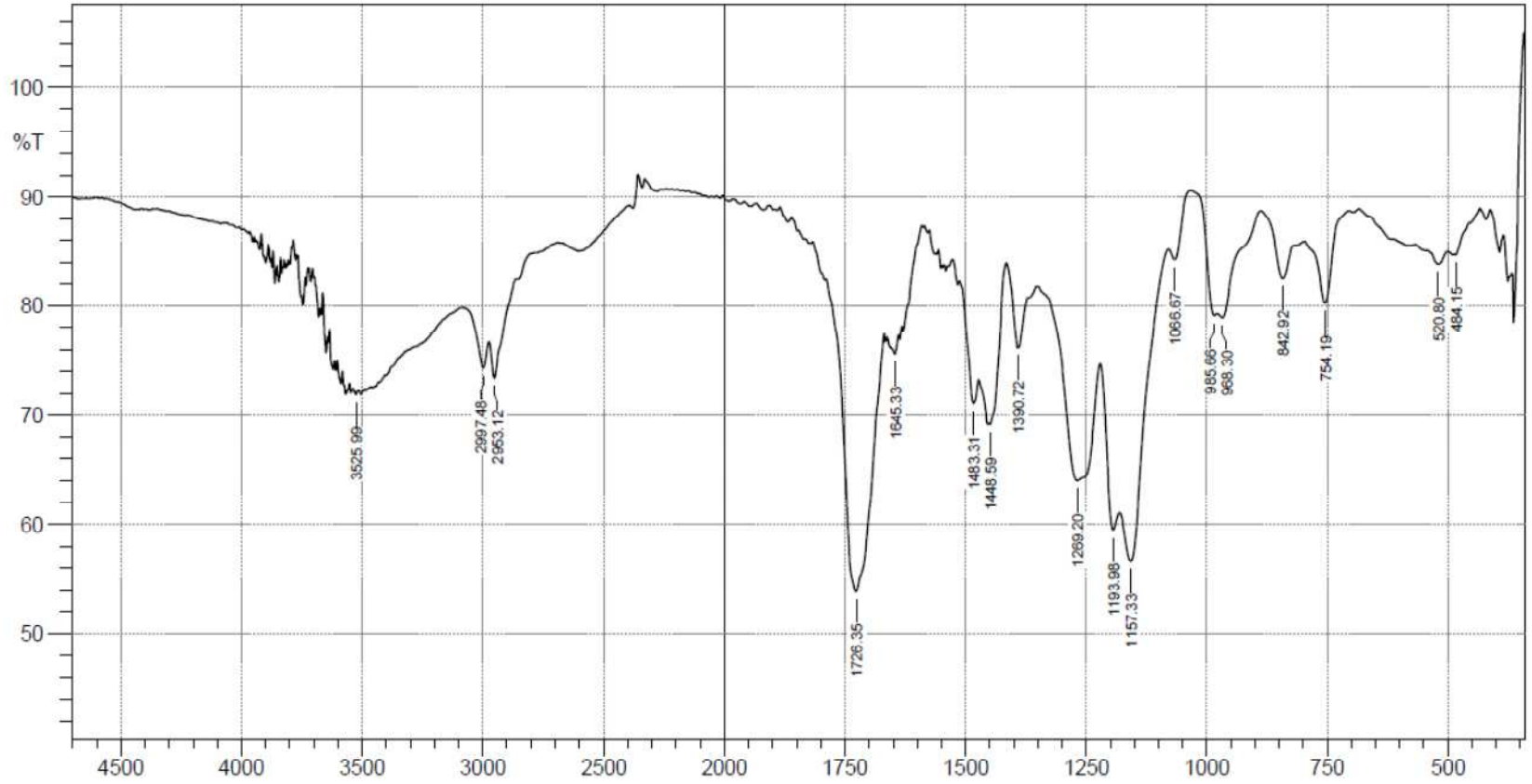

Figure 22 c FT-IR Spectra of Eudragit S 100

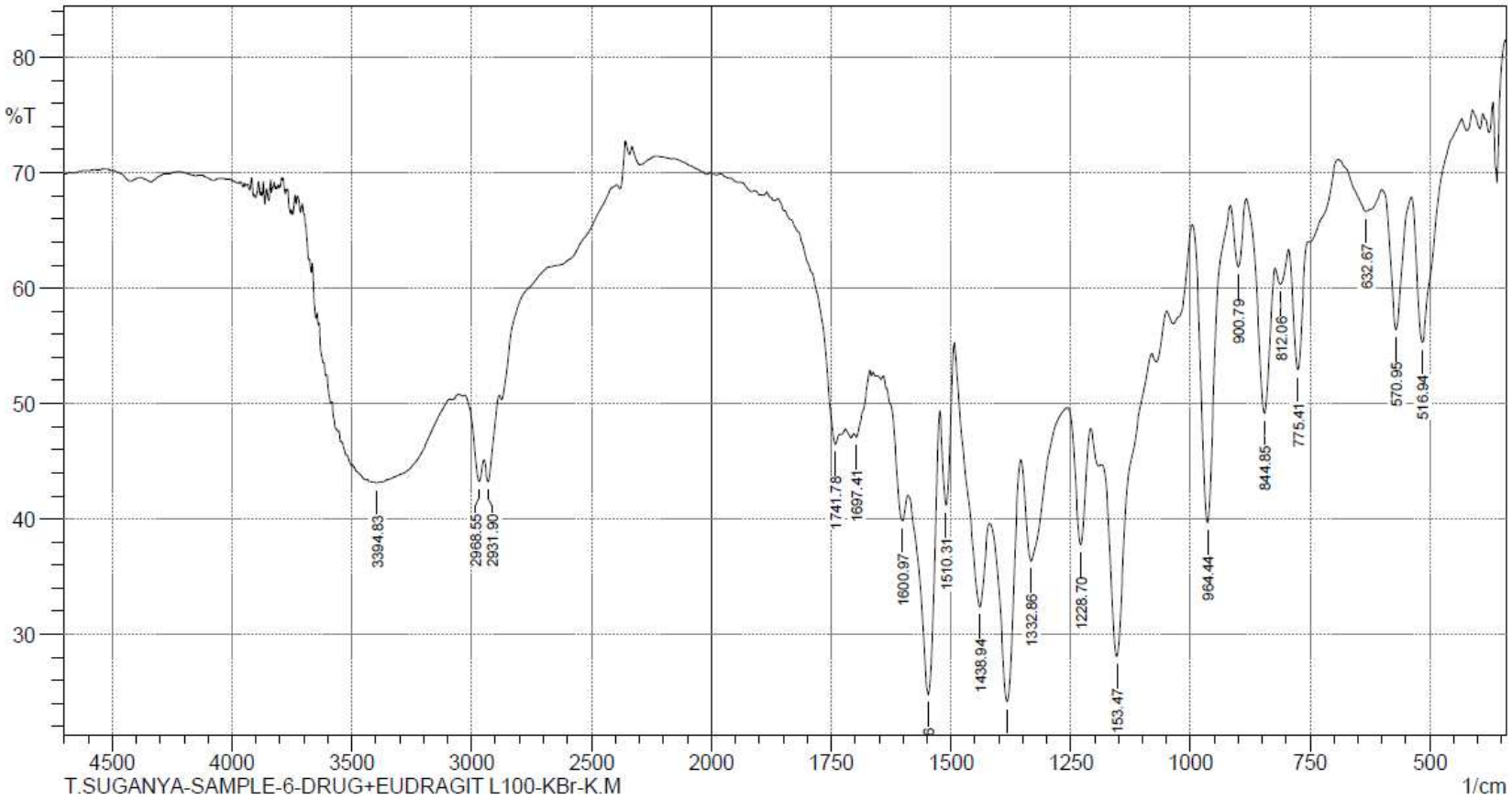

Figure 22d FT-IR Spectra of Physical Mixture of Rosuvastatin Calcium and Eudragit L100

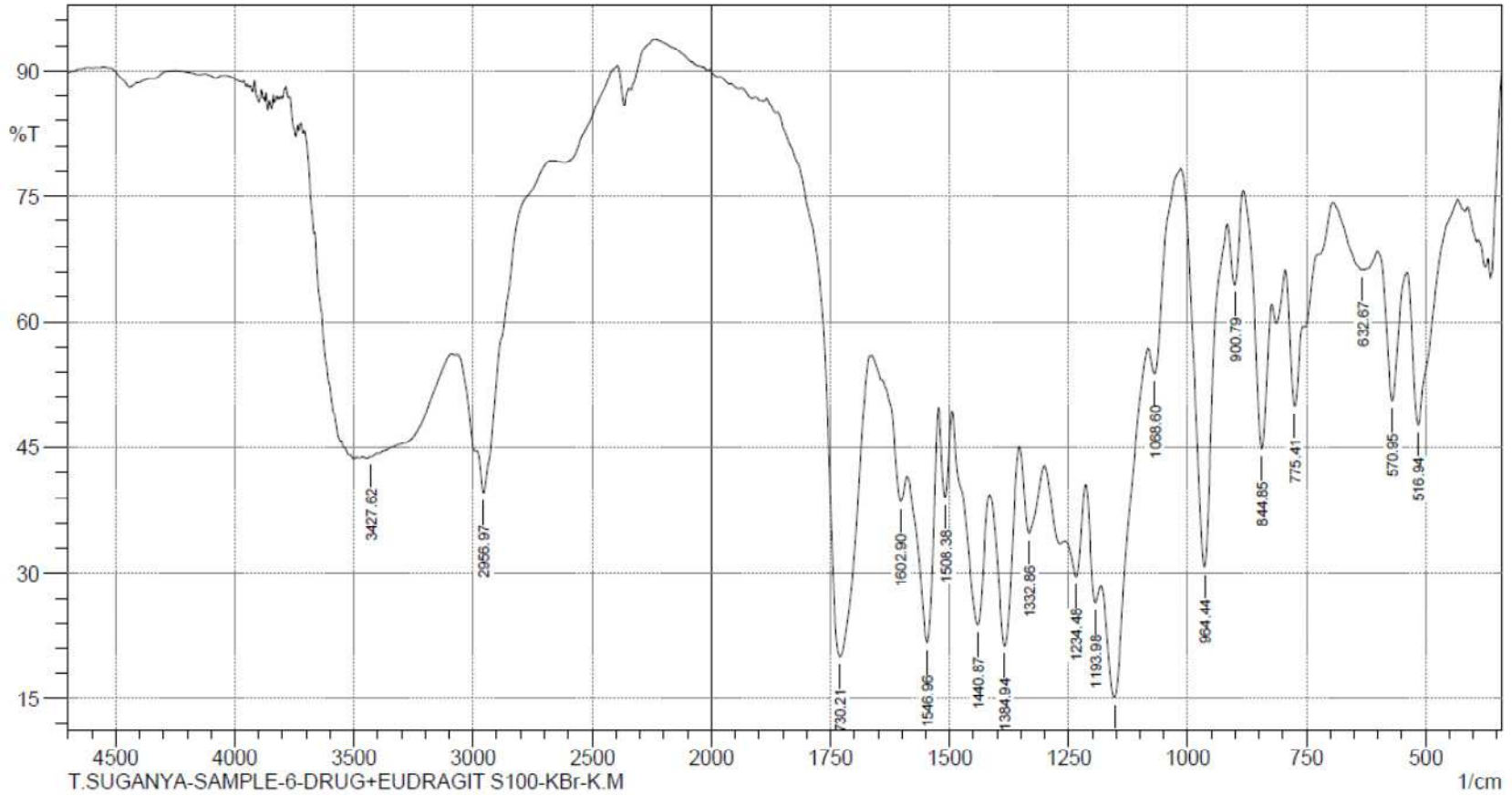

Figure 22 e FT-IR Spectra of Physical Mixture of Rosuvastatin Calcium and Eudragit S100

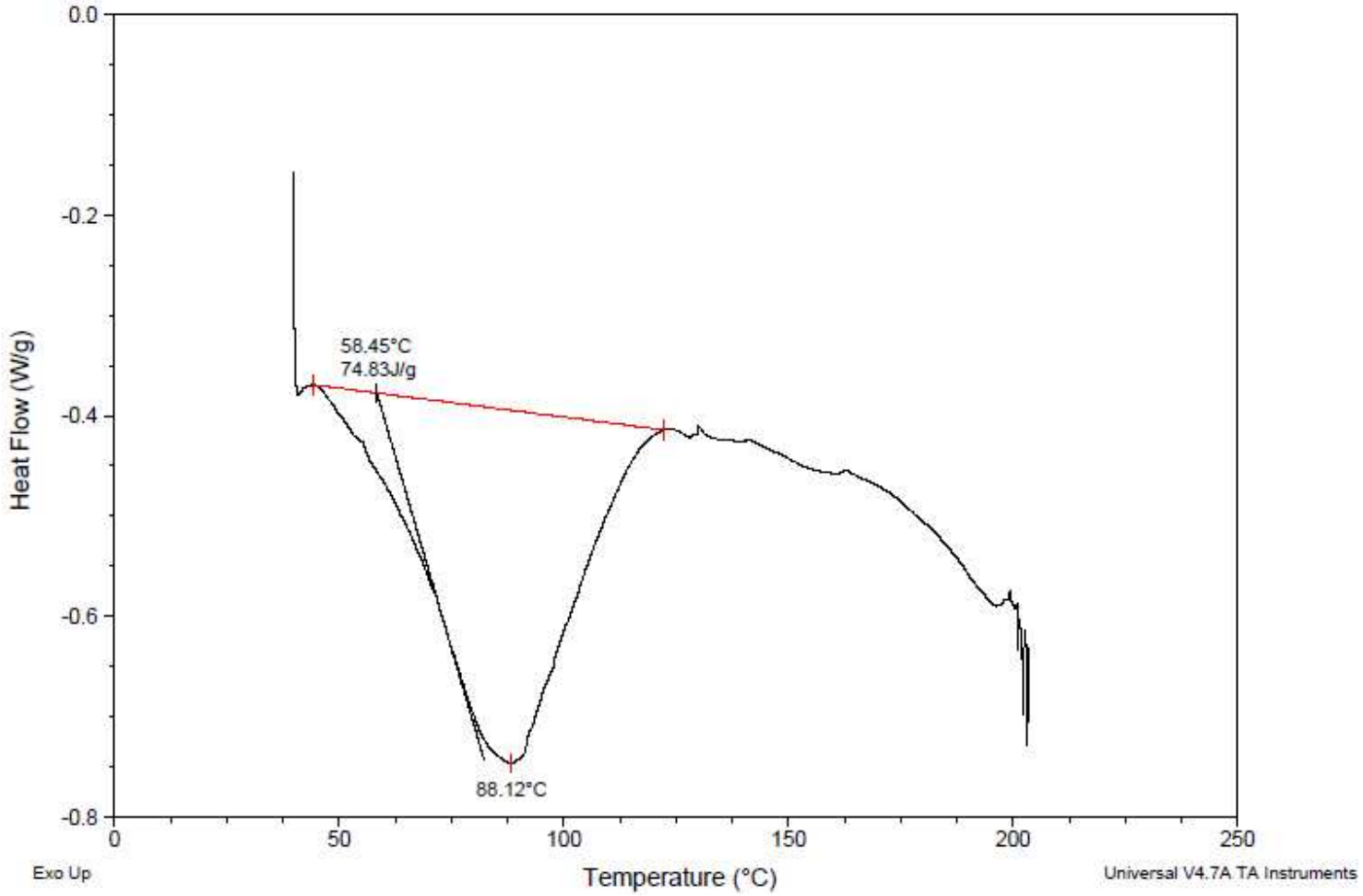

Figure 23 a DSC Thermogram of Rosuvastatin Calcium

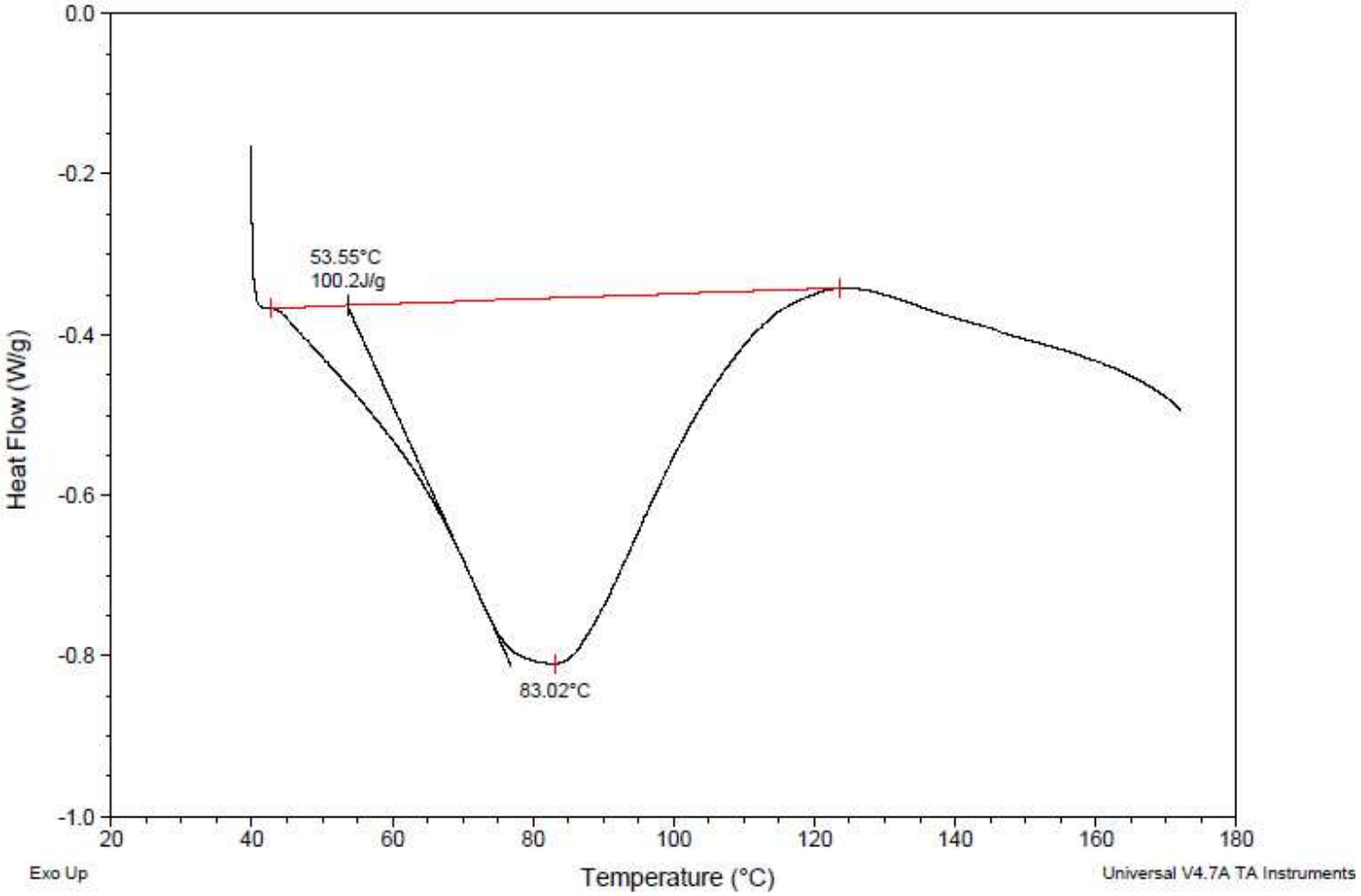

Figure 23 b DSC Thermogram of Eudragit L 100

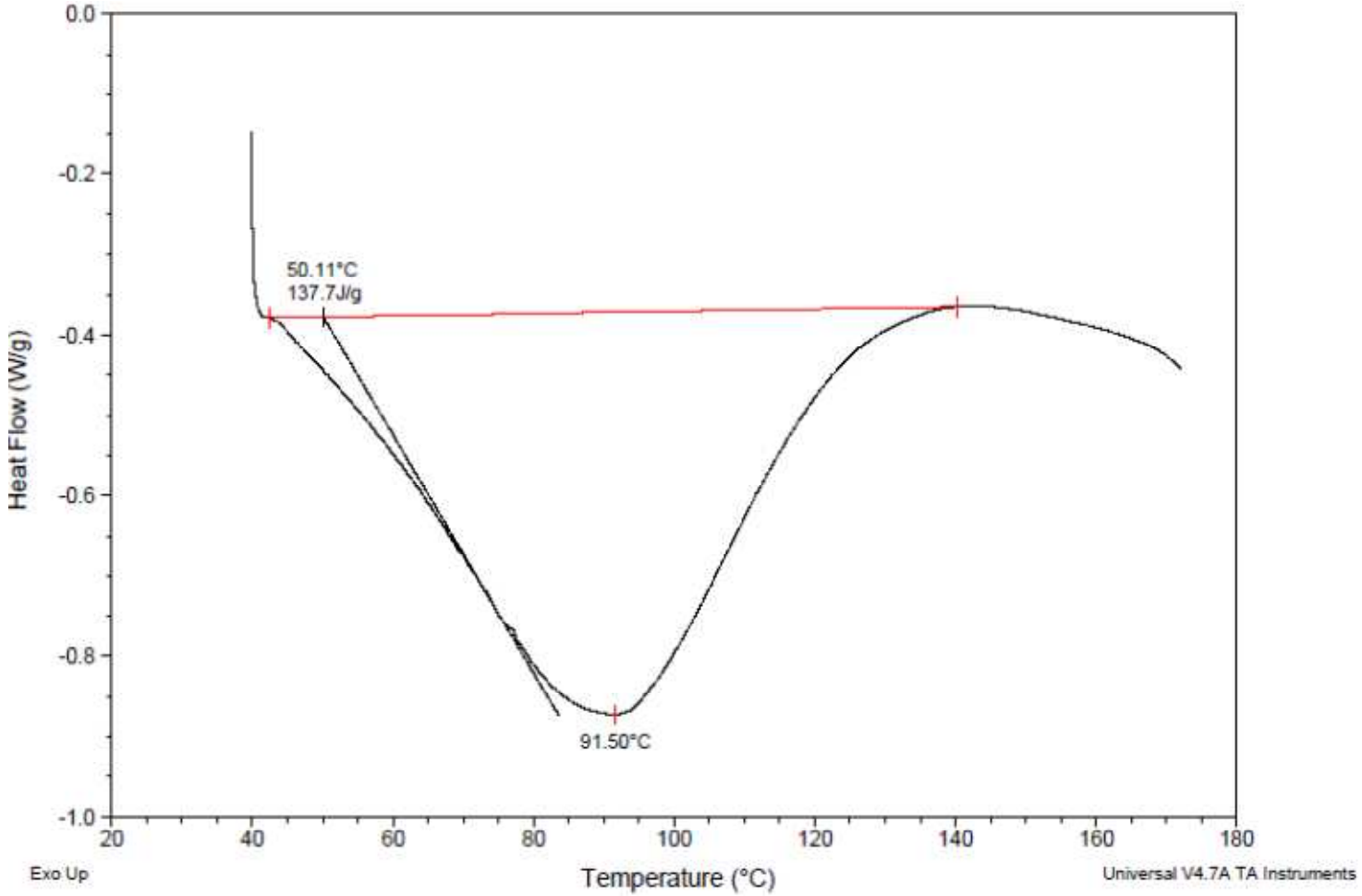

Figure 23 c DSC Thermogram of Eudragit S 100

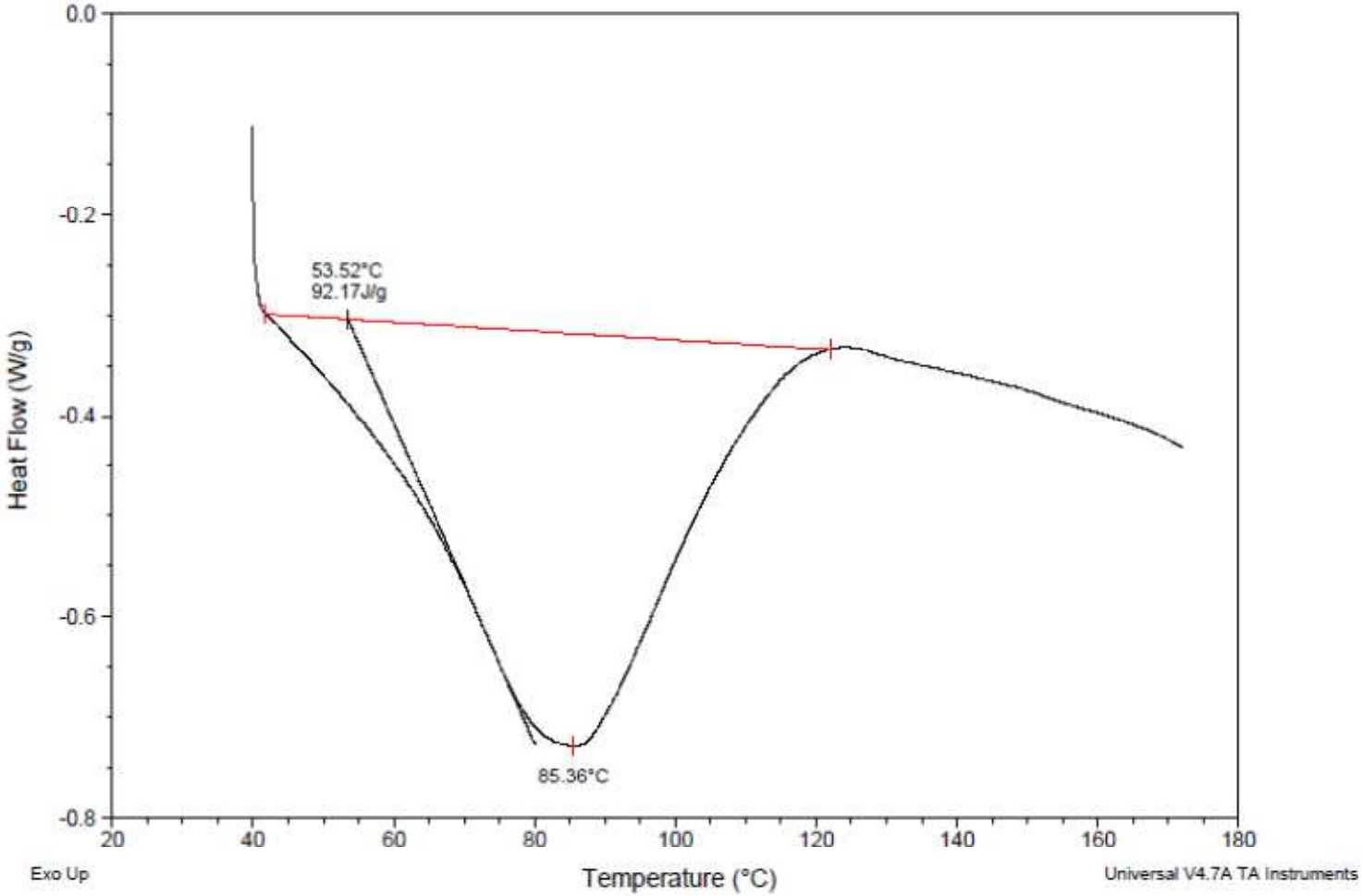

Figure 23 d DSC Thermogram of Physical Mixture of Rosuvastatin Calcium and Eudragit L100

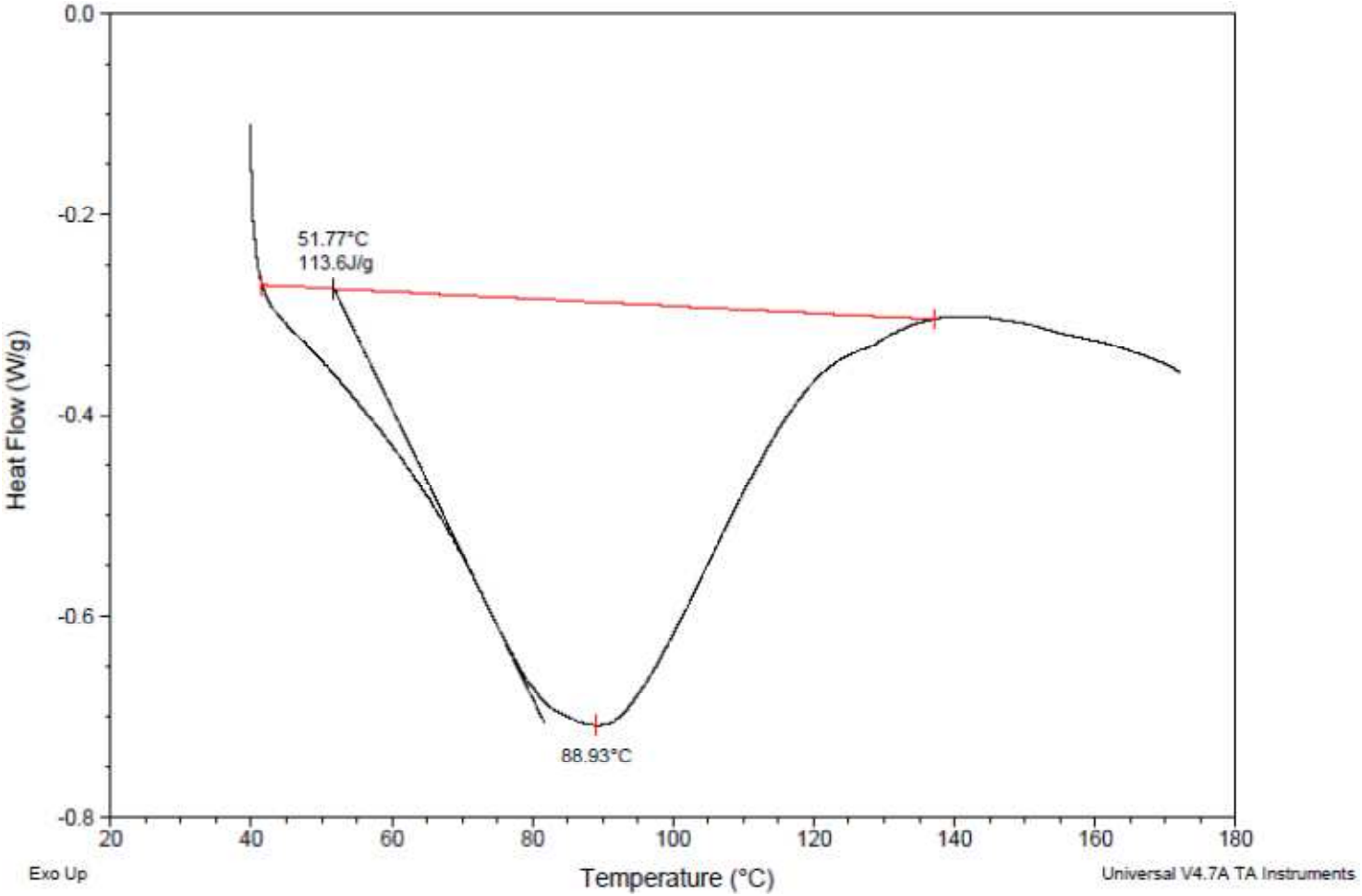

Figure 23 e DSC Thermogram of Physical Mixture of Rosuvastatin Calcium and Eudragit S100

Results

			Diam. (nm)	% Intensity	Width (nm)
Z-Average (d.nm):	125.9	Peak 1:	162	100.0	53.5
PdI:	0.095	Peak 2:	0.00	0.0	0.00
Intercept:	0.954	Peak 3:	0.00	0.0	0.00
Result quality :	GOOD				

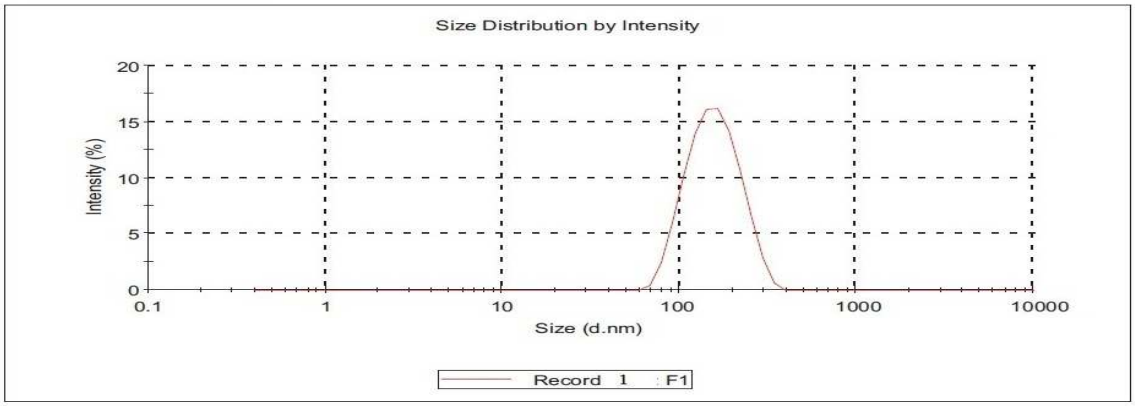

F1 (EL 100 1:10, PLURONIC F68 1%)

Results

			Diam. (nm)	% Intensity	Width (nm)
Z-Average (d.nm):	142.2	Peak 1:	146	95.3	54.6
PdI:	0.092	Peak 2:	0.00	0.0	0.00
Intercept:	0.969	Peak 3:	0.00	0.0	0.00
Result quality :	Good				

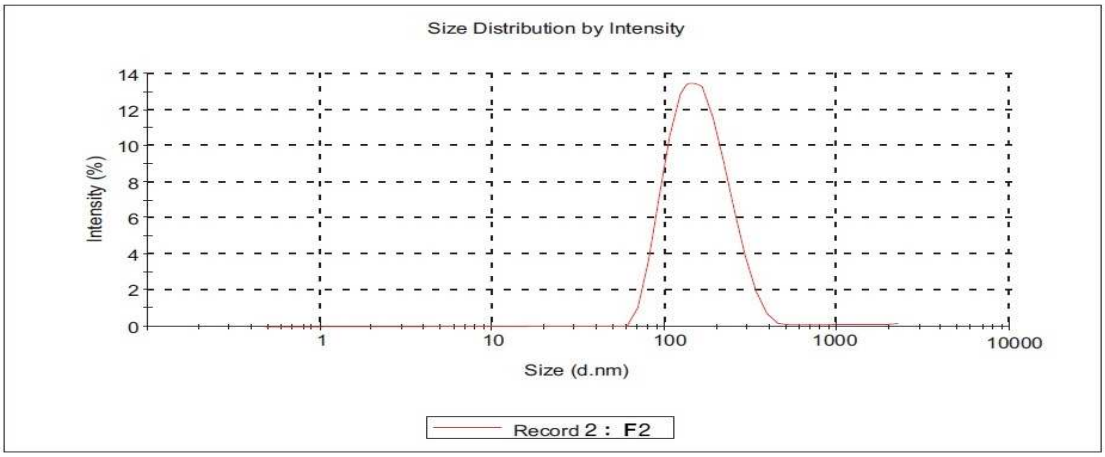

F2 (EL 100 1:20, PLURONIC F68 1%)

Figure 24 a Particle size distribution curve of formulations F1 and F2

Results

		Diam. (nm)	% Intensity	Width (nm)
Z-Average (d.nm): 166.2	Peak 1:	194	99.8	68.4
PdI: 0.162	Peak 2:	0.00	0.0	0.00
Intercept: 0.972	Peak 3:	0.00	0.0	0.00

Result quality : Good

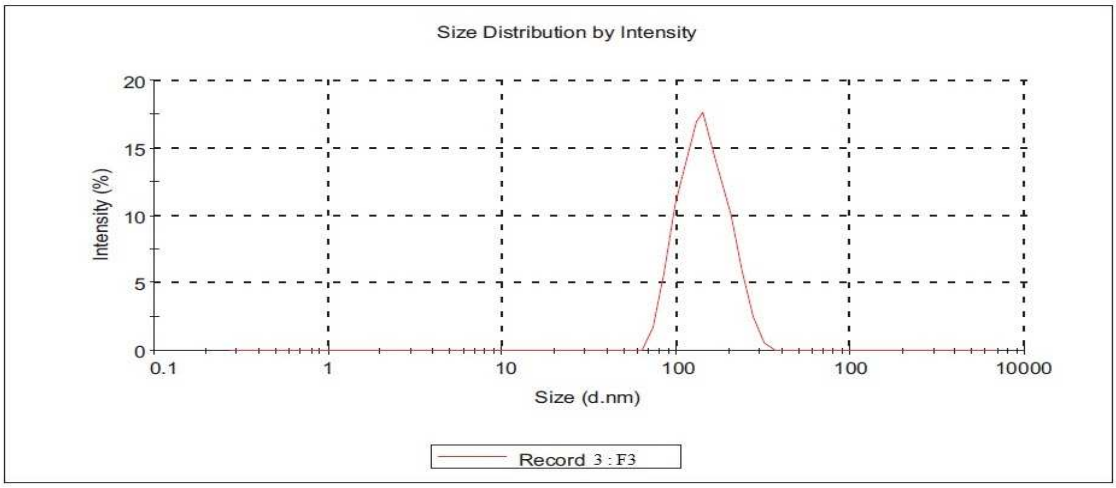

(EL 100 1:30, PLURONIC F68 1%)

Results

		Diam. (nm)	% Intensity	Width (nm)
Z-Average (d.nm): 178.5	Peak 1:	198	98.2	68.8
PdI: 0.185	Peak 2:	0.00	0.0	0.00
Intercept: 0.964	Peak 3:	0.00	0.0	0.00

Result quality : Good

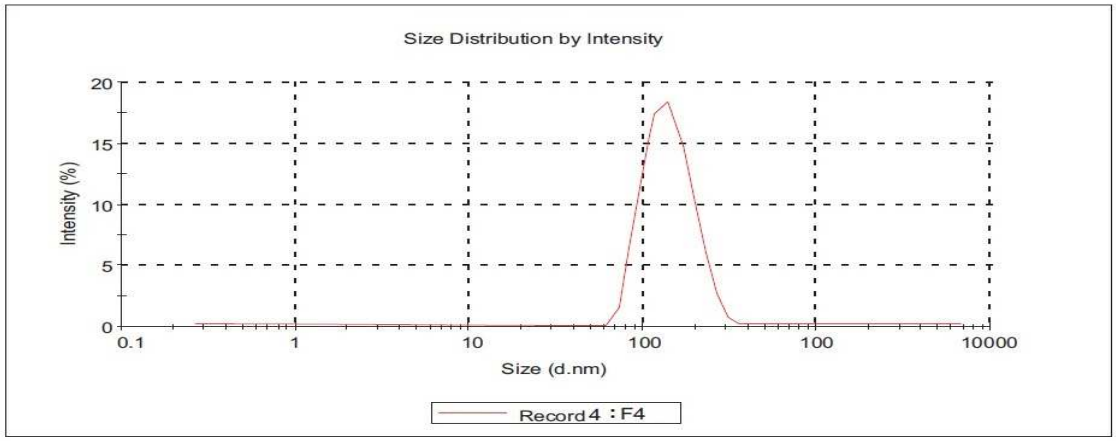

F4 (EL 100 1:40, PLURONIC F68 1%)

Figure 24 b Particle size distribution curve of formulations F3 and F4

Results

		Diam. (nm)	% Intensity	Width (nm)
Z-Average (d.nm): 191.9	Peak 1:	216	100.0	68.7
PdI: 0.109	Peak 2:	0.00	0.0	0.00
Intercept: 0.953	Peak 3:	0.00	0.0	0.00

Result quality : Good

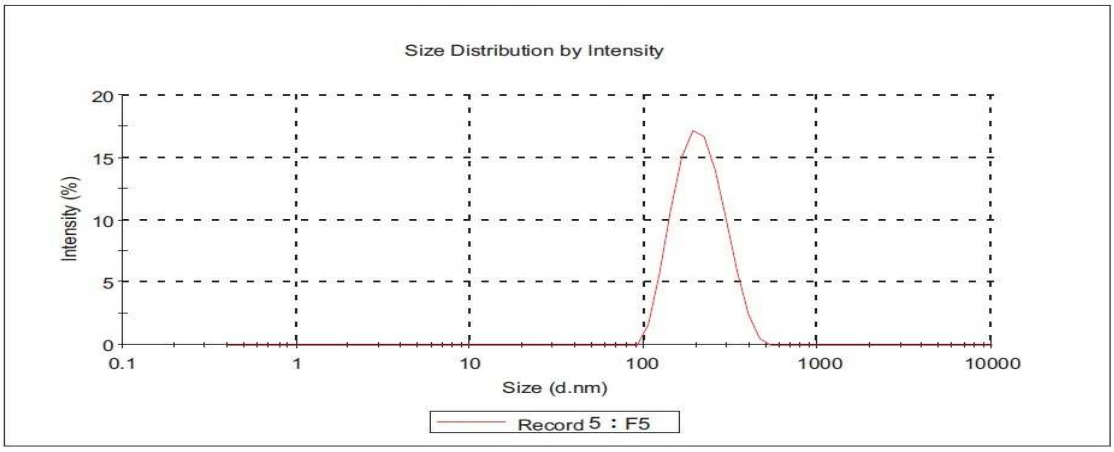

F5 (EL 100 1:50, PLURONIC F68 1%)

Results

		Diam. (nm)	% Intensity	Width (nm)
Z-Average (d.nm): 110.5	Peak 1:	162	100.0	53.5
PdI: 0.095	Peak 2:	0.00	0.0	0.00
Intercept: 0.954	Peak 3:	0.00	0.0	0.00

Result quality : Good

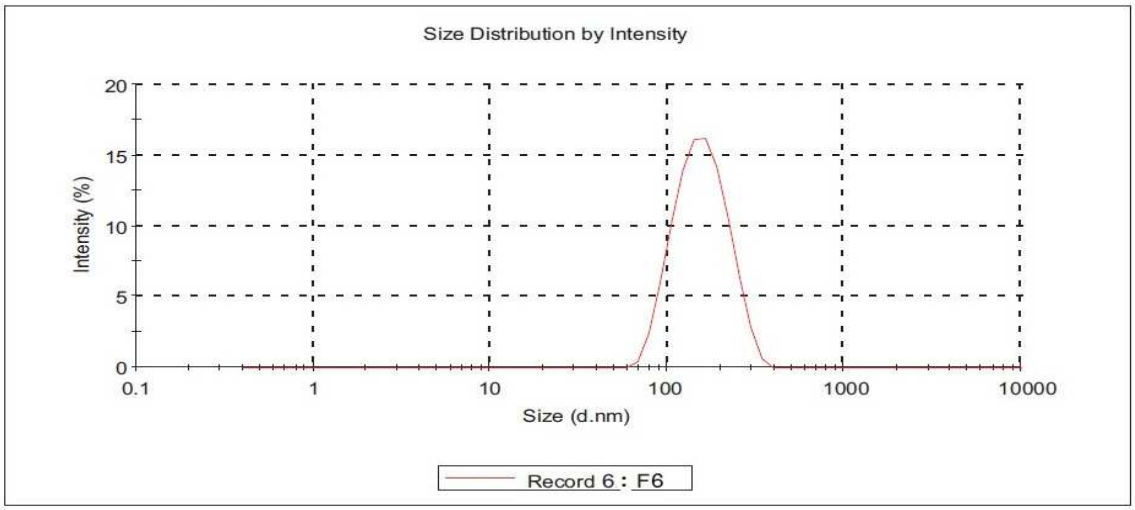

F6 (EL 100 1:10, PLURONIC F68 2%)

Figure 24 c Particle size distribution curve of formulations F5 and F6

Results

		Diam. (nm)	% Intensity	Width (nm)
Z-Average (d.nm): 133.9	Peak 1:	167	88.3	69.2
PdI: 0.159	Peak 2:	0.00	0.0	0.00
Intercept: 0.935	Peak 3:	0.00	0.0	0.00

Result quality : Good

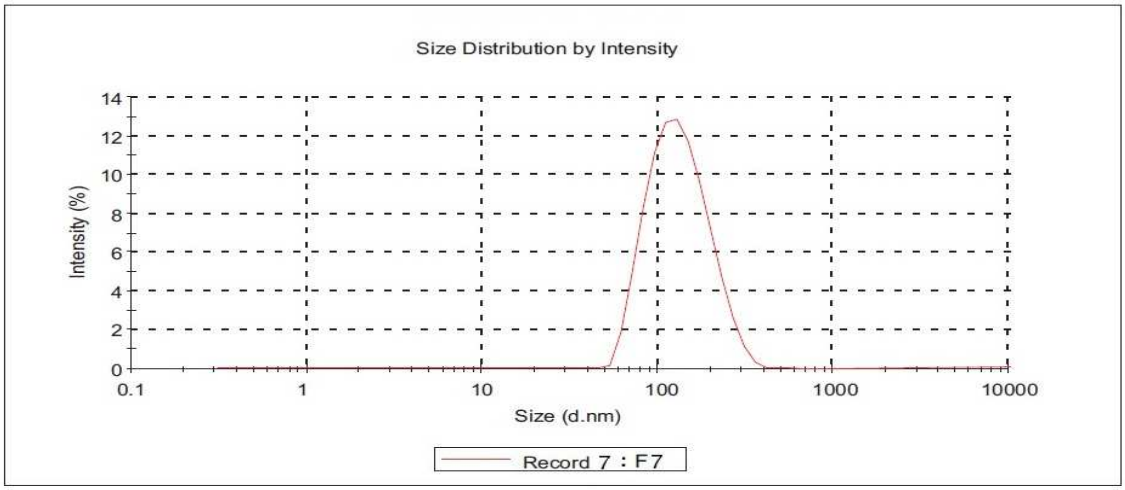

F7 (EL 100 1:20, PLURONIC F68 2%)

Results

		Diam. (nm)	% Intensity	Width (nm)
Z-Average (d.nm): 152.2	Peak 1:	185	100.0	68.7
PdI: 0.132	Peak 2:	0.00	0.0	0.00
Intercept: 0.953	Peak 3:	0.00	0.0	0.00

Result quality : Good

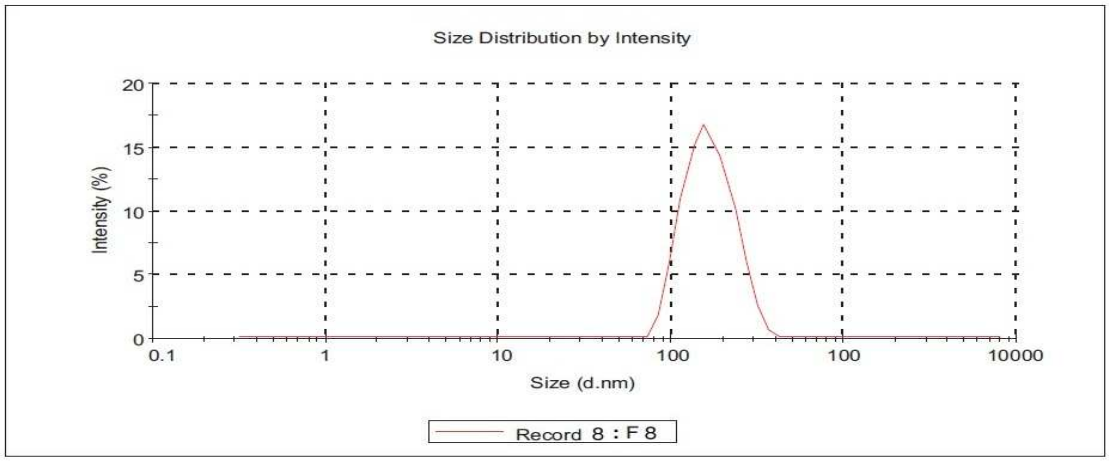

F8 (EL 100 1:30, PLURONIC F68 2%)

Figure 24 d Particle size distribution curve of formulations F7 and F8

Results

		Diam. (nm)	% Intensity	Width (nm)
Z-Average (d.nm): 168.3	Peak 1:	181	100.0	53.5
PdI: 0.123	Peak 2:	0.00	0.0	0.00
Intercept: 0.974	Peak 3:	0.00	0.0	0.00

Result quality : Good

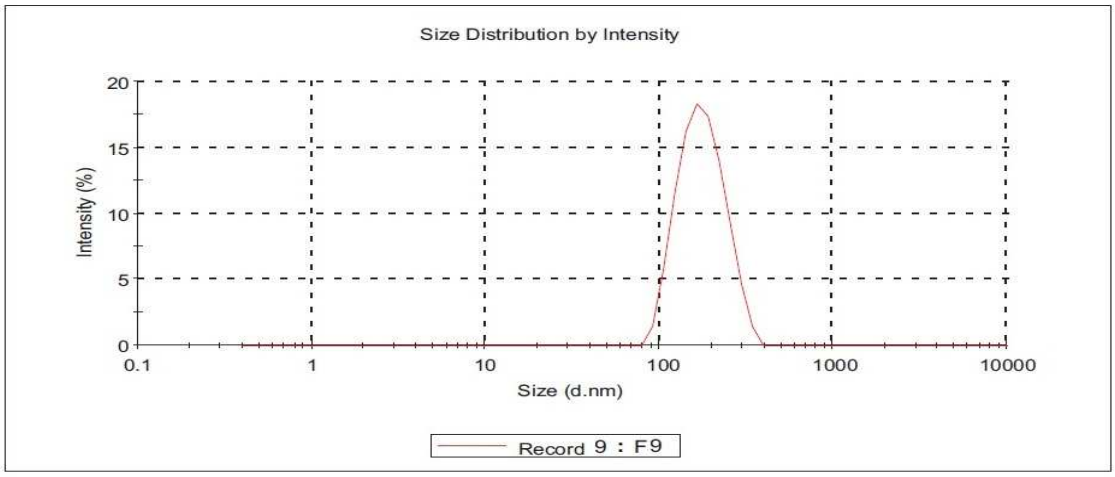

F9 (EL 100 1:40, PLURONIC F68 2%)

Results

		Diam. (nm)	% Intensity	Width (nm)
Z-Average (d.nm): 182.8	Peak 1:	198	98.2	65.7
PdI: 0.192	Peak 2:	0.00	0.0	0.00
Intercept: 0.971	Peak 3:	0.00	0.0	0.00

Result quality : Good

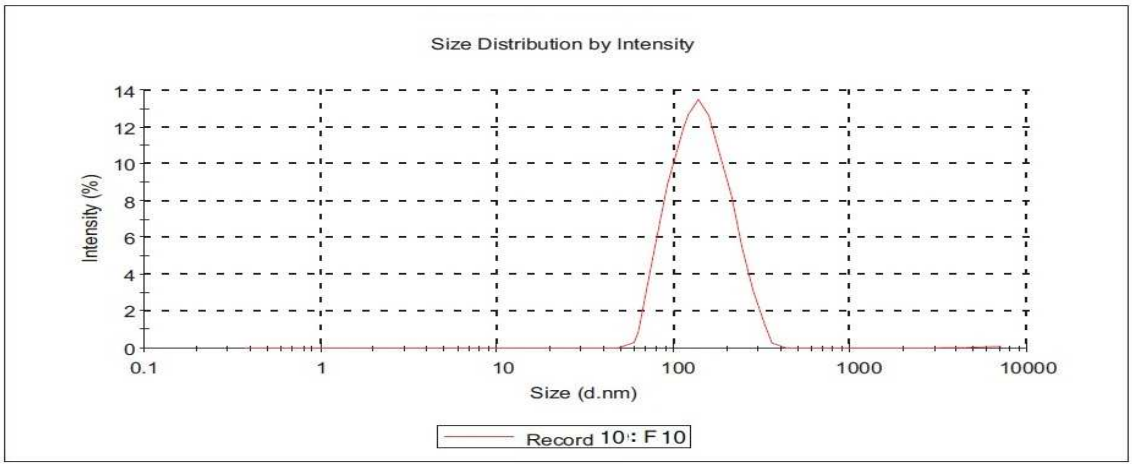

F10 (EL 100 1:50, PLURONIC F68 2%)

Figure 24 e Particle size distribution curve of formulations F9 and F10

Results

		Diam. (nm)	% Intensity	Width (nm)
Z-Average (d.nm): 135.9	Peak 1:	167	88.3	69.2
PdI: 0.159	Peak 2:	0.00	0.0	0.00
Intercept: 0.935	Peak 3:	0.00	0.0	0.00

Result quality : Good

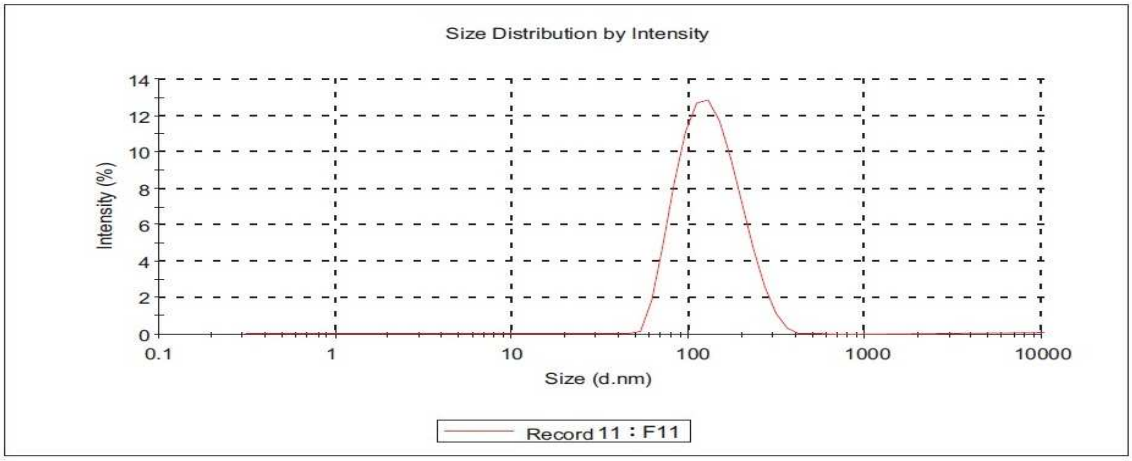

F11 (EL 100 1:10, PVA 1%)

Results

		Diam. (nm)	% Intensity	Width (nm)
Z-Average (d.nm): 151	Peak 1:	179	100	80.0
PdI: 0.161	Peak 2:	0.00	0.0	0.00
Intercept: 0.942	Peak 3:	0.00	0.0	0.00

Result quality : Good

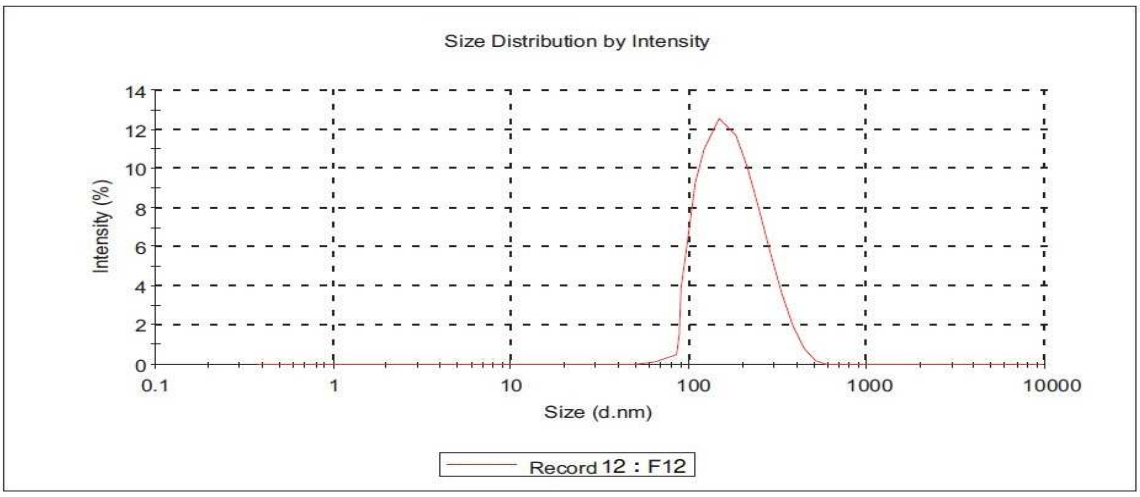

F12 (EL 100 1:20, PVA 1%)

Figure 24 f Particle size distribution curve of formulations F11 and F12

Results

		Diam. (nm)	% Intensity	Width (nm)
Z-Average (d.nm): 174.1	Peak 1:	178	98.7	64.1
PdI: 0.173	Peak 2:	0.00	0.0	0.00
Intercept: 0.985	Peak 3:	0.00	0.0	0.00

Result quality : Good

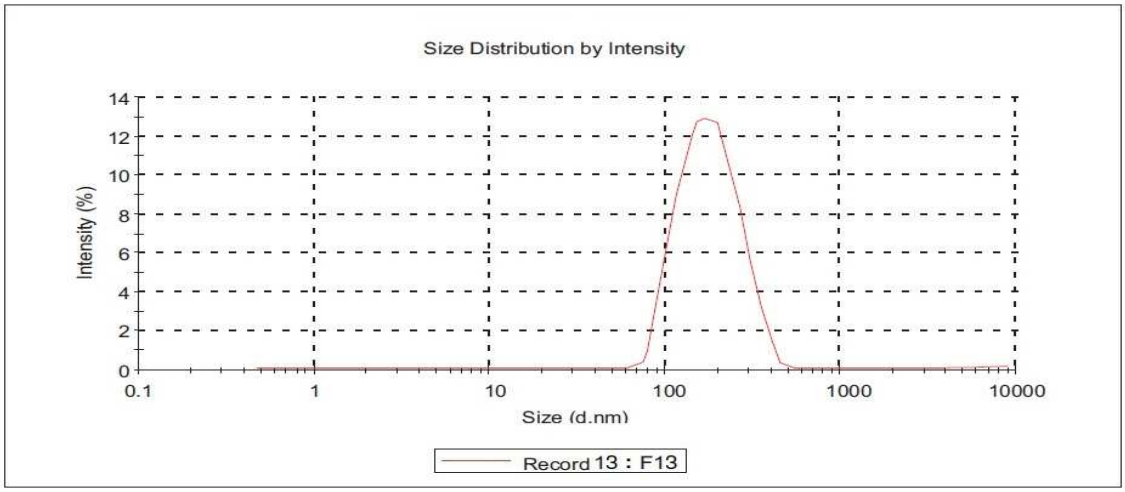

F13 (EL 100 1:30, PLURONIC F68 1%)

Results

		Diam. (nm)	% Intensity	Width (nm)
Z-Average (d.nm): 187	Peak 1:	212	98.4	65.5
PdI: 0.175	Peak 2:	0.00	0.0	0.00
Intercept: 0.976	Peak 3:	0.00	0.0	0.00

Result quality : Good

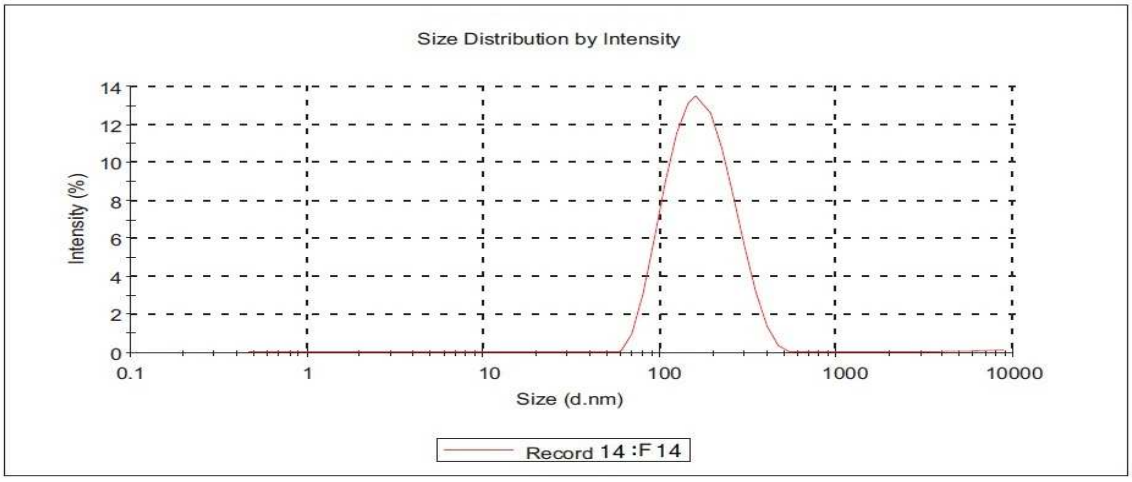

F14 (EL 100 1:40, PVA 1%)

Figure 24 g Particle size distribution curve of formulations F13 and F14

Results

		Diam. (nm)	% Intensity	Width (nm)
Z-Average (d.nm): 209.3	Peak 1:	170.9	100.0	28.79
PdI: 0.192	Peak 2:	0.000	0.0	0.000
Intercept: 0.668	Peak 3:	0.000	0.0	0.000

Result quality : Good

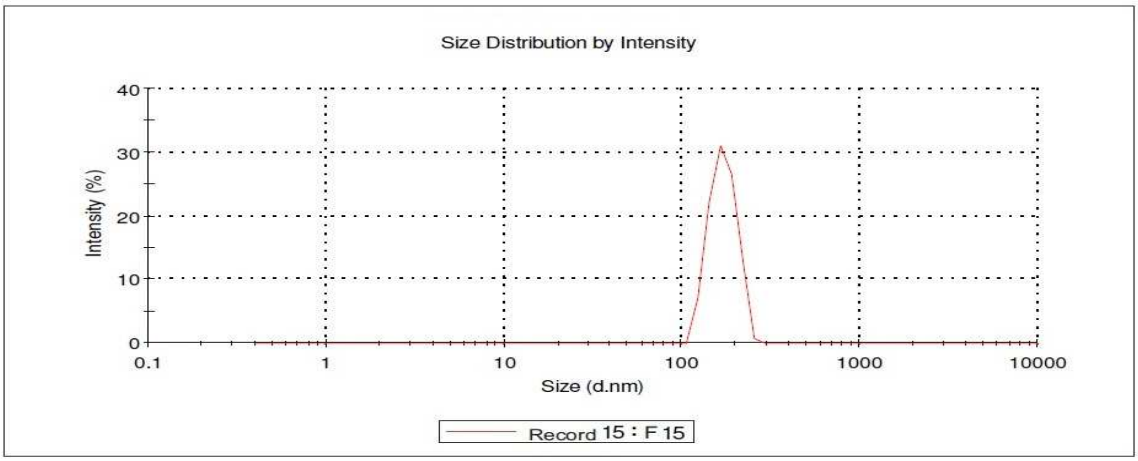

F15 (EL 100 1:50, PVA 1%)

Results

		Diam. (nm)	% Intensity	Width (nm)
Z-Average (d.nm): 127	Peak 1:	142	95.0	54.1
PdI: 0.167	Peak 2:	0.00	0.0	0.00
Intercept: 0.977	Peak 3:	0.00	0.0	0.00

Result quality : Good

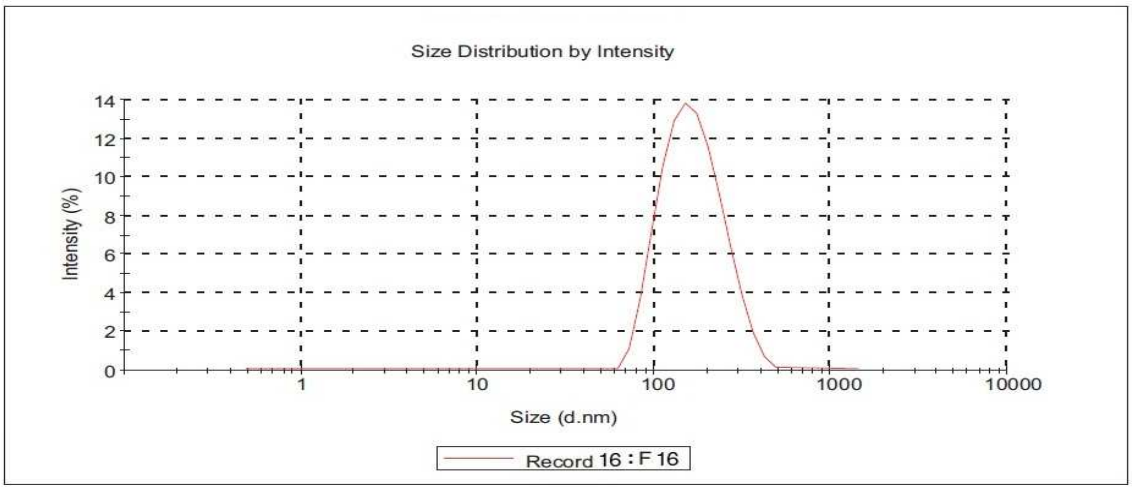

F16 (EL 100 1:10, PVA 2%)

Figure 24 h Particle size distribution curve of formulations F15and F16

Results

		Diam. (nm)	% Intensity	Width (nm)
Z-Average (d.nm): 145	Peak 1:	171	100.0	80.0
PdI: 0.159	Peak 2:	0.00	0.0	0.00
Intercept: 0.954	Peak 3:	0.00	0.0	0.00

Result quality : Good

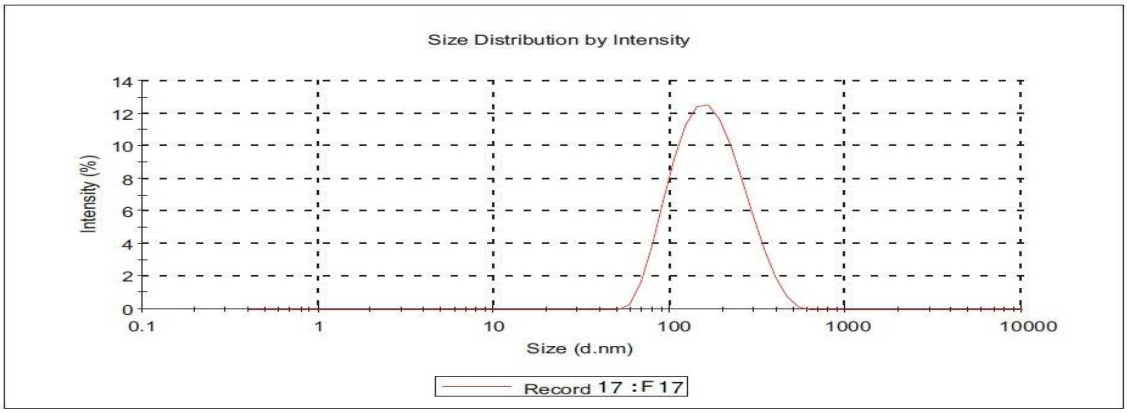

F17 (EL 100 1:20, PVA 2%)

Results

		Diam. (nm)	% Intensity	Width (nm)
Z-Average (d.nm): 168	Peak 1:	181	100.0	53.5
PdI: 0.123	Peak 2:	0.00	0.0	0.00
Intercept: 0.974	Peak 3:	0.00	0.0	0.00

Result quality : Good

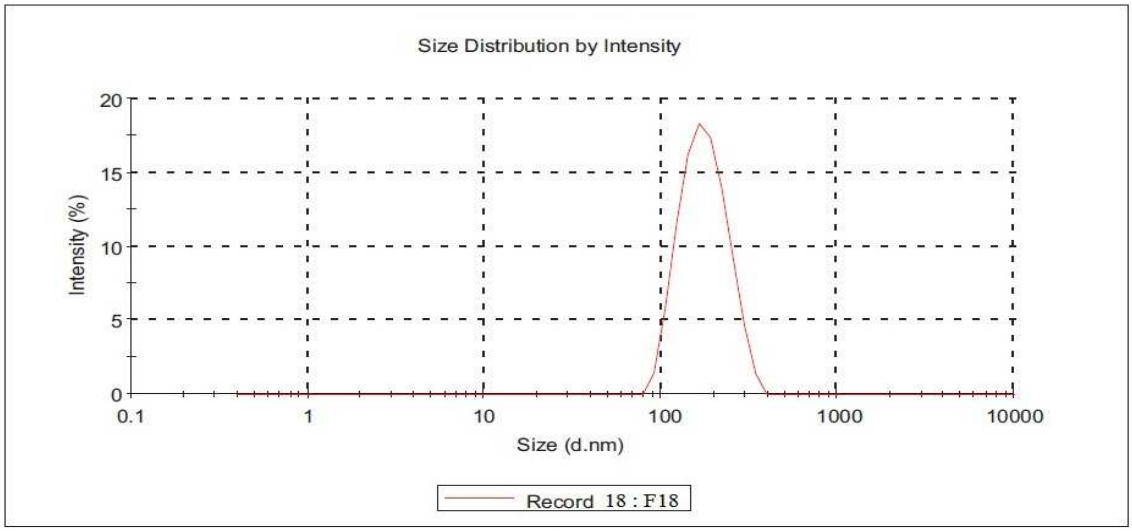

F18 (EL 100 1:30, PVA 2%)

Figure 24 i Particle size distribution curve of formulations F17 and F18

Results

		Diam. (nm)	% Intensity	Width (nm)
Z-Average (d.nm): 174	Peak 1:	178	98.7	64.1
Pdl: 0.173	Peak 2:	0.00	0.0	0.00
Intercept: 0.985	Peak 3:	0.00	0.0	0.00

Result quality : Good

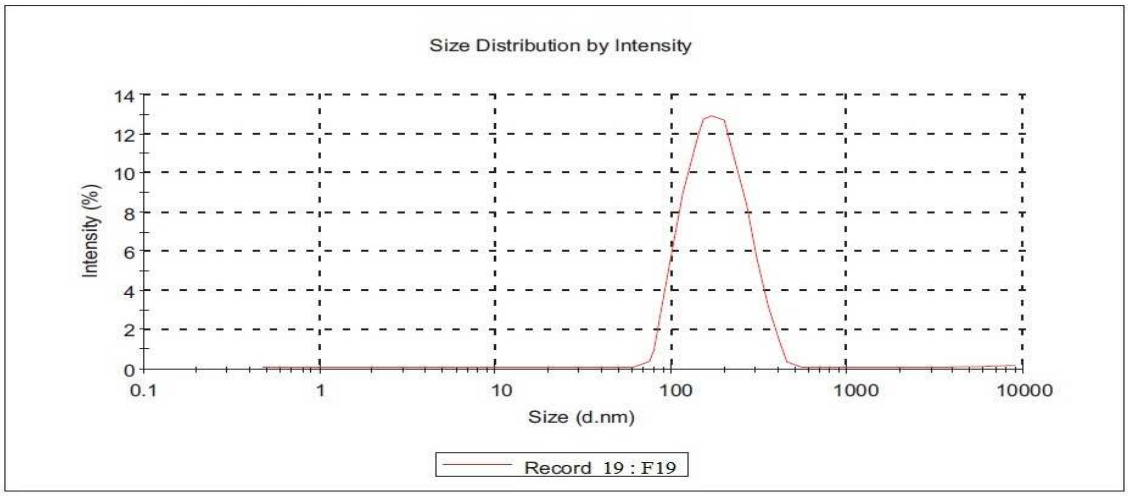

F19 (EL 100 1:40, PVA 2%)

Results

		Diam. (nm)	% Intensity	Width (nm)
Z-Average (d.nm): 190.1	Peak 1:	212	98.4	65.5
Pdl: 0.175	Peak 2:	0.00	0.0	0.00
Intercept: 0.976	Peak 3:	0.00	0.0	0.00

Result quality : Good

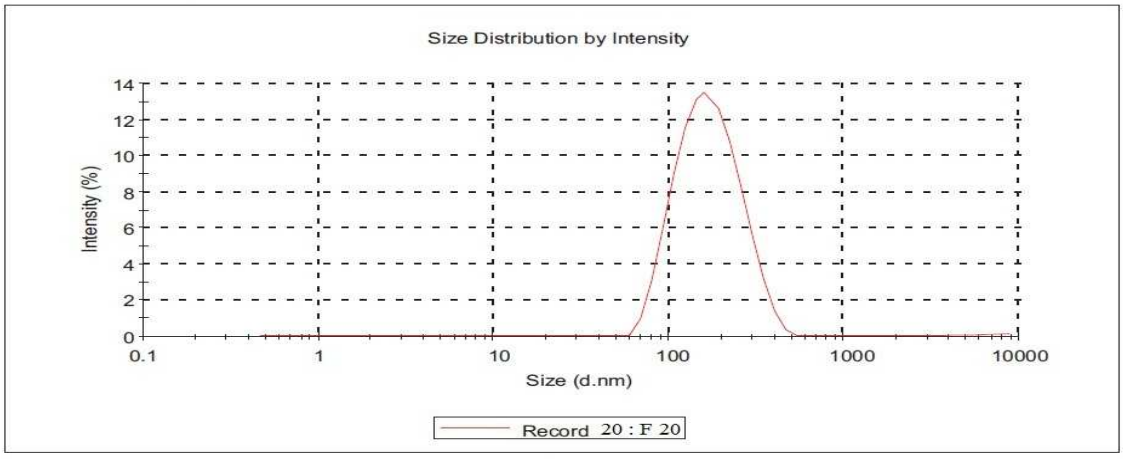

F20 (EL 100 1:50, PVA 2%)

Figure 24 j Particle size distribution curve of formulations F19 and F20

Results

		Diam. (nm)	% Intensity	Width (nm)
Z-Average (d.nm): 139.2	Peak 1:	146	95.3	54.6
PdI: 0.092	Peak 2:	0.00	0.0	0.00
Intercept: 0.969	Peak 3:	0.00	0.0	0.00

Result quality : Good

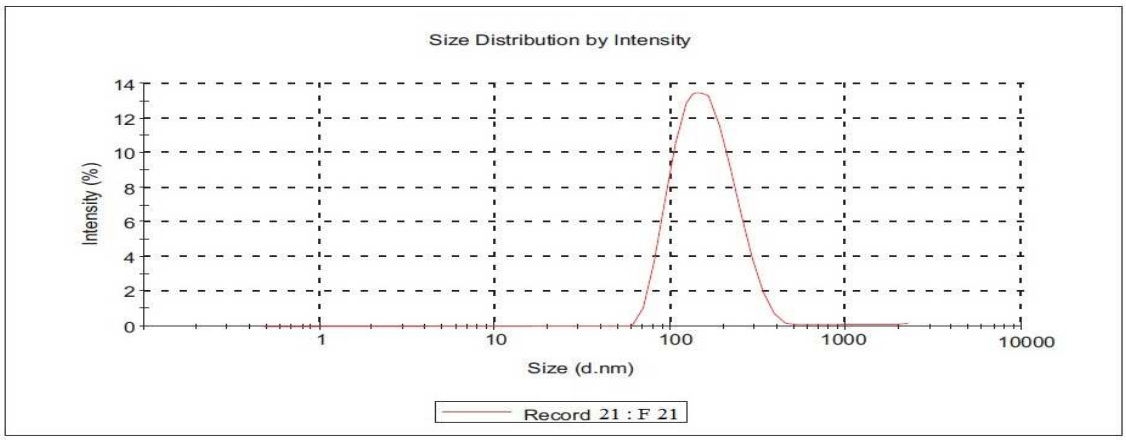

F21 (ES 100 1:10, PLURONIC F68 1%)

Results

		Diam. (nm)	% Intensity	Width (nm)
Z-Average (d.nm): 157.1	Peak 1:	175	98.3	62.2
PdI: 0.174	Peak 2:	0.00	0.0	0.00
Intercept: 0.972	Peak 3:	0.00	0.0	0.00

Result quality : Good

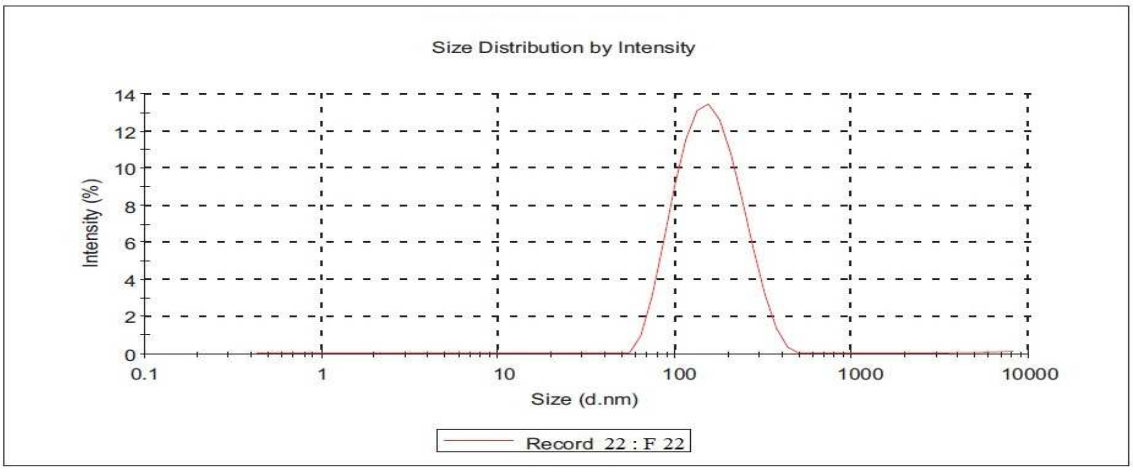

F22 (ES 100 1:20, PLURONIC F68 1%)

Figure 24 k Particle size distribution curve of formulations F21 and F22

Results

		Diam. (nm)	% Intensity	Width (nm)
Z-Average (d.nm): 174.1	Peak 1:	189	100.0	61.3
PdI: 0.164	Peak 2:	0.00	0.0	0.00
Intercept: 0.981	Peak 3:	0.00	0.0	0.00

Result quality : Good

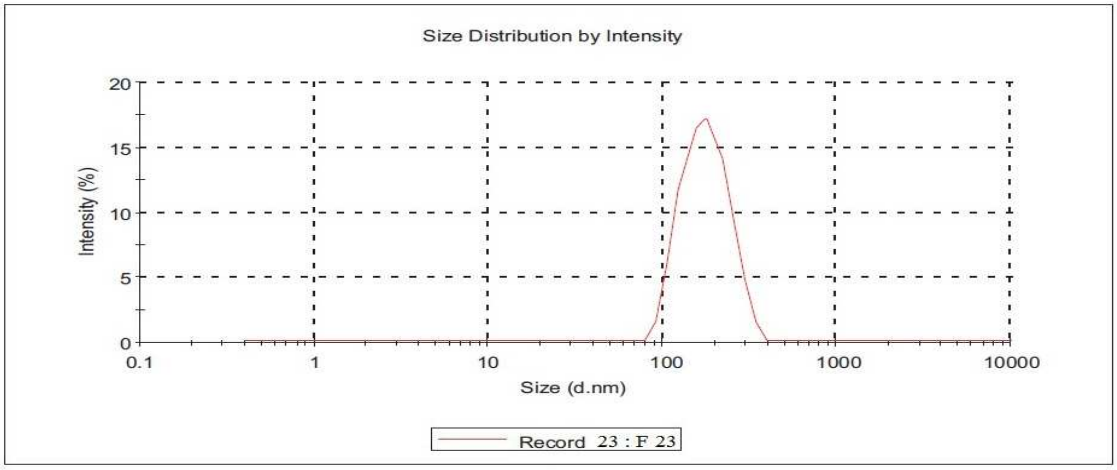

F23 (ES 100 1:30, PLURONIC F68 1%)

Results

		Diam. (nm)	% Intensity	Width (nm)
Z-Average (d.nm): 192	Peak 1:	212	98.4	65.5
PdI: 0.175	Peak 2:	0.00	0.0	0.00
Intercept: 0.976	Peak 3:	0.00	0.0	0.00

Result quality : Good

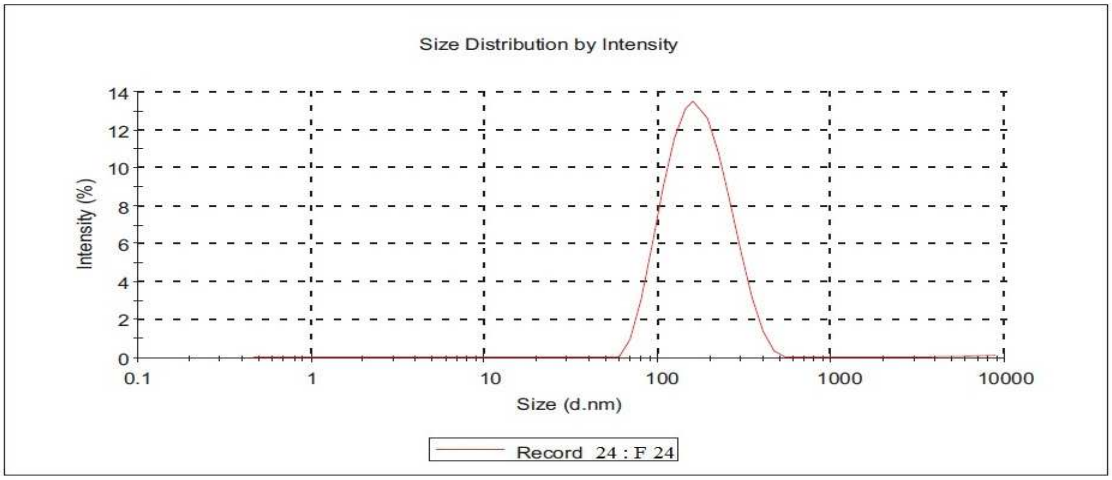

F24 (ES 100 1:140, PLURONIC F68 1%)

Figure 24 l Particle size distribution curve of formulations F23 and F24

Results

		Diam. (nm)	% Intensity	Width (nm)
Z-Average (d.nm): 229.3	Peak 1:	170.9	100.0	28.79
PdI: 0.175	Peak 2:	0.000	0.0	0.000
Intercept: 0.668	Peak 3:	0.000	0.0	0.000

Result quality : Good

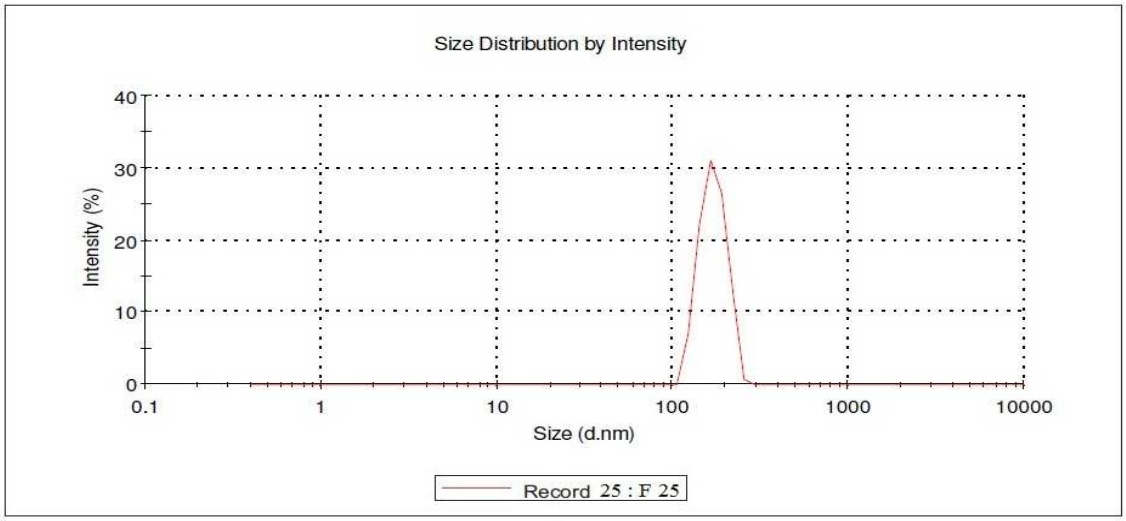

F25 (ES 100 1:50, PLURONIC F68 1%)

Results

		Diam. (nm)	% Intensity	Width (nm)
Z-Average (d.nm): 131	Peak 1:	167	88.3	69.2
PdI: 0.159	Peak 2:	0.00	0.0	0.00
Intercept: 0.935	Peak 3:	0.00	0.0	0.00

Result quality : Good

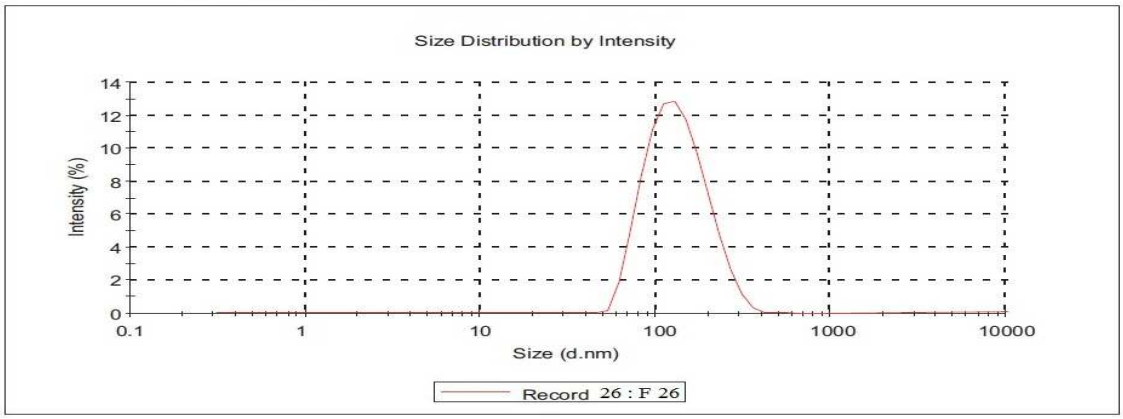

F26 (ES 100 1:10, PLURONIC F68 2%)

Figure 24 m Particle size distribution curve of formulations F25 and F26

Results

		Diam. (nm)	% Intensity	Width (nm)
Z-Average (d.nm): 145	Peak 1:	174	99.1	72.4
PdI: 0.176	Peak 2:	0.00	0.0	0.00
Intercept: 0.945	Peak 3:	0.00	0.0	0.00

Result quality : Good

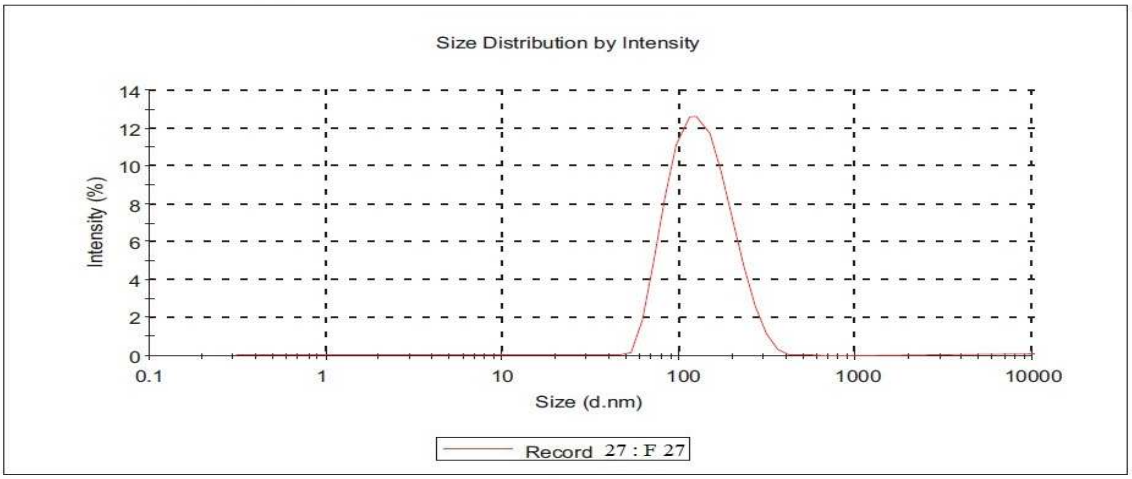

F27 (ES 100 1:20, PLURONIC F68 2%)

Results

		Diam. (nm)	% Intensity	Width (nm)
Z-Average (d.nm): 164	Peak 1:	189	100.0	73.2
PdI: 0.182	Peak 2:	0.00	0.0	0.00
Intercept: 0.987	Peak 3:	0.00	0.0	0.00

Result quality : Good

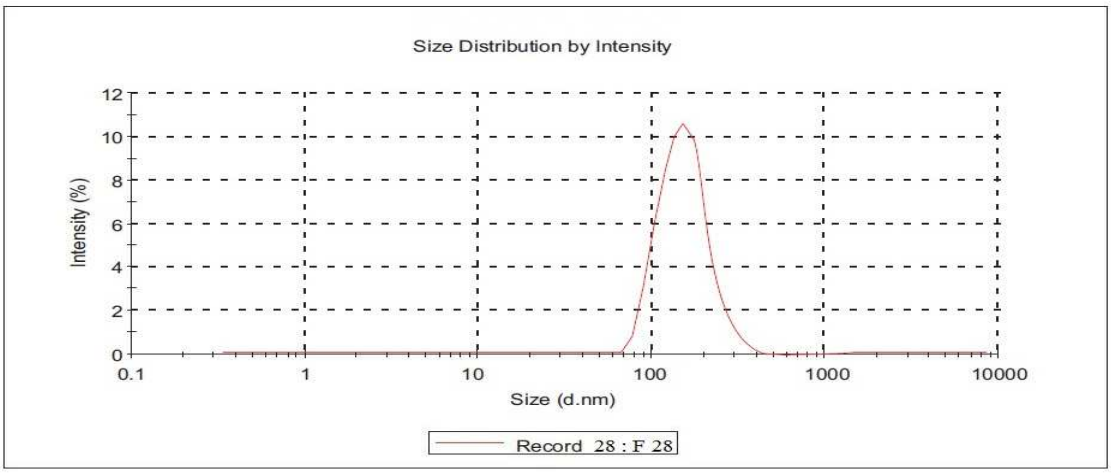

F28 (ES 100 1:30, PLURONIC F68 2%)

Figure 24 n Particle size distribution curve of formulations F27 and F28

Results

		Diam. (nm)	% Intensity	Width (nm)
Z-Average (d.nm): 179	Peak 1:	182	100.0	74.3
PdI: 0.169	Peak 2:	0.00	0.0	0.00
Intercept: 0.987	Peak 3:	0.00	0.0	0.00

Result quality : Good

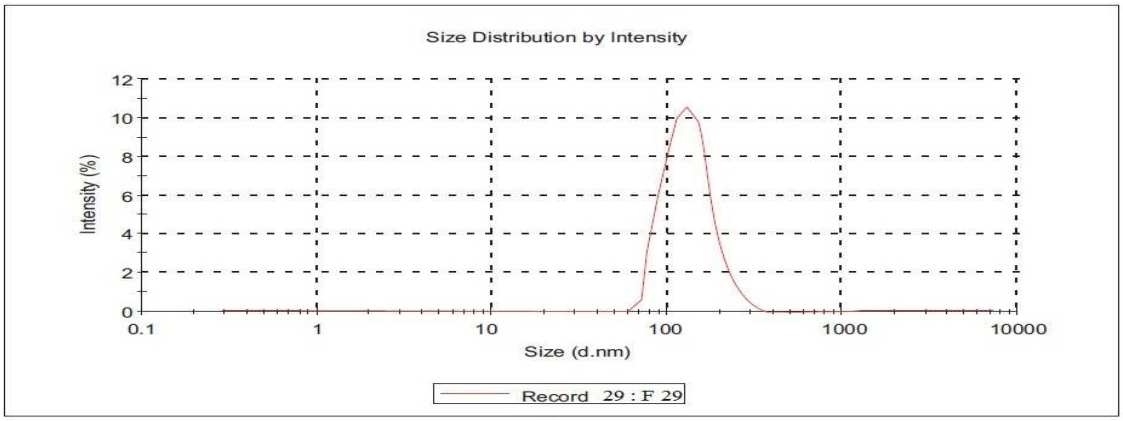

F29 (ES 100 1:40, PLURONIC F68 2%)

Results

		Diam. (nm)	% Intensity	Width (nm)
Z-Average (d.nm): 210.1	Peak 1:	216	100.0	68.7
PdI: 0.109	Peak 2:	0.00	0.0	0.00
Intercept: 0.953	Peak 3:	0.00	0.0	0.00

Result quality : Good

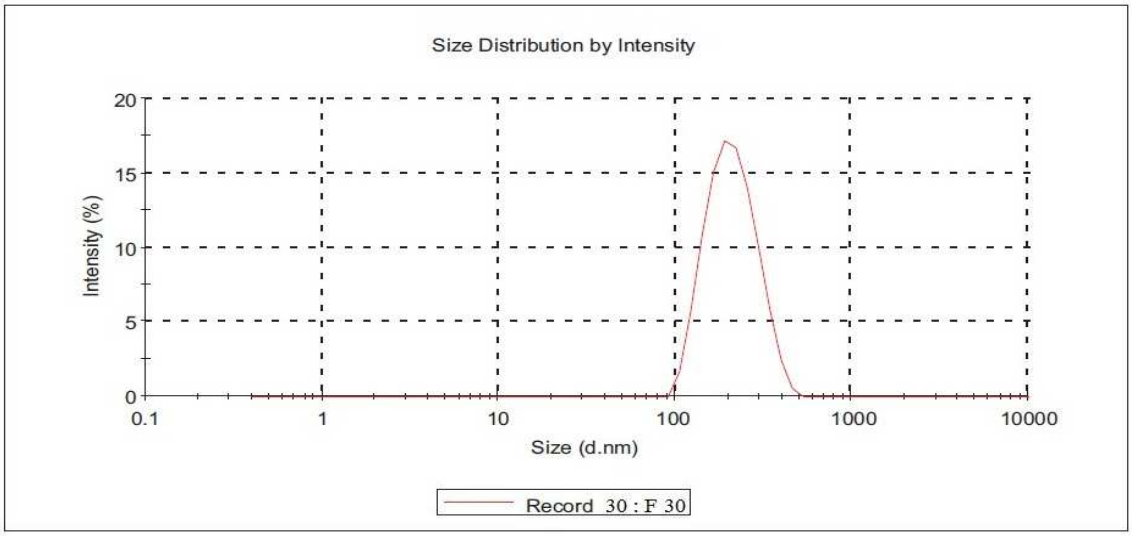

F30 (ES 100 1:50, PLURONIC F68 2%)

Figure 24 o Particle size distribution curve of formulations F29 and F30

Results

		Diam. (nm)	% Intensity	Width (nm)
Z-Average (d.nm): 149	Peak 1:	175	98.5	83.2
PdI: 0.161	Peak 2:	0.00	0.0	0.00
Intercept: 0.942	Peak 3:	0.00	0.0	0.00

Result quality : Good

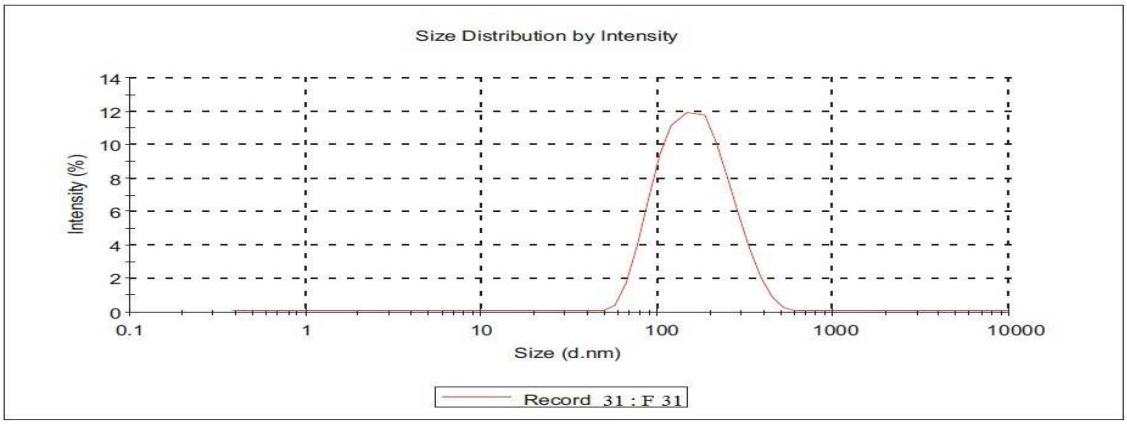

F31 (ES 100 1:10, PVA 1%)

Results

		Diam. (nm)	% Intensity	Width (nm)
Z-Average (d.nm): 161	Peak 1:	179	100.0	52.3
PdI: 0.141	Peak 2:	0.00	0.0	0.00
Intercept: 0.961	Peak 3:	0.00	0.0	0.00

Result quality : Good

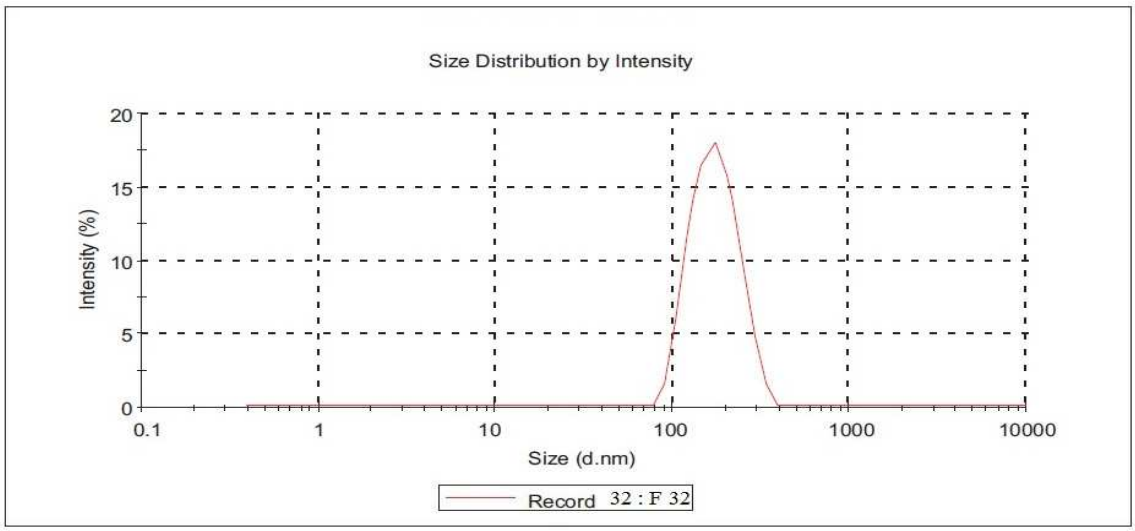

F32 (ES 100 1:20, PVA 1%)

Figure 24 p Particle size distribution curve of formulations F31 and F32

Results

		Diam. (nm)	% Intensity	Width (nm)
Z-Average (d.nm): 178	Peak 1:	192	100	83.0
PdI: 0.094	Peak 2:	0.00	0.0	0.00
Intercept: 0.969	Peak 3:	0.00	0.0	0.00

Result quality : Good

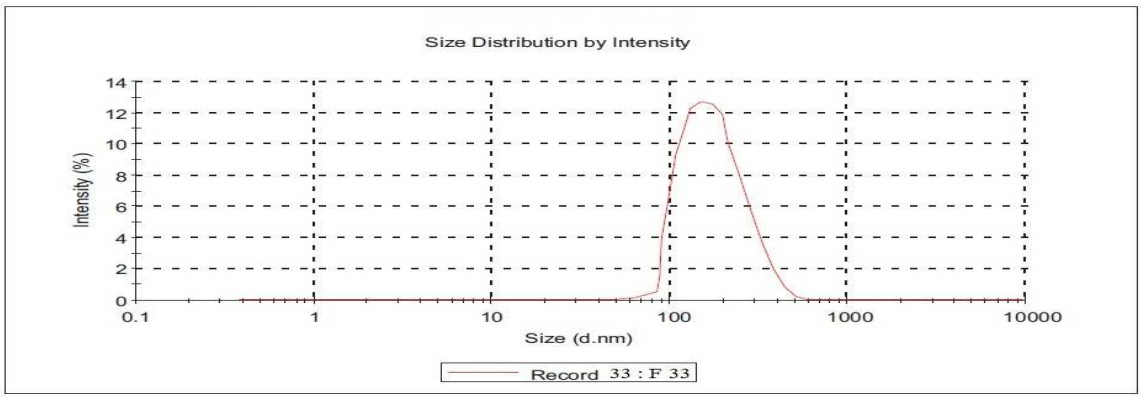

F33 (ES 100 1:30, PVA 1%)

Results

		Diam. (nm)	% Intensity	Width (nm)
Z-Average (d.nm): 199	Peak 1:	216	100.0	68.7
PdI: 0.109	Peak 2:	0.00	0.0	0.00
Intercept: 0.953	Peak 3:	0.00	0.0	0.00

Result quality : Good

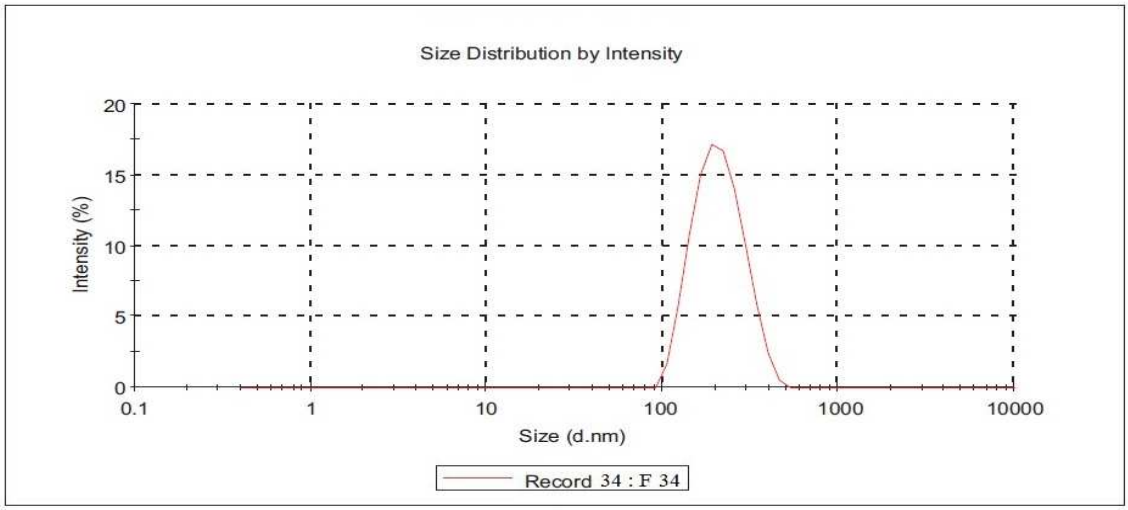

F34 (ES 100 1:40, PVA 1%)

Figure 24 q Particle size distribution curve of formulations F33 and F34

Results

		Diam. (nm)	% Intensity	Width (nm)
Z-Average (d.nm): 231	Peak 1:	212	98.4	65.5
PdI: 0.175	Peak 2:	0.00	0.0	0.00
Intercept: 0.976	Peak 3:	0.00	0.0	0.00
Result quality : Good				

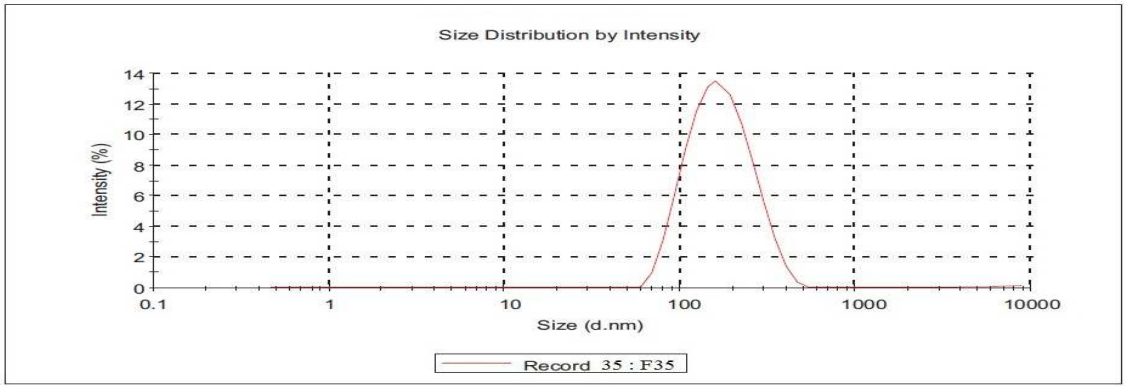

F35 (ES 100 1:50, PVA 1%)

Results

		Diam. (nm)	% Intensity	Width (nm)
Z-Average (d.nm): 137	Peak 1:	174	98.3	71.2
PdI: 0.163	Peak 2:	0.00	0.0	0.00
Intercept: 0.935	Peak 3:	0.00	0.0	0.00
Result quality : Good				

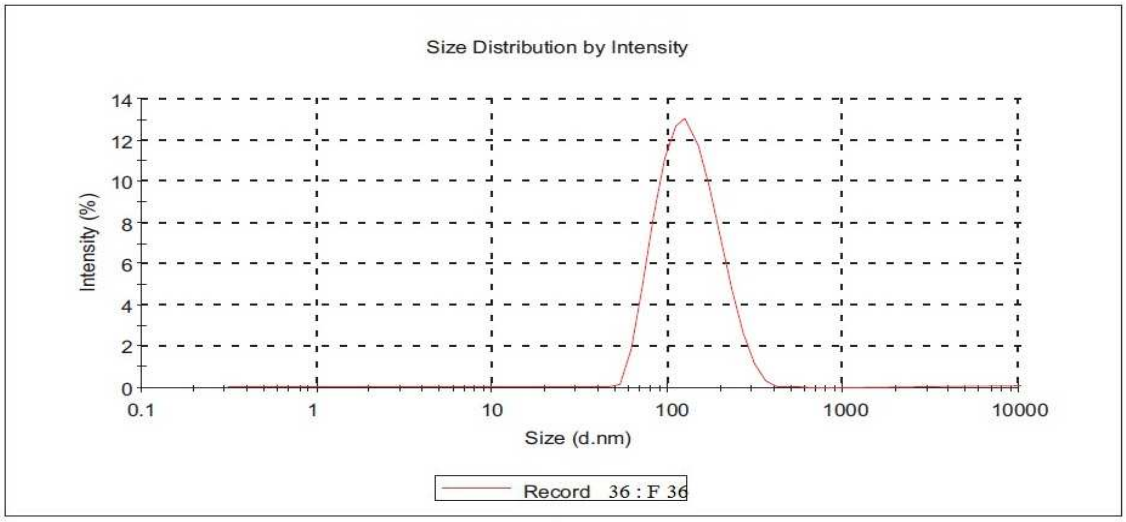

F36 (ES 100 1:10, PVA 2%)

Figure 24 r Particle size distribution curve of formulations F35 and F36

Results

		Diam. (nm)	% Intensity	Width (nm)
Z-Average (d.nm): 159	Peak 1:	186	100.0	80.0
PdI: 0.093	Peak 2:	0.00	0.0	0.00
Intercept: 0.961	Peak 3:	0.00	0.0	0.00

Result quality : Good

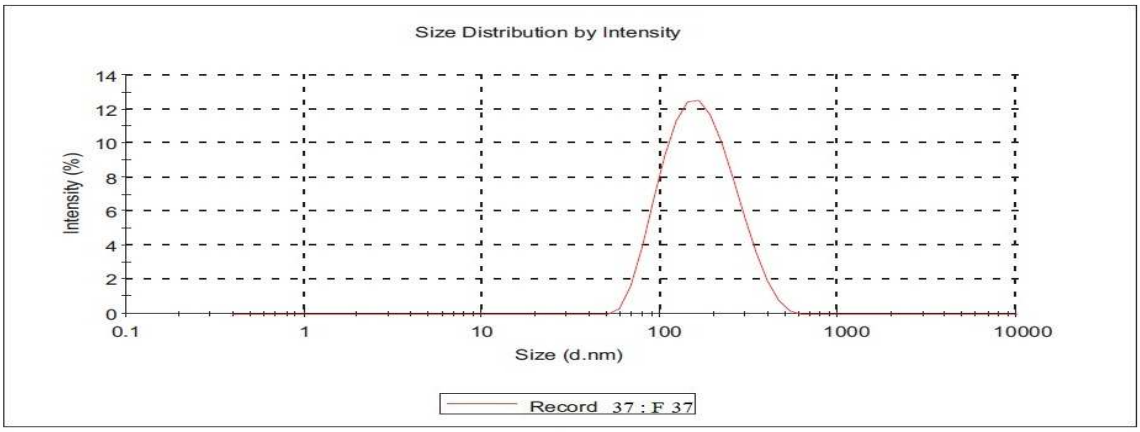

F37 (ES 100 1:20, PVA 2%)

Results

		Diam. (nm)	% Intensity	Width (nm)
Z-Average (d.nm): 165	Peak 1:	184	100.0	53.5
PdI: 0.135	Peak 2:	0.00	0.0	0.00
Intercept: 0.971	Peak 3:	0.00	0.0	0.00

Result quality : Good

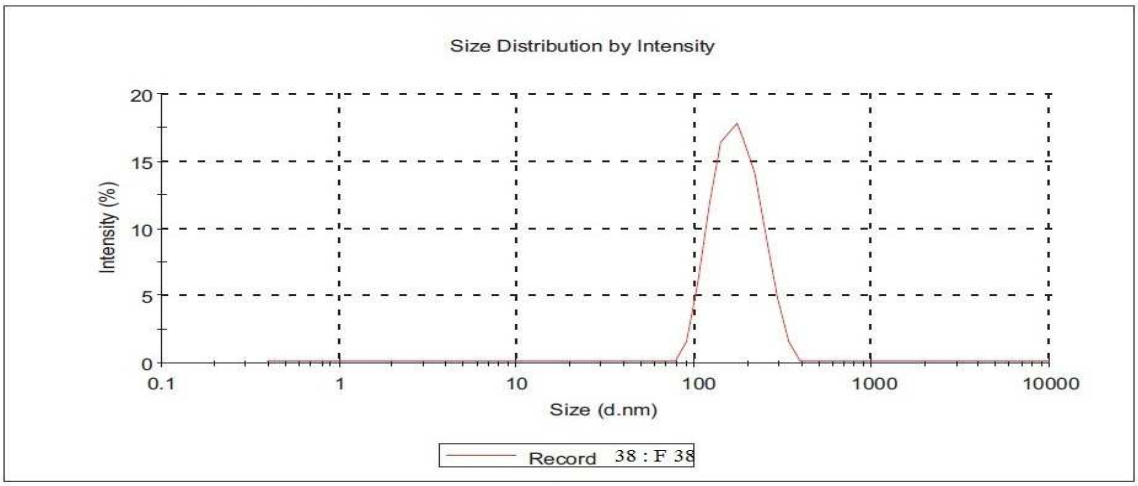

F38 (ES 100 1:30, PVA 2%)

Figure 24 s Particle size distribution curve of formulations F37 and 38

Results

		Diam. (nm)	% Intensity	Width (nm)
Z-Average (d.nm): 192.1	Peak 1:	212	98.4	65.5
PdI: 0.175	Peak 2:	0.00	0.0	0.00
Intercept: 0.976	Peak 3:	0.00	0.0	0.00

Result quality : Good

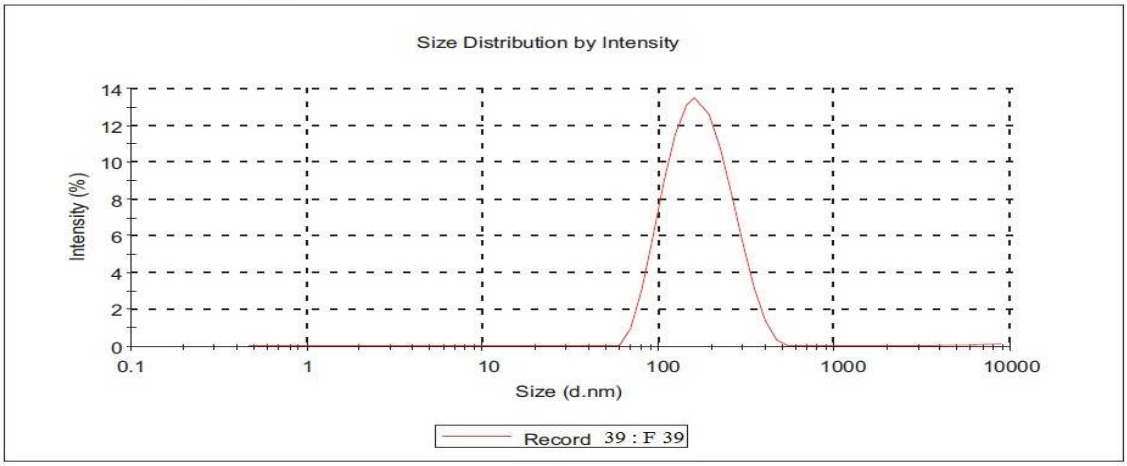

F39 (ES 100 1:40, PVA 2%)

Results

		Diam. (nm)	% Intensity	Width (nm)
Z-Average (d.nm): 229.5	Peak 1:	170.9	100.0	28.79
PdI: 0.175	Peak 2:	0.000	0.0	0.000
Intercept: 0.668	Peak 3:	0.000	0.0	0.000

Result quality : Good

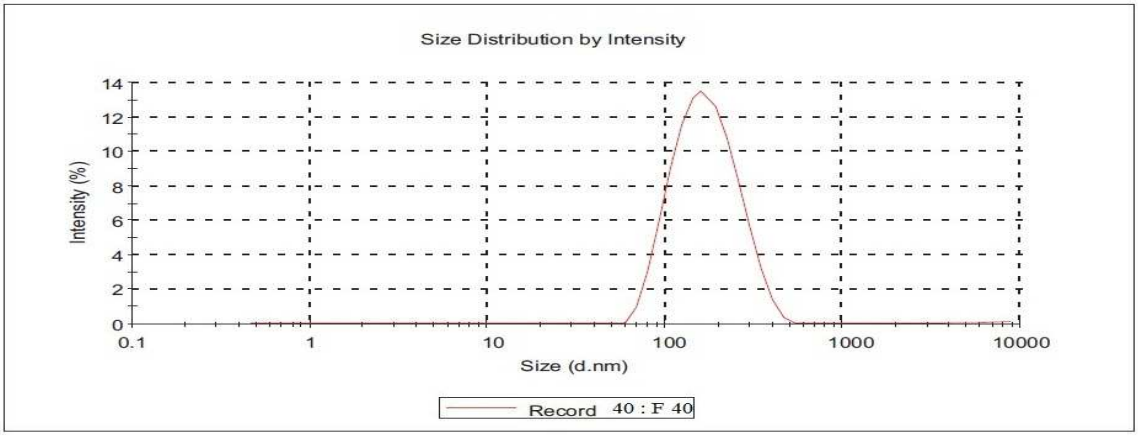

F40 (ES 100 1:50, PVA 2%)

Figure 24 t Particle size distribution curve of formulations F39 and F40

.

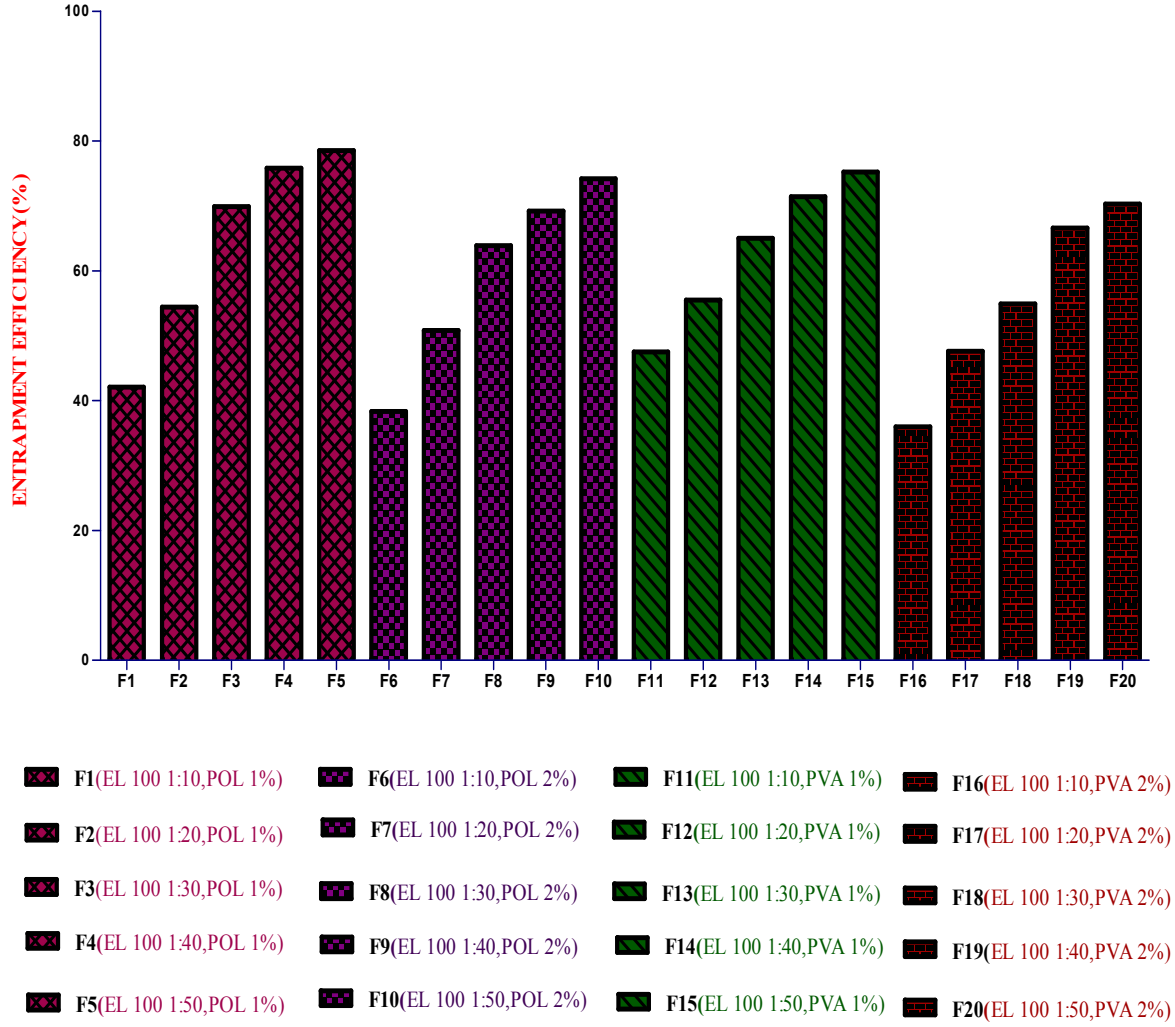

Figure 25 a Entrapment Efficiencies of Rosuvastatin Calcium Loaded EL 100 Nanoparticles

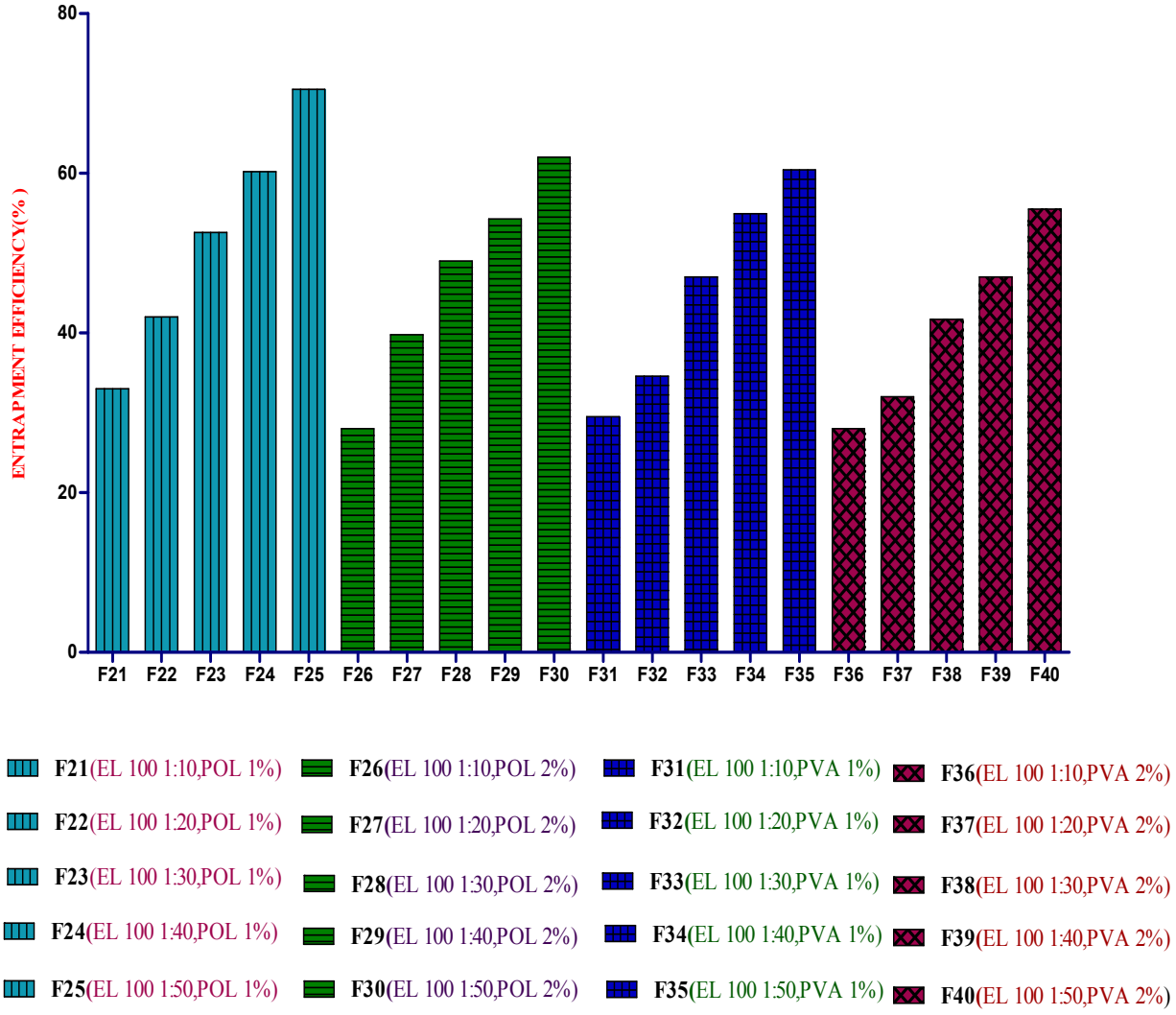

Figure 25 b Entrapment Efficiencies of Rosuvastatin Calcium Loaded ES 100 Nanoparticles

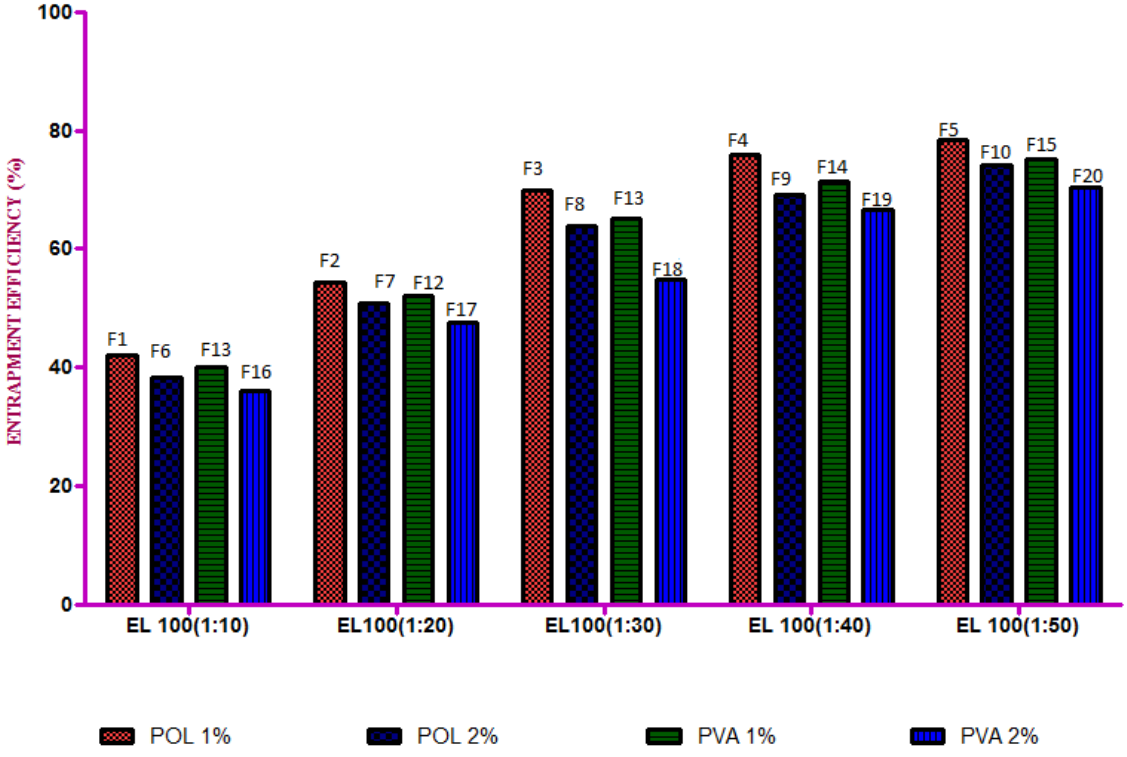

Figure 25 c Effect of Different Stabilizers at Different Concentrations on the Drug Entrapment Efficiencies of Rosuvastatin Calcium Loaded EL 100 Nanoparticles

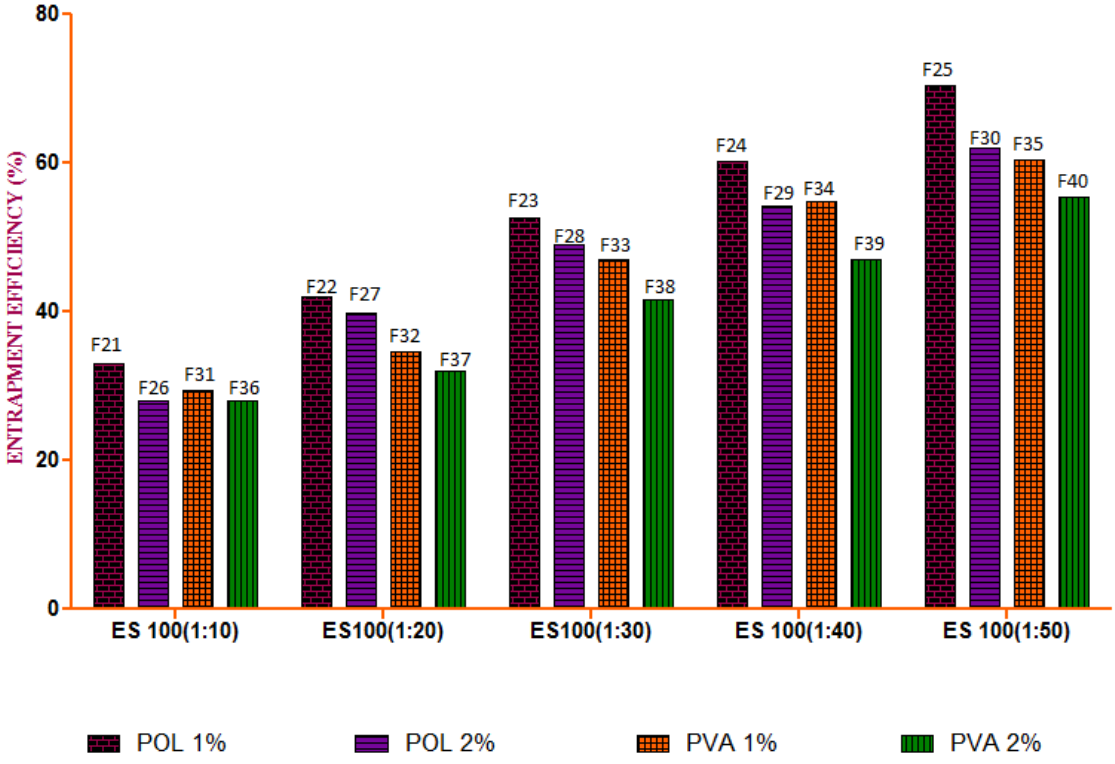

Figure 25 d Effect of Different Stabilizers at Different Concentrations on The Drug Entrapment Efficiencies of Rosuvastatin Calcium Loaded ES 100 Nanoparticles.

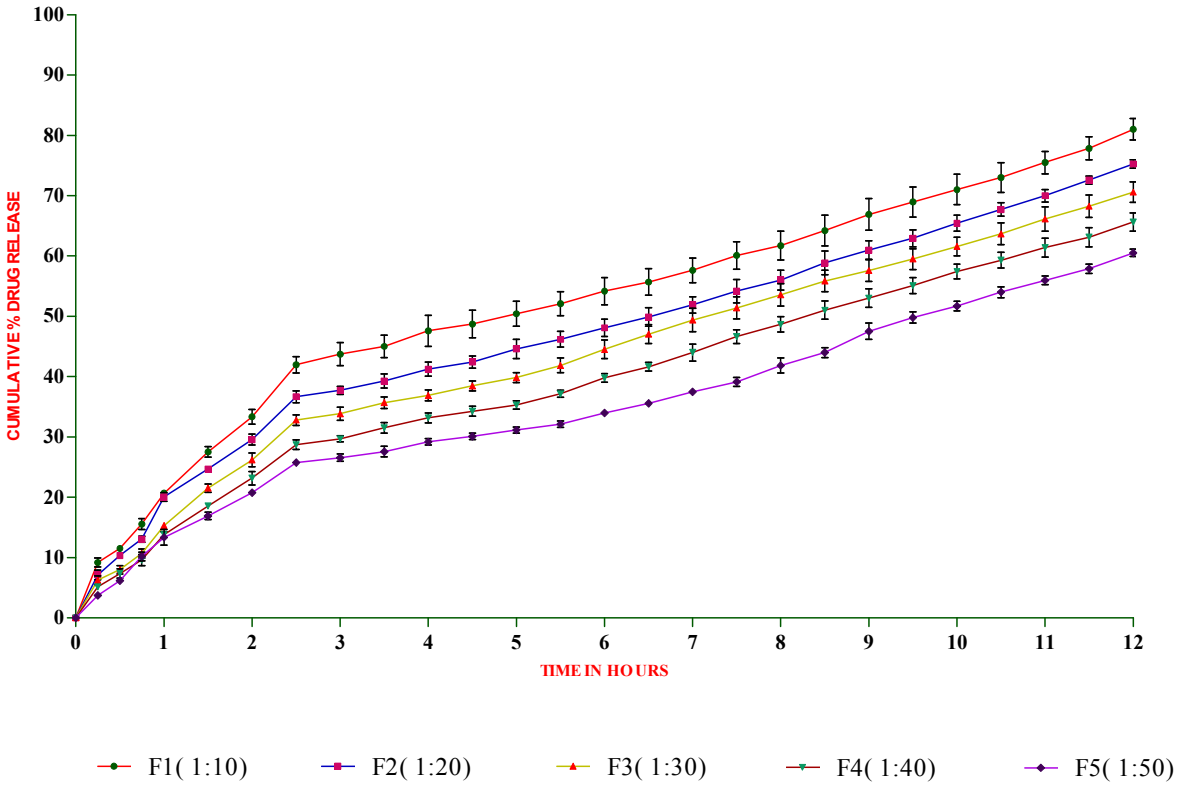

Figure 26 a Comparison of *Invitro* Release Profile of Rosuvastatin Calcium Loaded EL 100 Nanoparticles Containing Pluronic F68 1% Stabilizer

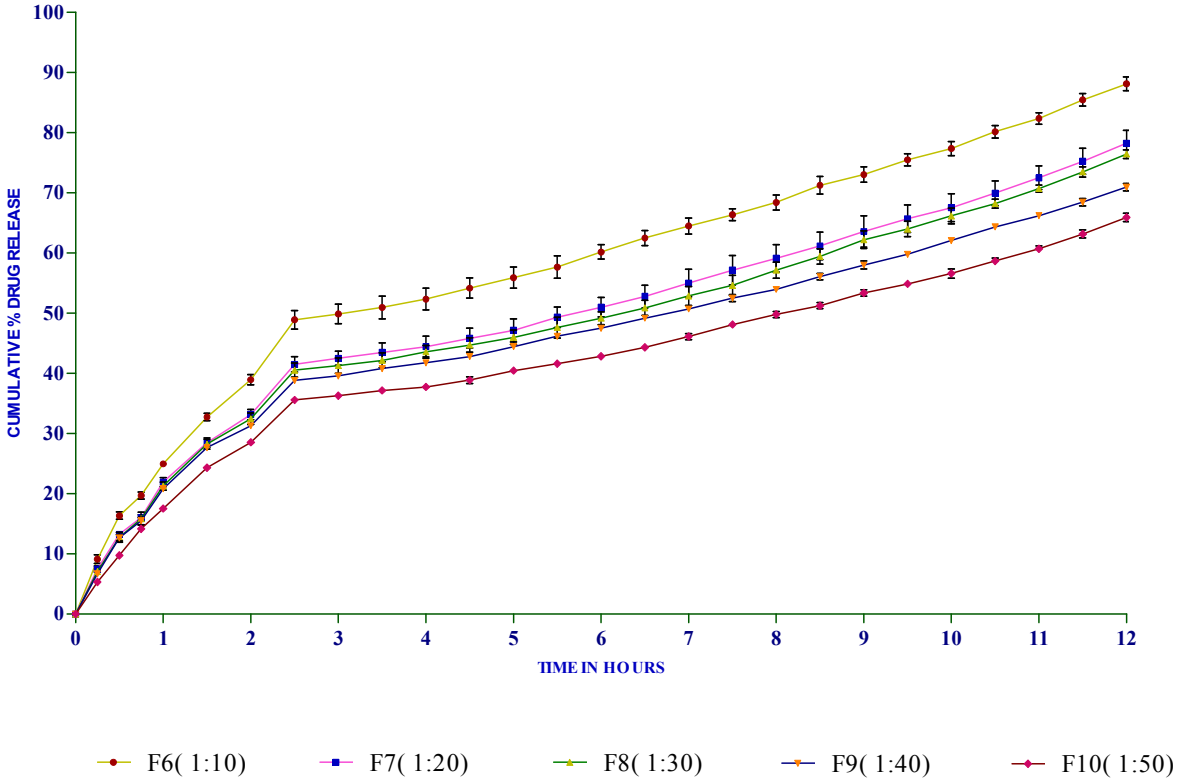

Figure 26 b Comparison of *Invitro* Release Profile of Rosuvastatin Calcium Loaded EL 100 Nanoparticles Containing Pluronic F68 2% as Stabilizer

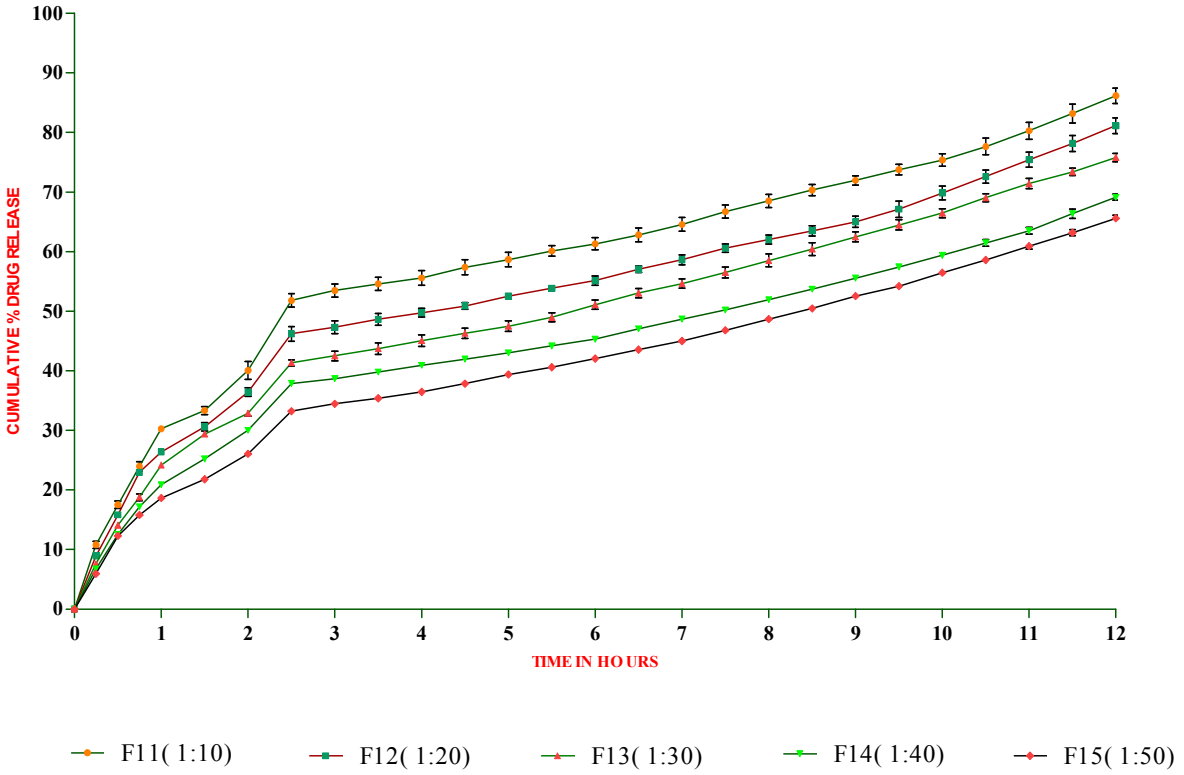

Figure 26 c Comparison of *Invitro* Release Profile of Rosuvastatin Calcium Loaded EL 100 Nanoparticles Containing PVA 1% as Stabilizer

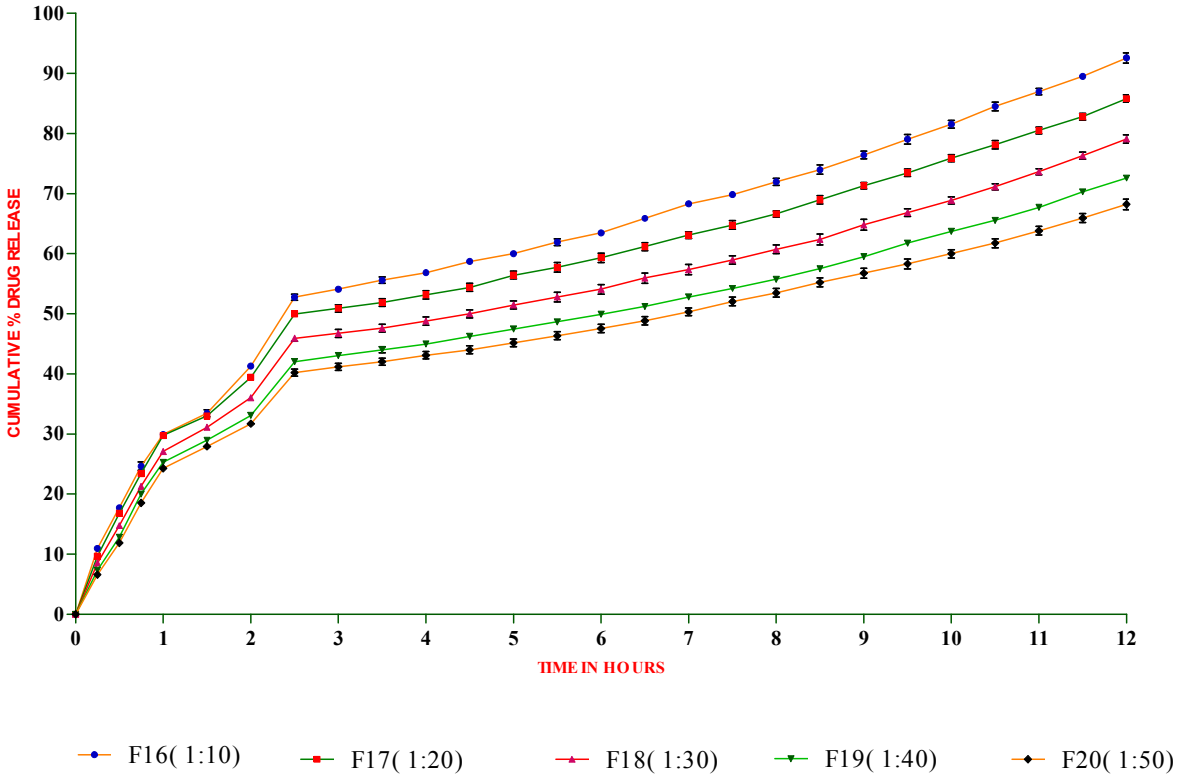

Figure 26 d Comparison of *Invitro* Release Profile of Rosuvastatin Calcium Loaded EL 100 Nanoparticles Containing PVA 2% as Stabilizer

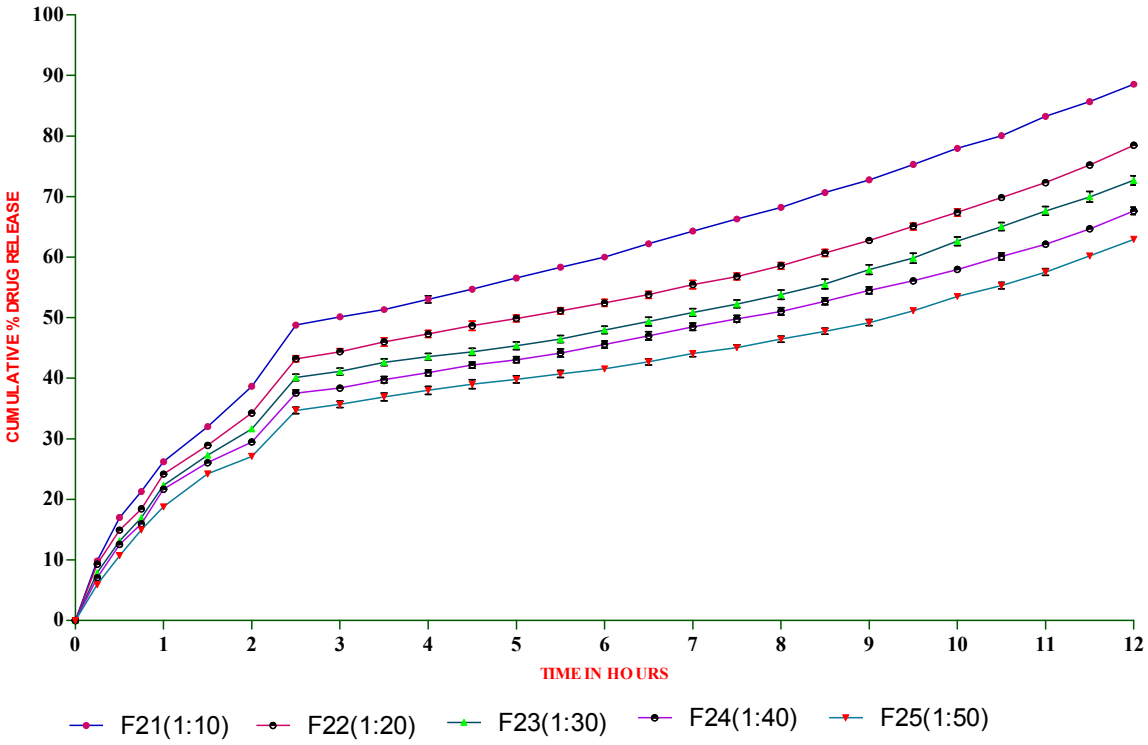

Figure 26 e Comparison of *Invitro* Release Profile of Rosuvastatin Calcium Loaded ES 100 Nanoparticles Containing Pluronic F68 1% as Stabilizer

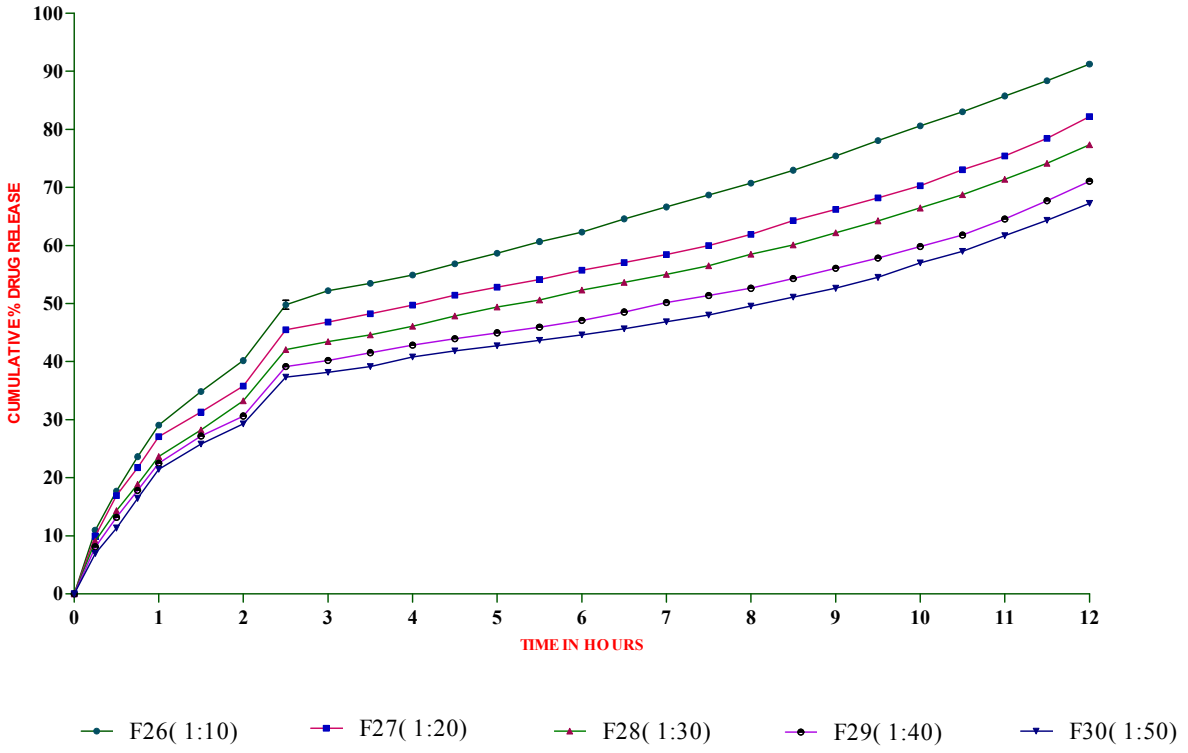

Figure 26 f Comparison of *Invitro* Release Profile of Rosuvastatin Calcium Loaded ES 100 Nanoparticles Containing Pluronic F68 2% as Stabilizer

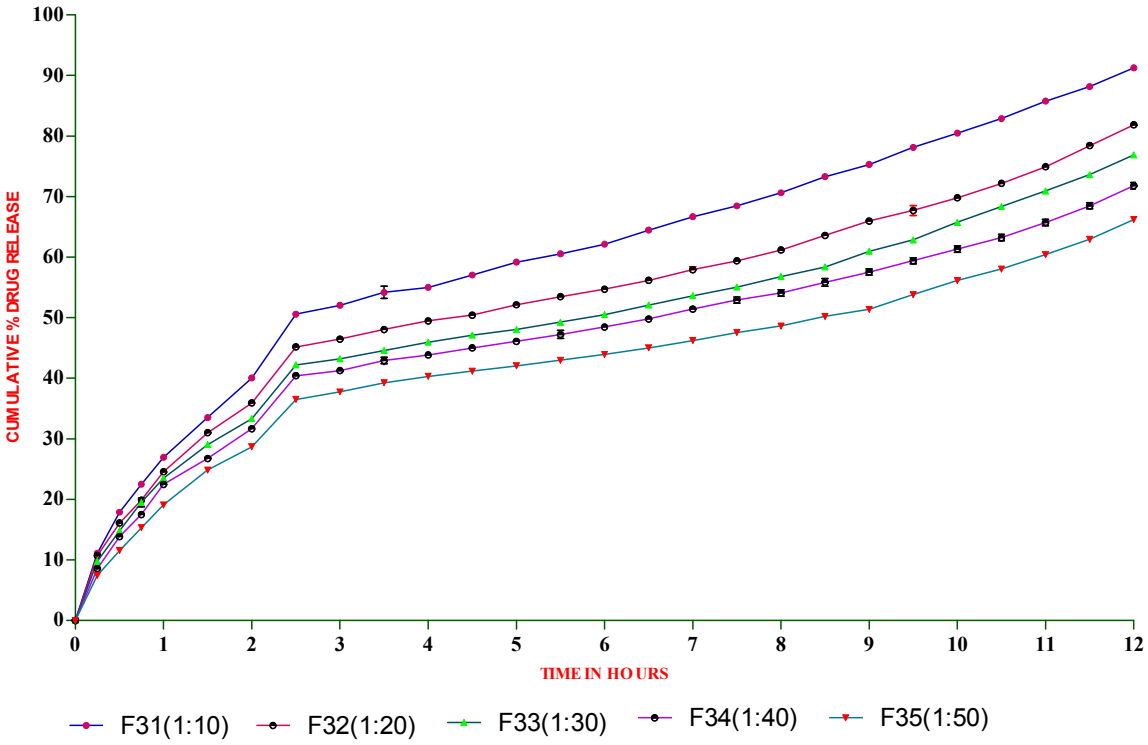

Figure 26 g Comparison of *Invitro* Release Profile of Rosuvastatin Calcium Loaded ES 100 Nanoparticles Containing PVA 1% as Stabilizer

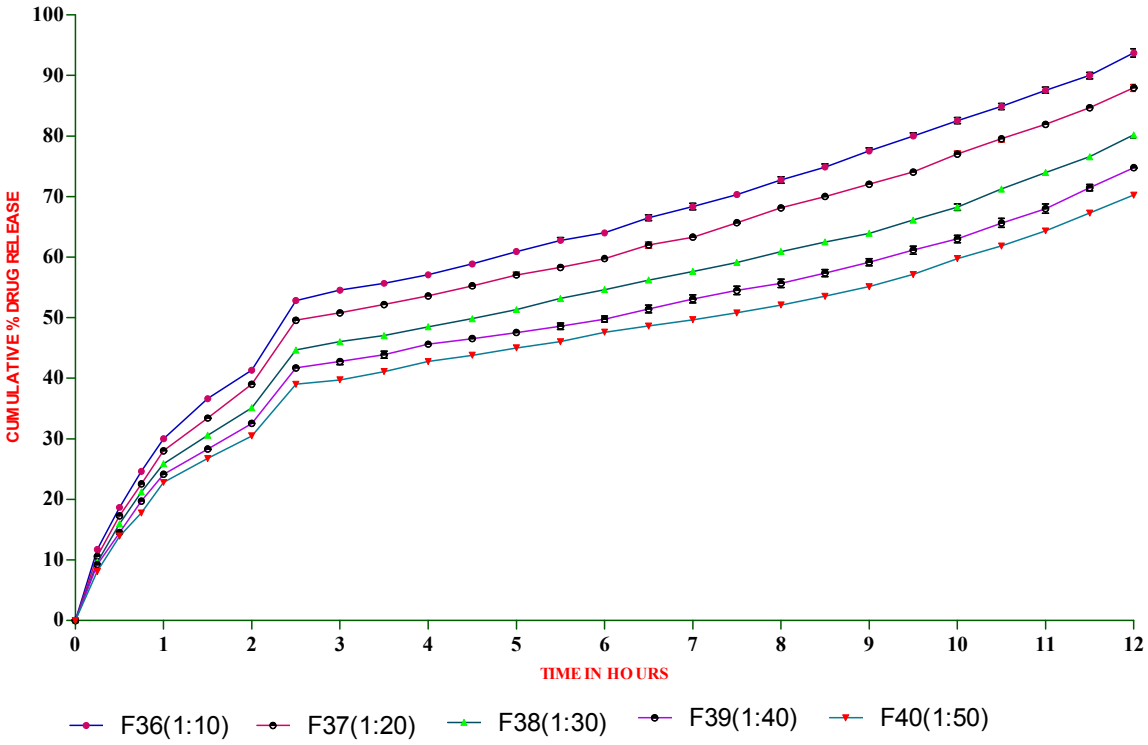

Figure 26 h Comparison of Invitro Release Profile of Rosuvastatin Calcium Loaded ES 100 Nanoparticles Containing PVA 2% as Stabilizer

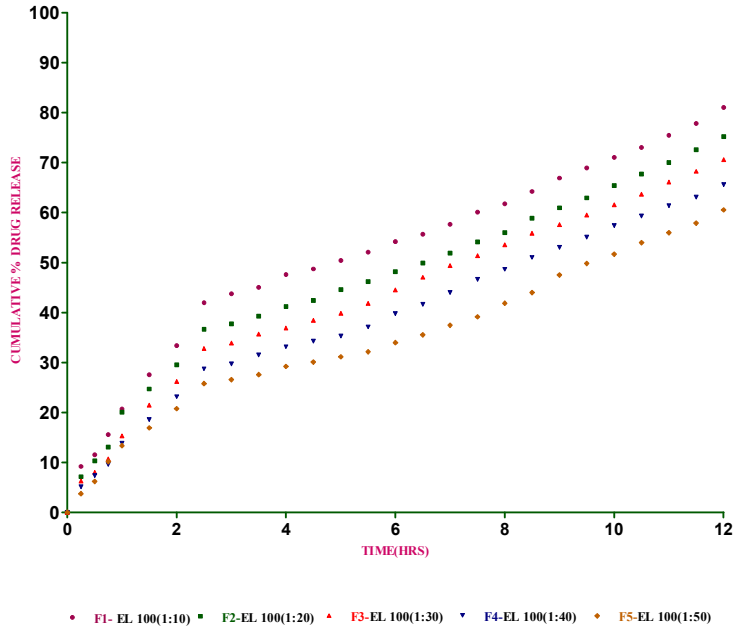

Figure 27 a **Comparison of *Invitro* Zero Order Release Kinetics of Eudragit L100 at Different Ratios Containing Pluronic F68 (1%) as Stabilizer**

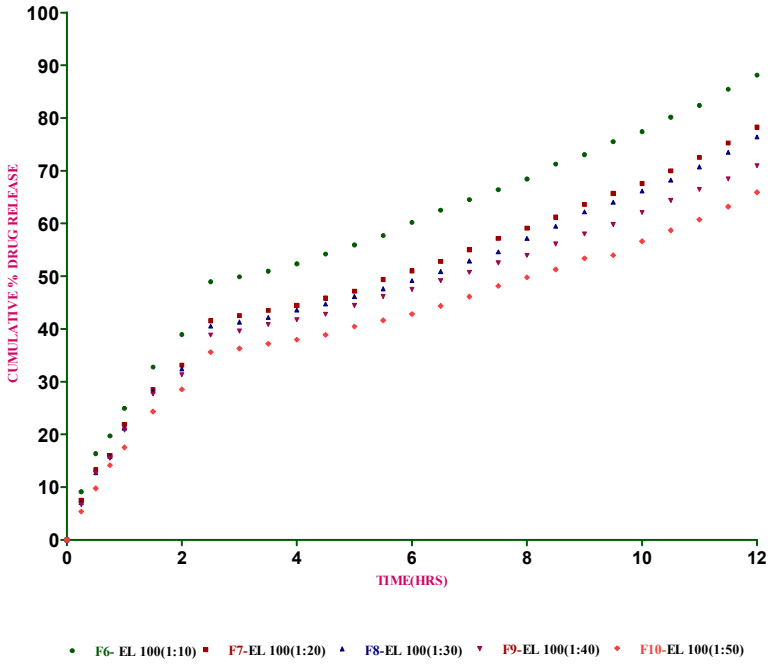

Figure 27 b **Comparison of *Invitro* Zero Order Release Kinetics of Eudragit L100 at Different Ratios Containing Pluronic F68 (2%) as Stabilizer**

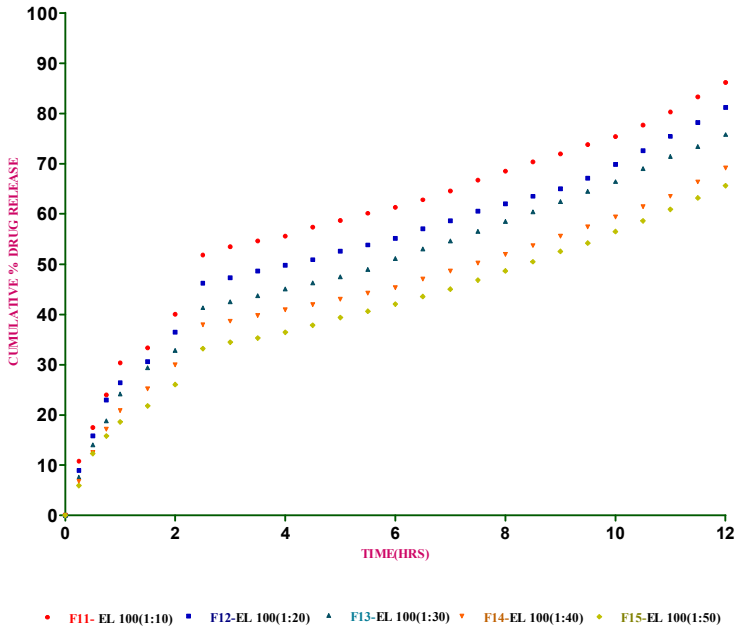

Figure 27 c **Comparison of *Invitro* Zero Order Release Kinetics of Eudragit L100 at Different Ratios Containing PVA (1%) as Stabilizer**

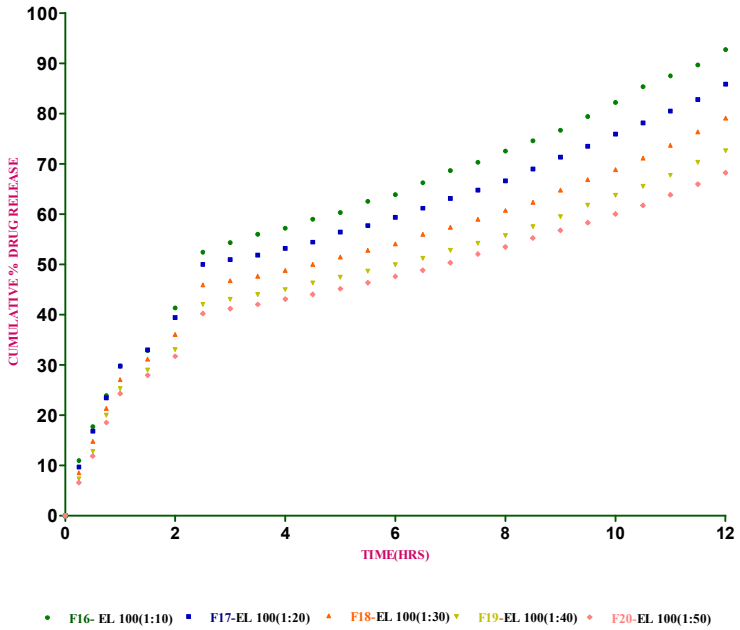

Figure 27 d **Comparison of *Invitro* Zero Order Release Kinetics of Eudragit L100 at Different Ratios Containing PVA (2%) as Stabilizer**

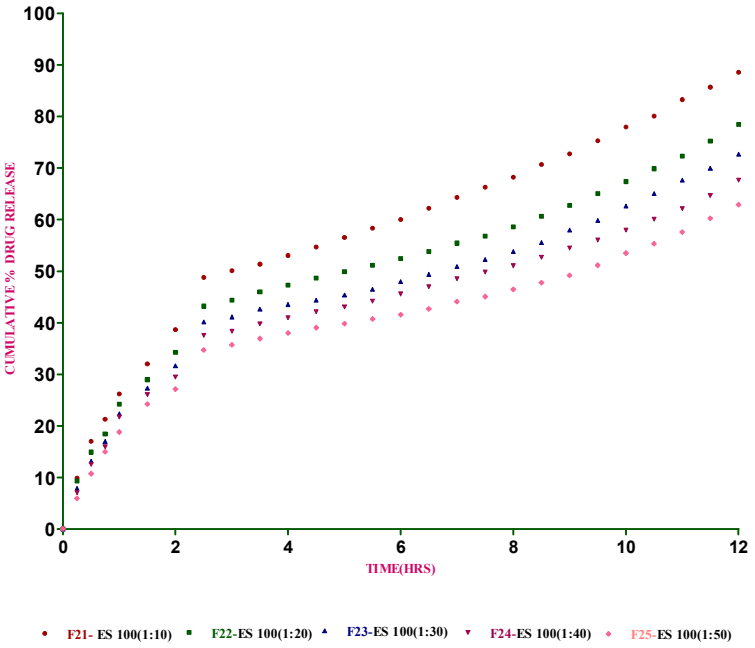

Figure 27 e **Comparison of *Invitro* Zero Order Release Kinetics of Eudragit S100 at Different Ratios Containing Pluronic F68 (1%) as Stabilizer**

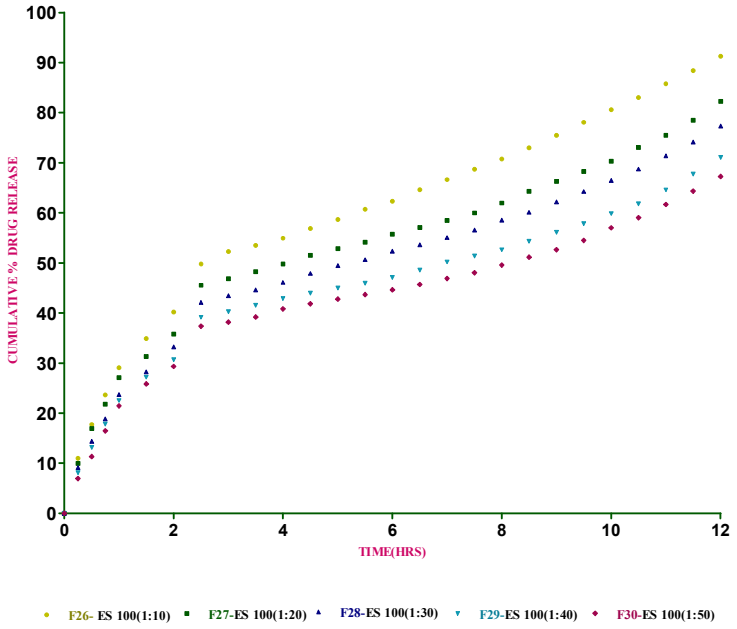

Figure 27 f **Comparison of *Invitro* Zero Order Release Kinetics of Eudragit S100 at Different Ratios Containing Pluronic F68 (2%) as Stabilizer**

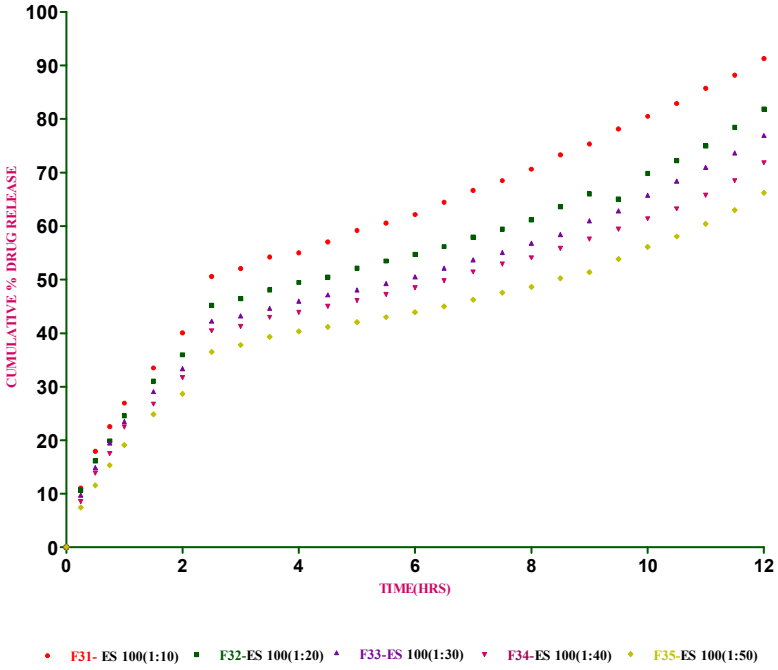

Figure 27 g **Comparison of *Invitro* Zero Order Release Kinetics of Eudragit S100 at Different Ratios Containing PVA (1%) as Stabilizer**

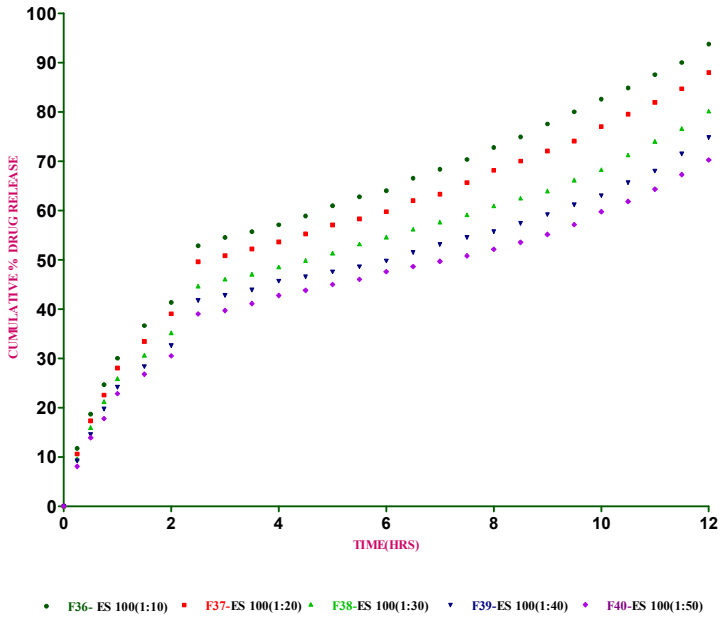

Figure 27 h **Comparison of *Invitro* Zero Order Release Kinetics of Eudragit S100 at Different Ratios Containing PVA (2%) as Stabilizer**

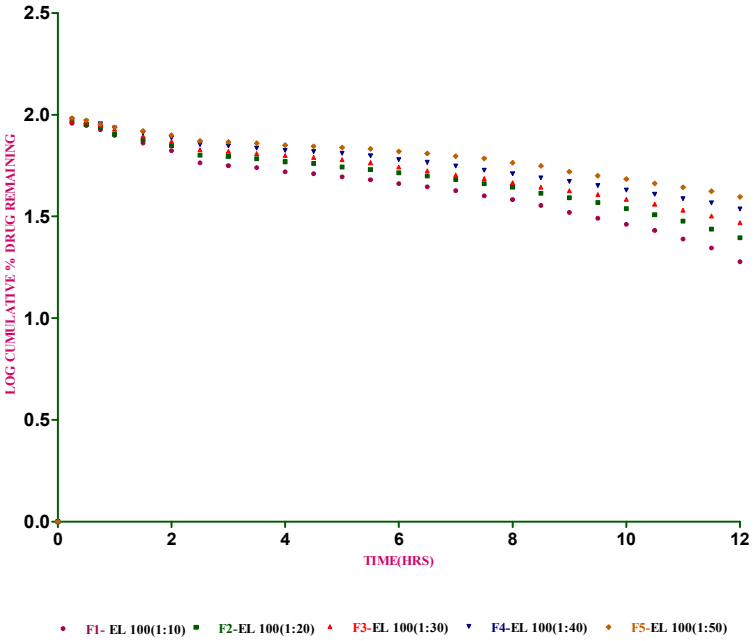

Figure 28 a **Comparison of *Invitro* First Order Release Kinetics of Eudragit L100 at Different Ratios Containing Pluronic F68 (1%) as Stabilizer**

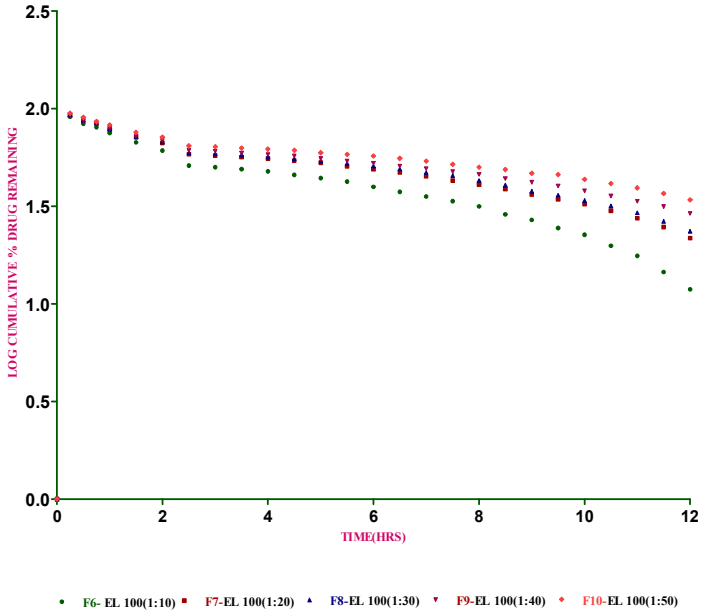

Figure 28 b **Comparison of *Invitro* First Order Release Kinetics of Eudragit L100 at Different Ratios Containing Pluronic F68 (2%) as Stabilizer**

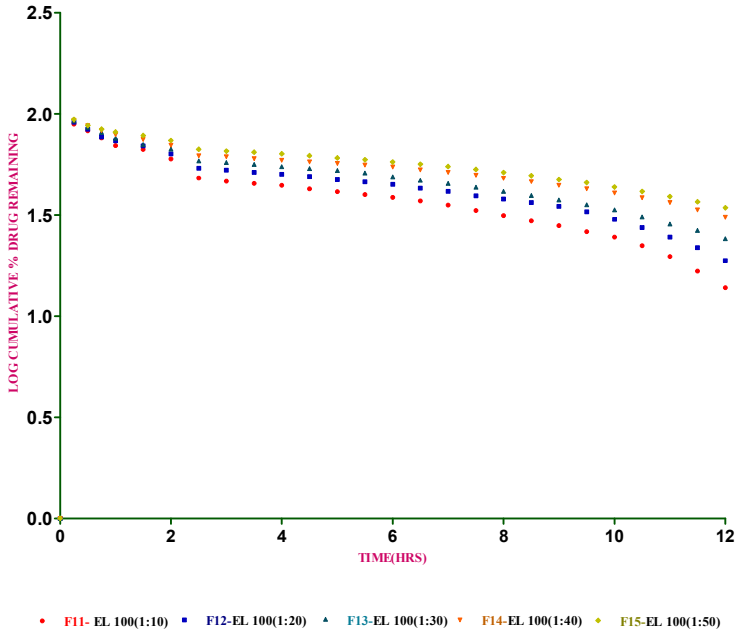

Figure 28 c **Comparison of *Invitro* First Order Release Kinetics of Eudragit L100 at Different Ratios Containing PVA (1%) as Stabilizer**

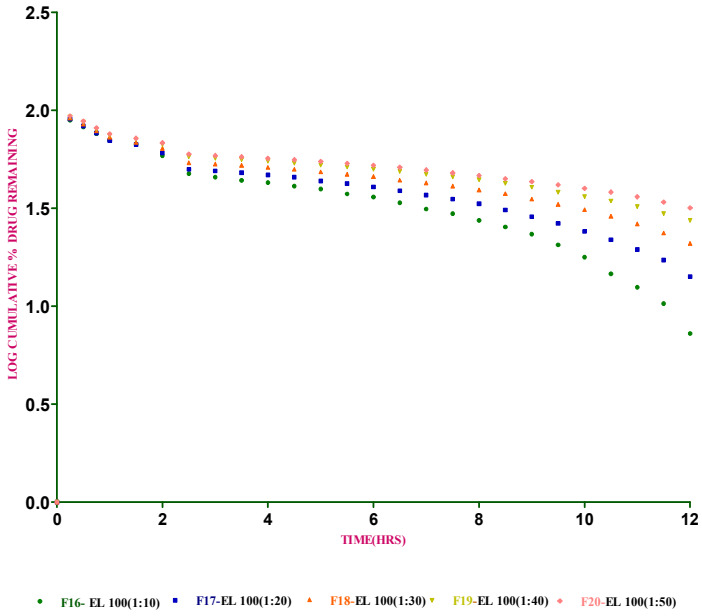

Figure 28 d **Comparison of *Invitro* First Order Release Kinetics of Eudragit L100 at Different Ratios Containing PVA (2%) as Stabilizer**

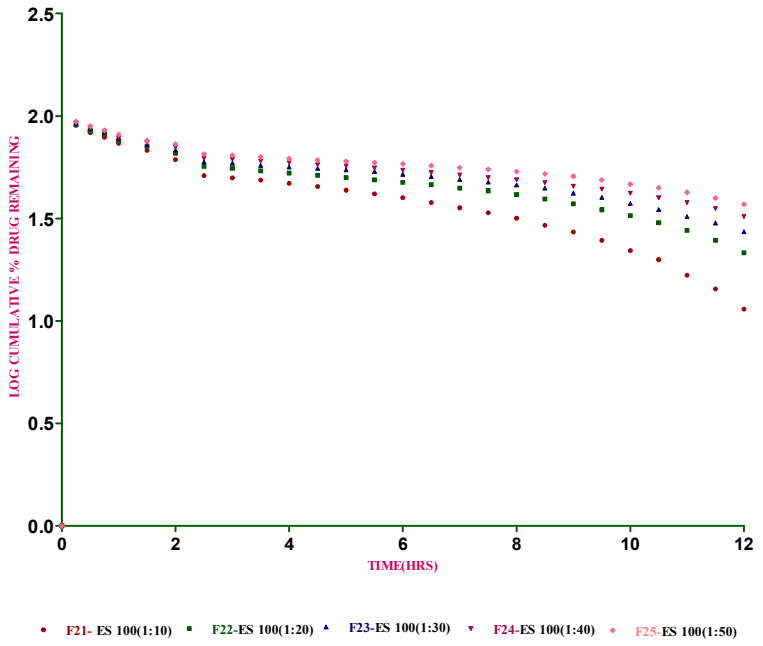

Figure 28 e **Comparison of *Invitro* First Order Release Kinetics of Eudragit S100 at Different Ratios Containing Pluronic F68 (1%) as Stabilizer**

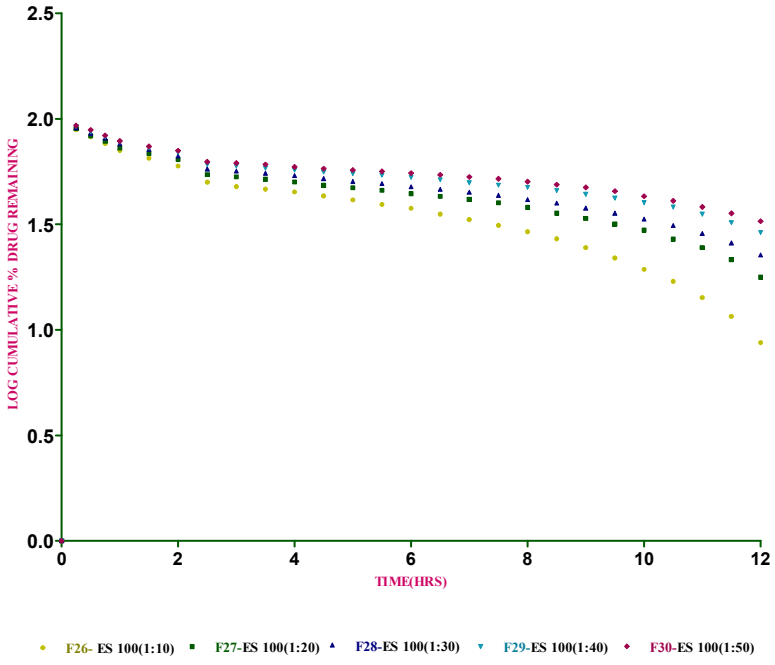

Figure 28 f **Comparison of *Invitro* First Order Release Kinetics of Eudragit S100 at Different Ratios Containing Pluronic F68 (2%) as Stabilizer**

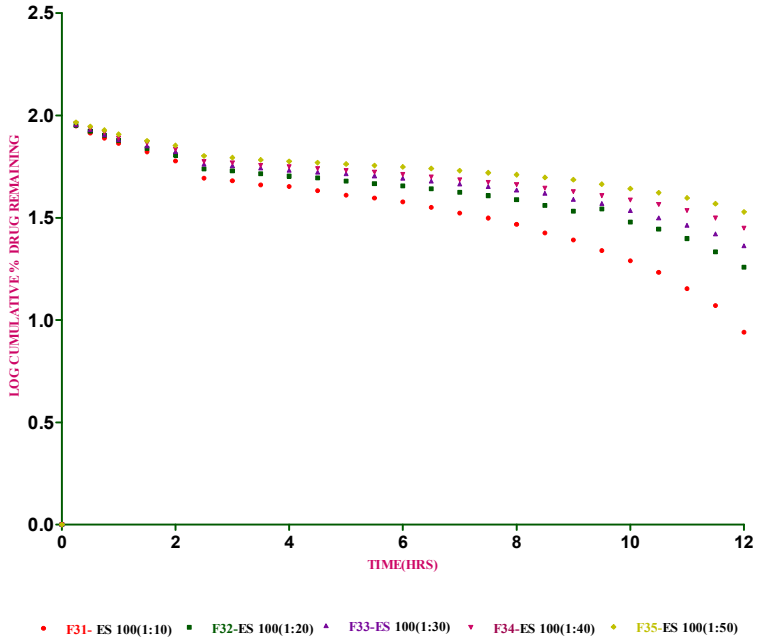

Figure 28 g **Comparison of *Invitro* First Order Release Kinetics of Eudragit S100 at Different Ratios Containing PVA (1%) as Stabilizer**

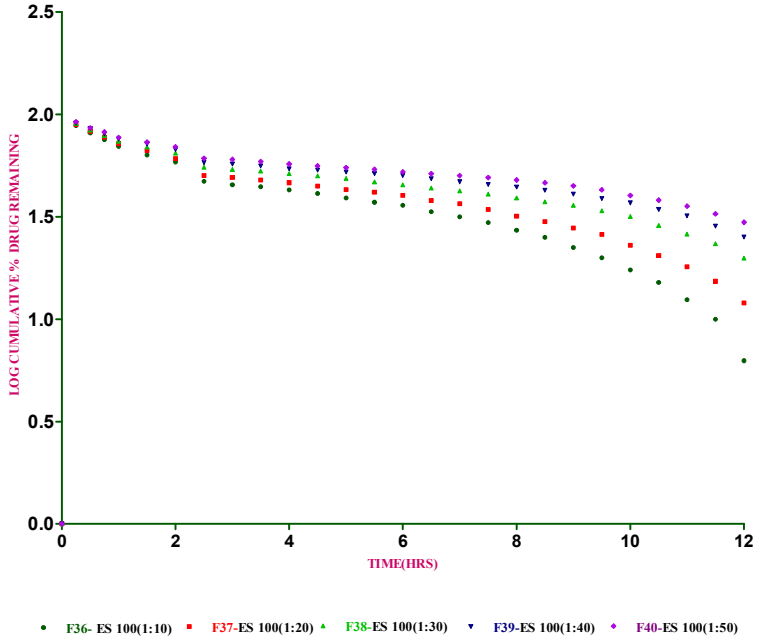

Figure 28 h **Comparison of *Invitro* First Order Release Kinetics of Eudragit S100 at Different Ratios Containing PVA (2%) as Stabilizer**

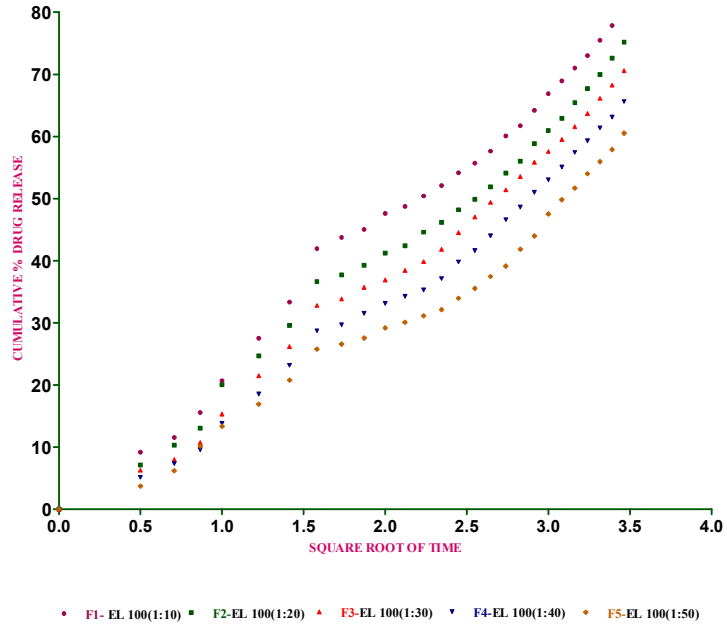

Figure 29 a **Comparison of *Invitro* Higuchi Model Release Kinetics of Eudragit L100 at Different Ratios Containing Pluronic F68 (1%) as Stabilizer**

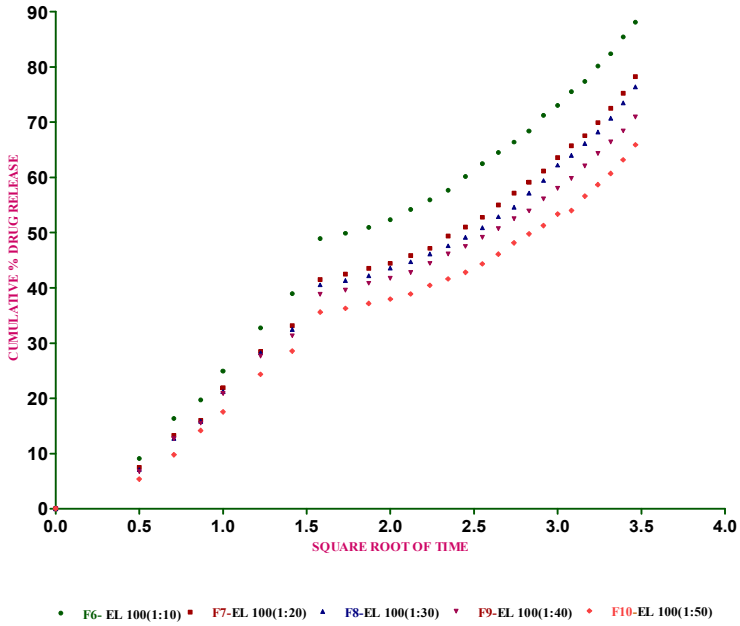

Figure 29 b **Comparison of *Invitro* Higuchi Model Release Kinetics of Eudragit L100 at Different Ratios Containing Pluronic F68 (2%) as Stabilizer**

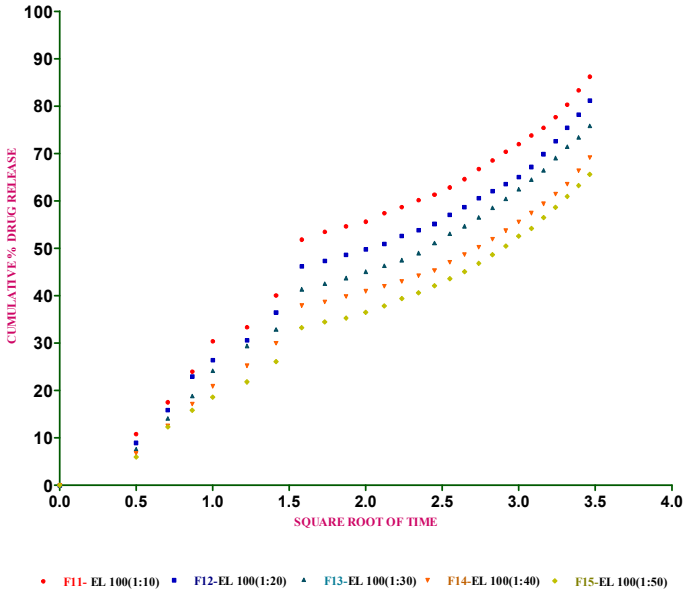

Figure 29 c **Comparison of *Invitro* Higuchi Model Release Kinetics of Eudragit L100 at Different Ratios Containing PVA (1%) as Stabilizer**

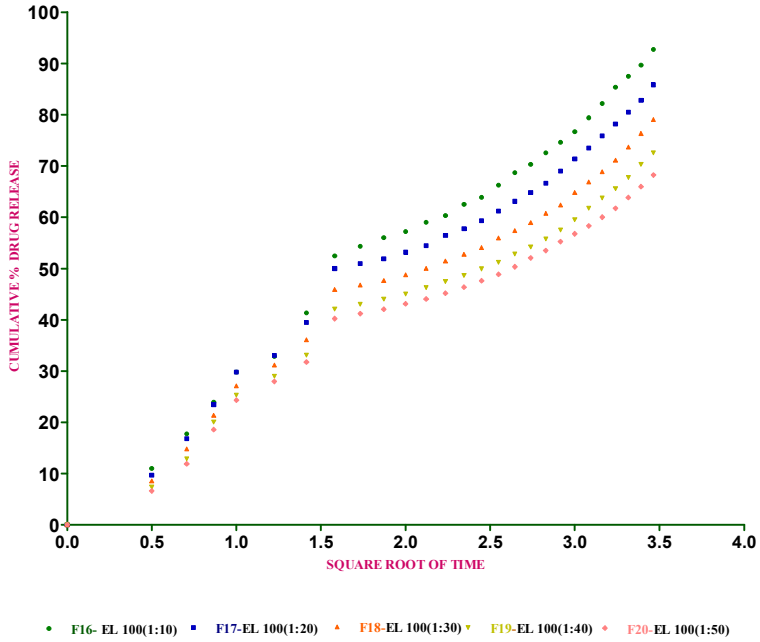

Figure 29 d **Comparison of *Invitro* Higuchi Model Release Kinetics of Eudragit L100 at Different Ratios Containing PVA (2%) as Stabilizer**

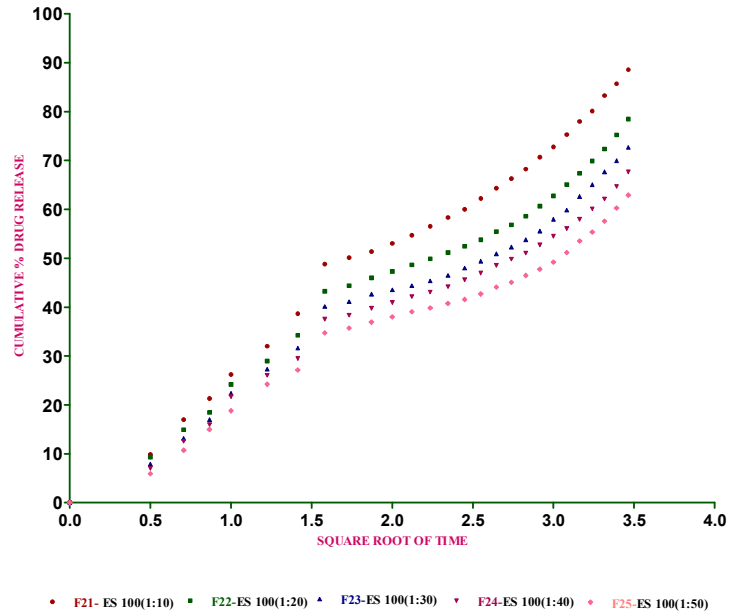

Figure 29 e **Comparison of *Invitro* Higuchi Model Release Kinetics of Eudragit S100 at Different Ratios Containing Pluronic F68 (1%) as Stabilizer**

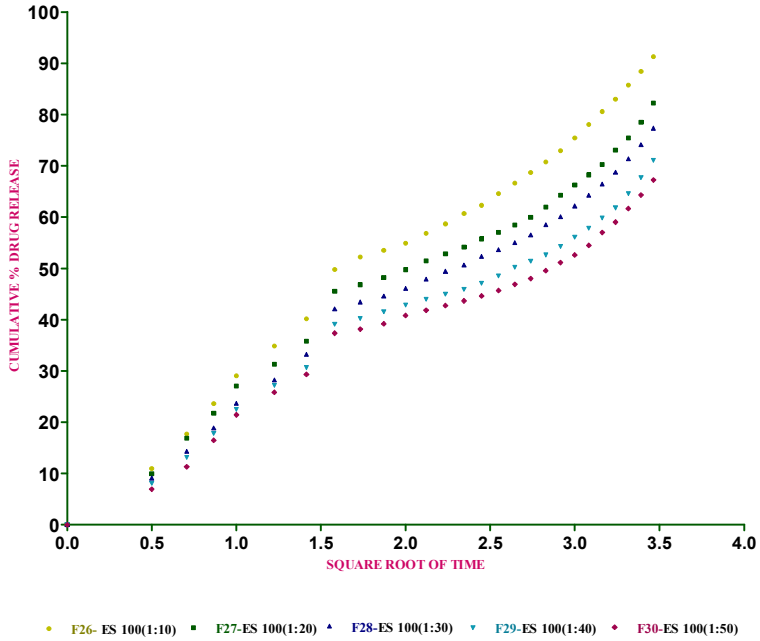

Figure 29 f **Comparison of *Invitro* Higuchi Model Release Kinetics of Eudragit S100 at Different Ratios Containing Pluronic F68 (2%) as Stabilizer**

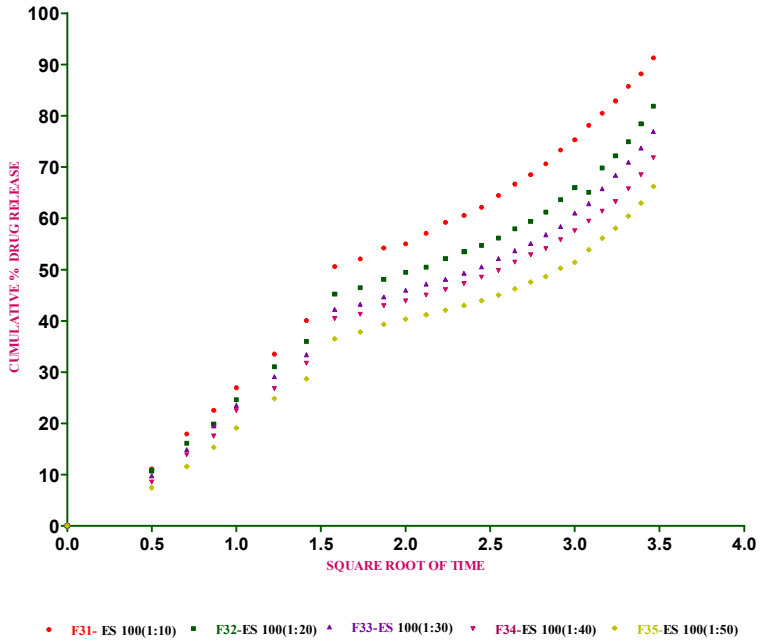

Figure 29 g **Comparison of *Invitro* Higuchi Model Release Kinetics of Eudragit S100 at Different Ratios Containing PVA (1%) as Stabilizer**

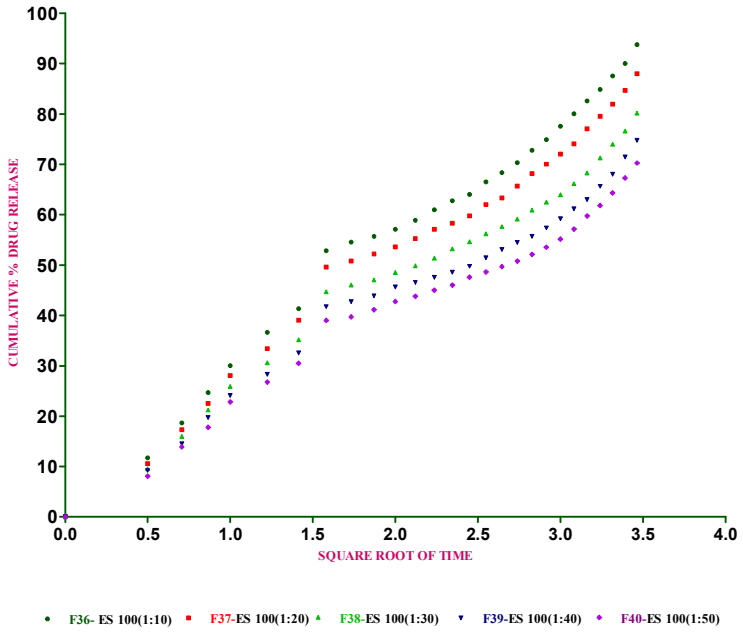

Figure 29 h **Comparison of *Invitro* Higuchi Model Release Kinetics of Eudragit S100 at Different Ratios Containing PVA (2%) as Stabilizer**

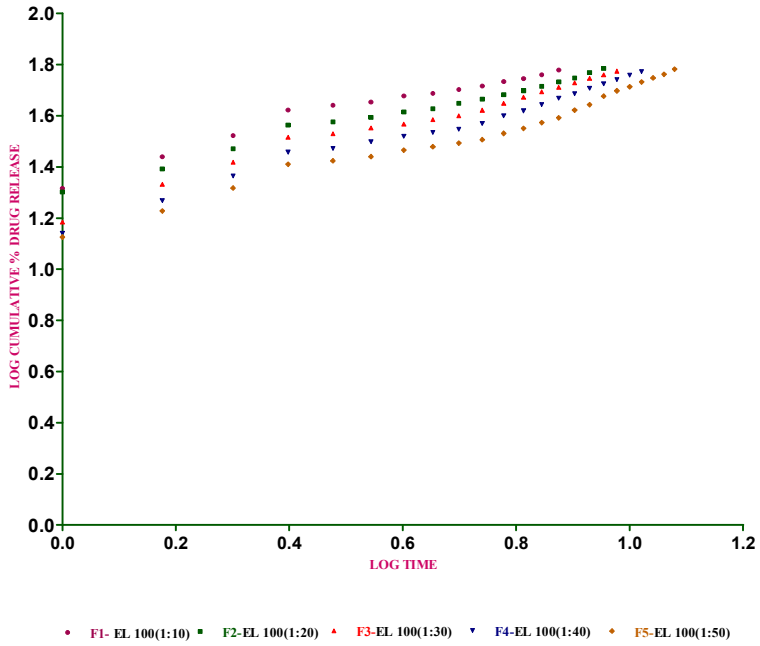

Figure 30 a **Comparison of *Invitro* Korsmeyer-Peppas Model Release Kinetics of Eudragit L 100 at Different Ratios Containing Pluronic F68 (1%) as Stabilizer**

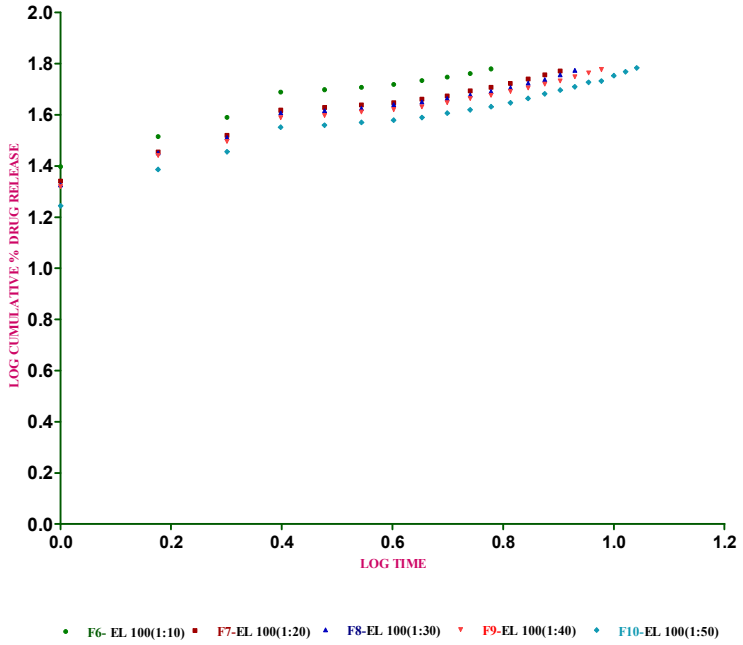

Figure 30 b **Comparison of *Invitro* Korsmeyer-Peppas Model Release Kinetics of Eudragit L100 at Different Ratios Containing Pluronic F68 (2%) as Stabilizer**

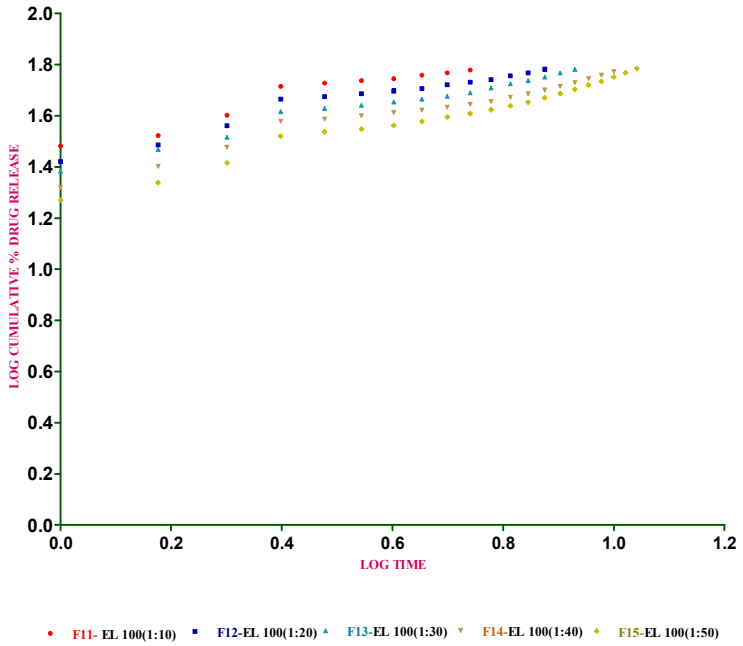

Figure 30 c **Comparison of *Invitro* Korsmeyer-Peppas Model Release Kinetics of Eudragit L100 at Different Ratios Containing PVA (1%) as Stabilizer**

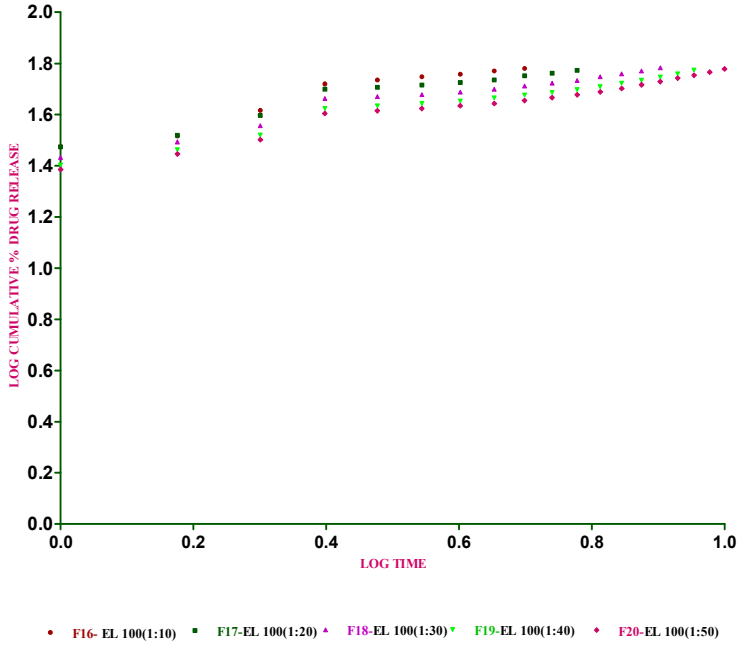

Figure 30 d **Comparison of *Invitro* Korsmeyer-Peppas Model Release Kinetics of Eudragit L100 at Different Ratios Containing PVA (2%) as Stabilizer**

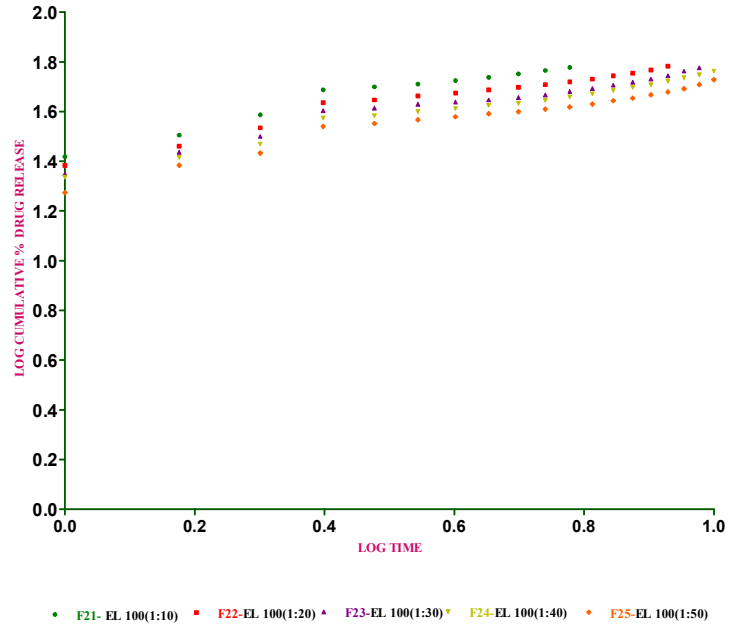

Figure 30 e **Comparison of *Invitro* Korsmeyer-Peppas Model Release Kinetics of Eudragit S100 at Different Ratios Containing Pluronic F68 (1%) as Stabilizer**

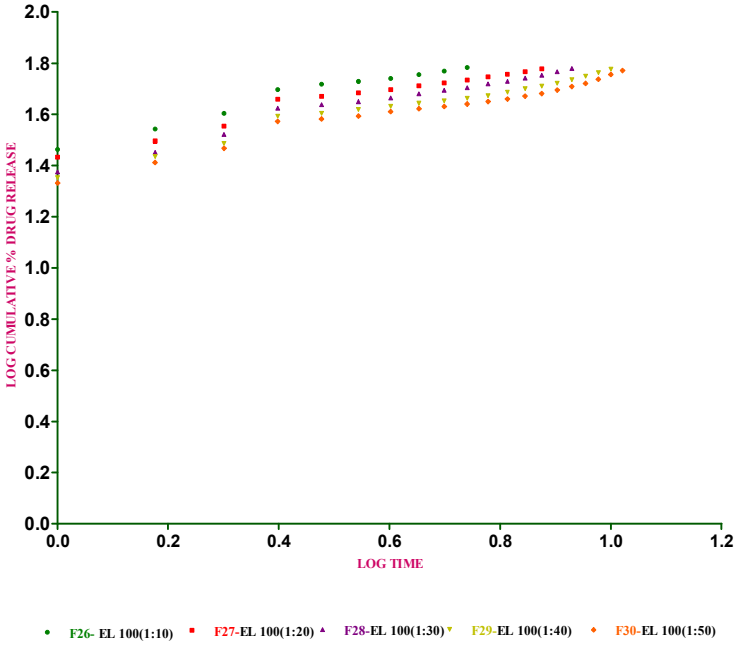

Figure 30 f **Comparison of *Invitro* Korsmeyer-Peppas Model Release Kinetics of Eudragit S100 at Different Ratios Containing Pluronic F68 (2%) as Stabilizer**

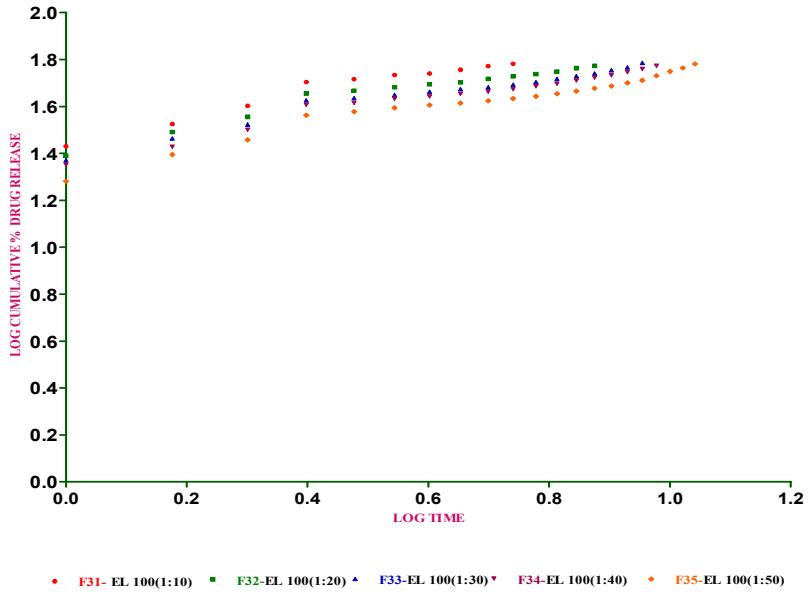

Figure 30 g **Comparison of *Invitro* Korsmeyer-Peppas Model Release Kinetics of Eudragit S100 at Different Ratios Containing PVA (1%) as Stabilizer**

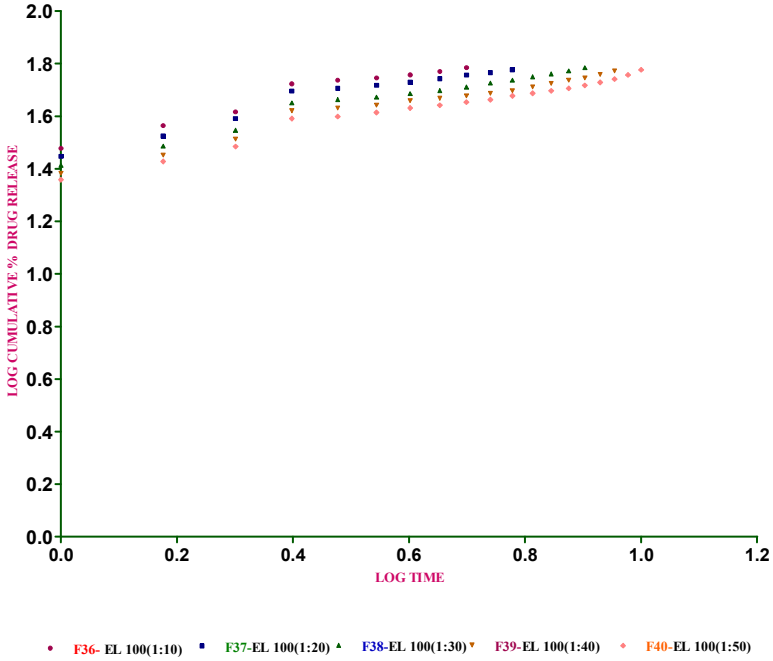

Figure 30 h **Comparison of *Invitro* Korsmeyer-Peppas Model Release Kinetics of Eudragit S100 at Different Ratios Containing PVA (2%) as Stabilizer**

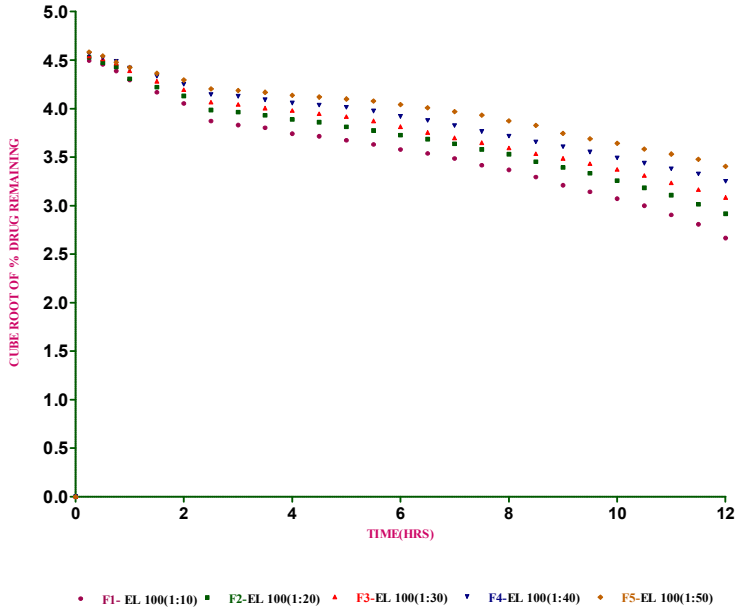

Figure 31 a **Comparison of *Invitro* Hixon-Crowell Model Release Kinetics of Eudragit L100 at Different Ratios Containing Pluronic F68 (1%) as Stabilizer**

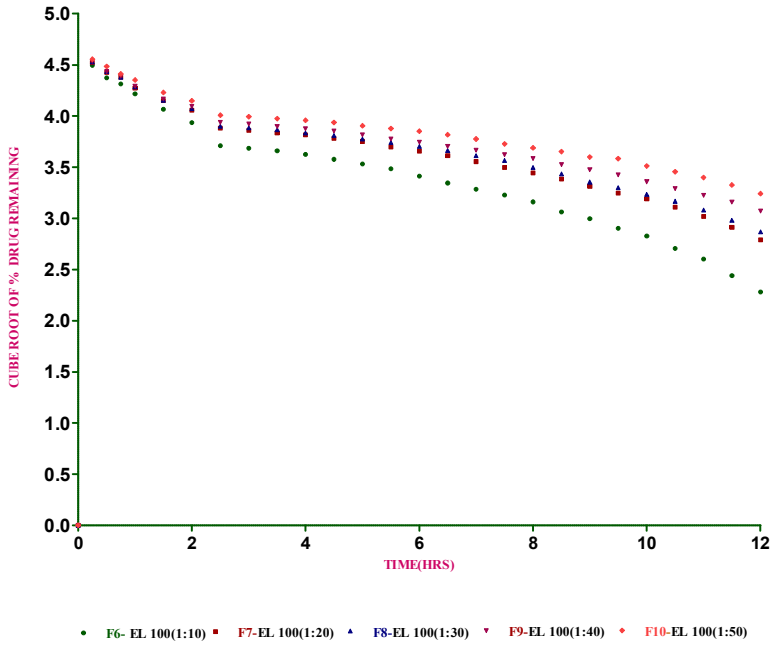

Figure 31 b **Comparison of *Invitro* Hixon-Crowell Model Release Kinetics of Eudragit L100 at Different Ratios Containing Pluronic F68 (2%) as Stabilizer**

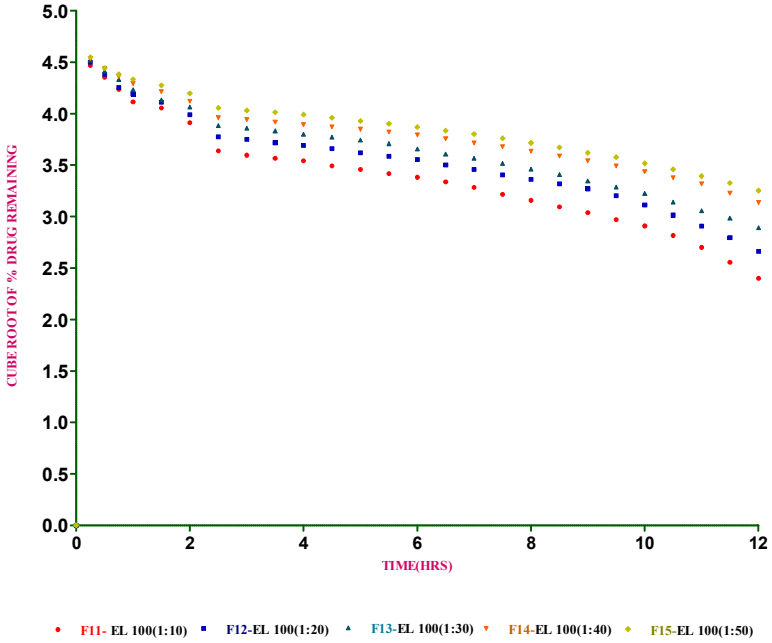

Figure 31 c **Comparison of *Invitro* Hixon-Crowell Model Release Kinetics of Eudragit L100 at Different Ratios Containing PVA (1%) as Stabilizer**

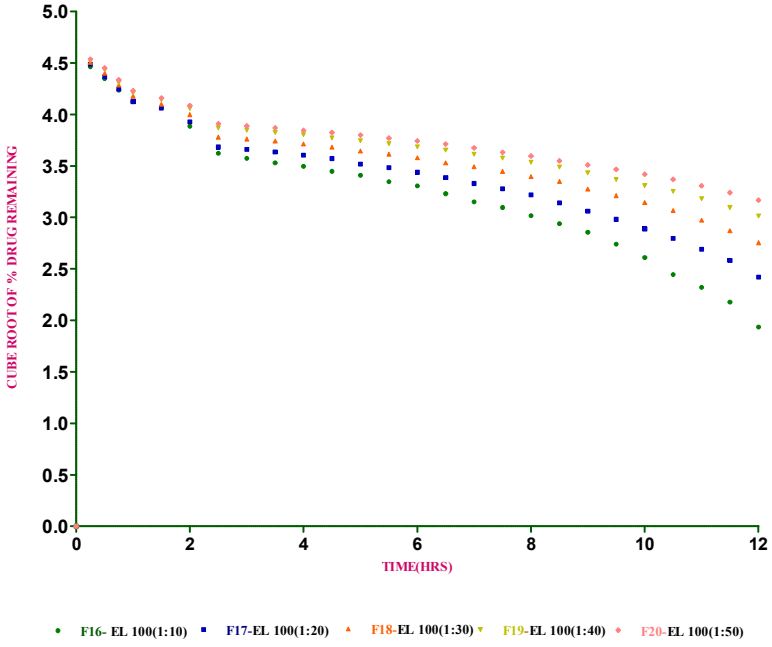

Figure 31 d **Comparison of *Invitro* Hixon-Crowell Model Release Kinetics of Eudragit L100 at Different Ratios Containing PVA (2%) as Stabilizer**

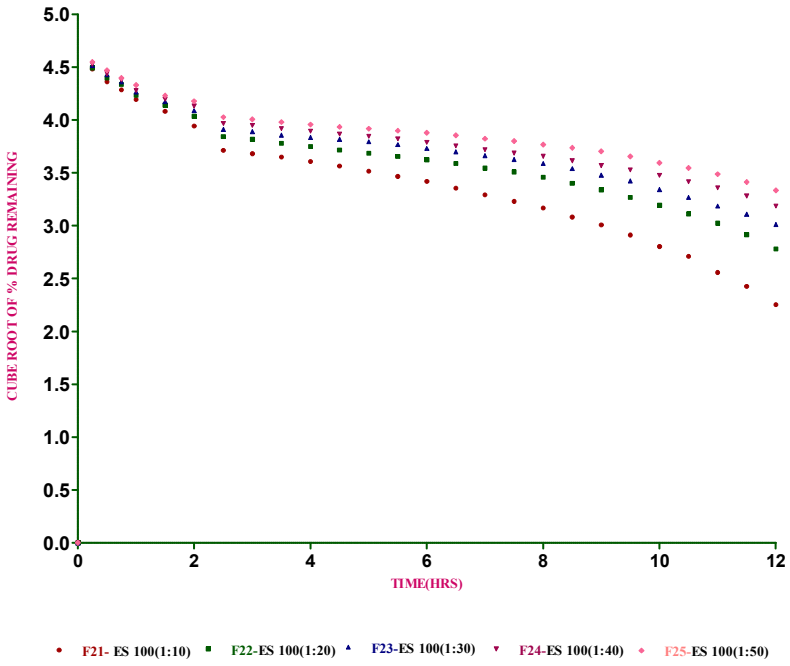

Figure 31 e **Comparison of *Invitro* Hixon-Crowell Model Release Kinetics of Eudragit S100 at Different Ratios Containing Pluronic F68 (1%) as Stabilizer**

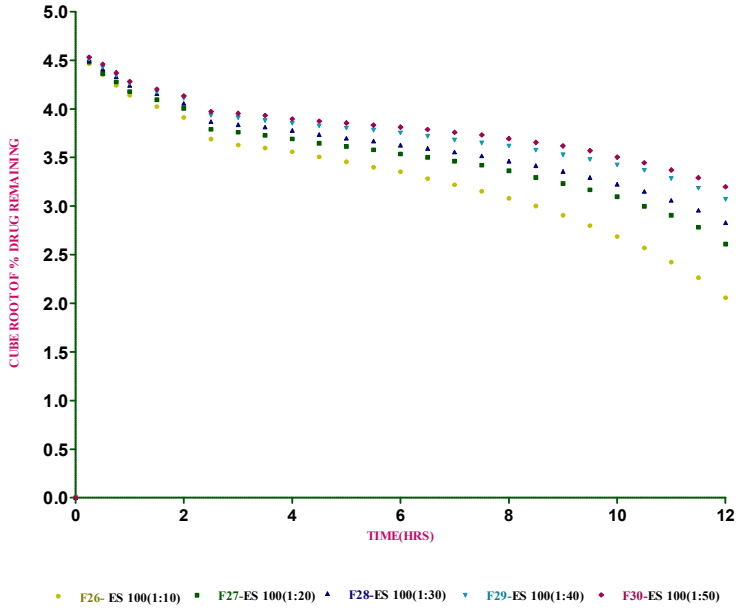

Figure 31 f **Comparison of *Invitro* Hixon-Crowell Model Release kinetics of Eudragit S100 at Different Ratios Containing Pluronic F68 (2%) as Stabilizer**

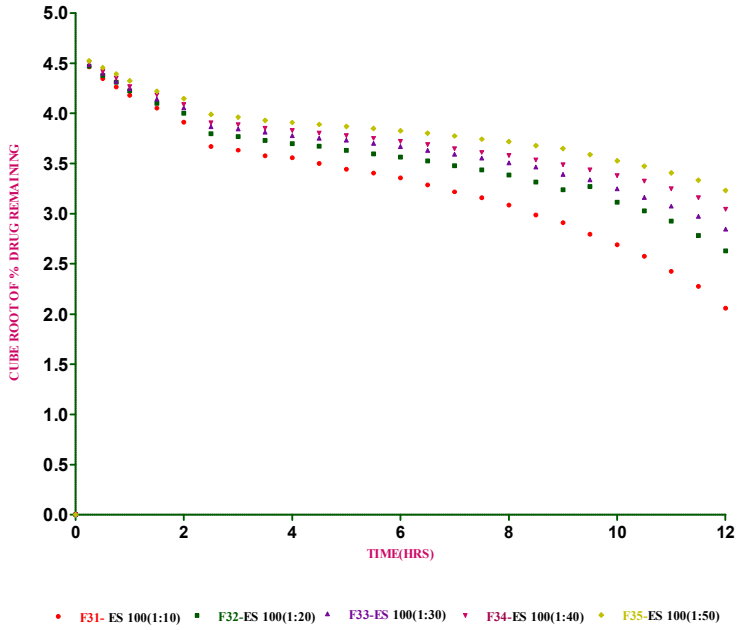

Figure 31 g Comparison of *Invitro* Hixon-Crowell Model Release Kinetics of Eudragit S100 at Different Ratios Containing PVA (1%) as Stabilizer

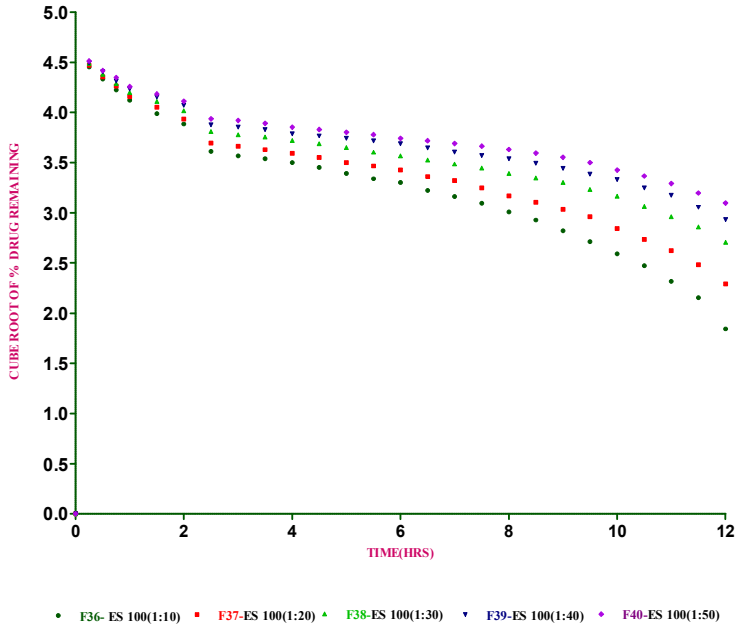

Figure 31 h Comparison of *Invitro* Hixon-Crowell Model Release Kinetics of Eudragit S100 at Different Ratios Containing PVA (2%) as Stabilizer

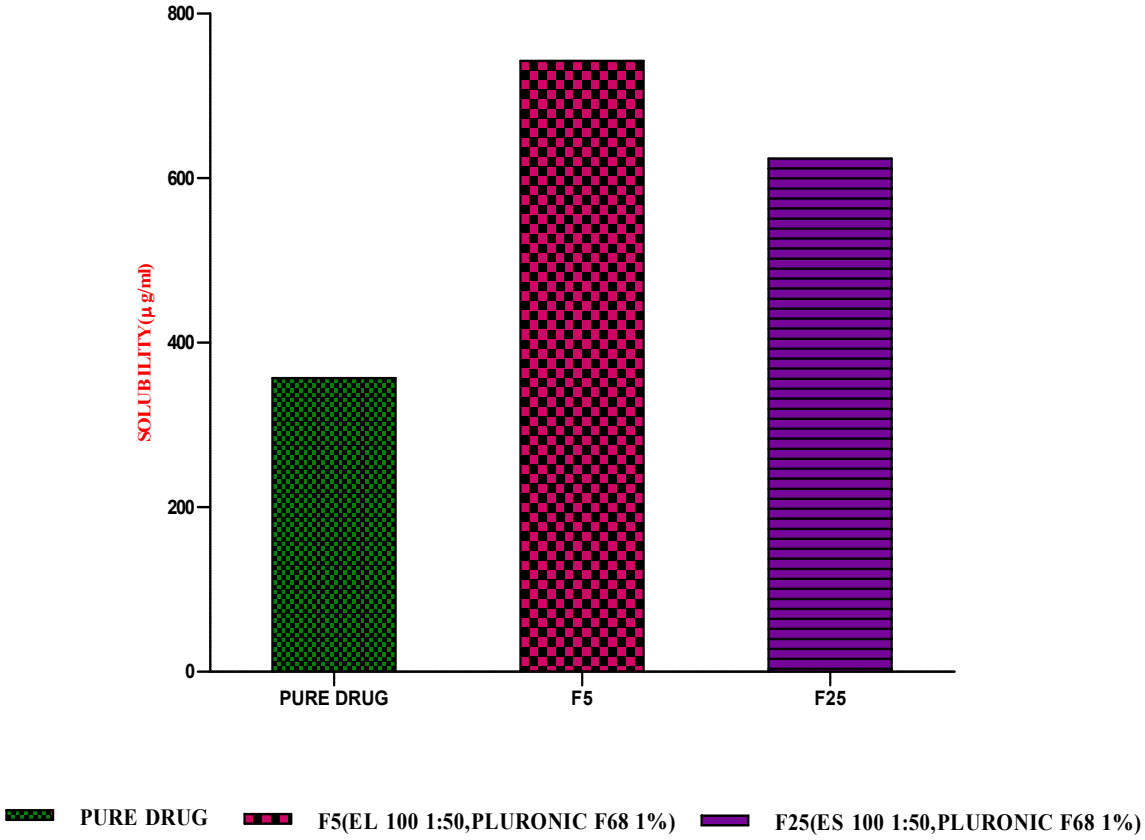

Figure 32 Comparison of Solubility of Best Formulations (F5, F25) with Pure Drug Solution

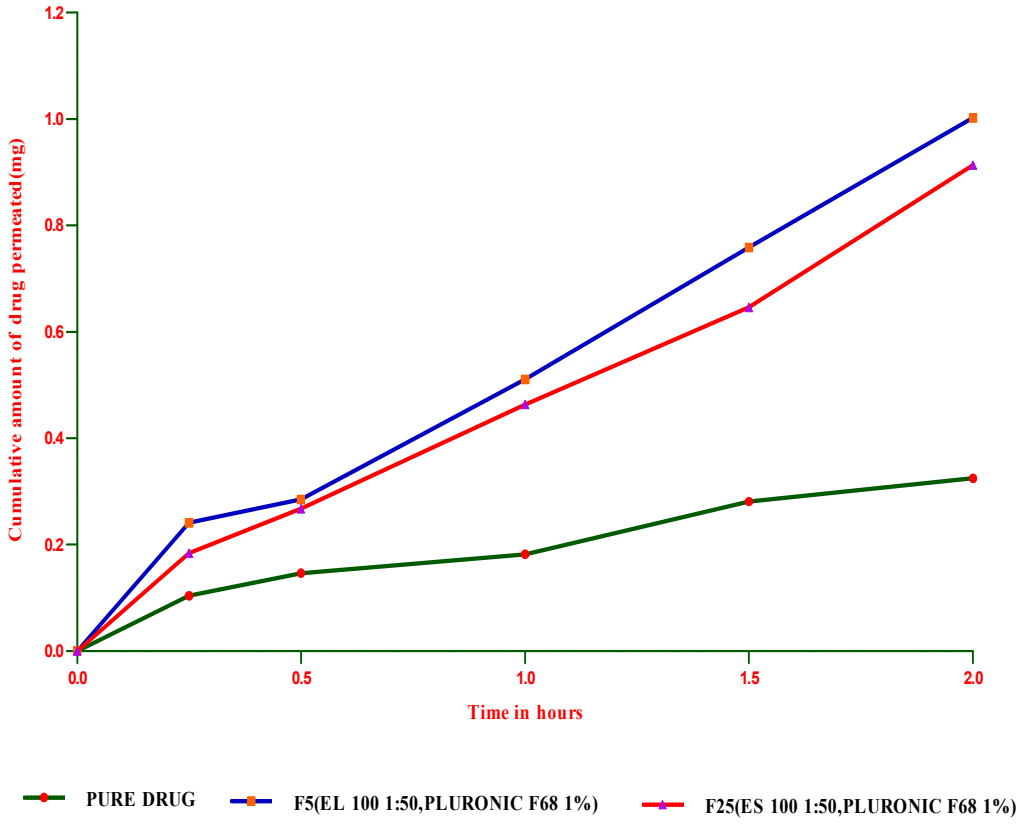

Figure 33 a Comparison of Cumulative Amount of Drug Permeated across Duodenum Segment.

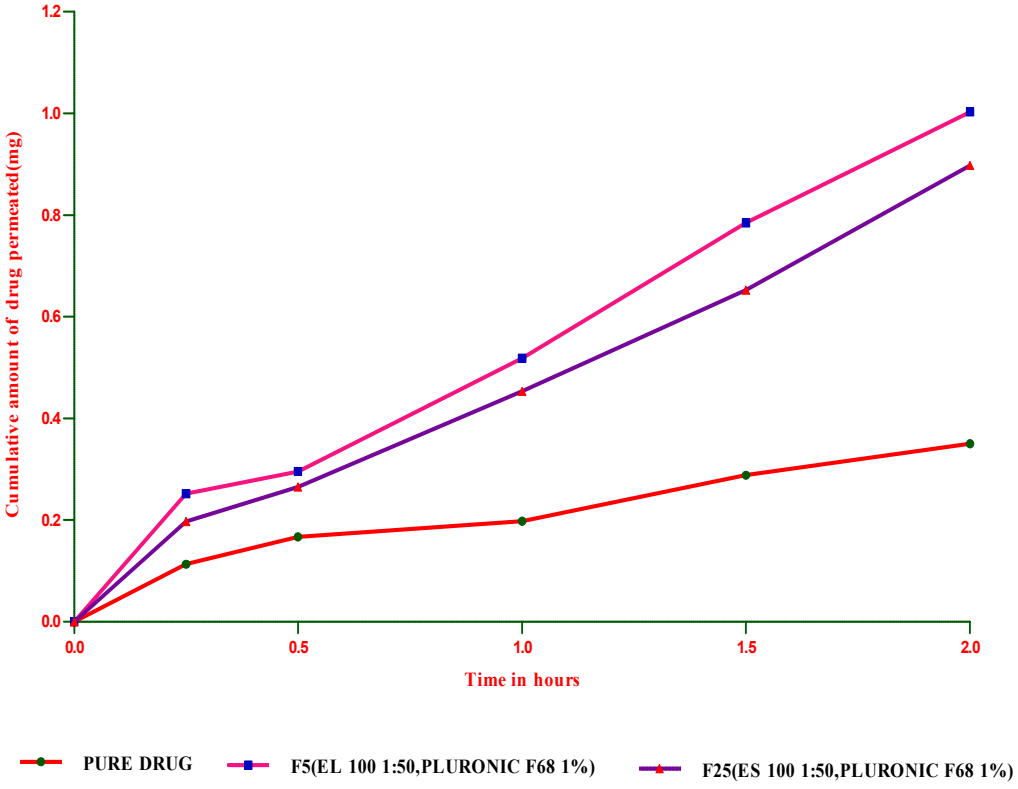

Figure 33 b Comparison of Cumulative Amount of Drug Permeated across Jejunum Segment

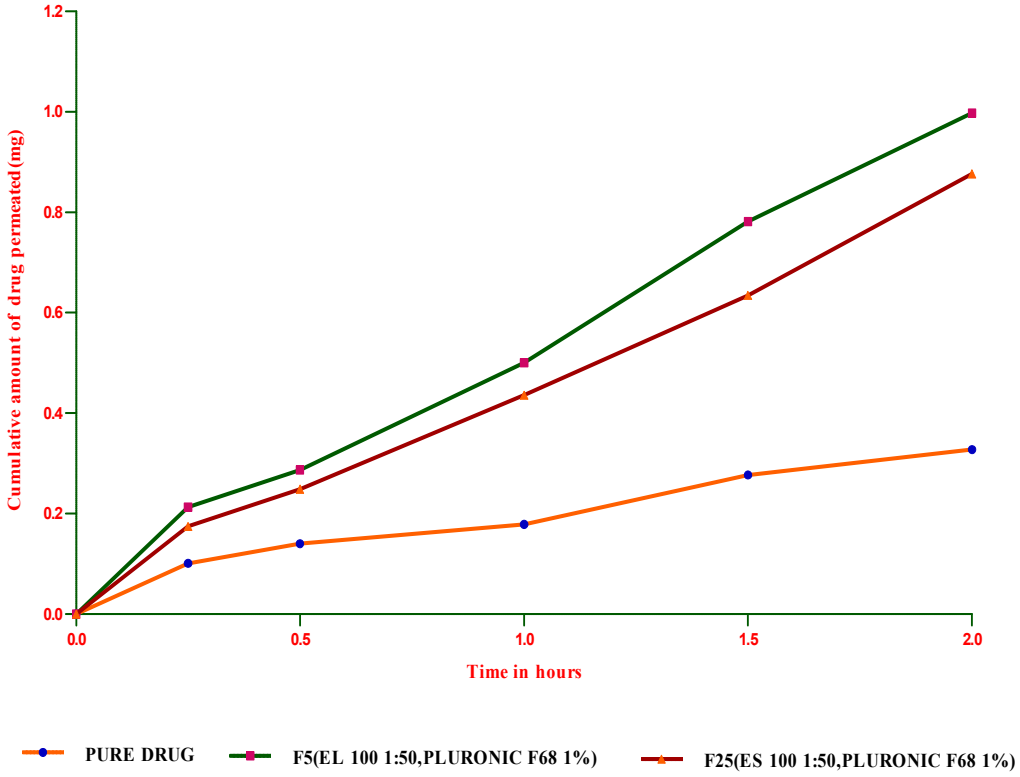

Figure 33 c Comparison of Cumulative Amount of Drug Permeated Across ileum Segment

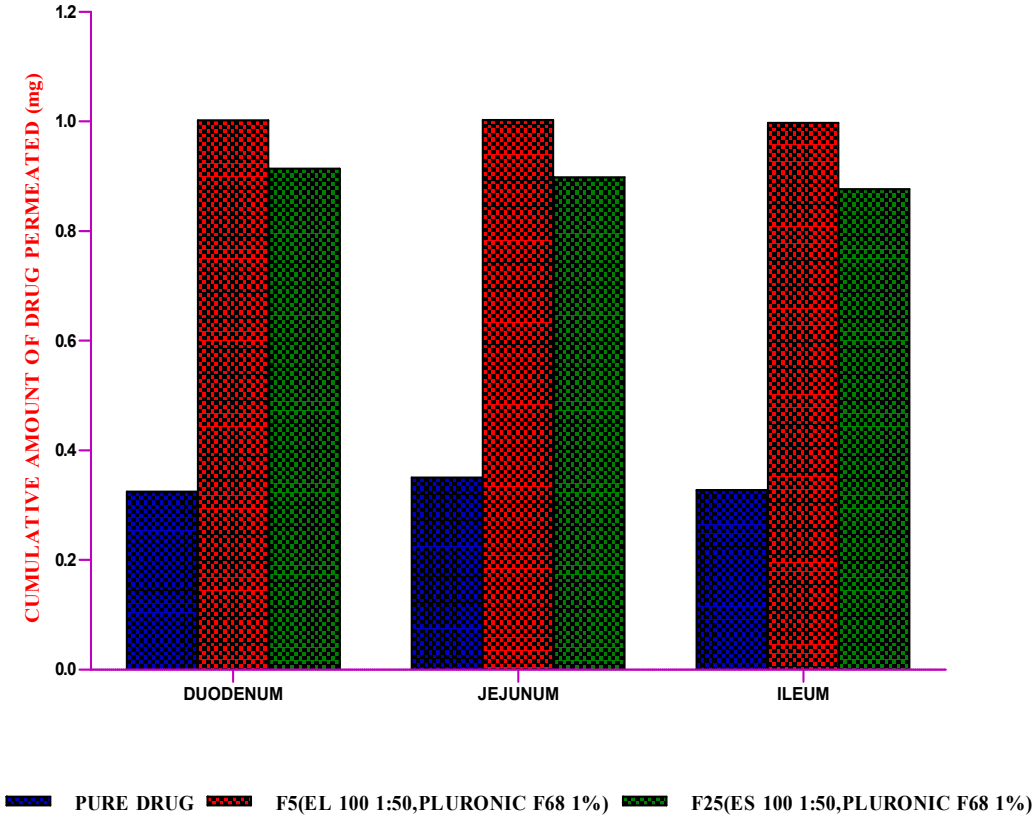

Figure 33 d Comparison of Cumulative Amount of Drug Permeated Through Small Intestinal Segments (At 2 Hour)

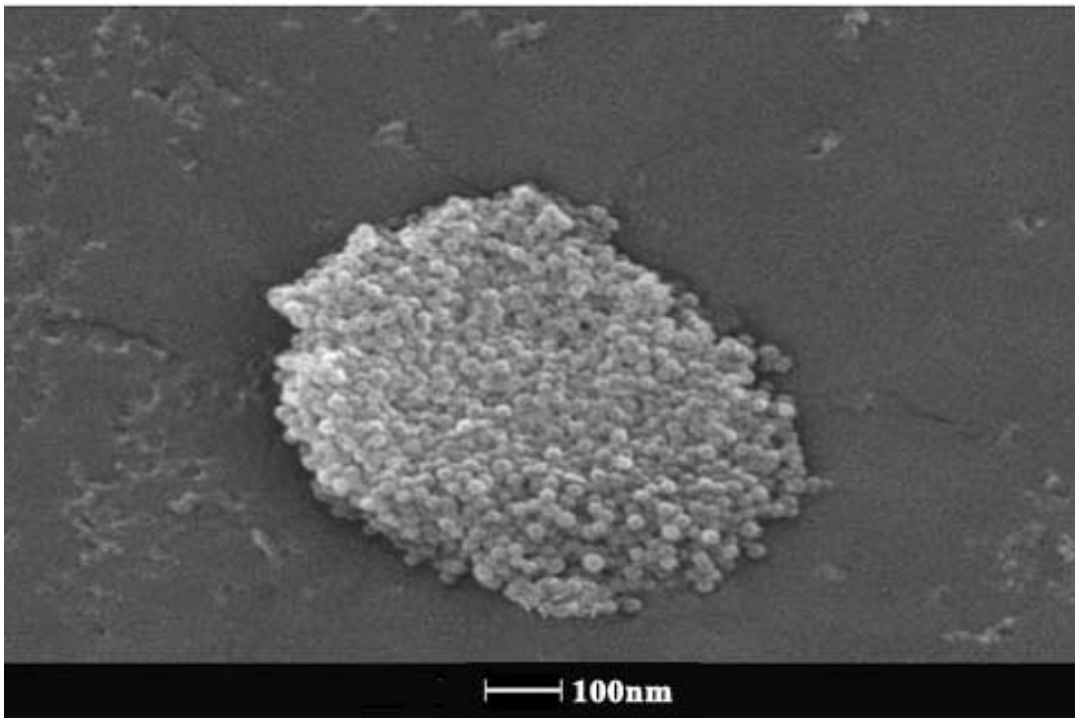

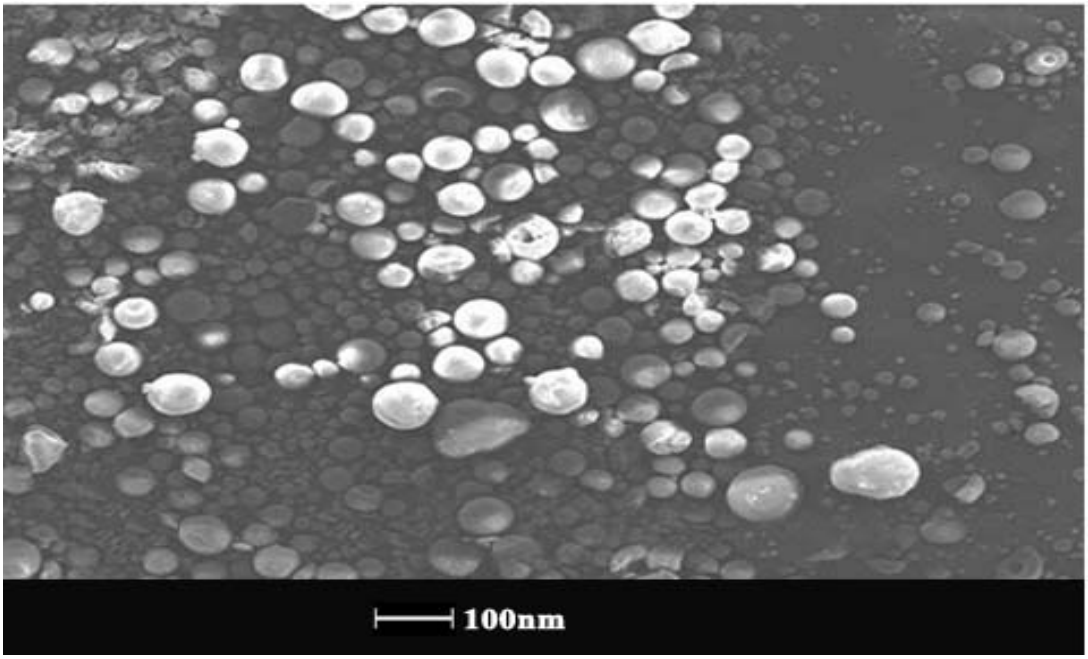

Figure 34 Transmission Electron Microscopy (TEM) Image of Best Formulation F5

CHAPTER-XI

SUMMARY AND CONCLUSION

- The λ_{max} of rosuvastatin calcium was found to be 241nm performed using phosphate buffer pH 6.8.
- The rosuvastatin calcium obeys the Beer's law within the concentration range of 2 to 20 µg/ml.
- FT-IR and DSC investigations confirmed that there was no interaction between drug and polymers.
- The rosuvastatin calcium loaded polymeric nanoparticles were successfully prepared by nanoprecipitation technique using Eudragit L100 and Eudragit S100 as polymers in the presence of stabilizers (Pluronic F68 and PVA).
- Malvern zeta sizer used to explore the particle size of rosuvastatin calcium loaded polymeric nanoparticle showed a suitable particle size in the range of 100-250 nm.
- The polydispersity index of nanoparticle formulation F1-F40 was less than 0.5, which indicated a relative homogenous dispersion.
- Malvern zeta sizer used to explore the zeta potential of rosuvastatin calcium loaded polymeric nanoparticle showed a negative surface charge due to the presence of terminal carboxylic groups in the polymers.
- The entrapment efficiency increased with increasing the concentration of polymers and decreased with increasing concentration of stabilizers.
- The presence of stabilizers made the nanoparticle formulations more stable with high entrapment efficiency.

- The *invitro* release studies displayed a similar biphasic drug release pattern with a burst release within 2 hours followed by sustained release at 12 hours.
- *Invitro* release kinetics showed sustained release and Fickian diffusion mechanism which describes that the drug release was purely diffusion controlled.
- The solubility of rosuvastatin calcium loaded polymeric nanoparticles increased two fold when compared to pure drug solution.
- The results of *ex vivo* intestinal permeability studies showed an increase in the permeation of rosuvastatin calcium loaded polymeric nanoparticles across small intestinal segments when compared to pure drug solution.
- TEM studies confirmed the morphology of the nanoparticle formulation.
- The stability studies confirmed that the developed rosuvastatin calcium polymeric nanoparticles are physically and chemically stable and retain their pharmaceutical properties at various temperature and humidity conditions over a period of 3 months.

Hence, it was concluded that the nanoprecipitation was a useful method for the successful incorporation of rosuvastatin calcium with high entrapment efficiency. The solubility and *ex vivo* intestinal permeability studies suggested that the nanoparticle formulations can improve the bioavailability of the rosuvastatin calcium by improving its solubility and permeability across intestinal membrane. Furthermore, it could be presumed that if the nanometer range particles were obtained, the bioavailability might be increased. Hence, we can conclude that polymeric nanoparticles enhance the bioavailability of poorly water soluble and low lipophilic drug like rosuvastatin calcium as a drug delivery system.

CHAPTER-XII

REFERENCES

A

Abdelwahed W., Degobert G., Stainmesse S., and Fessi H., (2006). Freeze-drying of nanoparticles: Formulation, process and storage considerations, *Adv.Drug.Deliv Rev*, 58(15), 1688-1713.

Abdullah M., Al- Mohizea., (2010). Influence of intestinal efflux pumps on the absorption and transport of furosemide, Saudi.PharmJ, 18, 97–101.

Adlin Jino Nesalin.J., Gowthamarajan.K. , Somashekhara.C.N., (2009). Formulation and evaluation of nanoparticles containing Flutamide, *Int.J.PharmTech.Res,* 1 (4), 1331-1334.

Akbari.B.V., Valaki.B.P., Maradiya.V.H., Akbari.A.K., Vidyasagar.G., (2011). Development and evaluation of orodispersible tablets of Rosuvastatin calcium-HP-β-CD inclusion complex by using different superdisintergrants, *Int.J.PharmTech,* 3(1), 1842-1859.

Albert. H. L., Ying Zheng., Zhong Zuo., Chow., (2006). Lack of effect of _-cyclodextrin and its water-soluble derivatives on in vitro drug transport across rat intestinal epithelium, *Int.J.Pharm, 309, 123*-128.

Alka Gupta., Mishra P., Shah K., (2009). Simple UV Spectrophotometric determination of rosuvastatin calcium in pure form and in pharmaceutical formulations, E.J.Chem, 6(1), 89-92.

Alle´mann .E., Leroux.J.C., Gurny. R., (1998). Polymeric nano-microparticles for the oral delivery of peptides and peptidomimetics, *Adv. Drug. Deliv.Rev,* 34(3), 171- 189.

Amarnath Maitra., Dhruba Jyoti Bharali., Sanjeeb Kumar Sahoo., Subho Mozumdar., (2003). Cross-linked polyvinylpyrrolidone nanoparticles: a potential carrier for hydrophilic drugs. *J.Colloid.Intface.Sci,* 258, 415-423.

Ammoury.N., Fessi.H., Devissaguet.J.P., Dubrasquet.M., Benita.S., (1991). Jejunal absorption, pharmacological activity, and pharmacokinetic evaluation of indomethacin-loaded poly (DL-lactide) and poly(isobutylcyanoacrylate) nanocapsules in rats, *Pharm. Res,* 8(1), 101- 105.

Angela Lopedota., Giuseppe Trapani., Adriana Trapani., Annalisa Cutrignelli., Laura Chiarantini., Elena Pantucci., Rosa Curci., Elisabetta Manuali., (2009). The use of Eudragit RS100/ cyclodextrin nanoparticles for the transmucosal administration of glutathione, *Eur.J.Pharm.BioPharm,* 72,509-520.

Annick Ludwig., Kathleen Dillen., Jo Vandervoort., Guy Van den Mooter., (2006). Evaluation of Ciprofloxacin – loaded Eudragit RS 100 or RL 100/ PLGA nanoparticles, *Int.J.Pharm,* 314, 72-82.

Arpan Chudasama., Chamanlal Shishoo., Vineetkumar Patel., Manish Nivsarkar ., (2011). A novel lipid – based oral drug delivery system of Nevirapine, *Int.J.PharmTech.Res,* 3(2), 1159-1168.

Arun Kumar.N., Deecaraman.M., Rani.C., Mohanraj.K.P., Venkates Kumar.K., (2009). Preparation and solid state characterization of Atorvastatin nano suspension for enhanced solubility and dissolution, *Int.J.PharmTech,* 1(4), 1725-1730.

Aslani P., Kennedy R.A., (1996). Studies on diffusion in alginate gels. I. Effect of cross-linking with calcium or zinc ions on diffusion of acetaminophen*, J. Control Release,* 42, (1), 75- 82.

Auvillain M., Cavé G., Fessi H., Devissaguet J.P., (1989). Lyophilisation devecteurs colloïdaux submicroniques, *STP Pharm. Sci.* 5, 738–744.

Avadi.M.R., Sadeghi.A.M.M., Naser Mohamadpour Dounighi., Dinarvand.R., Atyabi.F., Rafiee-Tahrani.M., (2011). Ex vivo evaluation of Insulin nanoparticles using chitosan and Arabic gum, *Int.Scholar.Res.Net*, 1-6.

Avgoustakis K., Beletsi A., Panagi Z., Klepetsanis P., Karydas A.G, Ithakissios D.S., (2002). PLGA-mPEG nanoparticles of cisplatin: In vitro nanoparticle degradation, in vitro drug release and in vivo drug residence in blood properties, *J.Control Release*, 79(1), 123-135.

Avgoustakis. K., (2004). Pegylated poly (lactide) and poly (lactide-coglycolide) nanoparticles: preparation, properties and possible applications in drug delivery, *Current Drug Delivery*, 1(4), 321–333.

B

Baba R., (2007). *Patent and Nanomedicine. Nanomed,* 2(3), 351-374.

Bae Y., Diezi T.A., Zhao A., Kwon G.S., (2007). Mixed polymeric micelles for combination cancer chemotherapy through the concurrent delivery of multiple chemotherapeutic agents, *J. Control Release,* 122(3), 324-330.

Barichello J. M., Morishita M., Takayama K., Nagai T., (1999). Encapsulation of hydrophilic and lipophilic drugs in PLGA nanoparticles by the nanoprecipitation method, *Drug. Develop. Industrial Pharm,* 25(4), 471–476.

Battaglia L., Trotta M., Gallarate M., Carlotti M. E., Zara G. P., Bargoni A., (2007). Solid lipid nanoparticles formed by solvent-in water emulsion–diffusion technique: Development and influence on insulin stability, *J. Microencap,* 24(7), 660–672.

Belbella. A., Vauthier.C., Fessi.H., Devissaguet.J.P., Puisieux.F., (1996). In vitro degradation of nanospheres from poly (D,Llactides) of different molecular weights and polydispersities, Int. *J. Pharm,* 129(1), 95–102.

Bhattacharya.R., Mukherjee.P., (2008). Biological properties of "naked" metal nanoparticles, *Adv. Drug. Deliv. Rev,* 60 (11), 1289-1306.

Bivash Mandal., Kenneth.S., Alexander., Alan T.Riga., (2010). Sulfacetamide loaded Eudragit RL 100 nano suspension with potential for ocular delivery, *J.Pharmacy.Pharm.Sci,* 13(4), 510-523.

Bodmeier.R., Chen.H., (1990). Indomethacin polymeric nanosuspensions prepared by microfluidization, *J. Controlled. Release,* 12(3), 223- 233.

Bouchemal.K., Briançon.S., Fessi.H., Chevalier.Y., Bonnet.I., Perrier E., (2006). Simultaneous emulsification and interfacial polycondensation for the preparation of colloidal suspension of nanocapsules, *Material. Sci.Eng.* 26, (2), 472–480.

Bouchemal.K., Briancon.S., Perrier.E., Fessi.H., Bonnet.I., Zydowicz.N.,(2004). Synthesis and characterization of polyurethane and poly(ether urethane) nanocapsules using a new technique of interfacial polycondensation combined to spontaneous emulsification, *Int.J.Pharm,* 269, 1 89- 100.

Brigger.I., Chaminade. P., Desmaële. D., Peracchia. M. T. J., Angelo., Gurny. R., Renoir. M., Couvreur. P., (2000). Near infrared with principal component analysis as a novel analytical approach for nanoparticle technology, Pharm. Res, 17(9), 1124–1132.

C

Calvo.P., Remunan-Lopez.C., Vila-Jato.J.L.,AlonsoM.J., (1998). Novel hydrophilic chitosanpolyethylene oxide nanoparticles as protein carriers, *J. Applied. Polymer Sci,* 63(1), 125-132.

Chacon.M., Berges.L., Molpeceres.J., Aberturas.M.R., (1996). Optimized preparation of poly DL-(lactic-glycolic) microspheres and nanoparticles for oral administration, *Int.J. Pharm,* 141(1), 81–91.

Chi H.Lee., Jin-Wook Yoo., Namita Giri., (2011). pH- sensitive Eudragit nanoparticles for mucosal drug delivery, *Int.J.Pharm,* 403, 262-267.

Christine Vauthier., Kawthar Bouchemal., (2009). Methods for the preparation and manufacture of polymeric nanoparticles, *Pharm.Res.* 26(5), 1025-1057.

Christine vauthier., Philippe Legrand., Sylviane Lesieur., Amelie Bochot., Ruxandra Gref., Wouter Raatjes., Gillian Barratt., (2007). Influence of polymer behaviour in organic solution on the production of poly lactide nanoparticles by nanoprecipitation, *Int.J.Pharm,* 344, 33-43.

Coffin M.D., McGinity J.W., (1992). Biodegradable pseudolatexes: the chemical stability of poly (D, L-lactide) and poly (ε-caprolactone) nanoparticles in aqueous media, *Pharm.Res,* 9, 200–205.

Couvreur.P., Barrat.G., Fattal.E., Legrand.P., Vauthier.C., (2002). Nanocapsule technology, *Critical Rev. Therap. Drug Carrier Sys,*19(2), 99- 134.

Couvreur.P., Dubernet.C., Puisieux.F., (1995). Controlled drug delivery with nanoparticles: current possibilities and future trends, *Eur. J. Pharm.Biopharm*, 41(1), 2 - 13.

D

Desai.M., Hilfinger.J., Amidon.G., Levy. R.J., Labhaset., Niwa.V., Futaki S., Kiwadar H., (1999). Immune response with biodegradable nanospheres and alum: Studies in rabbits using staphylococcal entertoxin localization signal: Qualitative and quantitative evaluation of Btoxoid, *J. Microencap,* 17, 215–225.

Desai.M.P., Labhasetwar.V., Amidon. G.L., Levy R.J., (1996). Gastrointestinal uptake of biodegradable microparticles: effect of particle size, *Pharm. Res,* 13(12), 1838—1845

Desai.M.P., Labhasetwar.V., Walter.E., Levy.R.J., Amidon. G.L., (1997). The mechanism of uptake of biodegradable microparticles in Caco-2 cells is size dependent, *Pharm. Res,* 14(11), 1568-1573.

Dhananjay S.Singare., Seshasai Marella., Gowthamrajan.K., Giriraj.T.Kulkarni., Rajesh Vooturi., Parchuri Srinivasas Rao., (2010). Optimization of formulation and process variable of nanosuspension: An industrial perspective, *Int.J.Pharm,* 402, 213-220.

Dhaval J.Patel., Jayvadan K.Patel., (2010). Mucoadhesive effect of polyethylene oxide on famotidine nanosuspension prepared by solvent evaporation method,*Int.J.Pharmacy.Pharm.Sci,*2(2),122-127.

Duclairoir.C., Nakache.E., Marchais.H., Orecchioni. A. M., (1998). Formation of gliadin nanoparticles: influence of the solubility parameter of the protein solvent, *Colloidal Polymer. Sci,* 276(4), 321–327.

Duclairoir.C., Orecchioni. A.M., Depraetere. P., Nakache. E., (2002). Tocopherol encapsulation and in vitro release from wheat gliadin nanoparticles, *J. Microencap,* 19(1), 53 - 60.

Dunne.M., Corrigan.O.I., Ramtoola.Z., (2000). Influence of particle size and dissolution conditions on the degradation properties of polylactide-co-glycolide particles, *Biomaterials,* 21, (16), 1659-1668.

E

Ekman. B., (1978)., Improved stability of proteins immobilized in microparticles prepared by modified emulsion polymerization technique, *J. Pharm. Sci,* 67(5), 693 - 696.

Elvassore. N., Bertucco A., Caliceti P., (2001). Production of insulin-loaded poly (ethylene glycol)/poly (l-Lactide) (PEG/PLA) nanoparticles by gas antisolvent techniques, *J. Pharm. Sci,* 90(10), 1628- 1636.

F

Ferrari M., (2005). Cancer nanotechnology: opportunities and challenges. Nature Reviews Cancer, 5, 161-171.

Fessi.H., Puisieux.F., Devissaguet.J.P., Ammoury.N., Benita.S., (1989). Nanocapsule formation by interfacial polymer deposition following solvent displacement, *Int.J.Pharm,* 55(1), R1–R4.

Francesco Castelli., Chiara Messina., Maria Grazia Sarpietro., Rosario Pignatello., Giovanna Puglisi., (2003). Eudragit as controlled release system for anti-inflammatory drugs A comparision between DSC and dialysis experiments, *Thermochinica. Acta,* 400,227-234.

G

Gershon Golomb., Einat Cohen-sela., Michael Chorny., Nickolay Koroukhov., Haim D. Dannenberg., (2009). Anew double emulsion solvent diffusion technique for encapsulating hydrophilic molecules in PLGA nanoparticles, *J.Controlled. Release* 133, 90-95.

Giuseppe Trapani., Angela Lopedota., Adriana Trapani., Annalisa Cutrignelli., Laura Chiarantini., Elena Pantucci., Rosa Curci., Elisabetta Manuali., (2009). The use of Eudragit RS100/ cyclodextrin nanoparticles for the transmucosal administration of glutathione, *Eur.J.Pharm.BioPharm,* 72,509-520.

Grislain.L., Couvreur.P., Lenaerts.V., Roland.M., Deprez- Decampeneere.D., Speiser.P., (1983). Pharmacokinetics and distribution of a biodegradable drug-carrier, *Int.J. Pharm,* 15(3), 335-345.

Gurny.R., Peppas.N.A., Harrington.D.D., Banker.G.S., (1981). Development of biodegradable and injectable lattices for controlled release of potent drugs, *Drug. Develop. Industrial. Pharm,* 7 (1) – 25.

Guterres.S.S., Fessi.H., Barrat.G., Devissaguet.J.P., Puisiex.F., (1995). Poly (DL-Lactide) nanocapsules containing diclofenac. Formulation and stability study, *Int.J.Pharm*, 113(1), 57–63.

H

Hans ML ., Lowman AM., (2002). Biodegradable nanoparticles for drug delivery and targeting. Curr. Opin. Solid State Materials Sci, 6, 319-327.

Harivardhan Reddy., Murthy., (2005). Etoposide-Loaded Nanoparticles Made from Glyceride Lipids: Formulation, Characterization, in Vitro Drug Release, and Stability Evaluation. *AAPS.Pharm.Sci.Tech.* 6(2), E158-E166**.**

Hatem Fessi., Sergio A.Galindo-Rodriguez., Francois Puel., Stephanie Briancon., EricAllemann., Eric Doelker., (2005). Comparative scale-up three methods for producing ibuprofen-loaded nanoparticles, *Eur.J.Pharm.Sci,* 25, 357-367.

http://www.emea.eu.int.

Hussain Kooshapur., Mandana Chaideh., (1999). Intestinal transport of human insulin in rat, *Med.J.Islamic.Acad.Sci,* 12(1), 5-11.

I

Ibrahim A.Alsarra., Ahmed A.Bosela., Abdullah M. Mohizea., Gamal M.Mahrous., Steven H.Neau**., (2005).** Modulating intestinal uptake of Atenolol using niosomes as drug permeation enhancers, *Sci. Pharm,* 73, 81-93.

Illum.L., Farraj.N.F., Davis.S.S., (1994). Chitosan as novel nasal delivery system for peptide drugs, *Pharm.Res*, 11(8,) 1186- 1189.

Indian Pharmacopoeia (1996). Government of India Ministry of Health and Family Welfare, Controller of Publication, Delhi, Volume II (P-Z, reference Spectra and Appendices), Appendix 13.2, A 144-147.

J

Jain, K.K., (2005). The role of nanobiotechnology in drug discovery, Drug Discovery Today, 10(21).1435-1442.

Janes.K.A., Calvo P., Alonso M.J.,(2001). Polysaccharide colloidal particles as delivery systems for macromolecules, Adv. Drug. Deliv, Rev. 47(1), 83-97.

Javed Ali., Vikas Bali., Mushir Ali., (2011). Nanocarrier for the enhanced bioavailability of a cardiovascular agent: In vitro, pharmacodynamic, pharmacokinetic and stability assessment. *Int.J.Pharm.* 403, 46-56.

Jawahar.N., Nagasamy Venkatesh.D., Suresh Kumar.R., Senthil.V., Ganesh.G.N.K., (2009). Development and characterization of PLGA - nanoparticles containing carvedilol,*J.Pharm.Sci.Res, 1*(3),123-128.

Ji Jingou., Hao Shilei., Liu Weiqi.,Wu Danjun., Wang Tengfei., Xu Yi., (2011). Preparation, characterization of hydrophilic and hydrophobic drug in combine loaded chitosan/cyclodextrin nanoparticles and in vitro release study.*Colloids.SurfaceB.Biointface*.83, 103-107.

Jiang.J., Oberdörster.G., Biswas.P., (2009). Characterization of size, surface charge, and agglomeration state of nanoparticle dispersions for toxicological studies, *J.Nanoparticle. Res,* 11(1) 177-189

Jundong Dai., Tsuneji Nagai., Xueqing Wang., Tao Zhang., Meng Meng., Qiang Zhang.,(2004). PH-sensitive nanoparticles for improving the oral bioavailability of cyclosporine A. *Int.J. Pharm*. 280, 229-240**.**

Jung.T., Kamm.W., Breitenbach.A., Kaiserling.E., Xiao.J.X., Kissel.T., (2005). Biodegradable nanoparticles for oral delivery of peptides: is there a role for polymers to affect mucosal uptake, *Eur. J. Pharm.Biopharm*, 50(1), 147- 160.

K

Karen I. Winey., Avinash Budhian., Steven J. Siegel., (2005). Production of haloperidol loaded PLGA nanoparticles for extended controlled drug release of haloperidol. *J.Microencap. 22(7), 773-785.*

Ken-Ichi Nezasa., Kazutaka Higaki., Tadahiko Matsumura., Kazuhiro Inazawa., Hiroshi Hasegawa., Masayuki Nakano., Masahiro Koike., (2002).Liver-specific distribution of rosuvastatin in rats: comparison with pravastatin and simvastatin. *The.American.Scoi.Pharmcol.Exp.Therap.* 30(11), 1158-1163.

Khopde.A.J., Jain. N.K., (2001). Dendrimer as potential delivery system for bioactive In: Jain NK, editor. Advances in controlled and novel drug delivery. *CBS publisher*, New Delhi, p. 361-380.

Khosro Adibkia., Yousef Javadzadeh., Siavoush Dastmalchi., Ghobad Mohammadi., Fatemeh Kari Niri., Mahmood Alaei- Beirami., (2011). Naproxen-Eudragit RS 100 nanoparticles: Preparation and physicochemical characterization. *Colloids. SurfacesB: Bio.Int*. 83,155-159.

Kimiko Makino., Hiroshi Teradaa., (2008). *In vitro* permeation of gold nanoparticles through rat skin and rat intestine: Effect of particle size, *Colloids and Surfaces B: Biointerfaces,* 65, 1–10.

Kreuter.J., (1983). Evaluation of nanoparticles as drug-delivery systems. I. Preparation methods. *Pharmaceutica Acta Helvetiae,* 58, 196-209.

Kreuter.J., (1994). Nanoparticles. In Colloidal drug delivery systems, J. K. Ed. Marcel Dekker: New York, 219-342

Kreuter.J., (2004). Nanoparticles as drug delivery system. In: Nalwa HS, editor. *Encyclopedia of Nanoscience.NanoTechn*. (7). New York: American Scientific Publishers. 161–180.

Kreuter.J., Ramge.P., Petrov.V., Hamm.S., Gelperina.S.E., Engelhardt.B., Alyautdin.R., Von Briesen.H., Begley.D.J.,(2003). Direct evidence that polysorbate-80-coated poly (butylcyanoacrylate) nanoparticles deliver drugs to the CNS via specific mechanisms requiring prior binding of drug to the nanoparticles, *Pharm. Res,* 20(3),409-416.

Kreuter.J., Zimmer.A., (1995). Microspheres and nanoparticles used in ocular delivery systems, *Adv. Drug. Deliv. Res,* 16(1), 61-73.

Kristl.J., P.Ahlin., Kristl.A., Vrecer.F.,(2002). Investigation of polymeric nanoparticles as carriers of enalaprilat for oral administration. *Int.J.Pharm*. 239,113-120.

Kubik.T., Bogunia-Kubik.K., Sugisaka. M., (2005). Nanotechnology on Duty in Medical Applications, *Current Pharm. Biotech,* 6, 17-33.

Kurt E.Geckeler., Prasad Rao.J., (2011). Polymer nanoparticles: Preparation techniques and size- control parameters, *Progress.Polymer.Sci,* 36,887-913.

L

Lambert.G., Fattal.E., Couvreur.P., (2001). Nanoparticulate system for the delivery of antisense oligonucleotides, *Adv. Drug. Deliv. Rev*, 47(1), 99 - 112.

Le Thi Mai Hoa., Nguyen tai Chi., Nguyen Minh Triet., Le Ngoc Thanh Nhan., Dang Mau Chien., (2009). Preparation of drug nanoparticles by emulsion evaporation method, *J.Physics,* 187, 1-4.

Legrand. P., Lesieur. S., Bochot. A., Gref. R., Raatjes.W., Barratt.G., Vauthier. C., (2007). Influence of polymer behaviour in organic solution on the production of polylactide nanoparticles by nanoprecipitation, *Int. J. Pharm*, 344, (1-2), 33–43.

Lemos- Senna E., Bernardy N., Romio AP., Barcelos EL., Dal Pizzel C., Araujo PH., Sayer C., (2010). Nanoencapsulation of quercetin via miniemulsion polymerization, J.Biomed.Nanotech, 6(2), 181-186.

Lenaerts.V., Labib. A., Chouinard. F., Rousseau. J., Ali H., Lier J., (1995). Nanocapsules with a reduced liver uptake: targeting of phthalocyanines to EMT-6 mouse mammary tumour in vivo, *Eur.J.Pharm.Biopharm,* 41, 38 - 43.

Lennernas., (2007). Animal data: The contribution of the using chamber and perfusion systems to predicting human oral drug delivery invivo,.*Adv.Drug.Deliv.Rev,*59, 1103-1120.

Li.V.H.K., Wood.R.W., Kreuter.J., Harmia.T., Robinson.J.R.,(1986). Ocular drug delivery of progesterone using nanoparticles, *J. Microencap*, 3(3), 213 - 218.

Liang Fang., Wei Li., Yonggang Yang., Yongshou Tianc., Xinlan Xua., Yang Chena., Liwei Mua.,Yaqiong Zhang., (2011). Preparation and in vitro/in vivo evaluation of revaprazan hydrochloride nanosuspension. *Int.J.Pharm.* 408.157-162.

Limayem.I., Charcosset.C., Fessi.H.,(2004). Purification of nanoparticle suspensions by a concentration/diafiltration process, *Separation and Purification Technology*, 38(1), 1-9.

Ljubimova.J.Y., Fujita.M., Khazenzon.N.M., Lee.B.S., Wachsmann-Hogiu.S., Farkas.D.L., Black K.L., Holler.E., (2008). Nanoconjugate based on polymalic acid for tumor targeting, *Chemico-Biological Interactions,* 171(2), 195-203.

M

Madaswamy S.Muthu., Sanjay Singh., Manoj K.Rawat., Amit Mishra., (2009). PLGA nanoparticles formulations of Risperidone: preparations and neuropharmacological evaluation, *J.NanoMed.NanoTech.Biology.Med,* 5,323-333.

Magneheim.B., Benita.S., (1991). Nanoparticles characterization: a comprehensive physicochemical approach, *STP Pharm. Sci*, 1, 221–241.

Mainardes.R.M., Evangelista.R.C., (2005).PLGA nanoparticles containing praziquantel: effect of formulation variables on size distribution, *Int. J. Pharm*, 290(1-2), 137- 144.

Maincent. P., Le Verge. R, Sado .P., Couvreur. P., Devissaguet. J.P., (1986). Disposition kinetics and oral bioavailability of vincamine-loaded polyalkyl cyanoacrylate nanoparticles, *J. Pharm.Sci,* 75(10), 955 - 958.

Mallikarjun Chitneni., **Kok Khiang Peh., Yusrida Darwis., Muthanna Abdulkarim., Ghassan Zuhair Abdullah., Mohammed Javed Qureshi., (2011).** Intestinal permeability studies of sulpiride incorporated into self- microemulsifying drug delivery system, *Pak.J.Pharm.Sci,* 24(2), 113-121.

Manchester.M., Singh.P., (2006). Virus-based nanoparticles (VNPs): Platform technologies for diagnostic imaging, *Adv.Drug. Deliv.Rev,*. 58(14), 1505-1522.

Manish K Gupta., Brahmeshwar Mishra., Deepak Prakash., Santosh K Rai., (2009). Nanoparticulate drug delivery system of cyclosporine. *Int.J.Pharmacy. Pharm. Sci.* 1(2), 81-92.

Mansouri.S, Lavigne.P, Corsi.K, Benderdour.M, Beaumont.E, Fernandes.J.C., 2004). Chitosan-DNA nanoparticles as non-viral vectors in gene therapy: strategies to improve transfection efficacy, *Eur. J. Pharm. Biopharm,*57(1), 1 - 8.

Mao H-Q., Roy K., Troung-Le VL., Janes. K.A., Lin.K.Y., Wang.Y., (2001). Chitosan-DNA nanoparticles as gene carriers: synthesis, characterization and transfection efficiency, *J. Control Release,* 70(3), 399- 421.

Martine Leroueil-Le Verger., **Philippe Maincent., Laurence Fluckiger., Young-II Kim., Maurice Hoffman., (1998).** Preparation and characterization of nanoparticles containing an anti hypertensive agent, *Eur.J.Pharm.BioPharm,* 46,137-143.

Matsumoto.J., Nakada.Y., Sakurai.K., Nakamura.T., Takahashi.Y., (1999). Preparation of nanoparticles consisted of poly(L-lactide) – poly(ethylene glycol) – poly(L-lactide) and their evaluation in vitro, *Int. J.Pharm,* 185(1), 93– 101.

Mbela.T.K.M., Poupaert. J.H., Dumont.P., (1992).Poly (diethylmethyldene malonate) nanoparticles as primaquine delivery system to liver, *Int. J. Pharm,* 79, 29 -38.

Mishra.B., Arya.,Tiwari.S., (2010). Investigation of formulation variables affecting yhe properties of lamotrigine nanosuspension using fractional factorial design,*Daru*,18(1),1-8.

Mohammad Reza Siahi Shadbad., Mohammad Barzegar-Jalali., Khosro Adibkia., Hadi Valizadeh., Ali Nokhodchi., Yadollah Omidi., Ghobad Mohammadi., Somayeh Hallaj Nezhadi., Maryam Hasan., (2008). Kinetic Analysis of drug release from nanoparticles. *J.Pharm.Pharmceut.Sci*. 11(1) 167-177.

Mohammed Anwar., Musarrat H. Warsi., Neha Mallick., Sohail Akhter., Sachin Gahoi., Gaurav K. Jain ., Sushma Talegaonkar., Farhan J. Ahmad., Roop K. Khar., (2011). Enhanced bioavailability of nano-sized chitosan–atorvastatin conjugate after oral administration to rats. *Eur.J.Pharm.Sci*.44, 241-249.

Mohammed Reza Avadi., Assal Mir Mohammad Sadeghi., Nasser Mohammad pour., Saideh Abedin., Fatemeh Atyabi., Rassoul Dinarvand., Morteza Rafice – Teharani., (2010). Preparation and characterization of insulin nanoparticles using chitosan and Arabic gum with ionic gelation method, *Nanomed. Nanotech. Biology and Medicine*. 6, 58 -63.

Mohanraj.V.J., Chen.Y., (2006). Nanoparticles-A Review,*Trop.J.Pharm.Res.*5(1),561-573.

Mohanty Sivasankar., Boga Pramod Kumar., (2010). Role of Nanoparticles in drug delivery system. *Int.J.Res.Pharm.BioMedSci*. 1(2), 41-66.

Mohantya .B., Aswalb. V.K., Kohlbrecherc.J., Bohidar.H.B., (2005). Synthesis of Gelatin Nanoparticles via Simple Coacervation, *J. Surface Science and Tech,* 21(3-4), 1-12.

Moinard-Chécot.D., Chevalier.Y., Briançon.S., Fessi.H., Guinebretière.S., (2006). Nanoparticles for drug delivery: review of theformulation and process difficulties illustrated by the emulsiondiffusion process, *J.Nanoscience. Nanotech.* 6(9–10), 2664–2681.

Molpeceres.J., Guzman.M., Aberturas.M.R., Chacon.M., Berges.L., (1996). Application of central composite designs to the preparation of polycaprolactone nanoparticles by solvent displacement *, J.Pharm.Sci,* 85(2), 206–213.

Mora CE – Huertas., Fessi.H., Elaissari.A., (2010). Polymer based Nano capsules for drug delivery, *Int.J. Pharm,* 385, 113 - 142.

Mukesh S.Patil., Kedar. R. Bavaskar., Ghanashyam.A.Girnar., (2011). Preparation and optimization of Simvastatin nanoparticles for solubility enhancement and invivo study, *Int.J.Pharm.Res.Develop,* 2(12), 219-225.

Muller. R.H., Jacobs.C., Kayser.O., (2001). Nanosuspensions as particulate drug formulations in therapy: Rationale for development and what we can expect for the future, *Adv. Drug. Deliv. Reviews,* 47(1), 3-19.

N

Nahar.M., Dutta. T., Murugesan.S., Asthana. A., Mishra.D., Rajkumar.V., Tare. M., Saraf. S., Jain.N.K., (2006). Functional polymeric nanoparticles: an efficient and promising tool for active delivery of bioactives, *Crit .Rev. Ther. Drug .Carrier. Syst,* 23(4), 259-318.

Némati.F., Dubernet.C., Fessi.H., Verdière.A. C., Poupon.M. F., Puisieux.F., Couvreur. P., (2004). Reversion of multidrug resistance using nanoparticles in vitro: influence of the nature of the polymer, *Int.J.Pharm*, 138(2), 237–246.

P

Paulo Costa., Jose´ Manuel Sousa Lobo., (2001). Modeling and comparison of dissolution profiles. *Eur.J.Pharm.Sci*.13, 23-33.

Peng Liu., Xinyu Rong., Johanna Laruc., Bert van Veenc., Juha Kiesvaarac., Jouni Hirvonena., Timo Laaksonena., Leena Peltonena., (2011). Nanosuspensions of poorly soluble drugs: Preparation and development by wet milling. *Int.J.Pharm*.411, 215-222.

Peracchia.M.T., Fattal E., Desmaele.D., Besnard.M., Noel.J.P., Gomis.J.M., Appel.M., Couvreur P., (1999). Stealth (®) PEGylated polycyanoacrylate nanoparticles for intravenous administration and splenic targeting, *J.Controlled. Release*, 60(1), 121-128.

Philippe Maincent., Martine Leroueil-Le Verger., Laurence Fluckiger., Young-II Kim., Maurice Hoffman., (1998). Preparation and characterization of nanoparticles containing an anti hypertensive agent, *Eur.J.Pharm.BioPharm,* 46,137-143.

Pieter Annaert., Joachim Brouwers., Ann Bijnens., Frank Lammert., Jan Tack., Patrick Augustijins., (2010). Exvivo permeability experiments in excised rat intestinal tissue and invitro solubility measurements in aspirated human intestinal fluids support age-dependent oral drug absorption, *Eur.J.Pharm.Sci,* 39, 15-22.

Pikal. M.J., Shah. S., Roy.M.L., Putman.R., (1990). The secondary drying stage of freeze-drying: drying kinetics as a function of temperature and chamber pressure, *Int. J. Pharm,* 60,203–217.

Poovi.G., Dhana Lekshmi.U.M., Narayanan.N., Neelakanta Reddy.P., (2011). Preparation and characterization of Repaglinide loaded chitosan polymeric nanoparticles, *Res.J.NanoSci.NanoTech,* 1(1), 12-24.

Praveen Kumar Gupta., Pandit.J.K.,Ajay Kumar., Pallavi Swaroop., Sanjiv Gupta., (2010). Pharmaceutical nanotechnology novel nanoemulsion- high energy emulsification preparation, evaluation and application,*The.Pharma.Res,*3,117-138.

Q

Qiang Zhang., Jundong Dai., Tsuneji Nagai., Xueqing Wang., Tao Zhang., Meng Meng., (2004). pH-sensitive nanoparticles for improving the oral bioavailability of cyclosporine A, *Int.J.Pharm,* 280,229-240.

Qiu S.X., Ruan.L.P., S. Chen.S., Yu B.Y., D.N. Zhu., Cordell.G.A., (2005). Prediction of human absorption of natural compounds by the non-everted rat intestinal sac mode, *Eur.J.Med.Chem,*41,605-610.

Quaroni .A., J. Hochmanb., (1996). Development of intestinal cell culture models for drug transport and metabolism studies, Adv.Drug.Del.Rev 22, 3-52.

Quintanar-Guerrero. D., Allémann.É., Doelker.É..Fessi.H., (1996). Influence of stabilizing agents and preparative variables on the formation of poly(-lactic acid) nanoparticles by an emulsification– diffusion technique, *Int.J.Pharm,* 143(2), 133–141.

Quintanar-Guerrero. D., Allémann.É., Doelker.É..Fessi.H., (1998). Preparation and characterization of nanocapsules from preformed polymers by a new process based on emulsification– diffusion technique, *Pharm. Res,* 15(7), 1056–1062.

Quintanar-Guerrero.D., Alle´mann.E., Fessi.H., Doelker.E., (1998). Preparation techniques and mechanism of formation of biodegradable nanoparticles from preformed polymers*, Drug Devlop. Industrial. Pharm,* 24(12), 1113-1128.

R

Ravi Kumar., Mittal., Sahana., Bhardwaj., (2007). Estradiol loaded PLGA nanoparticles for oral administration: Effect of polymer molecular weight and copolymer composition on release behavior in vitro and in vivo.*J.Controlled.Release.*119, 77-85.

Raymond C.Rowe., Paul J. Sheskey., Sean C.Owen., (2006). Handbook of Pharmaceutical excipients, Pharmaceutical press, London, 5th edition, 535-538,553-560 and 592-593.

Redhead.H.M., Davis.S.S., Illum.L., (2001).Drug delivery in poly (lactide-co-glycolide) nanoparticles surface modified with poloxamer 407 and poloxamine 908: in vitro characterisation and in vivo evaluation, *J. Controlled. Release,* 70(3), 353-363.

Reisch MS., (2007). Nano goes big time, Chem. Eng. News, 85(4), 22-25.

Rezaei Mokarram.A., Kebriaee zadeh. A., Keshavarz.M., Ahmadi.A.,Mohtat.B., (2010). Preparation and in-vitro evaluation of indomethacin nanoparticles, *Daru,* 18(3), 185-192.

Richard W. Korsmeyer., Robert Gumy., Eric Doelker., Pierre Buri., Nikolaos A. Peppas., (1983). Mechanisms of solute release from porous hydrophilic polymers.*Int.J.Pharm.*15, 25-35.

Ronald J.Neufeld., Catarina Pinto Reis., Antonio J.Ribeiro., Francisco Veiga., (2006). Nanosuspension Methods for preparation of drug – loaded polymeric nanoparticles, *J.NanoMed.NanoTech.Biology.Med,* 2, 8-21.

Ruolan Xiong., Weigen Lu., Jun Li., Peiquan Wang., Rong Xu., Tingting Chen., (2008). Preparation and characterization of intravenously injectable nimodipine nanosuspension. *Int.J.Pharm*. 350, 338-343.

S

Sa´nchez.A., Vila Jato.J.L., Alonso.M.J., (1993). Development of biodegradable microspheres and nanospheres for the controlled release of cyclosporine, *Int.J.Pharm,* 99(2-3) 263- 273.

Sanjeeb K.Sahoo., Suphiya Parveen., Ranjita Misra., (2011). Nanoparticles boon to drug delivery, therapeutics, diagnostics and imaging, *J.NanoMed.NanoTech.Biology.Med,* 1-20.

Seijo B., Fattal.E., Roblot-Treupel.L., Couvreur .P., (1990). Design of nanoparticles of less than 50 nm diameter: preparation, characterization and drug loading, *Int.J.Pharm*, 62(1), 1 - 7.

Senthilkumar.M., Subramanian.G., Ranjitkumar.A.,Nahar.M., Mishra.P. Jain N.K., (2007). PEGylated Poly (Lactide-co-Glycolide) (PLGA) nanoparticulate delivery of Docetaxel: synthesis of diblock copolymers, optimization of preparation variables on formulation characteristics and in vitro release studies, *J Biomed Nanotech,* 1, 52-60.

Shishu., Manjul Maheshwari.,(2010). Comparative bioavailability of curcumin, turmeric and Biocurcumax in traditional vehicles using non-everted rat intestinal sac model.*J.Fuct.Foods*.2, 60-65.

Singh.S., **Muthu.M.S., (2009).** Poly (D, L-Lactide) Nanosuspensions of Risperidone for Parenteral delivery: Formulation and in vitro evaluation, *Current.Drug.Delivery,* 6, 62-68.

Sinha.N., Yeow.J.T.W., (2005). Carbon Nanotubes for Biomedical Applications. IEEE Transactions on Nanobioscience, 4(2), 180-195.

Sivabalan.M., Anto Shering., Phaneendhar Reddy., Vasudevaiah., Anup Jose., Nigila.G., (2011). Formulation and evaluation of 5-Fluorouracil loaded chitosan and Eudragit Nanoparticles for cancer therapy. *Int.J.Compren.Pharm*. 1(7), 1-4.

Skiba.M., Morvan C., Duchene.D., Puisieux.F.,Wouessidjewe.D., (1995). Evaluation of gastrointestinal behaviour in the rat of amphiphilic β-cyclodextrin nanocapsules, loaded with indomethacin, *Int. J.Pharm*, 126(2), 275–279.

Skiba.M., Wouessidjewe.D, Puisieux.F., Duchène.D., Gulik. A., (1996). Characterization of amphiphilic fl-cyclodextrin nanospheres, *Int.J.Pharm*, 142(1), 121–124.

Snjezana Stolnik., Thirumala Govender., Martin C.Garnett., Stanley S.Davis., (1999). PLGA nanoparticles prepared by nanoprecipitation: drug loading and release studies of a water soluble drug, *J.Controlled.Release* 57,171-185.

Soppimath.K.S., Aminabhavi.T.M., Kulkarni.A.R., Rudzinski.W.E., (2001). Biodegradable polymeric nanoparticles as drug delivery devices, *J. Controlled. Release*, 70(1) 1-20.

Suvakanta Dash., Padala Narasimha Murthy., Lilakanta Nath., Prasanta Chowdhury., (2010). Kinetic Modelling on drug release from controlled drug delivery systems, *Acta.Poloniac.Pharm,* 67(3)217-223.

Swarnali Das., Preeti K.Suresh., Rohitas Desmukh., (2010). Design of Eudragit RL100 nanoparticles by nanoprecipitation method for ocular drug delivery, *J.NanoMed.NanoTech.Biology.Med,* 6,318-323.

Syam Potnuru., Sundaramoorthy.K., Vetrichelvan.T., (2011). Design of biodegradable polymer nanoparticles for oral drug delivery of stavudine: *in- vitro* dissolution studies and characterization, Int.J.Pharm.Tech, 3(1), 1360-1372.

T

Tang.X., Pikal.M.J., (2004). Design of freeze-drying processes for pharmaceuticals: practical advice, *Pharm. Res,* 21(2), 191–200.

Thote.A.J., Gupta.R.B., (2005). Formation of nanoparticles of a hydrophilic drug using supercritical carbon dioxide and microencapsulation for sustained release, *Nanomedicine: Nanotech. Biology. Medicine,* 1(1), 85-90.

Tice.T.R., Gilley.R.M., (1985). Preparation of injectable controlled-release microcapsules by solvent-evaporation process, *J. Controlled. Release*, 2, 343 - 352.

U

Ubrich.N., Schmidt.C., Bodmeier.R., Hoffman.M., Maincent.P., (2005). Oral evaluation in rabbits of cyclosporine- loaded Eudragit RS or RL nanoparticles, *Int.J.Pharm,* 288, 169-175.

Ueda.H., Kreuter.J., (1997). Optimization of the preparation of loperamide loaded poly (l-lactide) nanoparticles by high pressure emulsification solvent evaporation, *J.Microencap,* 14(5), 593- 605.

Ugo Bilati., Eric Allemann., Eric Doelker., (2005). Development of a nanoprecipation method intended for the entrapment of hydrophilic drugs into nanoparticles. *Eur.J.Pharm.Sci*. 24, 67-75.

Vasir, J. K., Reddy M.K., Labhasetwar V. D., (2005). Nanosystems in Drug Targeting: Opportunities and Challenges. Current Nano.sci, 1, 47-64.

Vaughn. J.M., (2006). Single dose and multiple dose studies of itraconazole nanoparticles, *Eur. J. Pharm.Biopharm,* 63(2), 95–102

Vauthier.C., Bouchemal.K.,(2009). Methods for the Preparation and Manufacture of Polymeric Nanoparticles, *Pharm. Res*, 26(5), 1025- 1058.

Vauthier.C., Dubernet.C., Fattal.E., Pinto-Alphandary.H., Couvreur.P., (2003). Poly (alkylcyanoacrylates) as biodegradable materials for biomedical applications, *Adv. Drug Deliv. Rev*, 55(4), 519- 548.

Vijaykumar N., Venkateswarlu., Raviraj., (2010). Development of oral tablet dosage form incorporating drug nanoparticles. *Res.J.Pharm.Bio.ChemSci*.1 (4), 952-963.

Vila. A., Sanchez. A., Tobio. M., Calvo. P., Alonso M.J., (2002). Design of biodegradable particles for protein delivery, *J.Controlled. Release,* 78(1) 15-24.

Vishal V., Rajkondwar., Pramila Maini1., Monika Vishwakarma., (2009). Characterization and method development for estimation and validation of Rosuvastatin Calcium by UV – visible spectrophotometry. *Int.J. Theoretical. Applied. Sci.*1 (1)48-53.

Wadke PA., Jacobson S. Preformulation testing In: Liebermann HA, Lachman L, Editors. Pharmaceutical Dosage Forms – Tablets. New York: Marcel Dekker Inc; 1980.

W

Wang.N., Wu.X.S., Mesiha.M., (1995).A new method for preparation of protein-loaded agarose nanoparticles, *Pharm. Res,*12, S257.

Wang.Y., Dave.R.N., Pfeffer.R., (2004). Polymer coating/encapsulation of nanoparticles using a supercritical anti-solvent process, *J.Supercritical Fluids,* 28, 85- 99.

Watnasirichaikul. S., Davies. N.M., Rades.T., Tucker. I.G., (2000). Preparation of biodegradable insulin nanocapsules from biocompatible microemulsions, *Pharm. Res,* 17(6), 684- 689.

Wickline.S.A., Lanza.G.M., (2002). Molecular Imaging, Targeted Therapeutics, and Nanoscience, *J .Cellular. Biochem. Supp,*9, 90–97.

Williams.N.A., Polli.G.P., (1984). The lyophilization of pharmaceuticals: a literature review, *J.Parenter. Science .Technology*, 38(2), 48–59.

Wissing.S.A., Kayser.O., Muller.R.H., (2004). Solid lipid nanoparticles for parenteral drug delivery, *Adv.Drug. Deliv. Rev*, 56(9), 1257-1272.

www.drugbank.com

X

Xiangrong Song., Shixiang Hou., Yu Zhao., Fangyuan Xu., Rongli Zhao., Junyao He., Zeng Cai.,Yuanbo Li., Qiuhong Chen., (2008). Dual agents loaded PLGA nanoparticles: Systematic study of particle size and drug entrapment efficiency, *Eur.J.Pharm.BioPharm,* 69,445-453.

Xuenong Zhang., Qiang Hong., Yang., Zhigang Fang., Yagen Chen., (2011). The pharmacokinetic profile of Freeze- dried Cyclosporine A- Eudragit S100 Nanoparticles formulation in dogs, *Nano.Biomed.Eng*. 3(1), 53-56.

Y

Ya-Ping L., Yuan-Ying.P., Xian-Ying.Z., Zhou-Hui Gu., Zhao-Hui.Z., Wei-Fang.Y., Jian-Jun.Z., Jian-Hua.Z., Xiu-Jian.G., (2001).PEGylated PLGA nanoparticles as protein carriers: synthesis, preparation and biodistribution in rats, *J. Controlled. Release,* 71(2), 203-211

Yoshioka.T., Hashida.M., Muranishi.S., Sezaki.H., (1981). Specific delivery of mitomycin C to the liver, spleen, and lung: nano- and microspherical carriers of gelatin, *Int.J.Pharm*, 8(2), 131 - 141.

Z

Zimmermann.E., Müller.R.H., Mäder.K., (2000). Influence of different parameters on reconstitution of lyophilized SLN, *Int.J.Pharm,* 196(2), 211–213.